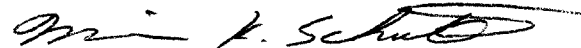
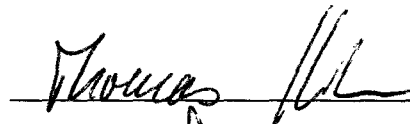


INVESTIGATION OF THE ALLOSTERIC MODULATORS
DESFORMYLFLUSTRABROMINE AND 4-(2-HYDROXYETHYL)-1-
PIPERAZINEETHANESULFONIC ACID (HEPES) INTERACTIONS ON NICOTINIC
ACETYLCHOLINE RECEPTORS

By
Maegan M Daniello-Weltzin

RECOMMENDED:



Advisory Committee Chair



Chair, Department of Chemistry and Biochemistry

APPROVED:



Dean, College of Natural Science and Mathematics



Dean of the Graduate School

Date

July 27, 2011

**INVESTIGATION OF THE ALLOSTERIC MODULATORS
DESFORMYLFLUSTRABROMINE AND 4-(2-HYDROXYETHYL)-1-
PIPERAZINEETHANESULFONIC ACID (HEPES) INTERACTIONS ON NICOTINIC
ACETYLCHOLINE RECEPTORS**

A
THESIS

Presented to the Faculty
of the University of Alaska Fairbanks
in Partial Fulfillment of the Requirements
for the Degree of

DOCTOR OF PHILOSOPHY

By

Maegan M Daniello-Weltzin, B.S.

Fairbanks, Alaska

August 2011

UMI Number: 3484666

All rights reserved

INFORMATION TO ALL USERS

The quality of this reproduction is dependent upon the quality of the copy submitted.

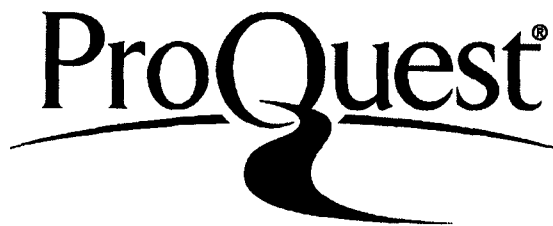
In the unlikely event that the author did not send a complete manuscript and there are missing pages, these will be noted. Also, if material had to be removed, a note will indicate the deletion.



UMI 3484666

Copyright 2011 by ProQuest LLC.

All rights reserved. This edition of the work is protected against unauthorized copying under Title 17, United States Code.



ProQuest LLC
789 East Eisenhower Parkway
P.O. Box 1346
Ann Arbor, MI 48106-1346

Abstract

Neuronal nicotinic acetylcholine receptors (nAChRs) are members of the Cys-loop super family of ligand gated ion channels. Dysregulation of nAChRs can lead to pathologies such as Alzheimer's disease, Parkinson's disease, Autism and nicotine addiction. Possible new therapeutic avenues are positive allosteric modulators (PAMs).

The natural product desformylflustrabromine (dFBr), a tryptophan metabolite of the marine bryozoan *Flustra foliacea*, was found to be PAM of $\alpha 4\beta 2$ nAChR. Evaluation of our synthetic water soluble dFBr salt by two-electrode voltage clamp of *Xenopus laevis* oocytes expressing human nAChR confirmed that synthetic dFBr displayed similar properties as the natural product. Low concentrations of the synthetic dFBr enhanced ACh's efficacy on $\alpha 4\beta 2$ receptors. At higher dFBr concentrations, dFBr inhibited ACh potentiated responses. On $\alpha 7$ receptors, dFBr inhibited ACh induced currents.

Further pharmacological characterization of dFBr revealed that dFBr was able to enhance partial agonist potencies and efficacies. Evaluation of dFBr on antagonists showed no effect on antagonist inhibition. The mechanisms of biphasic modulation (potentiation and inhibition) of dFBr on $\alpha 4\beta 2$ nAChR were also investigated. Enhanced efficacy of ACh induced currents by dFBr appeared to be accomplished by dFBr stabilization of the open receptor conformation by destabilization of the desensitized state. The inhibition of ACh potentiated currents by dFBr appeared to involve open-channel block.

To better understand dFBr mechanisms, its putative binding site was examined. Alanine mutations were made in non-orthosteric clefts on the $\beta 2+$ and $\alpha 4-$ faces. Results revealed residues located on these faces are involved in ACh induced conformational change of the receptor. In addition our data supports our hypothesis that allosteric modulation by dFBr interacts with residues located on the $\beta 2+$ and $\alpha 4-$ faces.

The new novel actions of (4-(2-hydroxyethyl)-1-piperazineethanesulfonic acid) (HEPES) as a $\alpha 4\beta 2$ stoichiometric PAM was discovered and characterized. We showed that HEPES, a common buffering agent, potentiated the high ACh sensitivity $\alpha 4\beta 2$ receptor while only inhibiting the low ACh sensitivity $\alpha 4\beta 2$ receptor. Mutagenesis results suggested that residue $\beta 2D217$ is a critical residue in the HEPES binding site.

Results from these studies will aid in the development of therapeutic ligands that will assist in the treatment of diseases where nAChRs are dysregulated.

Table of Contents

Signature Page	i
Title Page.....	ii
Abstract.....	iii
Table of Contents.....	iv
List of Figures	xiii
List of Tables.....	xvii
List of Appendices.....	xviii
Acknowledgements	xix
CHAPTER 1: Introduction.....	1
1.1. Gaps in Current Knowledge.	2
1.2. Gaps Addressed in Current Project.....	2
1.3. General Hypothesis.....	3
1.3.1. Specific Hypotheses.....	3
1.3.1.1. Desformylflustrabromine is an Allosteric Modulator of the $\alpha 4\beta 2$ nAChR.....	3
1.3.1.2. Desformylflustrabromine Binds at the $\beta 2+/\alpha 4$ - Interface on $\alpha 4\beta 2$ nAChR.....	4
1.3.1.3. HEPES is a positive allosteric modulator of $\alpha 4\beta 2$ nAChR.....	4
1.4. References.....	5
CHAPTER 2: Neuronal Nicotinic Receptors: Structure, Function and Therapeutic Opportunities.....	6
2.1. Introduction.	6

2.2.	A General Description of the Physiological Role of nAChRs.....	6
2.3.	The Ligand Gated Ion Channel Superfamily.....	7
2.3.1	Classification of LGICs.....	7
2.4.	Structure of the Cys-loop LGIC Family.....	9
2.5.	Predominant nAChR Subtypes.....	11
2.6.	Receptor Structure Described by Biochemical and X-ray Crystallography Studies.....	14
2.6.1	Extracellular Binding Domain.....	15
2.6.2	Transmembrane Domain.....	18
2.6.2.1	Transmembrane Domain Structure.....	18
2.6.2.2	Transmembrane Domain and Receptor Gating.....	20
2.6.3	Intracellular Domain.....	23
2.6.3.1	Ion Channel Selectivity.....	24
2.6.4	Comparison of Different Electron Diffraction and X-ray Crystallization of nAChR Structures.....	26
2.6.5	X-Ray Crystallography and Molecular Modeling of AChBP.....	27
2.6.5.1	AChBP Crystal Structure Bound to Orthosteric Ligands.....	29
2.6.5.2	AChBP Crystal Structure Bound to Allosteric Ligands.....	30
2.7.	Orthosteric and Allosteric Binding Sites.....	30
2.7.1	Characterized Binding Sites on the Serotonin Type 3 Receptor (5-HT3R).....	31
2.7.1.1	The 5HT3R Orthosteric Binding Site.....	31
2.7.1.2	The 5-Hydroxyindole Binding Site.....	34
2.7.2	Characterized Binding Sites on Gamma Amino Butyric Acid (GABA) Receptors.....	35
2.7.2.1	The Benzodiazepine Binding Site.....	35

2.7.2.2	The Neurosteroid Binding Site.....	37
2.7.2.3	The Anesthetic Binding Site.....	40
2.7.3	Characterized Binding Sites on Nicotinic Acetylcholine Receptors.....	41
2.7.3.1	The Physostigmine Binding Site.....	41
2.7.3.2	The Divalent Calcium Biding Site.	41
2.7.3.3	The NS-1738 and PNU-120596 Binding Sites.	42
2.7.3.4	The Galanthamine Binding Site.....	43
2.7.3.5	The 17 β -Estradiol Binding Site.....	45
2.7.3.6	The Zinc Binding Site.....	45
2.7.3.7	Channel Blockers.....	47
2.8.	Receptor Mechanism.....	48
2.8.1	Allostery.	48
2.8.2	Conformational Change Models.	51
2.9	Neurophysiological Role of Nicotinic Receptors.	53
2.10	Nicotinic Receptor Pharmacology.....	56
2.10.1	Selective α 4 β 2 Full and Partial Agonists.	57
2.10.1.1	Acetylcholine.....	57
2.10.1.2	Nicotine.....	57
2.10.1.3	Epibatidine.....	58
2.10.1.4	Cytisine.....	58
2.10.1.5	Varenicline.....	59
2.10.2	Selective α 4 β 2 Antagonists.	59
2.10.2.1	Mecamylamine.....	59

2.10.2.2 Methylcaconitine.....	60
2.10.2.3 Conotoxins.....	60
2.10.3 Selective $\alpha 4\beta 2$ Modulators.....	60
2.10.3.1 Galanthamine.....	61
2.10.3.2 Physostigmine.....	61
2.10.3.3 17- β -Estradiol.....	62
2.10.3.4 Zinc.....	62
2.10.3.5 Desformylflustrabromine.....	63
2.11 Assembly and Trafficking of Nicotinic Receptors.....	64
2.11.1 Assembly.....	65
2.11.2 Trafficking and Cell surface Localization.....	67
2.11.3 Post Translational Modifications.....	68
2.12. Distribution of nAChRs in the Central Nervous System.....	68
2.12.1 $\alpha 4\beta 2$ Expression.....	72
2.12.2 Other Heterpentameric nAChR.....	73
2.13 Pathological Conditions Associated with nAChRs.....	73
2.13.1 Alzheimer's Disease.....	74
2.13.2 Autism Spectrum Disorder.....	75
2.13.3 Nicotine Addiction.....	76
2.13.4 Cancer and Angiogenesis.....	78
2.14 References.....	82
CHAPTER 3: Pharmacological Characterization of the Allosteric Modulator Desformylflustrabromine and its Interaction with $\alpha 4\beta 2$ nAChR Orthosteric Ligands.....	111

3.1	Abstract.....	111
3.2	Introduction.....	112
3.3	Methods.....	113
3.3.1	Receptors and RNA.....	113
3.3.2	Two-Electrode Voltage Clamp.....	113
3.3.3	Electrophysiology Dose/Response Experiments.....	114
3.3.4	Exposure of dFBr Prior to Agonist Activation and During Agonist Induced Desensitization.....	114
3.3.5	Voltage Step Experiments.....	115
3.3.6	Data Analysis.....	115
3.4	Results.....	117
3.4.1	dFBr Inhibition Involves Open-Channel Block.....	117
3.4.2	dFBr Potentiates Low Efficacious Agonists More Than Full Agonists.....	118
3.4.3	dFBr Does Not Appear to Alter Inhibition by Antagonists.....	123
3.4.4	dFBr Can Reactivate Desensitized Receptors.....	126
3.4.5	dFBr Induced Currents Elicited on Desensitized Receptors Decline with Continuous Exposure to dFBr.....	128
3.5	Discussion.....	130
3.5.1	The Bell-Shaped Dose/Response of dFBr.....	130
3.5.2	The Effect of dFBr on the Action of Nicotinic Agonists and Partial Agonists.....	130
3.5.3	The Effect of dFBr on Inhibition of Responses by Nicotinic Antagonists.....	131
3.5.4	Recovery of Desensitized Receptors by dFBr.....	131
3.6	References.....	134

CHAPTER 4: Non-orthosteric Subunit Faces are Involved in $\alpha 4\beta 2$ nAChR Responses to Acetylcholine and Desformylflustrabromine in High- and Low-sensitivity Receptor Preparations.....	137
4.1 Abstract.....	137
4.2 Introduction.....	138
4.3 Materials and Methods.....	141
4.3.1 Receptors and mRNA.....	141
4.3.2 Experimental Chemicals and Test Compounds.....	141
4.3.3 <i>Xenopus laevis</i> Oocytes and Receptor Expression.....	141
4.3.4 Two-Electrode Voltage Clamp.....	142
4.3.5 Electrophysiology Dose-Response Experiments.....	142
4.3.6 Data Analysis and Statistics.....	143
4.4 Results.....	146
4.4.1 High- and Low- Sensitivity Wild-type $\alpha 4\beta 2$ Receptor Preparations.....	148
4.4.1.1 ACh Dose-Response on High- and Low- ACh Sensitivity $\alpha 4\beta 2$ Receptors.....	148
4.4.1.2 Effects of dFBr on Wild-Type Low- and High- ACh Sensitivity Receptors.....	152
4.4.2 $\beta 2$ B-Loop Mutations.....	153
4.4.2.1 Effects of $\beta 2$ B-loop Mutations on ACh Induced Responses.....	153
4.4.2.2 Effects of $\beta 2$ B-loop Mutations on dFBr Potentiation.....	155
4.4.2.3 Response Profiles Obtained With Co-application of dFBr and ACh on B-loop Mutant Receptors.....	156
4.4.3 $\beta 2$ C-loop Mutations.....	158
4.4.3.1 Effects of $\beta 2$ C-loop Mutation on ACh Induced Responses.....	158
4.4.3.2 Effects of $\beta 2$ C-loop Mutations on dFBr Potentiation.....	160

4.4.3.3	ACh Response Profiles of $\beta 2$ C-loop Mutations.	160
4.4.4	$\beta 2$ A-loop Mutations.	160
4.4.4.1	Effects of $\beta 2$ A-loop Mutation on ACh Induced Responses.	160
4.4.4.2	Effects of $\beta 2$ A-loop Mutations on dFBr Potentiation.....	163
4.4.4.3	Response Profiles Obtained with Co-application of dFBr and ACh on A-loop Mutant Receptors.	164
4.4.5	$\alpha 4$ D- and E- β -Sheet Mutations.	164
4.4.5.1	Effects of $\alpha 4$ D- and E- β -Sheet Mutations on ACh Induced Responses.....	164
4.4.5.2	Effects of $\alpha 4$ D- and E- β -Sheet Mutations on dFBr Potentiation.....	165
4.4.5.3	Response Profiles Obtained With Co-application of dFBr and ACh on $\alpha 4$ Mutant Receptors.....	167
4.5	Discussion.....	168
4.5.1	Stoichiometries of Receptors in LS and HS $\alpha 4\beta 2$ nAChR Preparations.	169
4.5.2	The $\beta 2+$ and $\alpha 4-$ Subunits Contain the dFBr Allosteric Binding Site.....	171
4.5.3	Summary.....	171
4.6	References.....	172
CHAPTER 5: Allosteric Modulation of High- and Low- Sensitivity $\alpha 4\beta 2$ Nicotinic Acetylcholine Receptors by HEPES.		176
5.1	Abstract.....	176
5.2	Introduction.	177
5.3	Materials and Methods.	178
5.3.1	Receptors and mRNA.	178
5.3.2	Test Compounds.....	179
5.3.3	<i>Xenopus laevis</i> Oocytes and Receptor Expression.....	179

5.3.4	Two-Electrode Voltage Clamp.....	180
5.3.5	Electrophysiology Dose-Response Experiments.....	181
5.3.6	Data Analysis and Statistics.....	181
5.4	Results.....	184
5.4.1	HEPES is an Allosteric Modulator of the High-sensitivity $\alpha 4\beta 2$ nAChR.....	184
5.4.2	Minimal Changes Were Observed in ACh Dose-Response Curves When HEPES and Phosphate ND-96 Recording Buffers.....	188
5.4.3	Tris Buffer.....	192
5.4.4	The $\alpha 7$ nAChR is Unaffected by HEPES.....	193
5.4.5	HEPES Effects Other PAM Interactions with $\alpha 4\beta 2$ nAChR.....	194
5.4.5.1	Desformylflustrabromine Modulation of High- and Low-sensitivity $\alpha 4\beta 2$ Receptors in HEPES ND-96 Recording Buffer.....	195
5.4.5.2	Zn ²⁺ Modulation of Low and High-sensitivity $\alpha 4\beta 2$ Receptors in HEPES ND-96 Recording Buffer.....	198
5.4.5.3	Zn ²⁺ Modulation of High- and Low-sensitivity $\alpha 4\beta 2$ Receptors in Phosphate ND-96 Recording Buffer.....	201
5.5	Discussion.....	202
5.5.1	HEPES Modulation of $\alpha 4\beta 2$ nAChR.....	202
5.5.2	HEPES Effects on $\alpha 7$ nAChRs.....	202
5.5.3	HEPES as a Therapeutic Lead Drug.....	203
5.5.4	Mounting Evidence That Good's Buffers Interact with Physiological Systems.....	203
5.5.5	HEPES Competition with Other PAMs.....	204
5.5.6	Summary.....	204
5.6	References.....	206
	CHAPTER 6: Discussion and Conclusions.....	209

6.1	General Overview	209
6.1.1	Pharmacological Characterization of Synthetic dFBr	211
6.1.2	Putative Binding Domain for Desformylflustrabromine	212
6.1.3	Allosteric Modulation of High- and Low- ACh Sensitivity $\alpha 4\beta 2$ Nicotinic Acetylcholine Receptors by HEPES.	214
6.2	Future Directions.....	215
6.2.1	Single Channel Studies.....	215
6.2.2	More Mutations and Scanning Cysteine Accessibility Method (SCAM).	216
6.2.3	The Development of the dFBr Binding Site on AChBP.....	217
6.2.4	Receptor Selectivity.	217
6.2.5	dFBr Analogues.	218
6.2.6	Further Studies of HEPES Potentiation.	219
6.3	Summary.....	219
6.4	References.....	221

List of Figures

Figure 2.1.	A diagram of a receptor belonging to the Cys-loop super family of LGIC emphasizing the location and amino acid composition of the cys-loop.....	8
Figure 2.2.	Ribbon structure of the Torpedo nAChR showing the extracellular, transmembrane and cytosolic domains.....	9
Figure 2.3.	The ancestral branch points of the modern day Cys-loop super family of LGIC.....	10
Figure 2.4.	$\alpha 7$ and $\alpha 4\beta 2$ nAChR subunit arrangements and ACh-induced response profiles.....	12
Figure 2.5.	Example of the Cys-loop receptor structure.....	15
Figure 2.6.	The 1.94Å crystal structure of the extracellular region of the mouse $\alpha 1$ nAChR.....	16
Figure 2.7.	Loop labeling and residues involved in the orthosteric binding site in the extracellular domain of nAChR.....	17
Figure 2.8.	Transmembrane helices in nAChR.....	18
Figure 2.9.	The ion channel pore of nAChR.....	19
Figure 2.10.	Illustrations of the contacts and movements that may occur between the extracellular and transmembrane domains of nAChR.....	21
Figure 2.11.	Auerbach and co-workers (2004) model of a conformational wave associated with agonist binding.....	23
Figure 2.12.	Ion translocation in nAChR.....	26
Figure 2.13.	AChBP structure overview.....	28
Figure 2.14.	AChBP with agonist and antagonist bound.....	30
Figure 2.15.	The orthosteric binding site of 5-HT ₃ AR.....	32
Figure 2.16.	Chemical structures of serotonin ligands.....	34
Figure 2.17.	Summary of the residues found benzodiazepine binding site on GABA _A R and the chemical structure of the benzodiazepines.....	36
Figure 2.18.	The neurosteroid binding sites in GABA _A R.....	38
Figure 2.19.	The chemical structures of the discussed anesthetic compounds.....	40
Figure 2.20.	Chemical structure of physostigmine.....	41
Figure 2.21.	The putative Ca ²⁺ binding site on $\alpha 7$ nAChR.....	42
Figure 2.22.	Chemical structures of NS-1738, PNU-120596 and LY-2087101.....	43
Figure 2.23.	Galanthamine and cocaine chemical structures.....	44
Figure 2.24.	The chemical structure of 17 β -estradiol.....	45

Figure 2.25.	The putative zinc potentiation and inhibition sites on $\alpha 4\beta 2$ nAChR.....	47
Figure 2.26.	Location of channel blocking ligand binding sites in the TM2.....	48
Figure 2.27.	Auerbach and Akk (1998) kinetic model of mouse muscle nAChR.....	50
Figure 2.28.	Free energy diagram of mouse muscle nAChR for activation, desensitization and recovery.....	51
Figure 2.29.	Chemical structure of acetylcholine.....	57
Figure 2.30.	Chemical structure of nicotine.....	58
Figure 2.31.	Chemical structure of epibatidine.....	58
Figure 2.32.	Chemical structure of cytisine.....	59
Figure 2.33.	Chemical structures of varenicline.....	59
Figure 2.34.	Chemical structure of mecamlamine.....	59
Figure 2.35.	Chemical structure for methylcaconitine.....	60
Figure 2.36.	Chemical structure of galanthamine.....	61
Figure 2.37.	Chemical structure of physostigmine.....	62
Figure 2.38.	Chemical structure for 17- β -Estradiol.....	62
Figure 2.39.	Chemical structure of desformylflustrabromine.....	63
Figure 2.40.	Components of nAChR trafficking highlighted in the text.....	65
Figure 2.41.	The three major cholinergic pathways found in the brain.....	70
Figure 2.42.	Locations of nAChR in the rat brain.....	71
Figure 3.1	Voltage dependence of potentiation and inhibition by dFBr.....	118
Figure 3.2	dFBr modulated responses to nAChR agonists and partial agonists.....	120
Figure 3.3	Dose response curves for agonists and partial agonists in the presence and absence of 1 μ M dFBr.....	122
Figure 3.4	Co-application of dFBr with nAChR antagonists.....	125
Figure 3.5	dFBr reactivates desensitized receptors.....	127
Figure 3.6	The amplitude of dFBr induced currents on desensitized receptors decline during long exposures to dFBr.....	129
Figure 4.1.	DNA sequence alignments for AChBP and nAChR subtypes.....	140
Figure 4.2.	DNA sequences for the binding- loops and - β -sheets for the nAChR subunits $\alpha 4$ and $\beta 2$ and GABA _A R subunits $\alpha 1$ and γ	147
Figure 4.3	ACh and dFBr dose-response curves for wild-type (WT) receptors expressed using the high-sensitivity (HS) and low-sensitivity (LS) receptor preparations.....	149

Figure 4.4.	ACh and dFBr dose-response curves for $\beta 2+$ face B-loop mutants and wild-type (WT) receptors expressed using the low- (LS) and high- (HS) sensitivity receptor preparation.....	154
Figure 4.5.	Response profiles that appeared different from wild-type receptors for co-application of varying concentrations of dFBr and ACh for $\beta 2+$ face B-loop mutant receptors expressed using the low- (LS) and high- (HS) sensitivity receptor preparations.....	157
Figure 4.6.	ACh and dFBr dose-response curves for $\beta 2+$ face C-loop mutant and wild-type (WT) receptors expressed using the low- (LS) and high- (HS) sensitivity receptor preparations.....	159
Figure 4.7	ACh and dFBr dose-response curves for $\beta 2+$ face A-loop mutant and wild-type (WT) receptors expressed using the low- (LS) and high- (HS) sensitivity receptor preparations.....	162
Figure 4.8	ACh and dFBr dose-response curves for $\alpha 4-$ face mutant and wild-type (WT) receptors expressed using the low- (LS) and high- (HS) sensitive receptor preparations.....	166
Figure 4.9	Response profiles for co-application of varying concentrations of dFBr and ACh for $\alpha 4-$ face mutant W88A expressed using the low- (LS) sensitive receptor preparation.....	168
Figure 5.1	HEPES dose-response curves on high- and low- sensitivity receptors.....	185
Figure 5.2	ACh dose-response curves in HEPES and phosphate ND-96 recording buffer	190
Figure 5.3	Tris concentration response curves for co-application of ACh and 1 μ M dFBr on high- (HS) and low- (LS) sensitivity $\alpha 4\beta 2$ receptors.....	193
Figure 5.4	$\alpha 7$ ACh dose-response curves obtained using HEPES or phosphate ND-96 recording buffers.....	194
Figure 5.5	dFBr concentration responses curves for high- (HS) and low- (LS) sensitivity $\alpha 4\beta 2$ nAChR obtained using HEPES or phosphate ND-96 buffers.....	196
Figure 5.6	Zn ²⁺ concentration responses curve obtained by co-application of Zn ²⁺ and ACh on high- (HS) and low- (LS) sensitivity $\alpha 4\beta 2$ nAChR using HEPES or phosphate ND-96 buffer.....	199
Appendix A.1	Response profiles for co-application of varying concentrations of dFBr and ACh for $\beta 2+$ face B-loop mutant receptors expressed using the low (LS) and high (HS) sensitive receptor preparations.....	223

Appendix A.2	Response profiles for co-application of varying concentrations of dFBr and ACh for $\beta 2+$ face C-loop mutant receptors expressed using the low (LS) and high (HS) sensitive receptor preparations.....	224
Appendix A.3	Response profiles for co-application of varying concentrations of dFBr and ACh for $\beta 2+$ face A-loop mutant receptors expressed using the low (LS) and high (HS) sensitive receptor preparations.....	225
Appendix A.4	Response profiles for co-application of varying concentrations of dFBr and ACh for $\alpha 4-$ face mutant receptors expressed using the low (LS) and high (HS) sensitive receptor preparations.....	226

List of Tables

Table 2.1	Currently known members of the Cys-loop super family of LGICs.....	11
Table 3.1.	dFBr induced effects on response kinetics for agonists and partial agonists	123
Table 4.1	Summary of the calculated results determined from ACh and dFBr potentiation of ACh dose-response results from wild-type (WT) and mutant $\alpha 4\beta 2$ receptors expressed using the low-sensitivity (LS) receptor preparation.....	150
Table 4.1	Summary of the calculated results determined from ACh and dFBr potentiation of ACh dose-response results from wild-type (WT) and mutant $\alpha 4\beta 2$ receptors expressed using the high-sensitivity (HS) receptor preparation.....	151
Table 5.1.	Summary of the calculated results determined from ACh dose-response curves in HEPES and phosphate ND-96 recording buffer.....	191
Table 5.2.	Summary of calculated results from dFBr concentration responses curves for high- (HS) and low- (LS) sensitivity $\alpha 4\beta 2$ nAChR obtained using HEPES or phosphate ND-96 buffers.....	197
Table 5.3.	Summary of calculated results from Zn ²⁺ concentration responses curve obtained by co-application of Zn ²⁺ and ACh on high- (HS) and low- (LS) sensitivity $\alpha 4\beta 2$ nAChR using HEPES or phosphate ND-96 buffer.....	200

List of Appendices

Appendix A: α 4 β 2 Mutant Traces.....	223
Appendix B: IACUC Assurance.....	227

Acknowledgements

I would like to thank my immediate family Denise Daniello, Jeff Weltzin and Jana Weltzin for their love, support and encouragement. I would also like to thank my fiancé Eli Sonafrank for his help, inspiration and love. I would like to thank my major advisor Dr. Marvin K. Schulte for his guidance and mentorship over the last five years. I would also like to thank Ms. Mary van Muelken for all her help with writing and finding funding. A special thanks to my financial support Alaska IDeA Networks of Biomedical Research Excellence (INBRE), the Institute of National Health and the Sloan Foundation. I am grateful to my advisory committee members and Dr. Tom Clausen, Dr. Brian Edmonds and Dr. Mike Harris who had to take time out of their busy schedules in order to guide and help me with my dissertation.

CHAPTER 1: Introduction

The role of nAChRs in pathological conditions is widespread and monumental. Neuronal Nicotinic Acetylcholine Receptors (nAChR) are being found not only in the Central Nervous System (CNS) but also in the Peripheral Nervous System (PNS), suggesting that nAChRs are important for many physiological processes throughout the body. Therapeutic ligands that selectively target nAChRs may be a good treatment strategy for diseases such as Alzheimer's disease, Autism, nicotine addiction and cancer (see Chapter 2 for background of nAChR). Chapter 2 is intended to provide an extensive background of nAChR to aid in the understanding of the later research based chapters of this thesis and is intended to be submitted as a review article in the near future.

The development of allosteric modulators is a potential and valuable treatment strategy in pathologies where nAChRs are dysregulated. Positive allosteric modulators (PAMs) affect the agonist evoked responses on nAChR. Because of PAMs' low intrinsic activity, these ligands only affect the receptors in presence of agonists such as the endogenous neurotransmitter. This allows the spatial and temporal relationship of cholinergic transmission to remain unaltered.

To understand PAMs actions, several studies investigating different components of how an allosteric modulator works must be conducted. Characterization of PAMs action in combination with orthosteric ligands, including full and partial agonists and antagonists, will lead to a better understanding of how PAMs function on nAChR. Studies investigating the timing of PAM application can also provide clues to how a PAM is able to alter the stability of various receptor states (closed vs. open vs. desensitized). Elucidation of PAM mechanism will facilitate in the development of drugs that are selective of nAChR subtypes and stoichiometries that have specifically tailored actions.

Identifying ligand binding sites broadens the understanding of nAChR structure and function as well as ligand-receptor interactions. Elucidation of ligand-receptor interactions leads to the development of selective ligands that are able to shape the receptor response to better treat a given pathology. Knowledge gained from characterizing ligand binding sites and understanding how a ligand shapes a receptor response will provide refinements to our current receptor models. Each step in the process provides a greater understanding of nAChR's structure and function, and facilitates the development of novel allosteric ligands. Allosteric modulators are potentially valuable as diagnostic and therapeutic treatment tools for CNS disorders.

In this thesis, we address how the PAMs, desformylflustrabromine (dFBr) and 4-(2-hydroxyethyl)-1-piperazineethanesulfonic acid (HEPES) work on various nAChR subtypes and

stoichiometries in presence of orthosteric ligands to better understand the mechanism of PAMs. These studies are then followed by the initial characterization of the binding site. The findings from this research will aid in the development and understanding of PAMs as therapeutic and diagnostic ligands.

1.1. Gaps in Current Knowledge.

nAChRs have become a heavily investigated subject in the last decade. There are many gaps in the current knowledge that need to be investigated including the development of new therapeutic ligands for both the diagnosis and treatment of pathologies. Potential therapeutic ligands which are selective for subtypes and stoichiometries of these receptors will aid in our understanding of how dysregulation of nAChR are associated with ailments. Furthermore selective ligands could also aid in the treatment of diseases where the densities of subtypes or stoichiometries of nAChR differ from normal brains. Characterization of the parent lead compound location and structure of the binding sites on nAChR would aid in the development of therapeutic ligands.

One possible therapeutic treatment avenue is the use of Positive Allosteric Modulators (PAMs). It is currently known that PAMs alter the apparent affinity and efficacy of agonist evoked responses and that PAMs are unable to activate the channels alone. PAMs appear to bind at allosteric binding sites throughout nAChRs (see Chapter 2). A more in-depth understanding of how PAMs interact with nAChR is needed so that this type of ligand can be used clinically. It is unknown if PAMs work by increasing the receptor p_{open} and/or alter the firing rate of the receptor. It also seems likely that different PAMs will perform differently on nAChR subtypes and stoichiometries. Studies investigating how PAMs interact with different pharmacological agents, mechanism of action and elucidation of their binding sites will aid in the understanding of how PAMs are able to alter agonist affinity and efficacy.

1.2. Gaps Addressed in Current Project.

This thesis focuses on the development of dFBr and HEPES as potential new therapeutic ligands (see Chapters 3-5). The compound dFBr is explored more thoroughly than HEPES. Exploration of the pharmacology of dFBr, mechanism of action and binding site location on $\alpha 4\beta 2$ nAChR is emphasized in this thesis (see Chapter 3 and 4). Chapter 3 is a manuscript that has been published (J Pharmacol Exp Ther. 2010 Sep 1;334(3):917-26.) and Chapter 4 has been submitted to Journal of Molecular Pharmacology. Results from these studies will aid in the understanding of how this parent lead compound interacts with $\alpha 4\beta 2$ nAChR. Information gained from these studies will aid in the development of dFBr analogues that are more selective and will have increased ACh affinity and efficacy with the lack of ability to inhibit ACh induced currents.

More importantly, these studies provide supportive evidence for developing dFBr-like molecules for therapeutic treatment strategies.

Initial HEPES pharmacology and functional binding site studies are also discussed (see Chapter 5). Chapter 5 is a manuscript has been submitted to the Journal of Pharmacology and Experimental Therapeutics. Here we present the findings that HEPES is a high-sensitivity (HS) $\alpha 4\beta 2$ nAChR ligand. On HS receptors, HEPES is a PAM that is able to enhance the ACh efficacy. On low-sensitivity receptors (LS), HEPES is a poor inhibitor of ACh evoked currents. The putative binding site of HEPES on HS receptors was found. Findings from these studies will further the understanding of $\alpha 4\beta 2$ selective PAMs pharmacology and binding sites.

1.3. General Hypothesis.

Members of LGICs include 5-HT₃R, nAChR, GABA_AandC_R and glycine receptors. On GABA_AR the allosteric modulators benzodiazepines and barbiturates have been prescribed to alleviate the symptoms of depression, epilepsy and anxiolytics. Despite nAChRs wide distribution throughout the human body, there are no allosteric modulators used therapeutically to selectively target nAChR subtypes. Based on preliminary molecular modeling and sequence comparisons between members of LGICs we **hypothesize that there are allosteric modulators for $\alpha 4\beta 2$ nAChRs and they bind in a similar region as benzodiazepines on GABA_ARs.**

1.3.1. Specific Hypotheses.

1.3.1.1. *Desformylflustrabromine is an Allosteric Modulator of the $\alpha 4\beta 2$ nAChR.*

This hypothesis is based on previous studies by Kim et al. (2007) and Sala et al. (2005), that dFBr selective potentiates $\alpha 4\beta 2$ nAChR and inhibits $\alpha 7$ receptors (Sala et al., 2005; Kim et al., 2007). In order to prove this hypothesis, three criteria must be met: 1) How does dFBr alter $\alpha 4\beta 2$ function in presence of pharmacological agents like full agonist, partial agonist and antagonist? 2) What is the mechanism of dFBr potentiation and inhibition? 3) Where does dFBr bind?

Results showed that dFBr was able to potentiate full and partial agonist induced $\alpha 4\beta 2$ nAChR responses (Weltzin and Schulte, 2010a). The inhibition of ACh induced currents by antagonists on $\alpha 4\beta 2$ nAChR was unaffected by dFBr. The mechanism of dFBr inhibition was shown to be voltage dependent, suggesting that dFBr inhibition of ACh-evoked currents was caused by open-channel block. The potentiation of dFBr appears to involve maintenance of the receptor open state either by destabilization of the desensitized state or stabilization of the open state. The potentiation mechanism of dFBr requires further investigation using more refined

techniques such as single-channel studies. Question 3 is addressed in specific hypothesis number two.

1.3.1.2. Desformylflustrabromine Binds at the $\beta 2+/\alpha 4-$ Interface on $\alpha 4\beta 2$ nAChR.

Chapter 4 of the thesis investigates the putative dFBr binding site on $\alpha 4\beta 2$ receptors. The putative binding location of dFBr was hypothesized to be at the $\beta 2+/\alpha 4-$ cleft. This region was chosen following sequence comparisons between other LGIC binding sites and molecular modeling studies. The putative dFBr binding site was explored by making single point alanine mutations and evaluating the effects of the mutations on ACh and dFBr induced responses. Mutagenesis results suggest that dFBr primarily binds to the $\beta 2+$ face. Additional results suggest that non-orthosteric subunit faces are involved in $\alpha 4\beta 2$ responses to ACh. Results from this study begin to elucidate the dFBr binding site on the $\beta 2+$ face and advances our understanding of $\alpha 4\beta 2$ nAChR function in response to ACh.

1.3.1.3. HEPES is a positive allosteric modulator of $\alpha 4\beta 2$ nAChR.

This hypothesis is based on the observation that the crystal structure of the Acetylcholine Binding Protein (AChBP) contains HEPES molecules in a similar region of the protein that binds ACh (Brejc et al., 2001). This led us to question the reactivity of HEPES with nAChR.

The characterization of HEPES actions on $\alpha 4\beta 2$ and $\alpha 7$ nAChR is studied in Chapter 5 of the thesis (Weltzin and Schulte, 2010b). Findings from this study demonstrate that HEPES is a stoichiometric selective PAM that potentiates and inhibits ACh induced currents on HS receptors. A point mutation on the C-loop of the $\beta 2+$ face eliminated the HEPES potentiation. On LS receptors, HEPES inhibits ACh evoked currents. Interestingly on $\alpha 7$ nAChR HEPES appears to have no effect on ACh currents. Furthermore this study investigated the use of other buffer systems and the how HEPES may have altered the interpretation of other modulators.

1.4. References

- Brejck K, van Dijk WJ, Klaassen RV, Schuurmans M, van Der Oost J, Smit AB and Sixma TK (2001) Crystal structure of an ACh-binding protein reveals the ligand-binding domain of nicotinic receptors. *Nature* **411**:269-276.
- Kim JS, Padnya A, Weltzin M, Edmonds BW, Schulte MK and Glennon RA (2007) Synthesis of desformylflustrabromine and its evaluation as an alpha4beta2 and alpha7 nACh receptor modulator. *Bioorg Med Chem Lett* **17**:4855-4860.
- Sala F, Mulet J, Reddy KP, Bernal JA, Wikman P, Valor LM, Peters L, Konig GM, Criado M and Sala S (2005) Potentiation of human alpha4beta2 neuronal nicotinic receptors by a *Flustra foliacea* metabolite. *Neurosci Lett* **373**:144-149.
- Weltzin MM and Schulte MK (2010a) Pharmacological characterization of the allosteric modulator desformylflustrabromine and its interaction with alpha4beta2 neuronal nicotinic acetylcholine receptor orthosteric ligands. *J Pharmacol Exp Ther* **334**:917-926.
- Weltzin MM and Schulte, MK (2010b) Allosteric modulation of high and low affinity alpha4beta2 nicotinic acetylcholine receptors by HEPES, in *Society for Neuroscience*, San Diego.

CHAPTER 2: Neuronal Nicotinic Receptors: Structure, Function and Therapeutic Opportunities.

2.1. Introduction.

Ligand gated ion channels (LGIC) are essential components of the central and peripheral nervous system (Taly et al., 2009). Family members of the Cys-loop super family are nicotinic acetylcholine (nAChR), GABA_AR, 5HT₃R and glycine receptors (Gotti and Clementi, 2004). LGICs play a critical role in synaptic transmission at the junctions between nerve cells (synapses) and between nerve and muscle cells by regulating the passage of ions into the cell (Gotti et al., 2006b). The regulation of synaptic transmission is important in learning, memory, gene transcription and muscle contraction. Dysregulation of nAChRs can lead to neurological disorders including Alzheimer's disease (Court et al., 2001; Nordberg, 2001), Schizophrenia (Adams and Stevens, 2007), Parkinson's disease (Aubert et al., 1992), Autism (Martin-Ruiz et al., 2004; Lippiello, 2006) and nicotine addiction (Picciotto et al., 2001). Using allosteric modulators to target ion channels is a promising therapeutic treatment for many neurological disorders.

2.2. A General Description of the Physiological Role of nAChRs.

nAChRs are located in the peripheral and autonomic nervous system (PNS and ANS) at the skeletal neuromuscular junction and in the Central Nervous System (CNS) at the neuronal synapses, mediating the rapid and brief effects of acetylcholine (ACh) across a wide range of acetylcholine (ACh) concentrations (ranging from nM to mM) (Dani and Bertrand, 2007). Neuronal synapses are junction points where both pre- and post- synaptic cells meet. The gap between the two neurons, otherwise known as the synaptic cleft, is about 100 nM wide. In addition to ACh, nAChRs respond to a range of endogenous and exogenous pharmacological agents including nicotine and organophosphates. Activation of nAChR produces an enhanced release of other neurotransmitters including dopamine, serotonin, glutamate and GABA (γ -aminobutyric acid).

The process of synaptic transmission begins with the generation of a wave of electrochemical excitation known as an action potential at the axon hillock. The generated action potential propagates down the axon of the pre-synaptic neuron until it reaches the synapse. The action potential depolarizes the membrane and causes calcium (Ca^{2+}) permeable ion channels to open. Calcium ions flow into the pre-synaptic cell producing a rapid increase in calcium concentration. The high concentration of calcium triggers activation of calcium-sensitive proteins attached to synaptic vesicles that contain neurotransmitters such as ACh. The vesicles fuse with the cell membrane by interacting with membrane proteins such as t- and v-SNARES and release

their neurotransmitters into the synaptic cleft. The neurotransmitters diffuse into the synaptic cleft where the molecules can either bind to receptors on the membrane of the post-synaptic cleft, be degraded or diffuse away from the cleft. The binding of neurotransmitters to receptors such as nAChR on the post-synaptic cell initiates the activation of the receptors allowing ions such as Ca^{2+} , Na^+ and K^+ to flow down their ion concentration gradient into the post-synaptic cell. If the translocation of ions results in a membrane potential change of about 15 mV, the action potential will be propagated.

The resulting magnitude and sign of the induced action potential depends on the charge and influx of the translocated ions. Since the conduction of a single input is passive, it takes multiple inputs occurring simultaneously to generate an action potential. A synaptic potential can be inhibitory or excitatory depending on the charge of the translocated ions, the receptor type, the concentration of permeant ions inside and outside of the cell and the cell's action potential threshold (Purves, 2004). Inhibitory post-synaptic potentials (IPSP) are caused by the conductance of anions and low concentrations of cations. IPSPs reduce the chances of generating an action potential by hyperpolarizing the post-synaptic membrane (Purves, 2004). The excitatory post synaptic potential (EPSP) are caused by the conductance of cations as in the case of nAChR and low concentrations of anions. EPSPs increase the possibility of generating an action potential by depolarizing the post-synaptic cell (Purves, 2004).

After a couple of milliseconds, the neurotransmitter will disassociate from the receptor (Dani and Bertrand, 2007). The remaining neurotransmitter will either be metabolically degraded or be reabsorbed by the pre-synaptic cell for future use.

2.3. The Ligand Gated Ion Channel Superfamily.

2.3.1 Classification of LGICs.

Ligand gated ion channels (LGIC) are divided into three subclasses; Cys-loop, ionotropic glutamate and ATP-gated receptors, based on their structure, genetic origin and function. The receptors are integral membrane proteins and have three distinct extracellular, transmembrane and intracellular domains (Figure 2.1). Cys-loop receptors are pentamers. The ionotropic glutamate receptors bind the neurotransmitter glutamate and are usually tetramers. Members include AMPA, Kainate and NMDA receptors. ATP-gated receptors respond to the nucleotide ATP. The only known ATP-gate receptor is the trimer PX2 receptor.

The Cys-loop superfamily contains a characteristic 15 amino acid loop containing two cysteine (Cys) residues forming a disulfide bond. The Cys-loop is located at the bottom of the

extracellular domain (Figure 2.1). Members of the Cys-loop super family include GABA_A and C, 5HT_{A-3}, glycine and muscle and neuronal types of nicotinic acetylcholine receptors (nAChR).

The Cys-loop superfamily is further divided into anion and cation conducting channels. In general, receptors which pass anions are inhibitory, while cation selective channels are excitatory. The acetylcholine receptors and the 5HT₃R are non-selective cation (K⁺, Ca²⁺ and Na²⁺) conducting channels. The A and C subtypes of GABA and glycine receptors are non-selective anion conducting (Cl⁻) receptors. Unlike types A and C, the B type of the GABAR is a G-protein receptor.

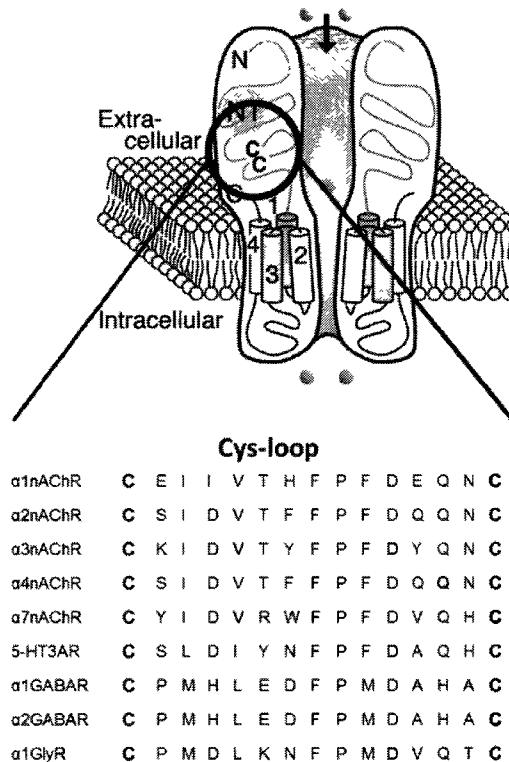


Figure 2.1. A diagram of a receptor belonging to the Cys-loop super family of LGIC emphasizing the location and amino acid composition of the cys-loop.

A representative side view of the receptor showing two of the five subunits is displayed above. The pore lumen, the neurotransmitter binding site (NT), the transmembrane topology and the conserved disulfide bridge (boldfaced C) are shown. All Cys-loop superfamily receptors share a similar amino acid composition of the Cys-loop (shown below). Amino acid sequences are from (Limapichat et al., 2010). (Top figure modified and used with permission from (Sunesen et al., 2006).)

2.4. Structure of the Cys-loop LGIC Family.

The Cys-loop LGICs have similar general structural features typified by the nicotinic acetylcholine receptor (nAChR) subfamily. Members of the Cys-loop super family have an extracellular or ligand binding domain, a transmembrane domain and a variable cytosolic loop (Figure 2.2).

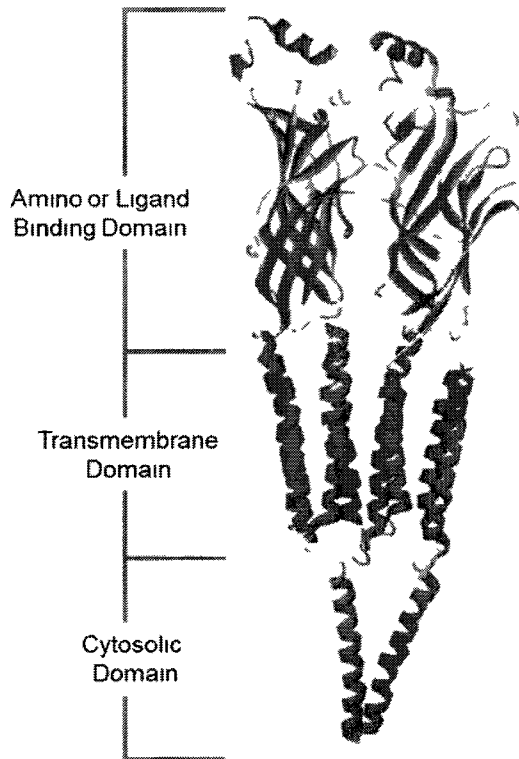


Figure 2.2 Ribbon structure of the Torpedo nAChR showing the extracellular, transmembrane and cytosolic domains.

(Image reprinted with permission from (Gay and Yakel, 2007).)

All members of the nAChR family respond to the exogenous agonist nicotine and the endogenous agonist acetylcholine, hence the name “nicotinic acetylcholine receptors.” Similarly, GABA_A and C, 5-HT₃ (serotonin, 5-hydroxytryptamine) and glycine receptors respond to their respective endogenous neurotransmitter γ -amino butyric acid, serotonin (5-hydroxytryptamine) and glycine. Figure 2.3 displays the ancestral branch points where new receptors were formed.

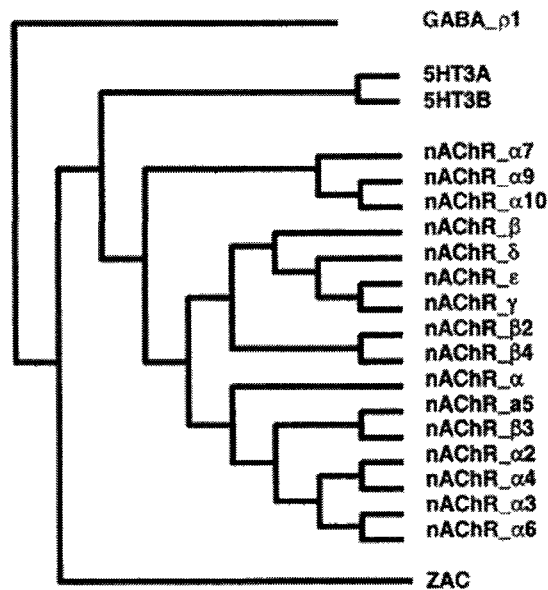


Figure 2.3 The ancestral branch points of the modern day Cys-loop super family of LGIC.

(Image reprinted with permission from (Davies et al., 2003)).

The Cys-loop receptors are pentameric receptors composed of different subunits. Muscle nAChR are heteromeric receptors composed of four different subunits, $\alpha 1$, $\beta 1$, δ , γ and ϵ , and are arranged in a $2\alpha:1\beta:1\delta:1\gamma$ or ϵ ratio (Barry and Lynch, 2005) (Table 2.1). The γ subunit is only expressed in the embryonic form of the receptor while the ϵ subunit is expressed in the adult receptor (Barry and Lynch, 2005). The neuronal nAChRs are composed of a broad range of combinations of α and β subunits (Gotti and Clementi, 2004). There are nine different α subunits ($\alpha 2$ -10) and three β ($\beta 2$ -4) subunits found in the CNS, collectively known as “neuronal” type subunits (Gotti and Clementi, 2004) (Table 2.1). Both homomeric and heteromeric receptors assemble to produce functional receptors. The multiple combinations of α and β subunits produce a large number of possible neuronal nAChRs, each with unique properties.

nAChRs are integral allosteric membrane proteins with a molecular mass of ~290 kDa and encoded by 17 genes (Taly et al., 2009). Of these, nine α and three β subunits are expressed in the brain. The various subunit combinations result in different pharmacological and kinetic properties and physiological locations.

Serotonin type 3 receptors (5HT₃R) consist of five different subunits ranging from A to E (Gaddum and Picarelli, 1957) (Table 2.1). 5HT₃R_A form homomeric receptors while types A and B

can combine and form hetero pentameric receptors. Types C, D and E have been described, but have yet to be characterized. GABA_A receptors are composed of combinations of 16 different subunits (α 1-6, β 1-3, γ 1-3, δ , ϵ , π and θ) (Olsen and Sieghart, 2008) (Table 2.1). Zinc activated ion channels (ZAC) have just recently been described and are known to consist of one subunit (Davies et al., 2003). Glycine receptors consist of α 1-4 and a single β subunit (Betz et al., 1999) (Table 2.1).

Table 2.1 Currently known members of the Cys-loop super family of LGICs.

Receptor	Ligand	Permeable Ions	Number of subunits known
Muscle nAChR	ACh	Cations	5
Neuronal nAChR	ACh	Cations	≥ 16
5-HT ₃ R	5-HT	Cations	≥ 2
ZAC	Zinc	Cations	1
GABA _A R	GABA	Anions	≥ 16
Glycine R	Glycine	Anions	≥ 5

2.5. Predominant nAChR Subtypes.

The predominant forms of nAChR found in the Central Nervous System (CNS) are the homomeric α 7 and heteromeric α 4 β 2 subtypes. The α 7 receptors contain five identical subunits arranged around a central cation conducting pore (Figure 2.4)(Taly et al., 2009). The α 4 β 2 receptors contain different combinations of α 4 and β 2 subunits, depending on the putative stoichiometry (Figure 2.4). The α 7 receptors are known to desensitize rapidly and have a higher Ca²⁺:Na⁺ permeability ratio compared to NMDA and other nAChR receptors (Albuquerque et al., 2009). The α 4 β 2 subtype exhibits slower desensitization kinetics and lower cation permeability compared to α 7 nAChR (Figure 2.4).

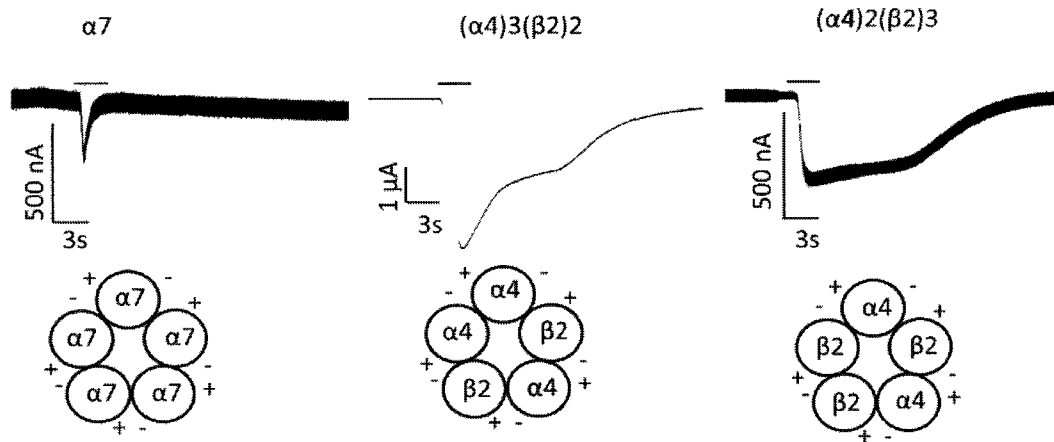


Figure 2.4 $\alpha 7$ and $\alpha 4\beta 2$ nAChR subunit arrangements and ACh-induced response profiles.

Left) Homomeric $\alpha 7$ ACh induced response profile and illustration of subunit arrangement. *Middle*) Heteromeric low ACh sensitive $\alpha 4\beta 2$ nAChR ACh induced response profile and illustration of putative subunit arrangement. *Right*) Heteromeric high ACh sensitive $\alpha 4\beta 2$ nAChR ACh induced response profile and illustration of putative subunit arrangement. The plus and minus signs designate the principal and complementary faces of each subunit.

Previous studies investigating $\alpha 4\beta 2$ nAChR injected in a 1:1 $\alpha:\beta$ ratio saw two-component dose response curves in response to varying concentrations of ACh, suggesting that two different populations of receptors existed in the preparation (Zwart and Vijverberg, 1998; Buisson and Bertrand, 2001; Moroni et al., 2006a; Zwart et al., 2006b). The estimated EC_{50} values were 0.3 - 2.8 μM for the high ACh sensitivity component and 66 - 142 μM for the low sensitivity component (Moroni et al., 2006a). Two putative stoichiometries of $\alpha 4\beta 2$ receptors have been observed *in vitro*, but have yet to be observed *in vivo*. The expression of $\alpha 4\beta 2$ stoichiometries in *Xenopus laevis* oocytes can be influenced by injecting 5 - 10 times higher concentrations of one subunit over the other (Zwart and Vijverberg, 1998; Moroni and Bermudez, 2006; Moroni et al., 2006a; Tapia et al., 2007). Previous studies have further suggested that the high-sensitivity receptor preparation predominantly forms receptors with two $\alpha 4$ and three $\beta 2$ subunits in the pentameric arrangement $\alpha\beta\alpha\beta\beta$ ($(\alpha 4)2(\beta 2)3$) (Nelson et al., 2003; Zhou et al., 2003; Briggs et al., 2006b; Moroni et al., 2006b; Zwart et al., 2006a; Tapia et al., 2007) (Figure 2.4). The high ACh-sensitive receptors in the presumed stoichiometry have two $\alpha+/\beta-$ clefts, two $\beta+/\alpha-$ clefts and one $\beta+/\beta-$ cleft. Several studies have suggested that receptors formed in the low-sensitivity receptor preparation are composed of three $\alpha 4$ and two $\beta 2$ subunits in the arrangement $\alpha\beta\alpha\alpha$ ($(\alpha 4)3(\beta 2)2$) (Nelson et al., 2003; Zhou et al., 2003; Briggs et al., 2006b; Moroni et al.,

2006b; Zwart et al., 2006a; Tapia et al., 2007) (Figure 2.4). The low ACh-sensitive receptor is thought to contain two α +/ β - clefts, two β +/ α - clefts and one α +/ α - cleft. It is likely that other arrangements are also expressing in both the high and low sensitivity receptor preparations.

The α 4 β 2 stoichiometries differ in their calcium permeability, functional pharmacology and pharmacological chaperones (Nelson et al., 2003; Tapia et al., 2007). The Ca^{2+} permeability has been demonstrated to be different between the two stoichiometries. Reversal potential experiments showed that the low sensitivity receptor permeates Ca^{2+} through the channel by 26.9 ± 1.3 mV. The high sensitivity receptor permeates Ca^{2+} through the channel at a much slower rate of 7.3 ± 2.2 mV (Tapia, et al., 2007). The higher Ca^{2+} permeability of the low sensitivity receptor is a result of a glutamate residue in the TM2 region of α 4 subunits. The β 2 subunits have a lysine residue at this position that reduces Ca^{2+} permeability (Tapia et al., 2007).

The high and low-sensitivity receptors differ in their response behavior to different pharmacological agents (Moroni et al., 2006a). Nicotine, epibatidine, TC-2559, A-85380 and 3-Br-cytisine produced concentration-dependent inward currents on oocytes expressing high and low-sensitivity receptors. Cytisine, 5-I-cytisine, 5-Br-cytisine and 5-Cl-cytisine acted as partial agonists and only evoked responses in oocytes expressing the low-sensitivity receptor. Nicotine, epibatidine and 3-Br-cytisine behaved as partial agonists on high-sensitivity receptors. TC-2559 and A-85380 were significantly more efficacious than ACh on high-sensitivity receptors. On low-sensitivity receptors epibatidine and A-85380 were significantly more efficacious than ACh (Moroni et al., 2006a). In addition, the low-sensitivity receptor stoichiometry appeared to be more sensitive to channel blocking drugs such as mecamylamine, chlorisondamine and d-tubocurarine (Briggs et al., 2006a), suggesting that the structure of the channel pore may differ from that of the (α 4) $_2$ (β 2) $_3$ stoichiometry.

The expression of nAChR can be mediated by pharmacological ligands. The expression of high-sensitivity α 4 β 2 receptors has been shown to increase after incubating transfected cells with nicotine (Buisson and Bertrand, 2001) and the amplified expression occurred independently from protein synthesis (Peng et al., 1994; Wang et al., 1998). Augmented expression resulted from increased receptor assembly (Wang et al., 1998) in combination with a reduced turnover rate of existing surface nAChRs (Peng et al., 1994). Functional studies have additionally revealed that the low-sensitivity receptor expression is mediated by post-translational modification of the α 4 subunit by chaperone protein 14-3-3 and protein kinase A (Exley et al., 2006). 3-24h exposure to nicotine caused up-regulation of the high α 4 β 2 sensitive receptors promoting the assembly of nAChR subunits from large pools of unassembled subunits (Kuryatov et al., 2005). The newly formed receptors had a 5-fold lifetime increase on the cell surface membrane. Membrane-

permeable ligands such as nicotine and choline (Kuryatov et al., 2005; Gahring et al., 2010) and less permeable quaternary amine cholinergic ligands (Kuryatov et al., 2005) can act as pharmacological chaperones within the endoplasmic reticulum aiding the assembly of nAChRs.

2.6. Receptor Structure Described by Biochemical and X-ray Crystallography Studies.

Cys-loop LGICs are found throughout the PNS and CNS (Taly et al., 2009). The Cys-loop superfamily of LGICs are composed of five membrane bound subunits arranged around an axis perpendicular to the cell membrane and form a pore that conducts ions from the outside to the inside of the cell (Figure 2.5). Each subunit contains a large amino terminal extracellular domain, a four segment transmembrane domain (TM1-TM4) and a variable cytoplasmic domain (Figures 2.2 and 2.5). Depending on the subunit composition, different types of receptors are formed. Homopentameric receptors contain the same subunits while heteropentameric receptors have different subunits (Figures 2.4 and 2.5). Different combinations of subunits result in the expression of receptor subtypes and stoichiometries with varying ligand selectivity and conductances (Figure 2.5) (Albuquerque et al., 2009).

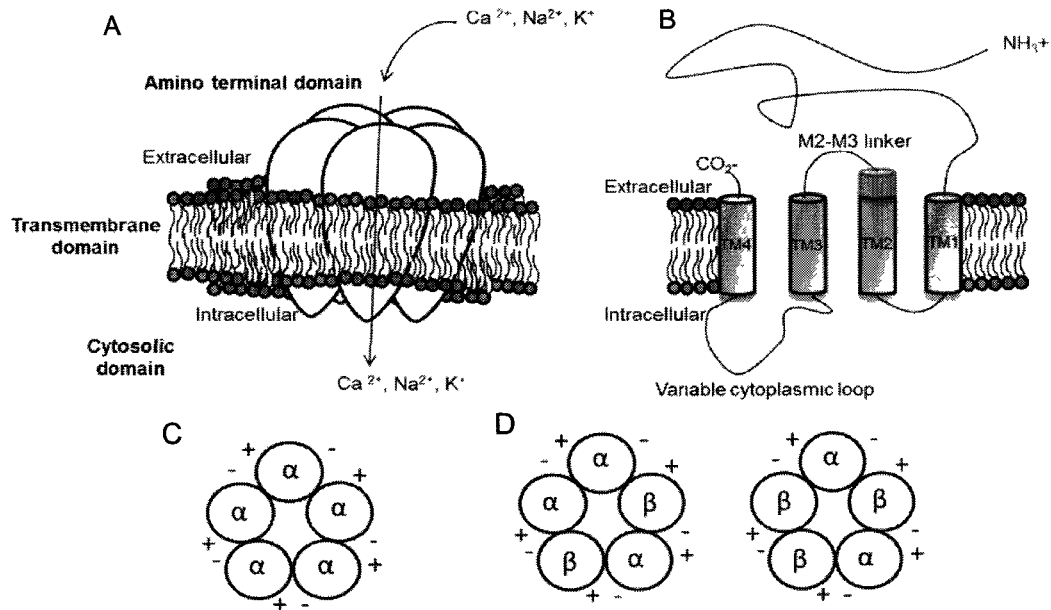


Figure 2.5 Example of the Cys-loop receptor structure.

A) This diagram shows the general structure of a Cys-loop structure. Note similarity to nAChR. The receptor is embedded in the cell membrane and in this example passes cations. **B)** The structure of each subunit. TM1-TM4 are the helices that comprises the transmembrane region. **C)** A general structure of a homopentameric receptor. The + designates the principal face and the – designates the complementary phase. **D)** A general structure of a heteropentameric receptor. The $\alpha_4\beta_2$ heteropentameric receptors can form two different stoichiometries based on the number of α_4 and β_2 subunits expressed (*left versus right*).

2.6.1 Extracellular Binding Domain.

To date, crystallography studies of nAChR and the Acetylcholine Binding Protein (AChBP) have been used to describe the structure of the amino terminal. A 4.6Å crystal structure of the Torpedo nAChR uncovered that the ion tunnel is framed by seven twisted β -sheet strands (Miyazawa et al., 1999). The recent 1.94Å resolution structure of the extracellular domain of the α_1 nAChR revealed a ten-stranded β -sandwich and an N-terminal α -helix (Dellisanti et al., 2007) (Figure 2.6). The sheet constructed from the strands β_1 , β_2 , β_3 , β_5 , β_6 and β_8 is referred to as the inner sheet, while β -strands β_4 , β_7 , β_9 and β_{10} are referred to as the outer sheet (Dellisanti et al., 2007) (Figure 2.6). Additional structural insights come from the 2.7Å crystallization of the *Lymnaea stagnalis* molluscan AChBP (Brejc et al., 2001) (see section 2.6.5).



Figure 2.6 The 1.94Å crystal structure of the extracellular region of the mouse $\alpha 1$ nAChR.

The crystal structure of mouse $\alpha 1$ nAChR subunit (cyan) bound to α -bungarotoxin. The carbohydrate chain is shown as a magenta stick structure. *Left*) Front view of the inner and outer sheets of the extracellular region. *Right*) The top view of the structure. (Image reprinted with permission from (Dellisanti et al., 2007)).

ACh is the endogenous ligand for nicotinic receptors. The location where the endogenous neurotransmitter binds is termed the “orthosteric site.” In nAChR, the orthosteric site has been shown to bind both agonist and antagonist and is located in the extracellular region between the principal face of the α and the complementary face of the α or β subunits (Figure 2.7)(Taly et al., 2009). The “principal” faces (denoted as the + face) comprise loops A (β -strands $\beta 4$ - $\beta 5$), B (β -strands $\beta 7$ - $\beta 8$) and C (β -strands $\beta 9$ - $\beta 10$) (Corringer et al., 1995; Unwin, 2005; Dellisanti et al., 2007) (Figure 2.7). The complementary face (designated the – face) contains the β -strands D, E and F (Figure 2.7) (Corringer et al., 1995).

Depending on the subunit composition of a nAChR, there are either two (heteropentameric) or five (homopentameric) ACh-binding sites within the extracellular domain. The ACh binding site is termed the “aromatic box” (Corringer et al., 2000; Brejc et al., 2001) (Figure 2.7B) and is primarily formed by five aromatic residues, Y93, W149, Y190 and Y198 located on the principal face, and W55, located on the complementary face (Figure 2.7B) (Corringer et al., 2000; Brejc et al., 2001).

Nicotinic agonists contain a cationic nitrogen and a hydrogen bond acceptor that interact with nAChRs (Glennon and Dukat, 2000; Glennon et al., 2004) (Figure 2.7C). In $\alpha 4\beta 2$ nAChR, there is evidence of a strong cation- π interaction between W149 and the ligands ACh and nicotine (Puskar et al., 2011). Nicotine also strongly interacts by hydrogen bonding with the

backbone carbonyl contributed by W149 (Puskar et al., 2011). The $\alpha 7$ nAChR has been shown to have a similar binding pattern to those of $\alpha 4\beta 2$ nAChR and it has been suggested that the $\alpha 7$ nAChR cation- π interaction is important for ligand recognition (Puskar et al., 2011). In $\alpha 4\beta 2$ receptors, this interaction is on W149 (Puskar et al., 2011). In $\alpha 7$ nAChR this cation- π interaction occurs with Y93 and the agonist (Puskar et al., 2011). Epibatidine, a nicotine analogue, forms a cation- π interaction with T198 (Puskar et al., 2011). A hydrogen bond involving the backbone NH of $\beta 2L119$ of $\alpha 4\beta 2$ nAChR has been shown to form with the ligands nicotine, ACh, epibatidine and carbamylcholine (Blum et al., 2010).

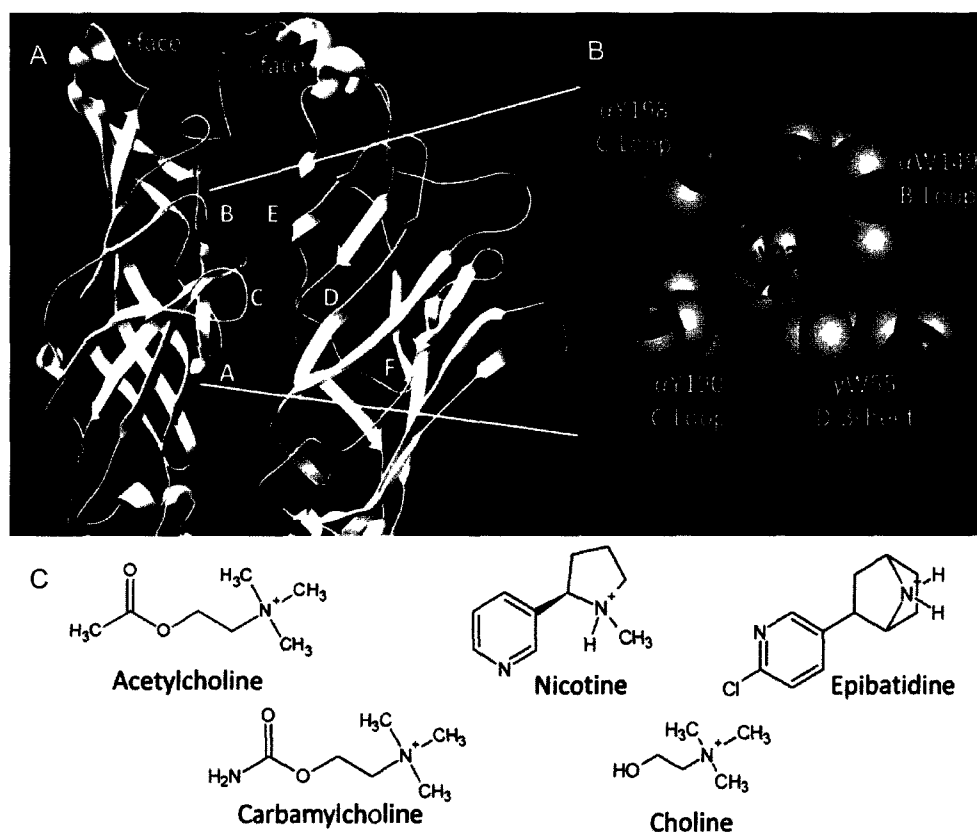


Figure 2.7 Loop labeling and residues involved in the orthosteric binding site in the extracellular domain of nAChR.

A) The designation of the loops and β -sheets on the principal (+) and complementary (-) faces. **B)** The orthosteric aromatic box. (Figure B reprinted with permission from (Lester et al., 2004)). **C)** Structures of important nicotinic ligands. Hydrogen bond acceptor groups are colored red and cationic nitrogens are colored blue.

2.6.2 Transmembrane Domain.

2.6.2.1 Transmembrane Domain Structure.

The transmembrane (TM) domain spans the 3 nm or so of the cell lipid bilayer membrane. There are four alpha helical transmembrane segments (TM1-TM4) in each subunit for a total of 20 transmembrane helices in the holoprotein (Figure 2.8). The TM2 helices line the channel pore and contain residues that form the ion channel gate. Crevices filled with water and cholesterol are formed between TM1, TM2 and TM3 of each subunit (Figure 2.8) (Wick et al., 1998; Bera et al., 2002; Bera and Akabas, 2005; Brannigan et al., 2008). The extracellular domain is linked to the TM1 domain (see Figure 2.5). There is a short intracellular loop which connects TM1 to TM2 (see Figure 2.5). TM2 and TM3 are connected via a short extracellular loop termed the TM2-TM3 linker (see Figure 2.5). A long intracellular loop connecting TM3 to TM4 may interact with cytoskeletal protein within the cell (Barry and Lynch, 2005) (see Figure 2.5).

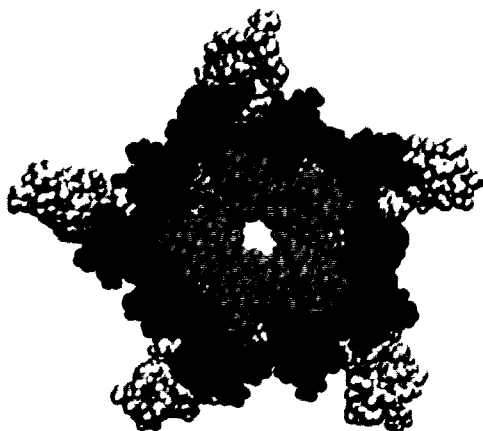


Figure 2.8 Transmembrane helices in nAChR.

The 20 transmembrane helices in a nAChR modeled after of N. Unwin (2005) 4Å template: TM1 is purple; TM2 is green; TM3 is blue and TM4 is cyan. Cholesterol was docked into the proposed binding sites (sites A (yellow), sites B (orange), sites C (red)). (Image reprinted with permission from (Brannigan et al., 2008).)

The ion channel is blocked by a gate constructed of leucines and valines on the TM2 helices (Figure 2.9). There are two rings, 9' leucines and 13' valines, that face into the channel and form a 6Å in diameter hydrophobic girdle that prevents ion flow (White and Cohen, 1992; Banks et al., 2000; Miyazawa et al., 2003; Arevalo et al., 2005; Unwin, 2005). A numbering system has been developed to compare TMs of the different subunits to each other (Miller, 1989). The conserved positively charged residues at the cytoplasmic end of TM2 are defined as 0' with

the numbers increasing toward the extracellular end which is designated as 20' (Miller and Smart, 2010). Hydrated Na^+ and K^+ ions (approximately 8Å in diameter) cannot pass due to their size. Smaller dehydrated ions also cannot pass due to insufficient polarity through the hydrophobic girdle (Miller and Smart, 2010). It is believed that the gate opens as a result of the TM2's tilting motion (Unwin, 1995).

The TM2 helix is an important structure that links the binding and gating events of the Cys-loop receptors. The TM2 extends two α -helix twists above the extracellular membrane in GABA_AR (Bera et al., 2002). The position of the TM2 does not parallel the cell membrane. Rather, the upper section of the helix tilts away from the helix's posterior part making it so that the top part of the channel (nearest to the extracellular domain) is wider than the bottom of the channel creating a 'kink' in the middle of each TM2 (Unwin, 1995).

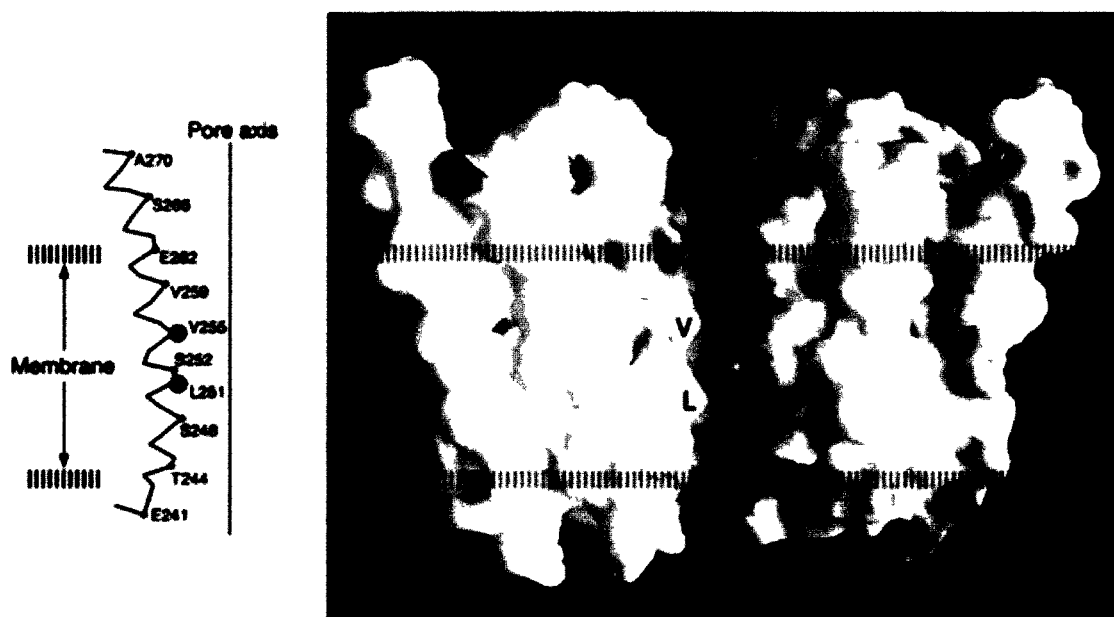


Figure 2.9 The ion channel pore of nAChR.

The pore facing side chains of the TM2 helix. Grey dots are residues that form the gate. The molecular surface of the pore domain cross sectional view with the front subunit removed. Red and blue colors correspond to areas with high negative (red) and positive (blue) charge. The yellow areas are hydrophobic regions containing the gate. Valines and leucines are identified (αV255 and αL251). The little light blue sphere located midway down the channel is the approximate size of a hydrated sodium ion. (Image reprinted with permission from (Miyazawa et al., 2003).

2.6.2.2 *Transmembrane Domain and Receptor Gating.*

There are several hypotheses regarding the conformational change within nAChR that link the ligand binding and gating events. Using electron microscopic structural studies of Torpedo nAChR, Unwin and colleagues proposed a receptor mechanism that links the binding and gating events (Unwin et al., 2002). They predicted that the binding of the agonist caused a clockwise rotation of each a region (likely the inner β -sheet) of the extracellular domain perpendicular to the cell membrane and through the Cys loop (Unwin et al., 2002) (Figure 2.10A). However, due to the tilt of the angle's rotation on each subunit's extracellular domain, the quaternary structure of the extracellular domain rotates anticlockwise (Bocquet et al., 2009). The rotation of each extracellular domain may create contact points between the β 1- β 2 loop and the TM2-TM3 linker (Unwin et al., 2002), a hypothesis that is supported by glycine mutations in the linker region (Lynch et al., 1997; Lewis et al., 1998; Shan et al., 2003) and mutagenesis studies demonstrating that the TM2-TM3 linker experiences backbone structural changes during gating (England et al., 1999; Bera et al., 2002) (Figure 2.10A and C). The movement of the TM2-TM3 linker (Figure 2.10B) torques the TM2 area, retracting TM2 from the pore and pushes it toward TM1, TM3 and TM4 causing the channel to open (Miyazawa et al., 2003). The channel is stabilized by contacts between neighboring TM1, TM2 and TM3 helices (Miyazawa et al., 2003). A water and/or cholesterol filled cavity separating TM2 from TM1 and TM3 additionally assists this movement (Figure 2.8) (Wick et al., 1998; Bera et al., 2002; Bera and Akabas, 2005; Brannigan et al., 2008). The TM1-TM2 and TM2-TM3 connecting loops contain conserved glycines that allow for increased flexibility of the TM2 movement (Miyazawa et al., 2003).

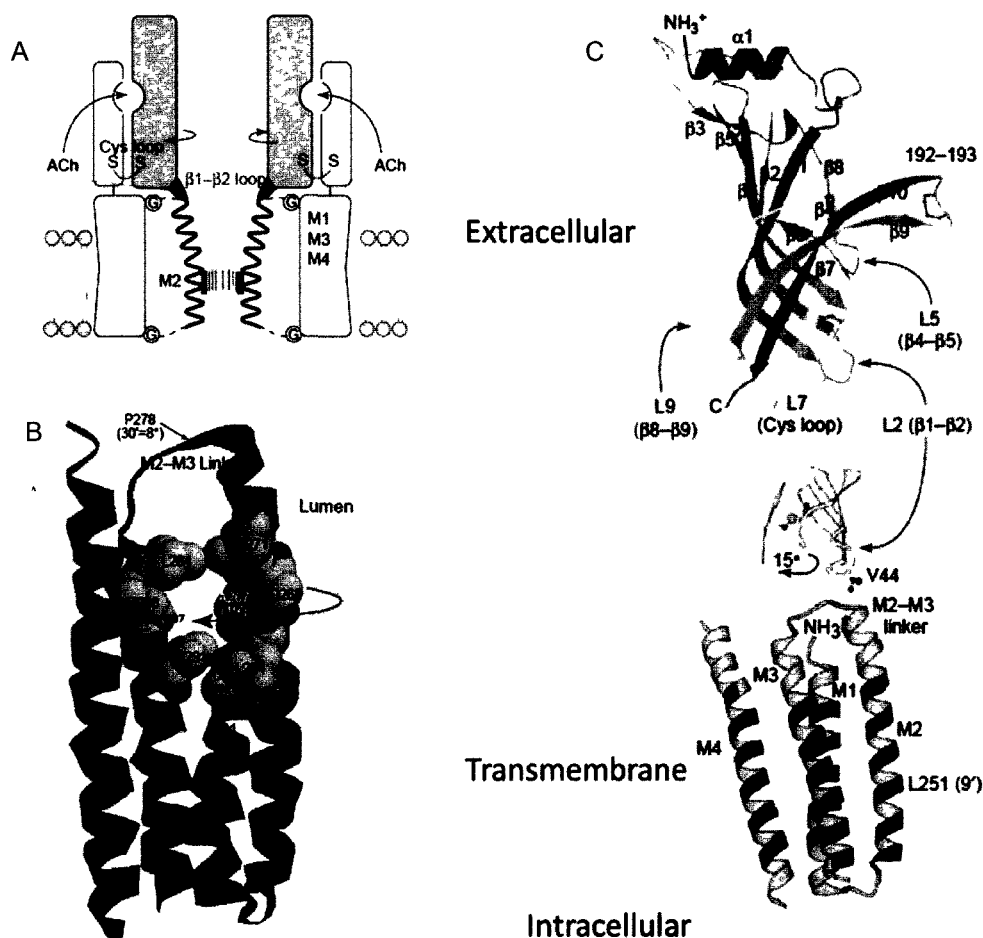


Figure 2.10 Illustrations of the contacts and movements that may occur between the extracellular and transmembrane domains of nAChR.

A) A model of nAChR structure and gating modeled after Neigel Unwin's investigations. The binding of the agonist induces clockwise rotation of the large shaded region which then torques the TM2 region causing the channel to open. The gate is represented by hatched lines in the transmembrane domain. **B)** The transmembrane structure of nAChR illustrates the postulated movement of the TM2 helix. Residue 19' has been shown to rotate into a more hydrophobic environment (Dahan et al., 2004). **C)** *Top*, Ribbon structure of one nAChR subunit. All the β -sheets are labeled. The red labels indicate the β -strands that might rotate with agonist binding. *Bottom*, A close up view of the transmembrane domain, postulated contact points and structural movements associated with agonist binding. The L251 is thought to lie at the TM2 gate. (Permission to reuse image granted by (Lester et al., 2004).

The timing of TM2 movement has been investigated by Auerbach and co-workers (Purohit et al., 2007). They predicted that the two α -subunit TM2s moved before the non- α subunits. The sideways TM2-TM2 interactions that stabilize the gate are possibly disrupted by the outward movement of the two α -subunit TM2s. This movement would cause the leucine gate to destabilize and move out of the way, allowing the passage of ions (Miller and Smart, 2010).

Recent studies demonstrated that as the channel opens a tagged fluorescent group attached near the top of the TM2 helix moves into a more hydrophobic environment (Dahan et al., 2004). This data is consistent with the clockwise rotation of the TM2 region. The rotation would move the chain at position 19' into contact with several hydrophobic side chains (Miyazawa et al., 2003). Previous data showing that the water-filled TM2-TM3 pocket changes shape during Cys-loop activation (Wick et al., 1998) is consistent with Unwin and colleagues' theory of conformational change (Unwin et al., 2002).

It has been proposed that the Cys loop may be the structural region that contacts the TM2-TM3 linker during conformational changes (England et al., 1997; Kash et al., 2003; Leite et al., 2003). Unwin has postulated that the β 1- β 2 loop contacts the TM2-TM3 linker (Unwin et al., 2002). In the AChBP, these regions are nearby which may explain the differing ideas. It is also possible that both of these regions are involved in gating. Kash et al., (2003) suggested that the Cys loop and the TM2-TM3 linker are involved in both the opening and closing events of the receptor.

Another theory proposed by Auerbach and co-workers suggests that a gradual series of transitions occurs in response to agonist binding (Grosman et al., 2000; Cymes et al., 2002) (Figure 2.11). Linear free-energy analysis of single point mutations investigated by single-channel recordings may indicate the position of the transition state for the gating event. A $\phi=0$ indicates the mutated receptor is in a 'closed-like state, while a $\phi=1$ indicates the receptor is more 'open-like' (Grosman et al., 2000; Cymes et al., 2002). There is a gradient of ϕ values from the agonist binding site to the transmembrane domain. These results suggest that conformation changes occur in a wave rather than a unified single movement (Akk et al., 1996; Grosman et al., 2000; Auerbach, 2005; Zhou et al., 2005; Purohit et al., 2007) (Figure 2.11).

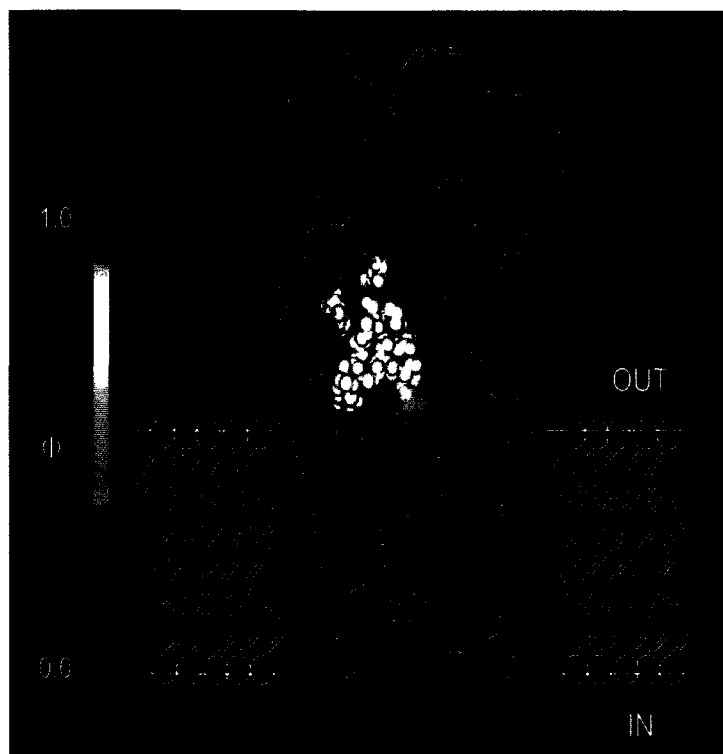


Figure 2.11 Auerbach and co-workers (2004) model of a conformational wave associated with agonist binding.

Structure is of nAChR α and δ subunits. The gradient ϕ value is shown on the left. During gating, red colored residues in loop 5 have $\phi=0.93$ and are the first residues to move. Loop 2/loop 7 in yellow ($\phi=0.80$) are the next to move, followed by residue α S269 (green $\phi=0.69$) in the TM2-TM3 linker region. The upper part of the δ TM2 are the next to move (blue, $\phi=0.32$) followed by the lower half of the δ TM2 (magenta, $\phi=0.0$). The extracellular domain is the AChBP (Brejc et al., 2001) and the transmembrane domain is from the *Torpedo* nAChR (Miyazawa et al., 2003). The ϕ values were estimated independently from Chakrapani et al., 2004. (The image is from (Chakrapani et al., 2004) and has been reused with permission).

2.6.3 Intracellular Domain.

The structure of the intracellular domain consists of a cytoplasmic loop that has not been extensively studied. Unwin's 4.6Å structure of the nAChR intracellular region predicted that there are transverse tunnels formed by α -helices in the channel wall (Miyazawa et al., 1999). However, Unwin's 4Å *Torpedo* nAChR structure did not reveal the cytoplasmic loop and was presumed to be disordered (Unwin, 2005).

Amino acid sequence comparison within the LGIC family of the intracellular region has revealed that this area is highly variable in amino acid residues and length. This loop of the

protein varies in length from 70 residues (in glutamate-gated Cl⁻ channels) to 271 residues (α 4 nAChR) (Keramidas et al., 2004). The diversity of the cytoplasmic loop sequence may suggest that this region is important for subunit specific behavior and possible interactions with cellular components.

The residues in the TM1 (Wang et al., 2002) and at TM4's extracellular and intracellular ends of α 1 nAChR (Roccamo and Barrantes, 2007) have been shown to control the assembly and targeting of the receptors to the cell surface. Mutation and deletion of residues near the intracellular end of TM4 in the cytoplasmic loop have been shown to reduce the assembly of the receptor subunits and cause both enhancement and reduction of ACh induced currents of nAChRs (Yu and Hall, 1994b; Valor et al., 2002; Kuo et al., 2005; Castelan et al., 2007). The diversity of the cytoplasmic loop sequence may suggest that this region is important for subunit specific behavior and the possible interactions with cellular components. It has been demonstrated that the cytoplasmic loop interacts with cytoplasmic transport machinery during nAChR trafficking to the synapse (Williams et al., 1998; Temburni et al., 2000; Keller et al., 2001; Ren et al., 2005; Xu et al., 2006). The mutation of residues in the TM1 (Wang et al., 2002) and at TM4's extracellular and intracellular ends of α 1 nAChR (Roccamo and Barrantes, 2007) have been shown to reduce the assembly and targeting of the receptors to the cell surface. The cytoplasmic loop interacts with the actin cytoskeleton resulting in cell surface expression (Bencherif and Lukas, 1993; Yu and Hall, 1994a; Shoop et al., 2000) and the resultant phosphorylation (Pacheco et al., 2003; Wiesner and Fuhrer, 2006) may reduce the time the receptor is desensitized (Huganir et al., 1986; Fenster et al., 1999), enhance or reduce receptor expression (Wang et al., 2004; Cho et al., 2005) and reduces cytoskeletal interactions (Colledge and Froehner, 1997). In α 7 nAChR, palmitoylation has been shown to aid in the formation of functional receptors (Drisdell et al., 2004; Huang and El-Husseini, 2005).

2.6.3.1 Ion Channel Selectivity.

The Cys-loop super family receptors contain ion selectivity filters that screen hydrated ions via a partial dehydration mechanism (Corringer et al., 1999b). Charged rings exist at the cytoplasmic and extracellular ends of the channels and are important for regulating channel conductances (Figure 2.12A) (Miller and Smart, 2010). In nAChR and 5HT₃R, the rings are negatively charged permitting the passage of cations (Keramidas et al., 2004) while GABA_A and C and glycine receptors have positively charged rings that allow anions to pass (Keramidas et al., 2004).

Voltage-gated ion channels have aided our understanding of the movement of ions through receptor pores. In voltage-gated channels, ions transverse down the ion channel by

dehydration of their water molecules by protein residues that mimic the interactions of water. The ions are then coordinated by the partial charges of the carbonyl groups found on the protein's backbone and "ping-pong" down the pore (Doyle et al., 1998; Zhou et al., 2001; Dutzler et al., 2003). Cys-loop receptors appear to have additional ion translocation mechanisms. For example, in muscle AChR cations are selected by the anionic residues located on either side of the TM2 (Imoto et al., 1988) and the transverse tunnels in the cytoplasmic domain (Kelley et al., 2003) (Figure 2.12). The hydrophobic α -helices reside in the TM2 form a narrow region of the AChR channel, providing little stabilization and thereby minimally slowing the passage of hydrated ions (Miyazawa et al., 2003). Studies have shown that in the course of translocation, individual ions are transiently stabilized by electrostatic attraction to rings of negatively charged residue along the extracellular part of the pore (Imoto et al., 1988; Wang et al., 2008a) (Figure 2.12). The cytoplasmic border rings (positions -2 to 2) of TM2 select monovalent cations over anions (Galzi et al., 1992; Corringer et al., 1999a; Gunthorpe and Lummis, 2001; Keramidas et al., 2004; Sunesen et al., 2006; Wotring and Weiss, 2008). By using molecular dynamics simulations to investigate the transport of ions through the muscle nAChR, Wang et al., (2008) suggested that ion selectivity is achieved by electrostatic interactions while the translocation is reliant on channel hydration (Wang et al., 2008a) (Figure 2.12B). This study demonstrated that selective cation translocation may occur in two stages. First, cations are selected through a series of oppositely charged residues in the protein vestibule leading down to a narrow hydrophobic constriction (presumably the gate). Second, hydration of the narrow region and protein movement enables the cation to pass through the pore (Wang et al., 2008a).

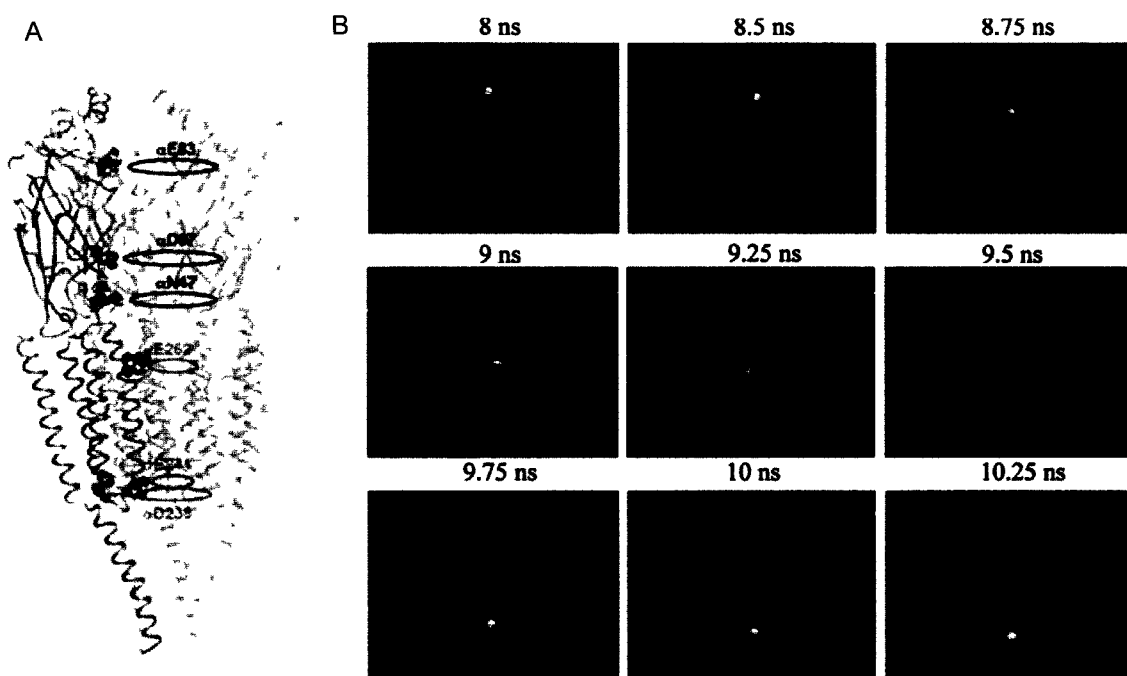


Figure 2.12 Ion translocation in nAChR.

A) A homology model of the human adult muscle nAChR. The rings of change are shown. The rings and labels in grey describe charged residues that affect conductances and selectivity as described in Imoto et al.'s, (1988) functional assay (Imoto et al., 1988). The rings and labels in black are identified residues associated with prolonged cation dwell times in molecular dynamic studies conducted by Wang et al. (2008) (Wang et al., 2008a). (Image reprinted from (Sine et al., 2010) and used with permission.) **B)** Molecular dynamic successive snapshots depict the translocation of a single cation through the nAChR channel. The water molecules inside the channel are shown in surface representation. The permeating ion is shown in yellow. Water molecules outside the channel are shown in line representation and other cations are shown as small yellow spheres (Image reprinted from (Wang et al., 2008a) and used with permission).

2.6.4 Comparison of Different Electron Diffraction and X-ray Crystallization of nAChR Structures.

Structures obtained by electron diffraction and X-ray crystallization techniques have contributed substantial information about the architecture and function of LGICs (Unwin, 1995; Miyazawa et al., 1999; Unwin, 2005; Dellisanti et al., 2007). Unwin's 4Å resolution of the *Torpedo* AChR is currently the best structure to date and assists in the homology modeling of other nAChRs (Unwin, 2005). This structure reveals that the N-terminal extracellular domain of each subunit has ten β -strands and one α -helix at the top of the channel pore, furthest from the cell membrane. The subunits are thought to contact each other in the extracellular domain primarily through polar contacts (Wells, 2008) while the transmembrane appears to make contacts mainly

through hydrophobic contacts (Wells, 2008). The Cys-loop and the β 1- β 2 loop of the N-terminal extracellular domain of a subunit interact with the short TM2-TM3 loop of the TM domain (Unwin, 2005). This interaction may be linked to channel gating as described in the above sections.

The mouse α 1 nAChR subunit bound to α -bungarotoxin was recently crystalized with a resolution of 1.94 Å (Dellisanti et al., 2007). In the extracellular region, the Cys loop and the previously unknown N-linked glycosylation moiety appeared to interact with the bound α -bungarotoxin (see Figure 2.6). Functional studies demonstrated that the carbohydrate chain is involved in α -bungarotoxin binding and channel gating (Dellisanti et al., 2007).

2.6.5 X-Ray Crystallography and Molecular Modeling of AChBP.

In 2001, the 2.7Å resolution X-ray crystal structure of the acetylcholine binding protein (AChBP) from the fresh water snail *Lymnaea stagnalis* was determined by Brejc et al., (2001) (Figure 2.13). To date, three different AChBP proteins have been isolated from freshwater mollusks *Lymnaea stagnalis* (Brejc et al., 2001), *Aplysia californica* (Hansen et al., 2004), *Bulinus truncates* (Celie et al., 2005). In the snail, AChBP is secreted into the synaptic cleft and is thought to regulate neurotransmission by quenching ACh (Smit et al., 2001). These pentameric water soluble proteins lack the transmembrane and cytosolic domains; therefore AChBP may only be a model of the binding and not the gating mechanism.

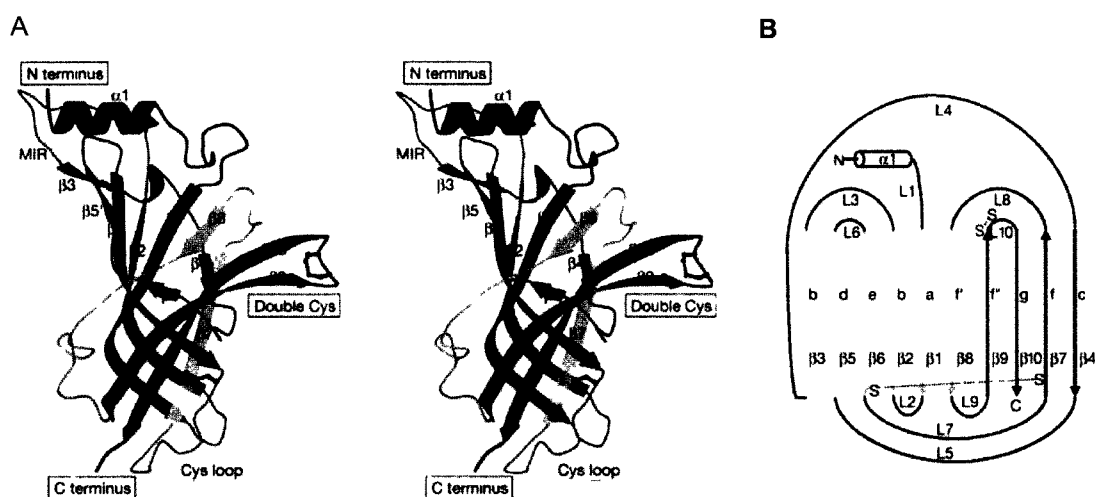


Figure 2.13 AChBP structure overview.

A) A stereo image of one subunit from the AChBP viewed from outside the pentameric ring. The N-terminus is colored blue while the C-terminus is colored red. The disulfide bridge found on the C-loop is colored in green ball-and-stick representation. The β -sheets are numbered. **B)** The topology of a AChBP subunit is shown. The Immunoglobulin-like folds have been labeled in alphabetical letters. The β -strands have been labeled $\beta 1$ -10 and the loops have been labeled L1-10. The disulfide bridge is labeled as S-S. (Image reprinted with permission from (Brejc et al., 2001).)

AChBP appears to be a good structural model of nAChR extracellular domain. The AChBP backbone is similar to nAChR with a comparative sequence of 20-40% homology (Wells, 2008). However, despite the low sequence homology, many other aspects of the tertiary and quaternary structures are similar. For example, nearly all of the conserved residues found in the nAChR family are also found in the AChBP (Brejc et al., 2001) and the AChBP binds similar agonist and antagonist such as ACh, nicotine, d-tubocurarine and α -bungarotoxin (Smit et al., 2001).

The Brejc et al., crystal structure of *Lymnaea* AChBP showed that the amino terminal of each subunit consists of an α -helix, two short 3_{10} helices and a core of ten β -strands forming a β -sandwich (Brejc et al., 2001) (Figure 2.13). The AChBP β -strands are considerably twisted with the β -sheets rotated against each other causing two separate hydrophobic cores to be formed (Brejc et al., 2001). Presumably, AChBP's hydrophobic cores are the same structures described as the inner and outer β -sheets in nAChR. The 210 amino acid sequence of each AChBP subunit is the same and is most similar to the $\alpha 7$ nAChR (Brejc et al., 2001). The Cys-loop contains 14 residues instead of the usual 15 (Brejc et al., 2001).

2.6.5.1 AChBP Crystal Structure Bound to Orthosteric Ligands.

In Brejc et al.'s *Lymnaea* AChBP structure, the ligand binding sites are occupied by HEPES, a common buffering agent used in electrophysiological experiments (Brejc et al., 2001) (Figure 2.14A). The *Lymnaea* AChBP crystal structure bound to the nicotinic agonists nicotine and carbamylcholine provides insights into the orthosteric binding site (Celie et al., 2004; Karlin, 2004). Usually negatively charged, the orthosteric site facilitates the interactions with the positively charged tertiary nitrogen of nicotine and the quaternary nitrogen of carbamylcholine (Dougherty and Stauffer, 1990; Dougherty, 1996; Zhong et al., 1998). The negative charges within the orthosteric site are formed by the π electrons from the aromatic residues W143, Y192, Y1185 and W53 and the backbone carbonyl of W143 (Dougherty and Stauffer, 1990; Dougherty, 1996; Zhong et al., 1998).

The C-loop in AChBP crystal structures suggests that this loop undergoes structural movements depending on the ligand bound in the orthosteric site (Figure 2.14B). The HEPES-, nicotine- and carbamylcholine- bound structure shows that the C-loop is positioned over the ligand (Brejc et al., 2001; Celie et al., 2004; Karlin, 2004). The *Lymnaea* AChBP with α -cobratoxin, an antagonist of nAChR, indicates a movement of the C-loop away from the binding site (Bourne et al., 2005). Comparison of AChBP structures free of ligand, agonists ((+)-epibatidine and lobeline) and antagonists (α -conotoxin Iml and methyllycaconitine) bound structures reveal that agonist binding induced C-loop closure (Hansen et al., 2004; Hansen et al., 2005) (Figure 2.14).

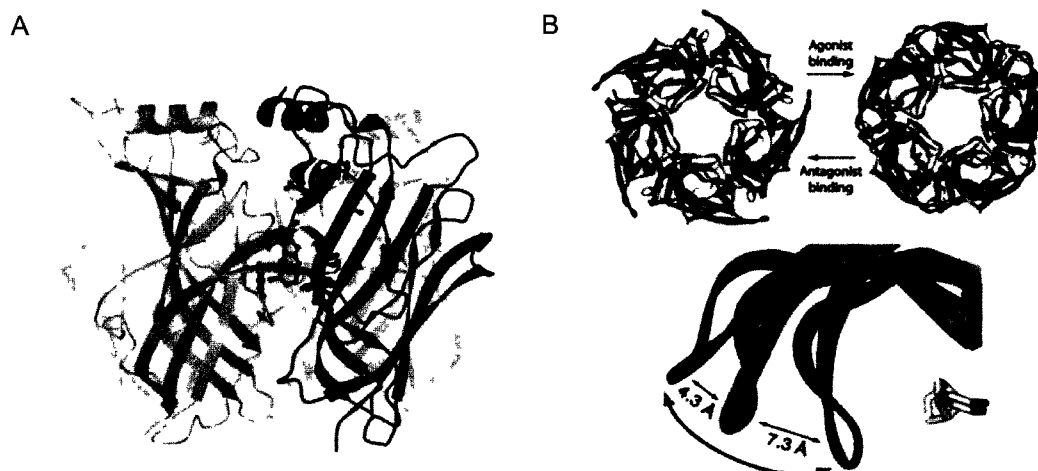


Figure 2.14 AChBP with agonist and antagonist bound.

A) AChBP side view. The ligand binding site (ball and stick representation) is shown between the yellow and blue subunits. (Image reprinted from (Brejc et al., 2001) and used with permission.) **B)** Conformational change mechanism and ligand selectivity. *Top:* The top view of the Iml-bound (C-loop red) and epibatidine bound *Aplysia* AChBP pentamers (C-loop blue). Structure shows how distant conformations for the agonists and antagonists bind. *Bottom:* The overlay of the C-loop in the apo (grey), Iml (red), methylcaconitine (green) and epibatidine (blue). The bound epibatidine ligand is shown in light grey. The arrow depicts the motion of the opening and closing of the C-loop upon antagonist and agonist binding. (Image reprinted from (Hansen et al., 2005) and used with permission.)

2.6.5.2 AChBP Crystal Structure Bound to Allosteric Ligands.

The crystal structure of *Aplysia* AChBP bound to galanthamine and cocaine, positive allosteric modulators of nAChRs, demonstrate that these ligands bind deeply into the subunit interfaces without contacting the C-loop tip (Hansen and Taylor, 2007). AChBP, from the *Bulinus truncates*, was crystalized using the common biochemistry buffer agent N-cyclohexyl-3-aminopropanesulfonic acid (CAPS) (Celie et al., 2005). CAPS molecules were found in four of the five ligand binding sites (Celie et al., 2005). These crystal structures may provide insight on the different conformational changes that occur in response to binding of different ligands.

2.7. Orthosteric and Allosteric Binding Sites.

The agonist binding site on LGIC is located between two receptor subunits (Figure 2.7). The binding site for the endogenous agonist is commonly referred to as the “orthosteric” binding site while the binding sites for allosteric modulators are commonly referred to as “allosteric” binding sites. The allosteric site includes loops A, B and C on the primary face and β -strands D, E and F on the complementary face (Figure 2.7). Both sites include highly conserved aromatic

residues. In general, the orthosteric site is negatively charged allowing favorable interactions between the positive charges of tertiary and quaternary nitrogens on nicotinic ligands (Dougherty and Stauffer, 1990; Dougherty, 1996; Zhong et al., 1998) (Figure 2.7). The negative charges within the orthosteric site are formed by the π electrons from the aromatic residues W143, Y192, Y1185 and W53 and W143's carbonyl backbone (Dougherty and Stauffer, 1990; Dougherty, 1996; Zhong et al., 1998).

A selective review of well-characterized binding sites and significant therapeutic ligands including the serotonin, GABA_A and Nicotinic receptors follows. Elucidation and characterization of ligand binding sites will lead to a greater understanding of the protein and the development of novel therapies.

2.7.1 Characterized Binding Sites on the Serotonin Type 3 Receptor (5-HT₃R).

5-HT₃R are involved in various physiological functions including cognitive processing, sensory transmission, regulation of autonomic function, integration of vomiting, reflex, pain processing and control of anxiety (Barnes and Sharp, 1999; Hu and Lovinger, 2008). 5-HT₃ receptors have two different subunits, 5-HT_{3A} and 5-HT_{3B}. 5-HT_{3A} forms α homomers while 5-HT_{3B} only forms $\alpha\beta$ heteromers. In the nervous system, 5-HT₃R mediates fast excitatory synaptic transmission and modulates neurotransmitter release (Hu et al., 2003).

2.7.1.1 The 5HT₃R Orthosteric Binding Site.

In 5HT₃R, the primary side chain interactions for the orthosteric binding site appear to come from loops A, B and C on the principal face (Figure 2.15). On the complementary face, amino acids on the D and E β -strands appear to play a role in ligand binding (Figure 2.15). The F β -strand has yet to be thoroughly investigated. The chemical structures of the discussed serotonin (5-HT) ligands are shown in Figure 2.16.

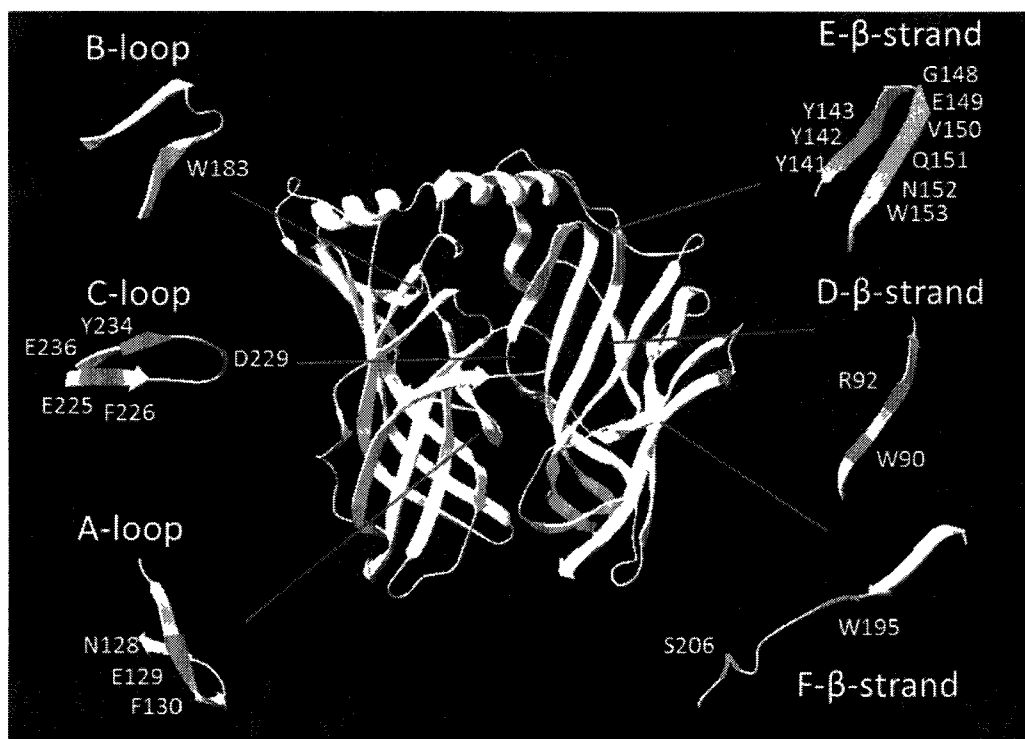


Figure 2.15 The orthosteric binding site of 5-HT_{3A}R.

Residues that have been demonstrated biochemically to participate in the binding and/or gating of 5-HT₃ agonist and/or antagonist. Extracellular region modeled after *Lymnaea stagnalis* AChBP (PDB ID 2ZJV). The position of the labeled residues is the approximate location.

In the A-loop, E129 or F130 faces into the binding pocket (Price et al., 2008) (Figure 2.15). Results reveal that a hydrogen bond forms between E129 and the hydroxyl group of 5-HT (Price et al., 2008). Other residues in the A-loop such as N128 and F130 may also play a role in receptor gating, but they do not participate in ligand binding (Price et al., 2008) (Figure 2.15).

W183 in loop B (W143 in AChBP) is entangled in ligand-receptor interactions and appears to be the core of the binding site (Spier and Lummis, 2000; Beene et al., 2002) (Figure 2.15). It has been postulated that W183 forms cation- π interactions with the amino group of 5-HT (Beene et al., 2002) or aromatic interactions with 5-HT (Suryanarayanan et al., 2005).

In the C-loop, residues E225, F226, D229, Y234 and E236 have been shown to be important residues in the orthosteric binding site (Figure 2.15). D229 and Y234 in the C-loop appear to be important binding residues (Beene et al., 2002; Suryanarayanan et al., 2005). This region of the receptor has little sequence homology with AChBP, making it difficult to align the

protein's sequences. Y234 appears to align best with AChBP Y192 (Celie et al., 2004). Y234 appears to play a role in 5-HT binding and/or gating, and is probably the most important residue in the binding pocket (Beene et al., 2004). Unnatural amino acid mutagenesis studies suggest that 5-HT orients itself so that the primary amine is located between W183 and Y234 (Beene et al., 2004). It has also been suggested that an inter-subunit contact forms between Y234 and Y143 in loop E (Maksay et al., 2003). D229 in the C-loop is another important residue aligning with C187 or Y185 (Celie et al., 2004). Alanine mutations of D229 in 5-HT₃R decreased 5-HT and granisetron, but not m-chlorophenylguanide (mCPBG) affinity (Suryanarayanan et al., 2005). These data suggest that interactions are formed between D229 and the ligands 5-HT and granisetron. Residues E225, F226 and E236 in the C-loop also appear to be involved in the orthosteric binding site. Mutagenesis studies of E225 have shown that E225 is involved in both 5-HT binding and gating of the receptor (Schreiter et al., 2003). F226 (similar in position to Y185 in AChBP) appears to be essential to 5-HT binding and receptor gating (Suryanarayanan et al., 2005). E236 (D194 AChBP equivalent) in 5-HT docking studies have shown that a salt bridge is formed between E236 and the 5-HT amino group (Schulte, 2006).

In the A-loop, E129 and F130 are involved in ligand binding (Figure 2.15). These residues have been shown to interact with the 5-HT ammonium group by ionic or hydrogen bond interactions (Boess et al., 1997; Steward et al., 2000). Residue F130 appears to be important for agonist selectivity and when mutated to the α 1 nAChR equivalent N, the F130N mutant 5-HT₃R become responsive to ACh (Steward et al., 2000).

On the complementary face, the binding site consists of the D, E and F β -strands (Figure 2.15). W90 and R92 reside on the D- β -strand and are involved in maintaining the proper binding site structure (Yan and White, 2002). A more recent study suggests that granisetron's orientation is such that the tropane ring interacts with W90 while R92 interacts with the indazole ring (Yan and White, 2005). Antagonist may directly interact with R92 (Yan and White, 2005).

In the E- β -strand, residues Y141, Y143, and Y153 are involved in the orthosteric site on 5-HT₃Rs (Figure 2.15). The ligands 5-HT and mCPBG interact with residue Y143, (+)-tubocurarine (dTC) with Y141 and lerisetron with Y143 and Y153 (Venkataraman et al., 2002a; Venkataraman et al., 2002b; Beene et al., 2004; Price and Lummis, 2004). The effects on 5-HT₃R antagonist binding affinity suggest that the E-loop region directly affects ligand binding (Venkataraman et al., 2002a; Venkataraman et al., 2002b). Residues L112 and M114 may also make hydrophobic interactions with nicotine (Celie et al., 2004) and dTC (Gao et al., 2005), respectively. Mutations of Y141, Y143 and Y153 have been demonstrated to significantly alter the binding of 5-HT₃R ligands (Beene et al., 2004). Residues Y142, G148, E149, V150, Q151, N152,

Y153 and K154 have been implemented to be important for granisetron binding (Venkataraman et al., 2002a) (Figure 2.15). Y143 and Y153 have been revealed to play a role in receptor function while Y153 is involved in ligand binding (Beene et al., 2004).

The structure of the F- β -strand has yet to be thoroughly investigated. Thompson et al., (2005) exhibited that residues W195 and S206 in mouse 5-HT₃R_s are critical for ligand binding, and may be involved in conformational changes within or close to the binding pocket (Thompson et al., 2005; Thompson et al., 2006) (Figure 2.15).

2.7.1.2 The 5-Hydroxyindole Binding Site.

The 5-HT binding site has been previously shown to bind a wide variety of ligands ranging from antagonists to agonists and may possibly include allosteric modulators (Kooyman et al., 1994; Yan et al., 1999). The positive allosteric modulator 5-hydroxyindole (5-HI) is a serotonin analogue (Figure 2.16) that displays biphasic behavior consisting of both competitive inhibition and allosteric potentiation actions on the homomeric 5-HT_{3A} receptor. This suggests that there are at least two distinct binding sites, one located at the orthosteric site and the other at a separate binding pocket (Kooyman et al., 1994). The mutation L293A on 5-HT_{3A} converted 5-HI to a partial agonist which was blocked by antagonist binding (Hu and Peoples, 2008). These results suggest that either 5-HI binds at the orthosteric site and/or that residue L293 is part of the 5-HI binding site. Studies have also shown that upon washout of 5-HI, rebound currents occur (Hu and Peoples, 2008). Rebound currents have been previously linked to open-channel block (Liu et al., 2008b), suggesting that 5-HI may also bind within the channel.

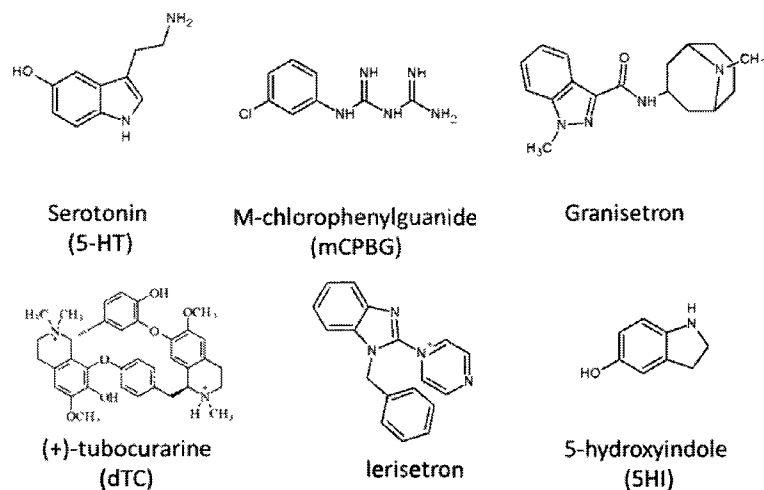


Figure 2.16 Chemical structures of serotonin ligands.

2.7.2 Characterized Binding Sites on Gamma Amino Butyric Acid (GABA) Receptors.

GABA_A receptors mediate synaptic inhibition in the CNS. One of the best characterized LGIC binding sites is the benzodiazepine site on GABA_ARs. The benzodiazepine binding site was reviewed by Sigel in 2002 so only a summary of the important findings discovered in the last nine years are discussed here (Sigel, 2002). In addition, the newly characterized neurosteroid and general anesthetic binding sites are summarized below.

2.7.2.1 *The Benzodiazepine Binding Site.*

Classical benzodiazepines (BZ) are positive allosteric modulators of the GABA_A receptor. BZ act primarily by increasing the affinity of the agonist GABA without affecting the maximal induced current amplitude (Sigel, 2002). It has recently been found that GABA evoked currents on GABA_ARs containing the $\alpha 4$ or $\alpha 6$ subunit can be potentiated by the BZs diazepam and flunitrazepam (You et al., 2010). The α and β subunits are sufficient to mediate GABA activated Cl⁻ currents while the γ subunit is needed for functional modulation by BZ as demonstrated with $\gamma 2$ knockout mice (Gunther et al., 1995). Research has demonstrated that the BZ binding site is located at the α and γ interface (Sigel and Buhr 1997). Non-BZD hypnotics used for treating insomnia also bind at the BZ binding cleft (Hanson et al., 2008). Only the key structural components of the BZ binding site structure are reviewed here (Figure 2.17). Reviews by Sigel and Buhr (1997) and Sigel (2002) are available for a more comprehensive coverage (Sigel and Buhr, 1997; Sigel 2002).

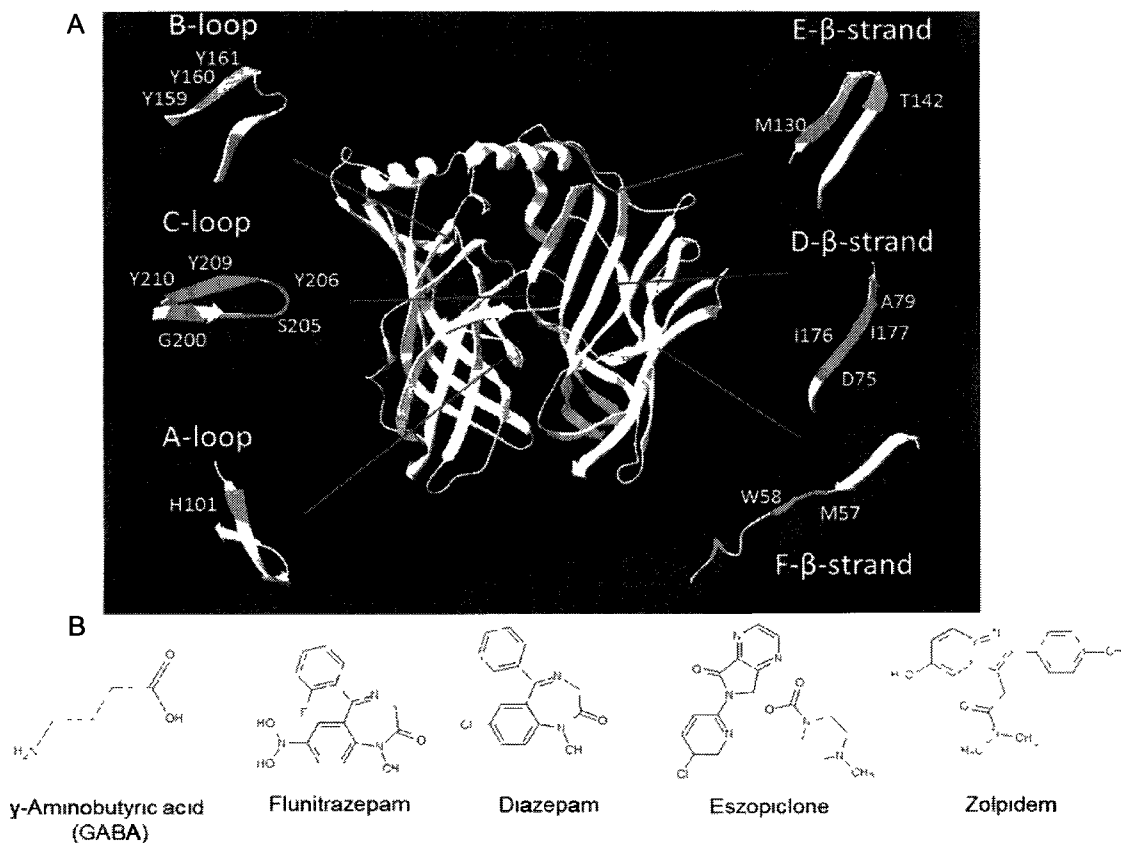


Figure 2.17 Summary of the residues found benzodiazepine binding site on GABA_AR and the chemical structure of the benzodiazepines.

A) A-loop shows residues that have been demonstrated biochemically to participate in the binding of benzodiazepines in GABA_AR. Extracellular region modeled after *Lymnaea stagnalis* AChBP (PDB ID 2ZJV). The position of the labeled residues is the approximate location. **B)** B-loop shows the chemical structures of the benzodiazepine ligands discussed in the text.

The $\alpha 1$ subunit is the main subunit that is photoaffinity labeled by the BZ flunitrazepam (Figure 2.17B for chemical structure). Specifically, H101 in loop A appears to be critical for flunitrazepam modulation (Duncliffe et al., 1996) and forms a covalent attachment at the C-7 position of diazepam as shown by radioactive ligand binding and two-electrode voltage clamp methods (Berezhnoy et al., 2004). The pendant phenyl group of flunitrazepam also interacts with α H101 (McKernan et al., 1998). When α Y159 in loop B was mutated to serine an impairment of diazepam modulation occurred (Amin et al., 1997). α Y159 and α Y161 in loop B, α T206 and Y209 in loop C have significant effects on BZ function whereas S205 and Y210 loop C are important for BZ selectivity (Sigel and Buhr, 1997; Wagner and Czajkowski, 2001). Mutating the α Y209 (C loop) residues nearly abolished flunitrazepam current stimulation (Buhr et al., 1997b). Other

studies show that when $\alpha 1Y209$ is mutated to a serine diazepam's EC_{50} is increased by >7-fold (Amin et al., 1997). Mutations of $\alpha 1G200$ and $\alpha 1T206$ in loop C alter affinities for BZ suggesting a role in the binding pocket (Schaerer et al., 1998) (Figure 2.17).

The region of $\gamma 2D75$, $\gamma 2I76$ and $\gamma 2I77$ in the D- β -sheet has been shown to drastically reduce allosteric modulation by flurazepam (Teissere and Czajkowski, 2001) (Figure 2.17). Residue $\gamma 1F77$ (D- β -sheet) is important for BZ direct interactions and selectivity (Buhr et al., 1997a). Displacement studies using the point mutation $\gamma 2F77Y$ caused a 250-fold reduction in diazepam affinity suggesting that the tyrosine hydroxyl group interferes with diazepam binding (Sigel et al., 1998). Using Substituted Cysteine Accessibility Method (SCAM), it has been shown that the region around $\gamma 2A79$ (D- β -sheet) in the BZ binding pocket becomes more accessible to MTSEA-biotin modification during GABA binding (Teissere and Czajkowski, 2001). These results suggest that at least a portion of the BZ binding pocket undergoes conformational change in response to GABA binding and channel gating (Teissere and Czajkowski, 2001). Amino acid residues $\gamma 2A79$ (D- β -sheet) and $\gamma 2M130$ (E- β -sheet) appear to be required for high affinity binding of various BZ, but does not alter BZ efficacy (Wingrove et al., 1997). Amino acid $\gamma 1T142$ (E- β -sheet) affects BZ efficacy suggesting a role in conformational change, facilitated possibly by a hydrogen bond with $\alpha Y160$ (loop B) (Mihic et al., 1994). $\gamma M57$ and $\gamma Y58$ (F- β -strand) are essential determinants for conferring high affinity BZ binding (Kucken et al., 2000) (Figure 2.17).

Alterations in zolpidem, eszopiclone (non-BZD hypnotics used for insomnia) and BZ-antagonist binding were studied using cysteine mutants in the BZ binding site (Hanson et al., 2008). Mutations in the $\gamma 2$ loop D and $\alpha 1$ loop A and B altered the affinity of all tested ligands demonstrating that these loops provide a structural framework for the BZ binding cleft. $\gamma 2$ loop E and $\alpha 1$ loop C mutants had various effects on ligand affinity suggesting that these loops are important for ligand selectivity. Molecular modeling of the binding site showed that docking of eszopiclone and zolpidem yielded a model stabilized by several hydrogen bonds. Alternatively, zolpidem docking showed the ligand binding via three equally populated orientations with few polar interactions. These results suggest that unlike eszopiclone, zolpidem binds in response to shape recognition of the BZ binding pocket rather than specific amino acid interactions, and may explain why zolpidem is $\alpha 1$ and $\gamma 2$ subunit selective (Hanson et al., 2008).

2.7.2.2 *The Neurosteroid Binding Site.*

The most potent endogenous modulators of $GABA_A$ receptors are neurosteroids, specifically allopregnanolone and tetrahydrodeoxycorticosterone, which are synthesized in neurons and glia cells from cholesterol (Hosie et al., 2007) (Figure 2.18B for chemical structures). At low nanomolar concentrations neurosteroids potentiate GABA responses (Stell et al., 2003)

and at sub to micromolar concentrations can directly activate the receptor (Majewska et al., 1986). The putative GABA_A neurosteroid binding sites have been recently reviewed (Hosie et al., 2007) and a brief summary follows (Figure 2.18).

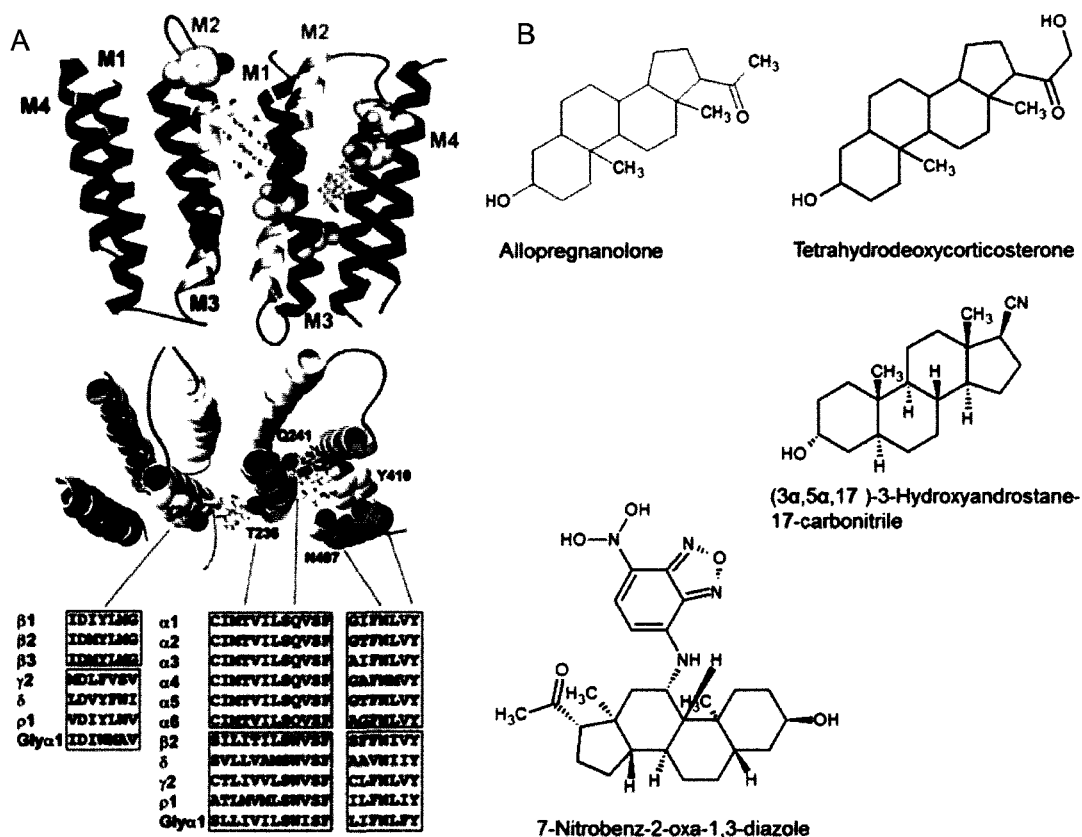


Figure 2.18 The neurosteroid binding sites in GABA_AR.

A) *Top:* A homology model for $\alpha 1$ and $\beta 2$ subunits of the GABA_AR. The TM2 domain is colored cream. The residues Q241, N407 and Y410 are shown in a space-filled layout. These residues have been shown to be important for the steroid potentiation site in the $\alpha 1$ subunit (green). $\alpha 1$ T236 and $\beta 2$ Y284 (blue) are located within the activating site. The tetrahydrodeoxycorticosterone molecules are shown docked into each site and viewed from within the plane of the membrane. *Bottom:* Same model of the binding sites, but viewed from a bird's eye perspective of only the transmembrane region. A primary sequence comparison of GABA_A, GABA_c $\rho 1$ and glycine $\alpha 1$ receptors for the major residues involved in steroid binding are compared in the tables. Red residues are involved in the activation site and blue residues are found in the potentiation site. (This image was modified and reprinted from (Hosie et al., 2007) with permission.) **B)** The chemical structures of the discussed steroids.

Based on studies using excised patches and the steroids 7-Nitrobenz-2-oxa-1,3-diazole and (3 α ,5 α ,17 β)-3-Hydroxyandrostane-17-carbonitrile, it appeared that steroids must accumulate in the cell membrane for modulation to occur (Akk et al., 2005) (Figure 2.18B). This strongly suggests a role of the transmembrane region in neurosteroid modulation (Akk et al., 2005). Specifically, mutation of β 2G219 located at the N-terminal of TM1 either reduced or enhanced the potentiation of GABA currents by various neurosteroids (Chang et al., 2003). Authors reasoned that G219 was more likely to be involved in the general mechanism of receptor modulation rather than contributing specifically to the binding site because mutations of β 2G219 failed to prevent direct gating by pentobarbital propofol, etomidate and alphaxalone. Amino acid residue ρ 1I307 located in TM2 was found to enhance and reduce anesthetic action in addition to altering the receptor's pharmacology suggesting that this residue may be involved in influencing allosteric modulation of the receptor function (Belelli et al., 1999; Morris and Amin, 2004) (Figure 2.18A).

Using *Drosophila* GABA_A receptor, the first two transmembrane domains of the α 1 subunit were found to be important regions for potentiation and direct receptor activation by various neurosteroids (Hosie et al., 2006a). Mutation of T236 was found to be critical for steroid activation. An I mutation of T236 markedly reduced receptor activation by tetrahydrodeoxycorticosterone and allopregnanolone, without affecting their potentiation responses to GABA (Hosie et al., 2006b). The Q241W mutation removed the potentiation of GABA currents and reduced the apparent neurosteroid agonist efficacy without altering the agonist EC₅₀ (Hosie et al., 2006b). The transmembrane region α Q241- α N407/ α Y410 has also been proposed to be involved in a neurosteroid potentiation site (Hosie et al., 2007). A neurosteroid activating site has been located in the region around α T236- β Y284 and there is at least one site for inhibitory sulphated steroids which likely involves the transmembrane 1 and 2 domains (Hosie et al., 2007). These results propose that there may be two to four neurosteroid binding sites on GABA_A receptors (Hosie et al., 2006b; Hosie et al., 2007) (Figure 2.18).

Homology modeling indicated that the polar residues T236 and Q241 are located in two discrete hydrophobic cavities that could each contain a steroid molecule implying the possibility for two binding sites (Hosie et al., 2006b) (Figure 2.18A). T236 is thought to be located on the outer surface of the receptor at the interface between the α and β subunits, but within the membrane. Q241 is thought to be located at the base of an aqueous pocket formed by the transmembranes 1-4 of the α subunit (Hosie et al., 2006b), which has also been proposed to interact with anesthetics (Mihic et al., 1997). Molecular modeling estimations of the steroid's molecular dimensions and mutagenesis suggest that N407 and Y410 in the TM4 of the α 1 subunit are involved in ligand binding (Hosie et al., 2006b) (Figure 2.18A). It is considered

unlikely that the β subunit contributes to the potentiation binding site although it may affect the efficacy of potentiation (Hosie et al., 2009).

2.7.2.3 The Anesthetic Binding Site.

General anesthetics, such as etomidate and propofol, have been shown to act by modulating LGIC such as GABA_A receptors possibly by the same putative binding pocket as neurosteroids (see Figure 2.18 above). The α 1 subunit appears to contribute L232 (TM1), S270 (TM2), A291 (TM3) as well as Y411, T414 and Y415 (TM4) (Mihic et al., 1997; Krasowski and Harrison, 1999; Mascia et al., 2000; Jenkins et al., 2001; Jenkins et al., 2002). In the β 2 and β 3 subunits, N265 (TM2) has been shown to be important for etomidate modulation but it is unclear if N265 is located within the binding pocket (Belelli et al., 1997; Moody et al., 1997; Moody et al., 1998) (Figure 2.19 for chemical structure). Using a radioactive etomidate analogue, α 1M236 in the TM1 and β 3M286 in TM3 were photolabeled suggesting the binding site is at the β and α transmembrane interface (Li et al., 2006).

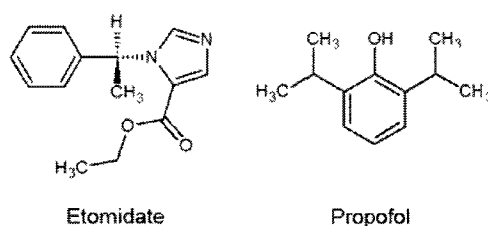


Figure 2.19 The chemical structures of the discussed anesthetic compounds.

The propofol cavity appears to be located closer to the membrane-extracellular interface between TM1 and TM4 (Figure 2.19 for chemical structure). Mutation of M286 to a tryptophan in the β 2 subunit abolished propofol potentiated GABA responses, but did not affect the direct activation of GABA_AR in absence of GABA (Krasowski et al., 2001). A hydrogen bond was predicted to form between Q224 and the propofol hydroxyl hydrogen atom. A π - π stacking interaction may occur between the Y448 phenyl ring and propofol. Other possible important sites of interaction include L223, T225 and Y226 in TM1, L285, F289 and F293 in TM3 and Y444 and W445 in TM4 (Campagna-Slater and Weaver 2007).

Recently, (Campagna-Slater and Weaver, 2007) used molecular modeling to further investigate this binding region in GABA_A receptors using the ligands etomidate and propofol. Models identified two cavities in the β 2 subunit. The etomidate binding sites appeared to be in the transmembrane domain between the TM1 and TM4 and between the TM3 and TM4. There appeared to be π - π stacking interactions formed between the imidazole ring of W237 (TM1) and

the phenyl group of etomidate. Other residues that may be important in etomidate binding include I230, L231, T233, I234 and S236 in TM1, M261 in TM2 and F293, L296, L287 and A300 in TM3 (Campagna-Slater and Weaver, 2007).

2.7.3 Characterized Binding Sites on Nicotinic Acetylcholine Receptors.

nAChR are excitatory receptors found in the CNS. Several allosteric binding sites have been characterized on the nAChR. The allosteric compounds physostigmine, divalent calcium, NS-1738 and PNU-120586 galanthamine, 17 β -estradiol and zinc are included in the following discussion.

2.7.3.1 The Physostigmine Binding Site.

Physostigmine is a cholinesterase inhibitor that stimulates both nicotinic and muscarinic receptors (Figure 2.20 for chemical structure). Only a single attempt to characterize the physostigmine binding site has been published. Using outside-out patches from cultured hippocampal neurons it was shown that α_7 nAChR residue α L125 appears to be essential to the physostigmine binding site (Pereira et al., 1993).

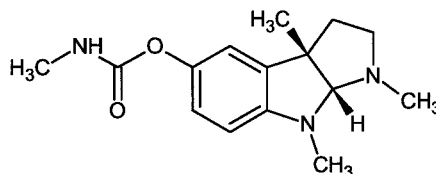


Figure 2.20 Chemical structure of physostigmine.

2.7.3.2 The Divalent Calcium Binding Site.

Divalent calcium (Ca^{2+}) is capable of modulating neuronal nAChRs by enhancing agonist affinity, efficacy and cooperativity (Hill coefficients) (Galzi et al., 1996). It has been suggested that the ACh and Ca^{2+} binding sites may be close together but occupy distinct locations (Galzi et al., 1996). Early work using $\alpha 7/5\text{-HT}_3$ receptor chimeras revealed that Ca^{2+} potentiated the chimera, but not the 5-HT_3 receptor. This observation indicated the allosteric effect of calcium ions was mediated by a binding site located on the N-terminus of $\alpha 7$ nAChR (Maricq et al., 1991). Later, use of the $\alpha 7/5\text{-HT}_3$ chimera combined with site directed mutagenesis uncovered ligand binding residues in the putative binding site (Galzi et al., 1996; Eddins et al., 2002). Mutations $\alpha 7\text{E18Q}$ and $\alpha 7\text{E44Q}$ abolished calcium enhanced agonist affinity, but maintained Ca^{2+} potentiation and cooperativity (Figure 2.21). Mutations in the region of $\alpha 7$ (161-172) (F- β -strand) had a variety of effects on Ca^{2+} modulation. Potentiation was enhanced by D163N and S169E (F- β -strand)

mutations while E161R, S165E and Y167F reduced or abolished (E172Q) the effects of calcium (Galzi et al., 1996; Eddins et al., 2002) (Figure 2.21). Molecular modeling of the $\alpha 7$ extracellular domain onto the crystal structure of the AChBP showed that E172 lines the “bottom” of the outer vestibule near the interface of the extracellular domain and the transmembrane domains (Figure 2.21). This model suggested that E172 is accessible to cations in the water filled vestibule (Eddins et al., 2002). The mutation E195Q was recently shown to be in the Ca^{2+} binding site and also reduces quercetin mediated enhancement of $\alpha 7$ ACh induced currents (Lee et al., 2010a). These results suggest that quercetin may also be binding in the same binding pocket as Ca^{2+} .

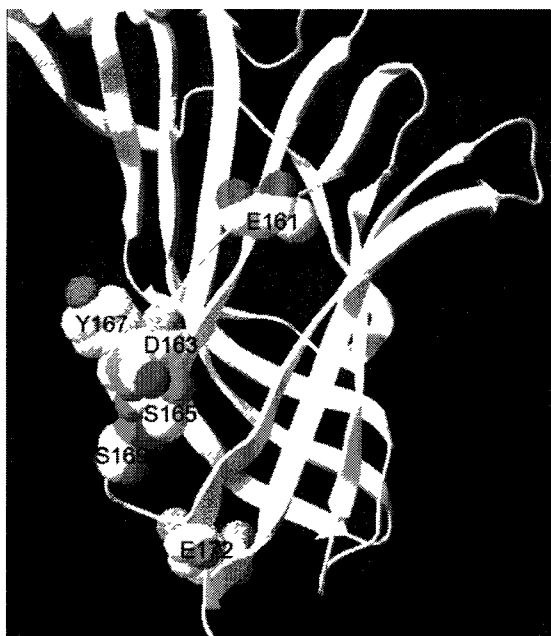


Figure 2.21 The putative Ca^{2+} binding site on $\alpha 7$ nAChR.

This diagram illustrates the location of the Ca^{2+} binding site on $\alpha 7$ nAChR. Residues labeled have been shown to alter Ca^{2+} potentiation. Residues are located on the F- β -strand on the complementary face of the $\alpha 7$ subunit.

2.7.3.3 The NS-1738 and PNU-120596 Binding Sites.

The $\alpha 7$ nAChR positive allosteric modulators (PAMs) 1-(5-chloro-2-hydroxyphenyl)-3-(2-chloro-5-trifluoromethylphenyl)urea (NS-1738) and 1-(5-chloro-2,4-dimethoxyphenyl)-3-(5-methylisoxazol-3-yl)urea (PNU-120596) have recently been shown to selectively potentiate, alter affinity and Hill coefficients of ACh-induced currents (Figure 2.22 for chemical structures). NS-1738 is

thought to be a type I modulator while PNU-120596 alters desensitization kinetics making it a type II modulator (Bertrand and Gopalakrishnan, 2007). Type 1 modulators are molecules that affect the induced peak current (Bertrand and Gopalakrishnan, 2007). A type II modulator is a ligand that alters both the peak current and the time course of the agonist evoked response (Bertrand and Gopalakrishnan, 2007). These two PAMs are structurally similar but have different functional effects on $\alpha 7$ nAChR suggesting that these modulators may act at allosteric binding sites (Bertrand et al., 2008). By using chimeras of $\alpha 7$ and 5-HT₃ receptor domains, the binding regions of these two modulators were narrowed down. Results suggested that the extracellular N-terminal domain of $\alpha 7$ plays a critical role in NS-1738 modulation while PNU-120596 probably interacts with one or more of the transmembrane domains of the receptor (Bertrand et al., 2008).

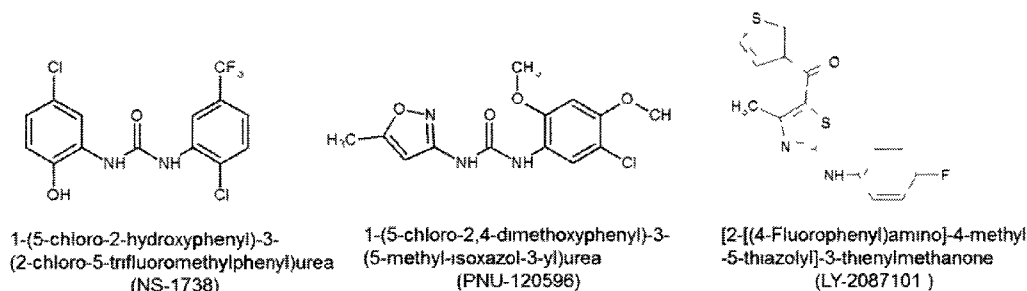


Figure 2.22 Chemical structures of NS-1738, PNU-120596 and LY-2087101.

Further studies investigating the role of the transmembrane domains in allosteric modulation concluded that the TM1-3 are the principal determinates of potentiation by the allosteric modulator PNU-120596. Specifically residues Ser222 (TM1), Ala225 (TM1), Met253 (TM2) and Phe455 and Cys459 (TM4) influenced potentiation by PNU-120596 (Young et al., 2008). Homology models of $\alpha 7$ and the crystal structure of the *Torpedo* nAChR showed that these amino acid residues are located centrally within the transmembrane helices and point towards the intra-subunit cavity located between the four helical domains. In contrast, residues that induce no effect on potentiation are positioned away from the central cavity. Blind docking studies suggest a role for these residues in binding of PNU-120596 and LY-2087101 (a type I modulator) (Young et al., 2008).

2.7.3.4 The Galanthamine Binding Site.

Galantamine, an approved drug for the treatment of Alzheimer's disease, is a dual action drug that inhibits acetylcholinesterase and is a allosteric modulator of $\alpha 3\beta 4$, $\alpha 4\beta 2$ and $\alpha 6\beta 4$ nAChR as demonstrated by whole-cell patch clamp studies using human embryonic kidney-293

cells (Figure 2.23 for chemical structure) (Samochocki et al., 2003). In an attempt to visualize the extracellular regions of heteromeric nAChRs bound to galanthamine and cocaine, the vicinal cysteines in the C-loop on AChBP were mutated to be more similar to the non α subunit interfaces of nAChR and other Cys-loop receptors (Hansen and Taylor, 2007). The 2.9 Å resolution crystal structures of *Aplysia* AChBP exposed galanthamine bound to four of the five subunits. In the binding sites that contained galanthamine the C-loop was against the ligand, but the vicinal cysteines were positioned away from the ligand. Galanthamine was found to be bound in two conformations in equal proportions. Galanthamine's amine nitrogen was positioned between W147 and either Y93 or Y55. The oxygen atom of galanthamine was positioned towards the C-loop in both conformations. In the cocaine bound 1.8 Å structure of *Aplysia* AChBP, cocaine occupied two of the five possible binding sites. The vicinal cysteines in one subunit contacted the benzene ring of cocaine (Hansen and Taylor, 2007).

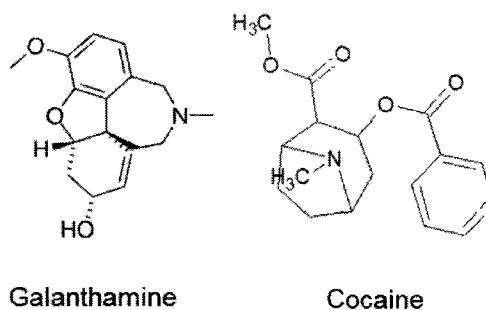


Figure 2.23 Galanthamine and cocaine chemical structures.

Using X-ray structures of cocaine and galanthamine bound to mutated AChBP revealed interactions deep within the non- α subunit interface and maintained little contact with the C-loop tip (Hansen and Taylor, 2007). Mutations were only made in the vicinal cysteines of the C-loop and results should be interpreted with caution. The data can only illustrate the events that occurred when the vicinal cysteines were not present. To further our understanding of the interactions occurring within the non- α subunits, this region in the AChBP could be mutated to residues found in nAChR and other Cys-loop receptors. Contrary to Hansen and Taylor's conclusions (2007), immune epitope mapping studies and photoaffinity labeling suggested that the galanthamine binding site is close to but distinct from the ACh binding site on the α nAChR subunit (Schrattenholz et al., 1993; Maelicke et al., 2000).

2.7.3.5 The 17 β -Estradiol Binding Site.

The steroid 17 β -estradiol selectively potentiates human α 4 β 2 neuronal nAChR while not potentiating rat α 4 β 2 nAChR (Figure 2.24 for chemical structure). The sequence AGMI at the end of the C-terminus of the human α 4 nAChR appears to form the binding site of 17 β -estradiol (Maelicke et al., 2000; Curtis et al., 2002). It appears that the steroid rings and/or the ethynyl group bind to the α 4 C-terminus and the two steroid hydroxyl groups are free to interact with other amino acids elsewhere in the protein (Paradiso et al., 2001).

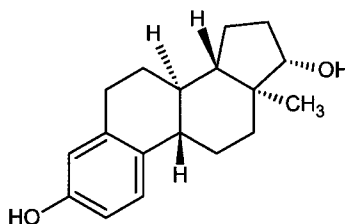


Figure 2.24 The chemical structure of 17 β -estradiol.

2.7.3.6 The Zinc Binding Site.

Zinc modulates heteromeric nAChR and potentiates α 2 β 2, α 2 β 4, α 3 β 4, α 4 β 2 and α 4 β 4, but not α 3 β 2. It was proposed that both the α and β subunits contribute to the zinc binding site (Hsiao et al., 2001). Using site directed mutagenesis, amino acid residues E59 and H162 on the rat α 4 subunit were identified as potential mediators of zinc potentiation (Hsiao et al., 2006). Cysteine mutations at α 4E59 (D- β -strand) and α 4H162 (F- β -strand) caused a reduction of zinc potentiation upon treatment with methanethiosulfonate reagents *N*-biotinoylaminoethyl methanethiosulfonate (MTSEA-biotin) and [2-(trimethylammonium)ethyl] methanethiosulfonate. The mutation α 4H162C compared to E59C was more effective at hindering the MTSEA-biotin reaction in presence of zinc, suggesting that H162 may participate in the binding site for zinc (Hsiao et al., 2006). Less robust effects were seen at the α 4E59C mutant, suggesting that α 4E59 may be near the zinc binding site. It was hypothesized that the zinc binding site occurred at the non-ACh binding site, the β 4- α 4 cleft and near the α 4 residues H162 and E59 (Hsiao et al., 2006).

The zinc binding site was further elucidated by attempting to express two different α 4 β 2 stoichiometries using a high and low ACh sensitive receptor preparation. It was presumed that the high-sensitivity receptor preparation formed receptors with the stoichiometry (α 4) $_2$ (β 2) $_3$. The low-sensitivity receptor preparation was assumed to form receptors with the stoichiometry (α 4) $_3$ (β 2) $_2$. It was noticed that zinc inhibited the “(α 4) $_2$ (β 2) $_2$ ” stoichiometry and depending on the

concentration, potentiated or inhibited “($\alpha 4$)₃($\beta 2$)₂” stoichiometry (Moroni et al., 2008) (Figure 2.25). These results suggest that the zinc potentiation binding site is located at the $\alpha 4(-)/\alpha 4(+)$ cleft. Alanine mutations of $\alpha 4$ H195 on the $\alpha 4(-)$ face and $\alpha 4$ E224 on the $\alpha 4(+)$ face reduced the zinc potentiation effects of zinc and $\alpha 4$ H195A shifted the zinc IC_{50} to the right. Authors reasoned that these residues are located in the zinc potentiation site. $\alpha 4$ H195 ($\alpha 4(-)$ face) interacted with both the inhibitory and potentiation zinc binding sites (Moroni et al., 2008). $\alpha 4$ H195A decreased the zinc IC_{50} in the high-sensitivity preparation. $\beta 2$ D218A (loop C) decreased the zinc IC_{50} receptors expressed using the high-sensitivity preparation. $\beta 2$ D218A receptors expressed in the high-sensitivity preparation had enhanced zinc potentiation compared to wild-type receptors. Authors reasoned that the $\beta 2(+)/\alpha 4(-)$ interface found in both receptor stoichiometries to be the location of the putative zinc inhibitory binding site (Moroni et al., 2008) (Figure 2.25). The conclusions regarding $\beta 2$ D218 are somewhat surprising. Moroni et al., (2008) reasoned that an increase in zinc potentiation indicated that this residue was located in the inhibition binding site. It seems more plausible that some other mechanism or ligand may be causing the increase in zinc potentiation (see Chapter 5 for further explanation).

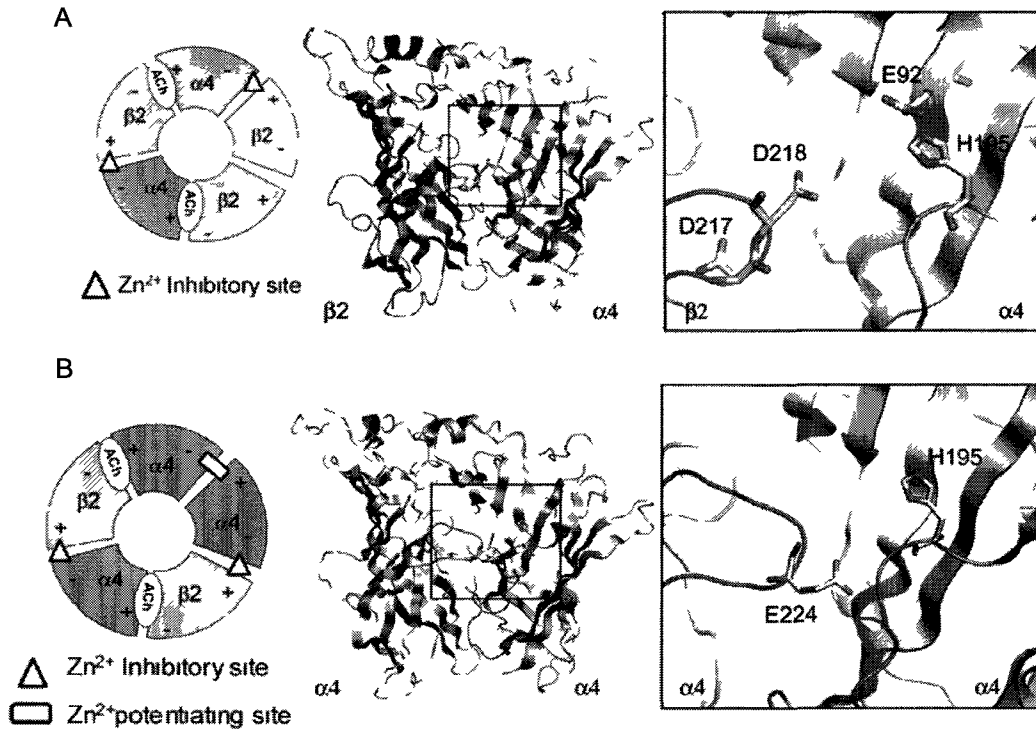


Figure 2.25 The putative zinc potentiation and inhibition sites on $\alpha 4 \beta 2$ nAChR.

A) These figures illustrate the zinc potentiation and inhibition sites. The far left diagram is the presumed stoichiometric arrangement of receptors formed in the high-sensitivity receptor preparation. Middle and right images are the putative potentiation binding site of zinc. **B)** The zinc inhibition site is illustrated below. The far left diagram is the presumed stoichiometric arrangement of receptors formed in the low-sensitivity receptor preparation. Middle and right images are the putative inhibition binding site of zinc. (Images are modified and used with permission from (Moroni et al., 2008).)

2.7.3.7 Channel Blockers.

A significant category of nicotinic drugs, channel blocking ligands may have therapeutic value in applications ranging from local anesthesia to smoking cessation. Channel blockers function by sterically blocking the channel pore thereby preventing ion flux and altering the allosteric transitions of the nAChR (Taly et al., 2009). Channel blockers have been shown, by affinity labeling experiments, to bind to key residues 2, 6, 9, 13 and 20 within in TM2 (Figure 2.26) (Giraudat et al., 1986; Blanton et al., 1998; Corringer et al., 2000). This is the face of TM2 that lines the inside of the channel pore. Various channel blocker binding sites have been shown to be located throughout the transmembrane channel. Binding sites have been mapped within the

gate in the closed conformation of the receptor and at the entrance of the ion selectivity filter, which consists of rings of hydrophilic residues at the cytoplasmic border.

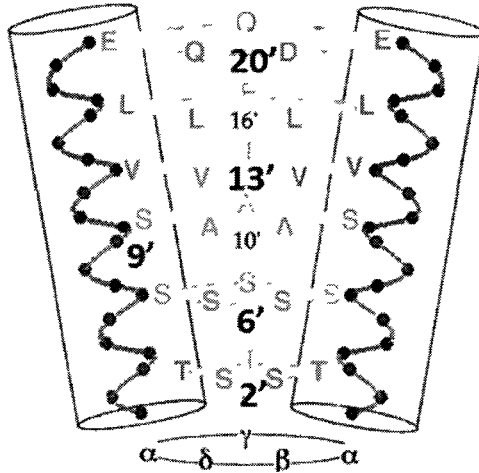


Figure 2.26 Location of channel blocking ligand binding sites in the TM2.

A diagram showing only the TM2 helix of two nAChR subunits. Channel blocker binding sites have been located within the gate in the closed conformation of the receptor and at the entrance of the ion selectivity filter. Residues at positions 2, 6, 9, 13 and 20 in the TM2 have been shown by affinity labeling to affect to bind channel blocking residues. (Image used with permission and significantly modified from (Miller, 2002).)

2.8. Receptor Mechanism.

2.8.1 Allostery.

Allostery is the property of proteins to adopt conformations or shapes induced by the adherence of two or more ligands. The binding events at one location can influence the coupling episodes on a different part of a protein through structural changes in the protein that may or may not alter the rate of binding of the second ligand to the protein. An increased binding rate of the second ligand is considered positive cooperativity. Conversely, negative cooperativity occurs when the rate of the second ligand is decreased. The quantification of cooperativity can be estimated using the Hill coefficient, which corresponds to a hypothetical number of ligands that would have to be bound to the protein in an all-or-none fashion for the protein to exhibit perfect cooperativity.

Allostery classically describes the events surrounding the binding of one ligand to a protein and provoking a large conformational change that alters the affinity of another site for its ligand. Recently Tsai et al., (2008) have shown dramatic backbone deformations are not an

essential characteristic of an allosteric effect (Tsai et al., 2008). It seems possible that allostery may arise from either large conformational changes or fluctuations in protein temporal dynamics. The conformational change of a protein is likely to be unique to the number and type of ligand(s) binding to the protein and the proteins structural composition.

The process of ion channel activation is a highly complicated mechanism that is only beginning to be understood. It is currently hypothesized that ligand binding a LGIC produces a conformational change in the protein and different types of ligands (agonists, partial agonists, antagonists, allosteric modulators, etc.) can induce different protein conformations. Ligand binding leads to an anticlockwise conformational wave (quaternary twist) that propagates through the protein causing the channel gate to open transiently and then close. The stabilization of each new conformation likely alters the structure of the orthosteric binding site and may modify the structure of allosteric subunit clefts as well.

LGICs can exist in at least three distinct conformations with different stabilization energies and are referred to as closed, open or desensitized. The closed state is the resting state of the receptor and is non-conducting whereas the open state actively conducts ions. The desensitized state is non-conducting and is distinct from the resting state. When exposed to low concentrations of ligand, it is most likely the receptor will enter an open (active) conformation or, although less likely, a desensitized state than remain in the closed state. Receptors have a high probability of existing in the desensitized state on continuous exposure to ligand. In the absence of ligand, the closed state predominates.

The conformational change of a protein may be driven by entropic effects which can be better understood through kinetic models. The process of a ligand binding to a protein may result in a decrease in the entropy of the system due to the translational and rotational degrees of freedom of the protein and the ligand no longer being independent. To better understand the biophysical characteristic of nicotinic receptors, kinetic models of receptor gating have and are currently being developed. Auerbach and Akk (1998) developed a kinetic model of the mouse muscle nAChR gating through single channel studies (Auerbach and Akk, 1998) (Figure 2.27). The receptor in the closed conformation (R) can bind two ACh molecules in two steps. The affinity for each site is relatively low but each site has a high forward rate constant $4 \times 10^{-8} \text{ M}^{-1} \text{ s}^{-1}$. A 125 μM concentration of ACh half saturates the two equivalent ACh binding sites. Binding of ACh produces a massive increase in the probability of the channel opening (O^*). In a diliganded mouse AChR, the gate will open approximately 50 times faster than the receptor closes. Comparatively, spontaneous channel opening events without a ligand can occur but the gate opens only about twice as fast as it closes (Auerbach and Akk, 1998). The calculated equilibrium

constant for spontaneous openings is approximately 3.0×10^{-6} . The mean open time of a mouse muscle nAChR bound with two ACh molecules is 670 μ S. The channel then closes with the two ACh molecules bound to the A_2D state. At this point, the receptor can either lose one ACh molecule or it can reopen with a probability of 0.5. If ACh is constantly present, the receptor can also move from the open (A_2O^*) to a desensitized (D) state. As the ACh comes off the channel, the receptor goes through a one ACh bound desensitized state and then to the closed state (Auerbach and Akk, 1998) (Figure 2.27).

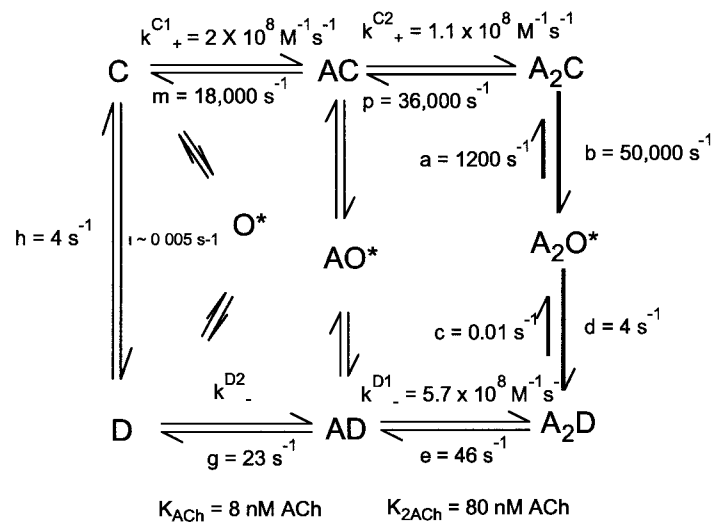


Figure 2.27 Auerbach and Akk (1998) kinetic model of mouse muscle nAChR.

The small alphabetical letters are the forward and reverse rate constants for the different receptor states. The k_{-} values are the agonist dissociation rate constants and the k_{+} values are the agonist association rate constants. $K_{2\text{ACh}}$ and K_{ACh} are the equilibrium dissociation constants (K_d) for double and single liganded states. Numerical values were taken from (Auerbach and Akk, 1998).

Equilibrium constants determined experimentally can be used to calculate the free energy differences between the receptor conformations using the relationship $\Delta G_0 = -RT \ln(K)$ (Auerbach and Akk, 1998). The equilibrium constants shown in Figure 2.27 were used to calculate the free energy diagram shown in Figure 2.28 (Auerbach and Akk, 1998). The A₂D state is -27.3 kT more stable than the resting state (C). During the nAChR recovery the receptor passes through the desensitized (D) state. The non-liganded D state is the only state that is less stable than the resting state of the receptor (Auerbach and Akk, 1998).

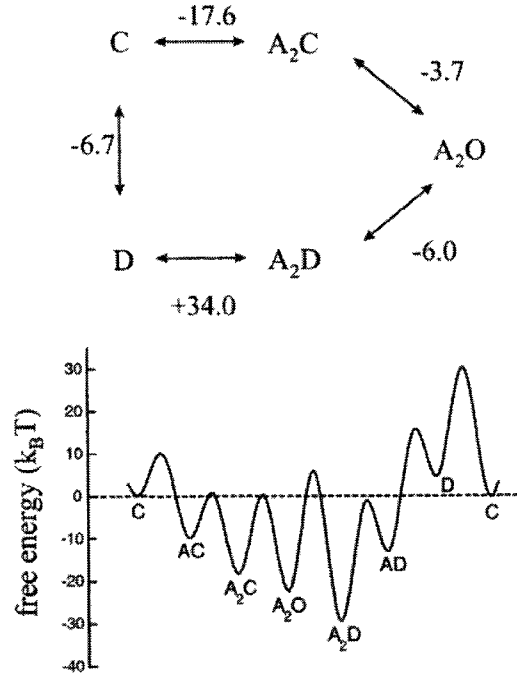


Figure 2.28 Free energy diagram of mouse muscle nAChR for activation, desensitization and recovery.

Top) The cyclic reaction of the receptor transition between the closed (C), open (O) and desensitized (D) states. For simplicity, the two agonist binding steps were condensed. The ΔG sign pertains to the clockwise direction. *Bottom)* A graphical representation of the calculated free energies of the different receptor states. The unliganded closed receptor is the ground state. Activation of receptors was accomplished by application of 1 M ACh. The A₂D state is the most stable conformation. The D state is the only state that is less stable than the C state. (Image reprinted from (Auerbach and Akk, 1998) and used with permission).

2.8.2 Conformational Change Models.

The signal transduction mechanism of the nAChR has been proposed to involve a global transition of the molecule, referred to as allosteric transition (Koshland, 1963; Changeux, 1964). Receptors are thought to transition between conformations by either the concerted or sequential models.

The concerted or the Monod-Wyman-Changeux (MWC) model was developed during an investigation of hemoglobin. The liganded and non-liganded forms of hemoglobin differ by 15° rotation of one pair of α and β subunits relative to the other two in the $\alpha_2\beta_2$ tetramer (Baldwin, 1980). The concerted model suggest that all subunits change conformation simultaneously resulting in only two conformational states, tense and relaxed (Monod et al., 1965). In this model the two conformations exist even in absence of ligand with the equilibrium constant L between the

two states. The ligand's apparent affinity for the protein is controlled by its ability to shift between the relaxed and tense states.

The MWC model accounts for signal transduction mediated by the nAChR between active, open-ligand bound conformations, resting and closed conformations and cooperative ligand binding (Taly et al., 2005). This model predicts that agonists, allosteric modulators and antagonists induced distinct conformations and accounts for spontaneous opening of the channel in absence of ligand.

The sequential or Koshland-Nemethy-Filmer (KNF) model proposes that each subunit can be in a different conformation depending on the number of agonists bound. The KNF model assumes that a protein is sufficiently flexible to allow the binding of one ligand to alter the protein conformation in a way that affects the affinity of the second site for the ligand. This model allows for intermediate states between closed and open to exist.

The two models differ in terms of protein conformations and the affinity of the ligands for each binding site. Both models suggest that binding of a ligand changes the protein conformation. In the sequential model, conformation change due to ligand binding leads to an effect on other binding sites and the ligand affinity for that site. In the concerted model the conformational change only alters the equilibrium between the protein's state (tense versus relaxed for hemoglobin or open versus closed for receptors). The models also differ in that the concerted model suggests that the two conformations are present (relaxed and tense) even in absence of ligand. The sequential model suggests that conformational change only occurs upon ligand binding. In general, the concerted model is the more restrictive of the two models particularly because it does not predict negative cooperativity. In the sequential model a ligand can only pull the conformational equilibrium towards the high affinity conformation.

Whether nAChRs function more like the concerted or sequential model is currently being debated. Crystallography studies have shown that the different subunits can exist in different conformations from each another with and without ligand being present in muscle nAChR (Unwin, 1995; Unwin, 2005; Hansen and Taylor, 2007) arguing in favor for the sequential model. Several AChBP crystallography studies have shown that different conformations are induced depending on the type of ligand bound to the protein (Unwin, 1995). It has also been observed that a change in one subunit conformation can affect other subunits causing a conformational wave within the protein (Auerbach, 2005), supporting the concerted model. nAChR have been shown to exist in open and closed states in absence of ligand (Jackson, 1984; Jackson, 1986), suggesting that the concerted model may explain nAChR function. However, nAChRs also experience different conformations besides open and closed such as the desensitized and the putative "flip" state

(Lape et al., 2009), arguing that nAChRs function more like the sequential model. The flip conformation is an intermediate conformation between the resting and open states (Lape et al., 2008) where the affinity and efficacy of a ligand for a receptor is determined by its ability to stabilize the conformation. This mechanism is different from the previous models which suggested that ligand affinity and efficacy depends on the ligand's ability to stabilize the open conformation.

It is likely that due to the complex nature of nAChR function that neither the sequential or concerted model fully explains nAChR conformational changes. A more expansive model that allows for conformational changes, variation in subunit conformations, different receptor states, etc. would be more appropriate.

2.9. Neurophysiological Role of Nicotinic Receptors.

In the CNS, acetylcholine activated nAChRs regulate processes such as transmitter release, cell excitability and neuronal integration (Gotti et al., 2006b). These processes are critical for network operations and influence physiological functions such as arousal, sleep, fatigue, anxiety, pain processing, food intake and several cognitive functions (Hogg et al., 2003; Gotti and Clementi, 2004; Hogg and Bertrand, 2004).

It has been proposed that the majority of the cortical and hippocampal cholinergic release sites are non-synaptic and contribute to diffuse volume transmission (Umbrico et al., 1994; Descarries et al., 1997) as has been observed for other modulatory neurotransmitters such as monoamines (Vizi, 2000). Other studies have suggested that nAChRs are principally located at presynaptic sites where they modulate neurotransmitter release or on cell bodies and dendrites where they mediate postsynaptic effects (Hogg et al., 2003; Dajas-Bailador and Wonnacott, 2004; Gotti and Clementi, 2004).

Spillover of ACh from the synapse or from non-synaptic release sites into the extracellular space is likely to be an important contributor to cholinergic volume transmission (Dani and Bertrand, 2007). The spread of ACh from the release site is determined by diffusion and the hydrolysis of ACh by the widely distributed CNS enzyme acetylcholinesterase (AChE) (Kawaja et al., 1990). ACh is synthesized from choline and acetyl-CoA by the enzyme acetyltransferase and is broken down by AChE into choline and acetate. The density and location of AChE does not always match the location of ACh release sites (Kawaja et al., 1990). Cholinergic volume transmission allows ACh to diffuse and act at lower concentrations at some distance from the release site. The amplitude, shape and time course of the ACh single depends on the local distribution and density of AChE relative to the ACh release sites (Dani and Bertrand, 2007).

The hydrolysis of ACh creates choline, which is a nAChR partial agonist (Castro and Albuquerque, 1995; Papke et al., 1996). It is estimated that choline has an $EC_{50} \sim 1.6$ mM and an $IC_{50} \sim 370$ μ M on $\alpha 7$ nAChRs (Alkondon and Albuquerque, 2006). The extracellular choline concentrations have been estimated to be around 3-5 μ M and reaches concentrations of 20 μ M or more under pathological conditions (Alkondon and Albuquerque, 2006). At a cholinergic synapse, vesicular release produces a millimolar ACh concentration for only a few milliseconds before diffusion and AChE removal of the neurotransmitter (Dani and Bertrand, 2007). An area that experiences a high frequency of ACh release and plentiful AChE would likely produce relatively high choline concentrations. Therefore ACh provides a diffuse, volume signal that continues as a choline signal (Dani and Bertrand, 2007).

Different nAChR subtypes are located throughout the CNS and respond differently to ACh and choline. $\alpha 7$ nAChRs have a lower ACh affinity (~ 100 μ M) compared to $\alpha 4\beta 2$ receptors which have two ACh affinities (ACh affinity ~ 1.6 μ M and 62 μ M) (Buisson and Bertrand, 2001). The two different ACh affinities in $\alpha 4\beta 2$ nAChR may be caused by the putative high- and low-ACh sensitivity $\alpha 4\beta 2$ stoichiometries. After neurotransmitter release at the synapse, high-sensitivity $\alpha 4\beta 2$ nAChR will open and desensitize with slower response kinetics than the rapidly desensitizing $\alpha 7$ nAChRs. Successive synaptic activity and volume transmission of ACh may provide a prolonged exposure of low agonist concentrations. This process produces a slow form of desensitization (Dani and Bertrand, 2007). Because $\alpha 4\beta 2$ have a high affinity for ACh, these receptors have a slower desensitization rate for agonist below 0.1 μ M. In comparison, $\alpha 7$ receptors are not effectively desensitized by agonist at concentrations below 1 μ M (Dani et al., 2000; Quick and Lester, 2002; Wooltorton et al., 2003). nAChRs which are exposed to a slow rising by sustained agonist concentrations may contribute to the modulation of the neuron activity when the cell is close to its resting potential (Dani and Bertrand, 2007).

Activation of presynaptic nAChRs can cause the release of many different types of neurotransmitters (McGehee et al., 1995; McGehee and Role, 1995; Gray et al., 1996; Role and Berg, 1996; Albuquerque et al., 1997; Alkondon et al., 1997; Lena and Changeux, 1997; Wonnacott, 1997; Guo et al., 1998; Radcliffe and Dani, 1998; Jones et al., 1999; Luetje, 2004; Sher et al., 2004). Nicotinic agonists applied exogenously enhance, while nicotinic antagonist generally reduce the release of ACh, dopamine (DA), norepinephrine, serotonin, glutamate and GABA (McGehee et al., 1995; McGehee and Role, 1995; Gray et al., 1996; Role and Berg, 1996; Albuquerque et al., 1997; Alkondon et al., 1997; Lena and Changeux, 1997; Wonnacott, 1997; Guo et al., 1998; Radcliffe and Dani, 1998; Jones et al., 1999; Luetje, 2004; Sher et al., 2004). The activity of presynaptic nAChRs directly and indirectly begins the intracellular calcium signal that enhances neurotransmitter release (McGehee et al., 1995; Gray et al., 1996; Role and Berg

1996; Wonnacott 1997). nAChRs mediate small direct calcium influx (Vernino et al., 1992; Seguela et al., 1993; Vernino et al., 1994; Castro and Albuquerque, 1995) that can cause the release of calcium from intracellular stores (Sharma and Vijayaraghavan, 2003). nAChR activity can also produce depolarization that can cause activation of voltage-gated calcium channels in the presynaptic terminal (Tredway et al., 1999). Presynaptic nAChR activity overall elevates intracellular calcium and causes increased neurotransmitter release.

Glutamate release is enhanced by nicotinic stimulation lasting from seconds to a few minutes (Radcliffe and Dani, 1998) and contributes to the ability of a neuronal synapse to change its connection strength in response to the usage of the synapse in synaptic pathways also known as synaptic plasticity (Wonnacott, 1997; Aramakis et al., 2000; Mansvelder and McGehee, 2000; Ji et al., 2001; Ge and Dani, 2005). The glutamate enhancement can last for several minutes or more and utilizes intra-terminal calcium elevation as a second messenger to indirectly modify glutamatergic synaptic transmission (Dani and Bertrand, 2007). The localized calcium signals, mediated by nAChRs, initiates enzymatic activity (i.e. protein kinases and phosphatases) that modify the glutamatergic synapse (Fisher and Dani, 2000; Hu et al., 2002). Presynaptic nAChR activity arriving just before electrical stimulation of glutamatergic afferents boosts the release of glutamate and enhance the induction of long-term synaptic potentiation (Dani and Bertrand, 2007).

nAChRs are found on preterminal, axonal, dendritic and somatic locations (Lena et al., 1993; Zarei et al., 1999). Preterminal nAChRs positioned before the presynaptic terminal bouton indirectly affect neurotransmitter release by activating voltage-gated ion channels and by possibly initiating action potentials (Lena et al., 1993; Alkondon et al., 1997; Albuquerque et al., 2000). Axonal, dendritic and somal nAChRs may modulate neurotransmitter release and affect local excitability in other ways. Activation of non-synaptic nAChRs alters the membrane impedance and changes the space constant of the cellular membrane (Dani and Bertrand, 2007) influencing the spread and efficiency of synaptic inputs to activate action potential outputs in the target neuron (Dani and Bertrand, 2007). Neuronal excitation can also be altered by directly exciting or slowing an action potential at junction, axonal or dendritic nAChRs (Dani and Bertrand, 2007). The widespread distribution in non-synaptic locations may also enable nAChRs to influence moment-to-moment membrane resting potentials thereby influencing the ease of reaching the threshold to generate an action potential (Dani and Bertrand, 2007).

nAChRs also appear to participate in other non-cholinergic neuronal systems. There has been mounting evidence that crosstalk occurs between GABA, dopamine and nAChRs. For example, by using hippocampal slices and electrophysiological recordings noradrenaline release

has been shown to be indirectly modulated by $\alpha 7$ nAChR located in glutamate afferents and γ -amino butyric acid (GABA)-containing interneurons. These results provide strong evidence that there is cross-talk amongst neurotransmitters in modulating noradrenalin release (Barik and Wonnacott, 2006). Cross-talk between neurotransmitter systems is likely to affect the properties of therapeutic ligands.

To summarize, synaptic and volume release of ACh activates and desensitizes nAChRs at synaptic and non-synaptic locations. nAChRs located at non-synaptic locations influences the excitability of a neuron (Dani and Bertrand, 2007). Continuous cholinergic activity causes depolarization of neurons and pushes the membrane potential to move towards the threshold for firing an action potential. nAChR activity contributes to calcium signals that regulates intracellular enzyme systems which shapes the response of the cell. Signaling by nAChRs causes subtype-dependent desensitization which influences the overall signal. The breakdown of ACh by AChE to produce choline assists in the shaping of the time and spatial dependence of nAChR signaling.

2.10. Nicotinic Receptor Pharmacology.

Each nAChR subtype has different ligand selectivity, affinity and efficacy. Selectivity delineates the specificity of a compound for different types of receptors. Affinity describes how tightly the ligand interacts with the receptor while the potency is measured by the EC_{50} or the effective drug concentration which elicits half of the maximum induced response. Efficacy is the ligand's ability to produce the maximum effect. For example, ACh induced responses produce 100% efficacy on nAChR. Partial agonists induce maximum responses with < 100% efficacy while PAMs may produce responses with > 100% efficacy.

There are different types of ligands such as full agonist, partial agonist, antagonist and allosteric modulators. Full agonists are ligands that bind to the orthosteric site and activate the receptor, displaying full efficacy of the receptor. Partial agonists bind at the orthosteric site, but are only able to cause partial efficacy of the receptor. Antagonists are ligands that do not induce a biological response, but reduce agonist mediated responses. Allosteric modulators are ligands which bind to non-orthosteric sites, resulting in conformational changes that may alter the protein's function. Positive and negative allosteric modulators (PAMs and NAMs) cause enhancement and inhibitory effects, respectively (Arias et al., 2006; Bertrand and Gopalakrishnan, 2007; Faghieh et al., 2008). Modulators can alter a ligand's affinity and/or efficacy. Enhancement of the agonist efficacy is known as potentiation.

Allosteric modulators typically have low intrinsic activity. A ligand which binds at an allosteric cleft and activates the channel without assistance would be classified as an allosteric non-competitive agonist or allosteric partial agonist. Allosteric modulators must be co-applied with

an agonist in order for the modulators to have an effect. PAMs selectively potentiate physiological activity, shifting the conformation equilibrium towards the receptor open state. There are two types of PAMs, type 1 and type 2. Type 1 modulators are molecules that affect the induced peak current (Bertrand and Gopalakrishnan, 2007) while a type 2 modulator is a ligand that alters both the peak current and the time course of the agonist evoked response (Bertrand and Gopalakrishnan, 2007). NAMs inhibit the agonist activity by shifting the conformation equilibrium towards the receptor closed state. The low intrinsic activity of allosteric modulators allows for the spatial and temporal synaptic patterning to remain unaltered. The data within this thesis is focused on $\alpha 4\beta 2$ nAChR. The following discussion is a brief description of $\alpha 4\beta 2$ nAChR pharmacology.

2.10.1 Selective $\alpha 4\beta 2$ Full and Partial Agonists.

2.10.1.1 Acetylcholine.

Acetylcholine (ACh) is a neurotransmitter in the PNS and CNS and acts as a full agonist on all nAChR subtypes (Figure 2.29). The ACh affinity on $\alpha 4\beta 2$ nAChR is approximately 21 μM ($\text{pEC}_{50} = 4.7 \pm 0.1$) (Weltzin and Schulte, 2010) while its efficacy is 100%.

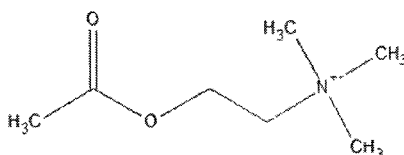


Figure 2.29 Chemical structure of acetylcholine.

2.10.1.2 Nicotine.

Nicotine, an alkaloid found in the botanical nightshade family (*Solanaceae*), is an nAChR targeted toxin that serves to defend the plant from predation (Albuquerque et al., 2009) (Figure 2.30). Until recently, nicotine was used as an insecticide. Nicotinic analogues such as imidacloprid have been found to be even more effective than nicotine as an insecticide. In addition to its toxic properties, nicotine is a highly addictive substance most commonly associated with tobacco products. Over the years, the concentration of nicotine has increased $\sim 1.6\%$ mg/cigarette/year from 1998-2005 to a current concentration of approximately 1 mg of nicotine/cigarette (Connolly et al., 2007). The American Heart Association has determined

nicotine addiction to be one of the most difficult addictions to break (American Heart Association, 2011).

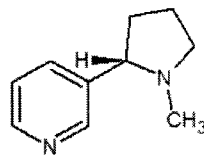


Figure 2.30 Chemical structure of nicotine.

A partial agonist on $\alpha 4\beta 2$ nAChRs, nicotine's affinity on $\alpha 4\beta 2$ nAChR is approximately 2.1 μM ($\text{pEC}_{50} = 5.7 \pm 0.3$) and its efficacy is approximately ~38% compared to ACh's efficacy (100%) (Weltzin and Schulte, 2010).

2.10.1.3 *Epibatidine.*

Epibatidine is an alkaloid found on the skin of the Ecuadorian tree frog *Epipedobates tricolor* (Daly et al., 2000; Dukat and Glennon, 2003) (Figure 2.31). It is a potent analgesic that has high affinity (~60 pM) to $\alpha 4\beta 2$ nAChR, but will also bind to other heteromeric nAChR subtypes with lower affinity (0.025 - 0.46 nM) (Xiao et al., 2004). Derivatives of Epibatidine are being explored for their therapeutic potential to treat diseases such as Alzheimer's disease (Dwoskin and Crooks, 2001).

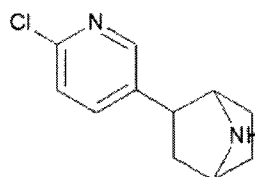


Figure 2.31 Chemical structure of epibatidine.

2.10.1.4 *Cytisine.*

Cytisine is a pyridine-like alkaloid that has similar pharmacological properties to nicotine (Figure 2.32). Plants belonging to the *leguminoae* family synthesize cytisine as a protective mechanism against predation (Marion and Cockburn, 1948). Cytisine is a $\alpha 4\beta 2$ nAChR partial agonist that has low efficacy (Coe et al., 2005). In eastern and central Europe, this compound is used as a smoking cessation treatment (Tutka and Zatonski, 2006).

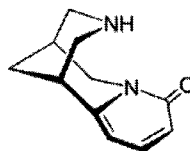


Figure 2.32 Chemical structure of cytisine.

2.10.1.5 *Varenicline.*

A derivative of cytisine, varenicline is an orally active compound used for smoking cessation that has also been shown to reduce alcohol consumption in humans (McKee et al., 2009) (Figure 2.33). Varenicline is a $\alpha 4\beta 2$ partial agonist (K_i value 0.06) (Coe et al., 2005; Rollema et al., 2007a).

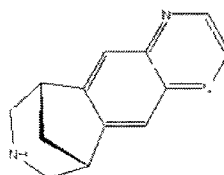


Figure 2.33 Chemical structures of varenicline.

2.10.2 Selective $\alpha 4\beta 2$ Antagonists.

2.10.2.1 *Mecamylamine.*

Mecamylamine is a non-competitive, non-specific nAChR antagonist displaying antidepressant-like effects in mice (Rabenstein et al., 2006) (Figure 2.34). Knockout mice lacking the $\beta 2$ or $\alpha 7$ subunits, this antidepressant effect was not observed (Ostroumov et al., 2008). Mecamylamine has also been shown to block physiological, behavioural and reinforcing properties of nicotine (Martin et al., 1989).

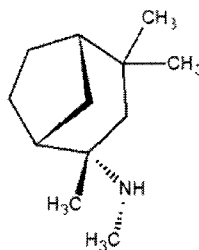


Figure 2.34 Chemical structure of mecamylamine.

2.10.2.2 Methylcaconitine.

An alkaloid derived from the larkspur flower, methylcaconitine or MLA is a potent and specific competitive antagonist that inhibits $\alpha 7$, $\alpha 6$ and $\alpha 3$ containing nAChRs (Alkondon et al., 1992; Pfister et al., 1999; Mogg et al., 2002) (Figure 2.35). MLA binds at the agonist binding site blocking access to the agonist binding site and inhibiting receptor activation. MLA is a selective and potent antagonist for $\alpha 7$ nAChR ($K_i = 1.4$ nM) (Ward et al., 1990).

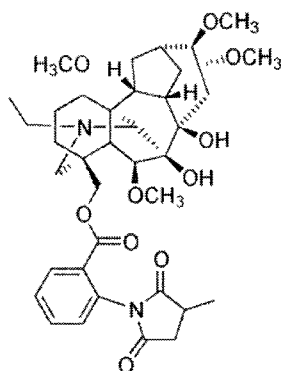


Figure 2.35 Chemical structure for methylcaconitine.

2.10.2.3 Conotoxins.

Derived from cone snails (genus *Conus*), conotoxins are a family of peptides and proteins used by the organism to paralyze other animals. These compounds work by disrupting multiple components of neurotransmission including voltage-gated Na^+ and K^+ channels and nAChRs (Dutertre and Lewis, 2006). α -Conotoxins are selective antagonists for different nAChR subtypes (Azam and McIntosh, 2009). The α -conotoxins share a common structural fold composed of a short helix stabilized by a disulfide bond. These ligands bind specifically to nAChR subtypes making them potentially useful therapeutic compounds.

2.10.3 Selective $\alpha 4\beta 2$ Modulators.

Allosteric modulators are ligands that bind at a different binding site than the endogenous agonist. Positive and negative allosteric modulators can exert activator or inhibitory effects respectively. Allosteric modulators have little or no stimulatory effects themselves, but enhance the activity of orthosteric acting agonists. The key advantage to using allosteric modulators is that alteration in receptor function only occurs on agonist binding. This allows for the spatial and temporal relationships in neurotransmission to remain unaltered, possibly presenting a new

avenue for therapeutic treatment of CNS disorders. Positive allosteric modulators (PAMs) have therapeutic potential in the possible restoration or improvement of nicotinic transmission compensating for altered expression of $\alpha 4\beta 2$ nAChR. PAMs can increase $\alpha 4\beta 2$ receptor responses and therefore may offset decreased receptor expression. A brief review of important nAChR PAMs follows.

2.10.3.1 Galanthamine.

Galanthamine is a drug that is used clinically to treat Alzheimer's disease symptoms (Scott and Goa, 2000) (Figure 2.36). It is an AChE inhibitor with a IC_{50} value $\sim 2.8 - 3.2 \mu M$ for the frontal cortex and hippocampus (Thomsen et al., 1991). By inhibiting AChE, galanthamine prolongs the time period in which ACh can interact on cholinergic systems. Galanthamine is not a selective PAM that potentiates $\alpha 3\beta 4$, $\alpha 6\beta 4$ and $\alpha 7$ nicotinic receptors. Galanthamine alters the apparent ACh affinity without changing the ACh apparent efficacy on $\alpha 4\beta 2$ nAChR (Samochocki et al., 2003). In the presence of $0.5 \mu M$ galanthamine, the ACh EC_{50} value decreased from 20 ± 1.7 to $10 \pm 1.8 \mu M$. The shift in the dose-response curve indicated that galanthamine may either act by increasing the binding affinity of ACh to $\alpha 4\beta 2$ nAChRs and/or facilitate the conversion of the ACh-bound receptor to the open conformation (Samochocki et al., 2003).

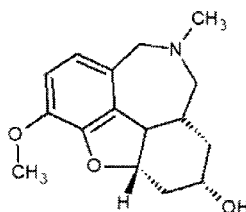


Figure 2.36 Chemical structure of galanthamine.

2.10.3.2 Physostigmine.

Physostigmine is not a selective PAM that potentiates $\alpha 7$ nAChR and other heteromeric subtypes (Figure 2.37). Physostigmine binds to a low affinity ACh binding site on $\alpha 4\beta 2$ receptors in presence of low concentrations of ACh (Smulders et al., 2005). Binding experiments have shown the potentiating physostigmine acts as a competitive ligand on $\alpha 4\beta 2$ nAChR, suggesting that ACh and physostigmine share a common binding site (Smulders et al., 2005).

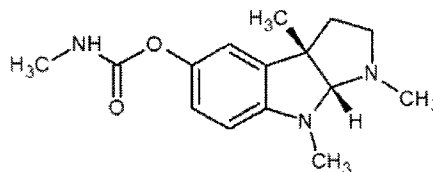


Figure 2.37 Chemical structure of physostigmine.

2.10.3.3 *17-β-Estradiol.*

17-β-Estradiol potentiates human $\alpha 4\beta 2$ nAChR, but inhibits rat $\alpha 4\beta 2$ receptors (Paradiso et al., 2000) (Figure 2.38). The difference in action between human and rat may be the result of having two 17-β-Estradiol binding sites on human $\alpha 4\beta 2$ nAChR and one on rat $\alpha 4\beta 2$ receptors. On human $\alpha 4\beta 2$ receptor, the 17-β-Estradiol potentiation binding site is located on the $\alpha 4$ subunit C-terminal end at the amino acid sequence WLAGMI. Single channel studies showed that 17-β-Estradiol works by increasing the opening probability of $\alpha 4\beta 2$ nAChR (Curtis et al., 2002). The binding site for 17-β-Estradiol's potentiation is not the same as its inhibition site. Mutation of the key W to an I or S removed the potentiation affect, but had no effect on progesterone inhibition (Paradiso et al., 2001). The inhibition site for 17-β-Estradiol may be located at the steroid binding site located within the transmembrane domain (discussed in section 2.7.2.2).

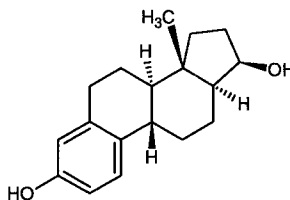


Figure 2.38 Chemical structure for 17-β-Estradiol.

2.10.3.4 *Zinc.*

Zinc (Zn^{2+}) modulates a number of LGIC receptors including $GABA_A R$, glycine and nAChRs (Krishek et al., 1998; Harvey et al., 1999). Zn^{2+} has been shown to inhibit $\alpha 7$ and $\alpha 3\beta 2$ nAChR subtypes and produces biphasic dose response curves on $\alpha 2\beta 2$, $\alpha 2\beta 4$, $\alpha 3\beta 4$, $\alpha 4\beta 2$ and $\alpha 4\beta 4$ (Hsiao et al., 2001). Zn^{2+} has also been shown to potentiate the $\alpha 4\beta 4$ receptors (Hsiao et al., 2008). Low micro molar concentrations of Zn^{2+} potentiated ACh induced currents on $\alpha 2\beta 2$, $\alpha 2\beta 4$, $\alpha 3\beta 4$, $\alpha 4\beta 2$ and $\alpha 4\beta 4$ receptors. At milli-molar Zn^{2+} concentrations, Zn^{2+} inhibited ACh induced responses on $\alpha 2\beta 2$, $\alpha 2\beta 4$, $\alpha 3\beta 4$, $\alpha 4\beta 2$ and $\alpha 4\beta 4$ receptors. Zn^{2+} potentiation is

apparently selective for the putative low ACh sensitivity $\alpha 4\beta 2$ stoichiometry (Moroni et al., 2008), while Zn^{2+} inhibition is non-selective, inhibiting both high and low-sensitivity stoichiometries. ACh responses on the low-sensitivity $\alpha 4\beta 2$ receptors were potentiated 260% by Zn^{2+} . The inhibition of Zn^{2+} on high-sensitivity $\alpha 4\beta 2$ receptors was voltage dependent while it was independent on low-sensitivity receptors. Site-directed mutagenesis studies suggested that the $\beta 2+/\alpha 4-$ interface contains the Zn^{2+} inhibition site. The putative potentiation site was presumed to be located at the $\alpha+/\alpha-$ binding cleft (Moroni et al., 2008).

2.10.3.5 Desformylflustrabromine.

Desformylflustrabromine (dFBr), a new compound extracted from North Sea bryozoan *Flustra foliacea*, has been shown to inhibit the growth of bacteria such as *Paenibacillus pabuli*; *Roseobacter* sp., *Sulfitobacter* sp., OI-14-4 (*Psychroserpens*-like bacterium) and *Halomonas marina* (Peters et al., 2003). In the *Flustra foliacea*, dFBr is a tryptophan metabolite (Lysek et al., 2002) (Figure 2.39). Other tryptophan derived metabolites of this organism were shown to have muscle relaxant properties (Sjoblom et al., 1983). Radioligand binding of dFBr on $\alpha 7$ and $\alpha 4\beta 2$ indicates an affinity of $> 50 \mu M$ on $\alpha 7$ nAChR and an affinity of 3.4 ± 0.5 on $\alpha 4\beta 2$ (Peters et al., 2004). Functional testing of dFBr on $\alpha 4\beta 4$, $\alpha 3\beta 2$, $\alpha 3\beta 4$, $\alpha 4\beta 2$ and $\alpha 7$ nAChR on *Xenopus* oocytes showed that with ACh, dFBr selectively potentiates $\alpha 4\beta 2$ nAChR (Sala et al., 2005). While dFBr did not potentiate the other tested subtypes, the compound did inhibit $\alpha 7$ nAChR. The induced response of dFBr on $\alpha 4\beta 2$ receptors was sigmoidal in nature. Low nM (up to $30 \mu M$) dFBr caused potentiation of ACh induced responses that were reversible and concentration dependent. Chapters 3 and 4 discuss our investigation and findings regarding the mechanisms of dFBr potentiation and inhibition. The selective nature of dFBr makes it an ideal molecule to probe novel binding sites on nAChRs and develop new potential therapeutic ligands. We have begun to characterize the dFBr binding site (see chapter 4) and have also begun to characterize analogues of dFBr. Results from these studies will be useful in developing $\alpha 4\beta 2$ nAChR subtype selective ligands that may be useful in treating pathologies.

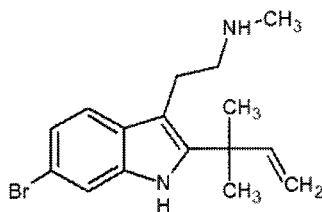


Figure 2.39 Chemical structure of desformylflustrabromine.

2.11. Assembly and Trafficking of Nicotinic Receptors.

nAChR subunits fold and assemble into pentameric receptors in the endoplasmic reticulum (ER) (Figure 2.40). A requirement for the proper folding and assembly of nAChR appears to be required before the receptors leave the ER (Smith et al., 1987; Gu et al., 1991; Kreienkamp et al., 1995; Keller et al., 2001). From there, the assembled proteins are transported to the Golgi apparatus and then to the plasma membrane (Figure 2.40). The maturation process has been estimated to take 2h (Merlie and Lindstrom, 1983) but the mechanism of nAChR maturation is poorly understood. Key proteins known to be involved in the process of nAChR maturation (Figure 2.40) are briefly summarized below.

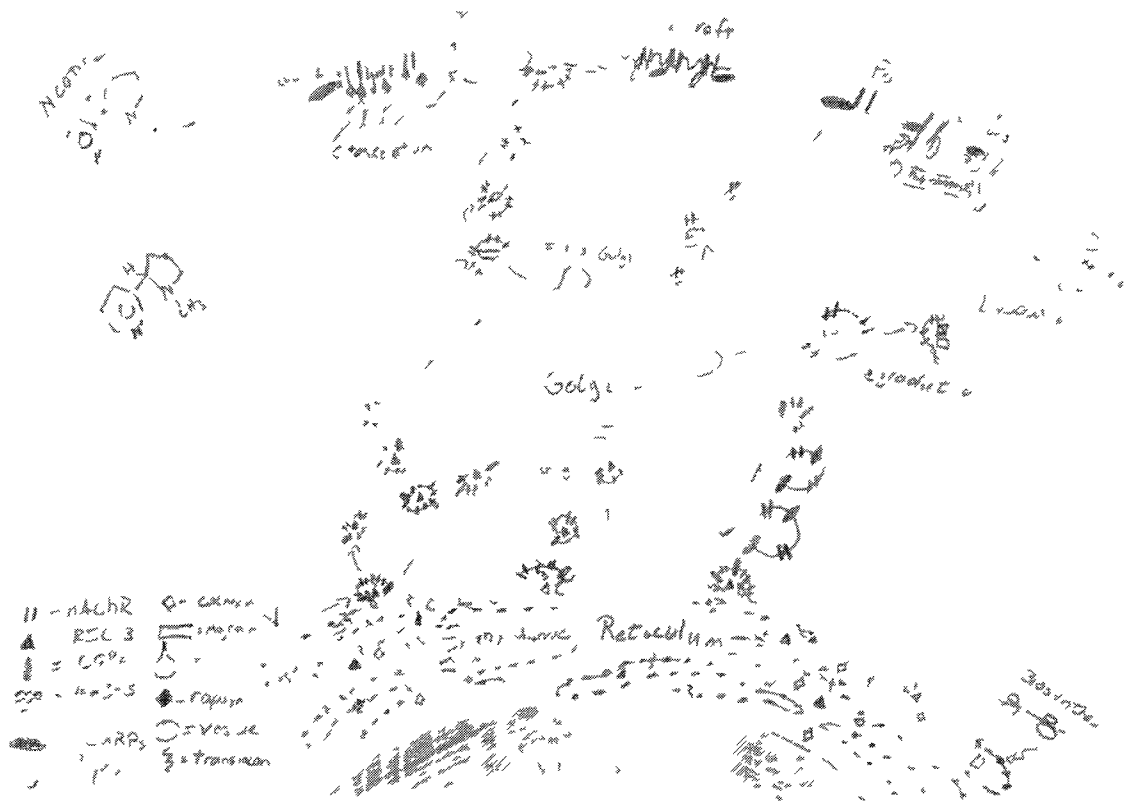


Figure 2.40 Components of nAChR trafficking highlighted in the text.

2.11.1 Assembly.

Several chaperones have been identified that are associated with and/or influence maturation of nAChRs. The most widely studied proteins include Ric-3 (Jeanclos et al., 2001; Halevi et al., 2002; Cheng et al., 2005), 14-3-3 (Jeanclos et al., 2001), BiP (Connolly et al., 1996) and Lynx-1 (Miwa et al., 2006) (Figure 2.40). These chaperones associate with immature nAChR subunits and enhance protein folding, assembly and surface expression. Ligands have also been shown to alter nAChR expression (Figure 2.40).

The protein Resistant to Inhibitors of Cholinesterase (RIC-3) has been identified as the first protein discovered that is specifically required for AChR maturation in *Caenorhabditis elegans* and has been hypothesized to function in the folding, assembly and/or transportation of nAChRs from the ER to the Golgi apparatus (Halevi et al., 2002; Treinin 2008) (Figure 2.40). RIC-3 has two transmembrane domains as well as extensive coiled-coil domains (Halevi et al., 2002)

and is expressed in both muscles and neurons within cell bodies. The RIC-3 protein appears to be localized in the ER where unassembled receptors accumulate and AChRs are assembled and miss-folded (Smith et al., 1987; Halevi et al., 2002). RIC-3 has additionally been shown to be an effective facilitator of $\alpha 7$ nAChR expression (Halevi et al., 2002; Treinin, 2008). However, contradictory results have been shown for RIC-3 in $\alpha 4\beta 2$ nAChR maturation (Halevi et al., 2003; Lansdell et al., 2005).

The 14-3-3 protein has also been shown to assist in nAChR trafficking. An adapter protein located at nicotinic synapses, the 14-3-3 protein binds at the cytoplasmic domain of the $\alpha 4$ nAChR subunit (Lin et al., 2002). The 14-3-3 protein allows or promotes the forward trafficking of multimeric membrane proteins, an action resulting from the 14-3-3 protein's masking or overriding the COPI recognition signals ensuring the protein's retention in the ER (Mrowiec and Schwappach, 2006) (Figure 2.40). COPI, or coat protein, is a protein complex that transports proteins back from the Golgi and preserves the proteins in the ER (Figure 2.40). In addition, the COPI protein allows the trafficking of unassembled subunits from the ER to the Golgi (St. John, 2009). Phosphorylation of the $\alpha 4$ nAChR subunit at the PKA consensus promotes the binding of 14-3-3 proteins and aids in the stabilization of $\alpha 4$ subunits in the ER (Bermudez and Moroni, 2006). This stabilization promotes the assembly of complete $\alpha 4\beta 2$ nAChRs which then releases the multimeric proteins from the ER and permits trafficking to the plasma membrane. While it is unknown if the 14-3-3 protein interacts with $\alpha 7$ nAChR, its involvement in the clustering of $\alpha 3$ -containing nAChRs has recently been determined (Rosenberg et al., 2008).

The immunological heavy chain-binding protein (BiP) is another chaperone protein that contributes to protein degradation (Plemper et al., 1997) and assists in the translocation of newly synthesized proteins across the ER membrane (Corsi and Schekman, 1997; McClellan et al., 1998) (Plemper et al., 1997; Brodsky et al., 1999) (Figure 2.40). BiP functions by ATP driven cycles of "binding to" and "release of" substrate proteins requiring ATP hydrolysis by BiP ATPase. The binding and release cycles promote protein folding by preventing aggregation (Gething, 1999).

The protein Lynx-1 may also play a role in the assembly and trafficking of LGICs (Figure 2.40). Lynx-1 is a GPI-anchored protein that co-localizes with nAChR and modulates nAChR affinity and desensitization (Miwa et al., 2006). Some associated proteins, such as HSP90 and P2X₇, may also exert the opposite effect by activating as negative regulators of receptor expression (Adinolfi et al., 2003).

Endogenous and exogenous ligands have also been shown to prompt changes in nAChR protein expression through up-regulation (Figure 2.40). For example chronic exposure to nicotine

causes up-regulation of nAChR by promoting the oligomerisation and maturation of high-sensitivity receptors (Kuryatov et al., 2005; Sallette et al., 2005). SLURP (secreted mammalian Ly-6/urokinase plasminogen activator receptor-related protein) -1 and -2 can modulate nAChR in non-neuronal tissues (keratinocytes, epithelial cells and immune cells) (Chimienti et al., 2003; Arredondo et al., 2006b; Moriwaki et al., 2007). SLURP-1 is a potent allosteric potentiator of human $\alpha 7$ nAChR (Chimienti et al., 2003). On $\alpha 3$ containing nAChR, SLURP-2 acts as a competitive antagonist (Arredondo et al., 2006b). The actions of SLURPs are thought to be important in modulating the autocrine cholinergic regulation of cell proliferation.

2.11.2 Trafficking and Cell surface Localization.

Synthesis, maturation and targeting have been comprehensively studied for muscle receptors yet the specifics of AChR ontogeny remain unknown. Muscle type nAChR subunits are translated by ER membrane-associated ribosomal complexes and co-transnationally inserted into the ER membrane by the translocon (Johnson and van Waes, 1999; Alder and Johnson, 2004) (Figure 2.40). The nascent subunit subsequently undergoes cleavage of its signal sequence, oxidation of its disulfide bonds (Mishina et al., 1985; Blount and Merlie, 1990) and N-glycosylation of specific residues (Merlie et al., 1982; Smith et al., 1987; Blount and Merlie, 1988). Chaperones like the binding protein BiP (Blount and Merlie, 1991; Paulson et al., 1991; Forsayeth et al., 1992) and calnexin (Gelman et al., 1995; Keller et al., 1998) promote the proper folding and maturation of AChR subunits (Figure 2.40). Miss folded and unassembled nAChR subunits are targeted for degradation by the ER-associated proteasomal degradation machinery (Wanamaker et al., 2003) and are then exported from the ER to the Golgi in vesicles coated in protein complex II (COPII) (Keller et al., 2001; Wang et al., 2002) (Figure 2.40). The trafficking from the ER to Golgi occurs presumably after the masking of specific ER retention signals and recognition of ER export motifs in properly folded and oligomerized AChR subunits.

Several trafficking motifs have been identified (Nishimura and Balch, 1997; Barlowe, 2003; Robinson, 2004) but little is known about the location or composition of these motifs in nAChR subunits. Alignment of the cytoplasmic domain of nAChR subunits reveals a large degree of conservation of hydrophobic residues (Ren et al., 2005). Mutagenesis studies have shown that these highly conserved hydrophobic residues are critical structural determinants for ER export of fully assembled nAChRs (Ren et al., 2005). Specifically mutations of leucine residues (L351A, L357A and L358A) in the $\alpha 4$ subunit attenuated nAChR cell surface expression, whereas mutations L342A, L343A, L349A and L350A in the $\beta 2$ subunit were sufficient to nearly abolish nAChR cell surface expression. These results suggest that the $\alpha 4$ AChR subunit has a

cooperative or regulatory role and the $\beta 2$ subunit has a role in functional interactions with the ER export machinery (Ren et al., 2005).

Clustering of nAChR at muscle endplates has shown nAChRs to be less susceptible to disassembly during maturation and increases the life time of the receptors in the membrane from hours to several days (Fambrough, 1979). Agrin activates the transmembrane receptor tyrosine kinase (MuSK) which can cause the clustering of nAChR by rapsyn, (Araud et al., 2010) a 43 kDa protein, that binds to nAChR and may tether receptors to the cytoskeleton (Antolik et al., 2007) (Figure 2.40). Studies have further suggested that rapsyn binds to the cytoplasmic loops of nAChR subunits (Lee et al., 2009).

The cytoplasmic loop on nAChRs is also an important regulator of cell surface expression. Co-localization of $\alpha 7$ nAChR with "lipid rafts" may be a determinate of nAChR surface expression (Figure 2.40). In PC12 cells, lipid rafts are essential for the co-localization of α receptors and adenylyl cyclase within the plasma membrane and for other regulation activities involving Ca^{2+} influx through α nAChR (Oshikawa et al., 2003).

2.11.3 Post Translational Modifications.

Post translational modifications are reversible modifications that can alter LGIC function, assembly, stability, etc. Phosphorylation, palmitoylation, sumoylation and ubiquitination are examples of post translational modifications that occur on nAChRs, although very little is known about palmitoylation and sumoylation of nAChRs.

Phosphorylation is a rapidly reversible modification that acts as a switch to influence LGIC function (ex. desensitization rate), subunit assembly, receptor aggregation, stability and synaptic strength (Araud et al., 2010). Attaching or removing phosphate groups on the receptors transpires by kinases or phosphatases (Figure 2.40). Phosphorylation at serine/threonine or tyrosine occurs at the intracellular loop. Tyrosine phosphorylation of the $\alpha 7$ nAChR by *src*-kinase on the receptor's cytoplasmic loop reduced ACh-evoked currents (Charpantier et al., 2005).

2.12. Distribution of nAChRs in the Central Nervous System.

nAChR are widely distributed in both the nervous system and non-neuronal tissues.. nAChRs are critically important during early pre- and post-natal circuit formation and age-related cell degeneration and are found along cholinergic pathways (Woolf, 1991; Gotti et al., 2006b). Cholinergic neurons in the basal forebrain generally located in an axis running from the cranial nerve nuclei of the brain stem to the medullary tegmentum and pons/mesencephalic tegmentum continuing rostrally through the diencephalon to the telencephalon (Woolf, 1991) (Figure 2.41). In the brain there are three cholinergic systems that reach from the brain stem to nearly every

neural area. The first major cholinergic system is found in the pedunclopontine tegmentum (ppt) and laterodorsal pontine tegmentum (ldt) providing a widespread innervation to the hindbrain, thalamus, hypothalamus, basal forebrain and midbrain dopaminergic areas and descending to the caudal pons and brain stem (Dani and Bertrand, 2007) (Figure 2.41). The second major system arises from various basal forebrain nuclei (the nucleus basalis group; nucleus basalis, substantia innominata and horizontal diagonal band: bas, si, hdb) that project throughout the neocortex, parts of limbic cortex and the amygdala (Dani and Bertrand, 2007) (Figure 2.41). These projections provide an extensive and sparse innervation throughout the brain. The third cholinergic system is composed of the medial septal group (medial septal nucleus and vertical diagonal band: ms and vdb) that project cholinergic axons to the hippocampus and parahippocampal gyrus (Dani and Bertrand, 2007) (Figure 2.41). In addition, this system makes up approximately 2% of the striatal neurons and innervates the striatum and olfactory tubercle (Zhou et al., 2002).

nAChRs are principally located at presynaptic or pre-terminal sites where they modulate neurotransmitter release or on cell bodies and dendrites where they mediate postsynaptic effects (Hogg et al., 2003; Dajas-Bailador and Wonnacott, 2004; Gotti and Clementi, 2004). Other studies suggest that nAChR are not found in abundance at the synapse and are more involved in diffuse volume transmission (Umbriaco et al., 1994; Descarries et al., 1997). It is not uncommon for structural studies to underestimate synaptic contacts due to the difficulty of observing every contact from every angle. It is becoming increasingly evident that alteration of nAChR neurotransmission can lead to pathologies during development, adulthood and aging.

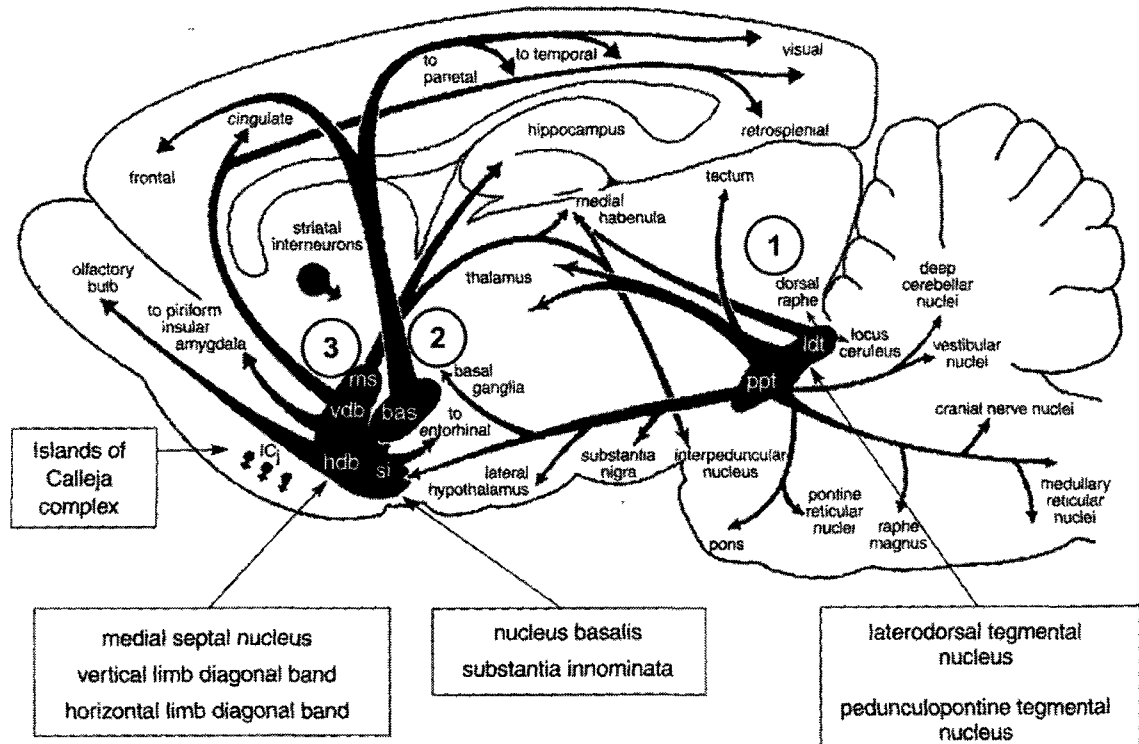


Figure 2.41 The three major cholinergic pathways found in the brain.

The cholinergic systems are located as described: (1) Cholinergic neurons in the pedunculo-pontine tegmentum (ppt) and laterodorsal pontine tegmentum (ldt) project into the hindbrain, thalamus, hypothalamus, basal forebrain and midbrain dopaminergic areas and descend to the caudal pons and brain. (2) Neurons located in the basal forebrain nuclei (the nucleus basalis group; nucleus basalis, substantia innominata and horizontal diagonal band: bas, si, hdb) extend throughout the neocortex, parts of the limbic cortex and the amygdala. (3) Cholinergic cells located in the medial septal group (medial septal nucleus and vertical diagonal band: ms and vdb) extend cholinergic axons to the hippocampus, parahippocampal gyrus, striatum and olfactory tubercle. The brain illustration is modeled after a rat brain. (Image was used with permission from (Woolf 1991) and was modified.)

In situ hybridization results of $\alpha 4$, $\beta 2$ and $\alpha 7$ indicate subunit mRNA is widely distributed throughout the brain with receptor location and varies among different vertebrate species (Gotti et al., 2006b). α -bungarotoxin sensitive receptor subtypes ($\alpha 7$ -10) are highly expressed in the cortex, hippocampus and subcortical limbic regions and are expressed at low levels in the thalamic regions and basal ganglia (Gotti et al., 2006b) (Figure 2.42).

The α -bungarotoxin sensitive $\alpha 9$ and $\alpha 10$ subtypes have not been found in the brain. Their co-expression as $\alpha 9$ homomers and $\alpha 9\alpha 10$ heteromomers appears to be limited to the cochlea and a few ganglia (Gotti et al., 2006a).

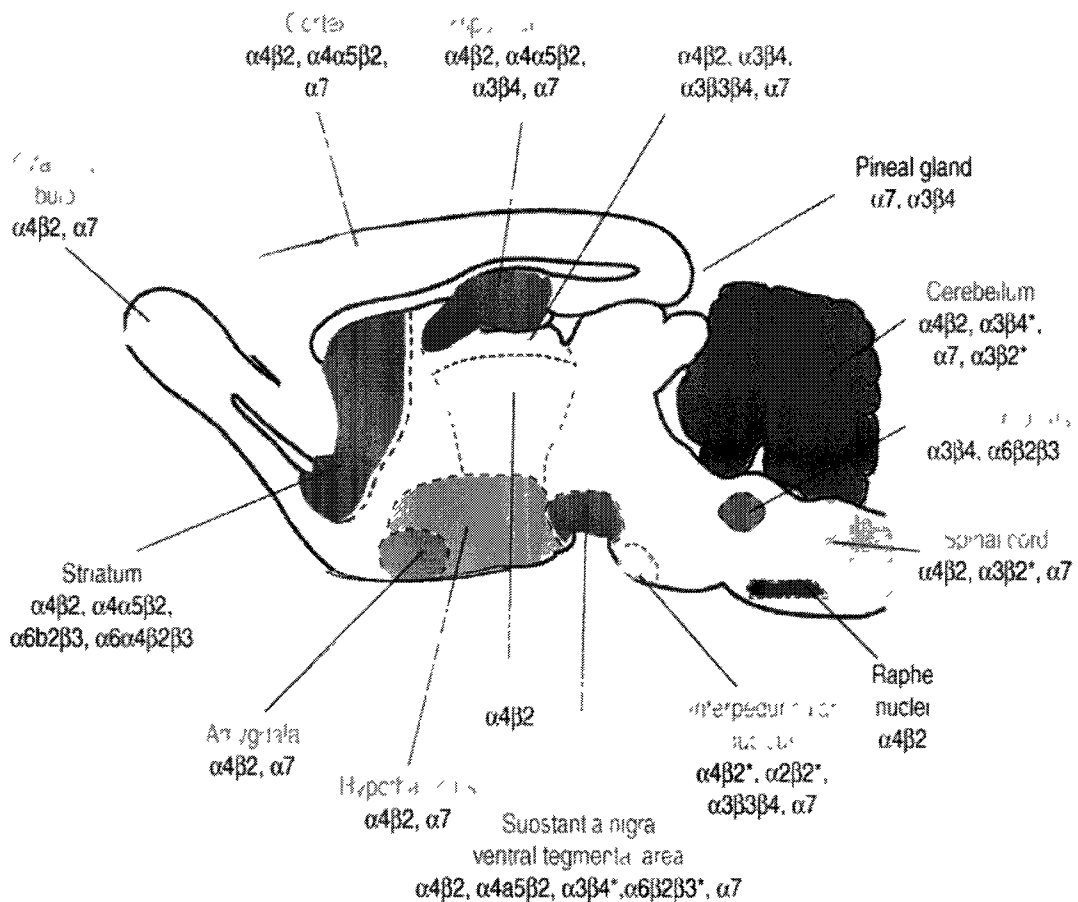


Figure 2.42 Locations of nAChR in the rat brain.

(Image reprinted from (Gotti et al., 2006b) and used with permission.)

2.12.1 $\alpha 4\beta 2$ Expression.

The $\alpha 4\beta 2$ subtype appears to be found in subregions such as the cortex, striatum, superior colliculus, lateral geniculate nucleus and cerebellum (Picciotto and Zoli, 2002; Gotti and Clementi, 2004; Gotti et al., 2005; Turner and Kellar, 2005) (Figure 2.42). In mice, radioligand binding using L-[^3H]nicotine has shown high levels of binding in the interpeduncular nucleus, medial habenula, thalamic nuclei, ventral lateral and dorsal lateral geniculate nuclei and optic tract nucleus. Moderate binding was found in many areas of the brain including the parietal cortex, cingulate cortex, subiculum, substantia nigra, superior colliculus, medial geniculate nucleus, optic nerve dorsal raphe, laterodorsal tegmental nucleus and retrosplenial cortex. Low levels of binding have been found in the medial septum, nucleus accumbens, caudate putamen, hippocampus and olfactory tubercle. Virtually no binding was found in the cerebellum (Marks et al., 1992).

The L-[^3H] nicotine labeling correlates well with $\alpha 4$ mRNA expression in the CNS (Wada et al., 1989; Marks et al., 1992). Discrepancies might be due to the protein being localized to axons and synaptic terminals while mRNA resides in the soma. $\beta 2$ nAChR subunit MAb270 immunolabeling displays a similar expression pattern to the L-[^3H]nicotine labeling (Clarke et al., 1985; Swanson et al., 1987). MAb270 immunolabeling indicates discrete expression at all levels of the rat brain and spinal cord with strong labeling in the interpeduncular nucleus, medial habenula, thalamus and superior colliculus.

Both $\alpha 4$ and $\beta 2$ subunit mRNA are detected in the CNS and PNS as early as E11 in rats. The expression of $\alpha 4$ is down-regulated in the PNS to undetectable levels by E15 whereas $\beta 2$ mRNA expression levels are maintained until adulthood (Zoli et al., 1995).

It has been found that GABAergic and dopaminergic neurons express similar nAChR mRNA (Klink et al., 2001). Both $\alpha 4$ and $\beta 2$ mRNAs are expressed in nearly all dopaminergic and GABAergic neurons in the ventral tegmental area, whereas $\alpha 2$ are not expressed (Klink et al., 2001). Specifically, the $\alpha 7$ nAChR subunit mRNA is found in 40% of the dopaminergic and GABAergic neurons while $\beta 4$ is sparsely found in the GABAergic (25%) and dopaminergic (12%) neurons. The $\alpha 5$, $\alpha 6$ and $\beta 3$ mRNA expression levels are lower in GABAergic (< 25%) than dopaminergic (> 70%) neurons.

The ventral tegmental area and substantia nigra pars compacta contain moderate to high levels of $\alpha 4\beta 2$ nAChR mRNA (Wada et al., 1989). Antibody labeling of $\alpha 4$ and $\beta 2$ subunits in the soma and dendrites of the substantia nigra pars compacta shows co-localization in > 90% of dopaminergic neurons (Arroyo-Jimenez et al., 1999; Jones et al., 2001). Immunoelectron microscopic studies have shown that $\alpha 4$ subunits are located in the perikarya and dendritic

shafts, but not in the spines and are scarcely found in postsynaptic membranes of dopaminergic neurons (Arroyo-Jimenez et al., 1999). The $\beta 2$ subunit shows a similar localization pattern in dopaminergic neurons found in the substantia nigra pars compacta and in presynaptic membranes of dopaminergic axonal terminals in the dorsal striatum (Jones et al., 2001).

2.12.2 Other Heterpentameric nAChR.

Studies have shown that the same neuronal population can express multiple nAChR subtypes. The nAChR subunits $\alpha 2$, $\alpha 3$, $\alpha 6$, $\beta 2$ and $\beta 4$ can either form heteropentameric complex subtypes. For example, $\alpha 4\alpha 6\beta 2^*$ are found in the striatum and visual pathways, $\alpha 3\alpha 4\beta 2$ or $\alpha 3\alpha 4\beta 4$ in the cerebellum (Turner and Kellar, 2005) and $\alpha 2\alpha 4\beta 2^*$ in the retina (Moretti et al., 2004; Marritt et al., 2005). Reasons for this heterogeneity are only partially understood. Specific characteristic of the subtypes, like high versus low Ca^{2+} permeability or slow versus fast desensitization rates, might make co-expression of the various subtypes relevant. Alternatively, the various subtypes may be critical for preferential targeting to different cell compartments (Gotti et al., 2006b).

2.13. Pathological Conditions Associated with nAChRs.

Implicated in many pathological conditions, nAChR subtypes and densities change depending on the disease. Neurological conditions with strong nAChR components include Alzheimer's disease (AD), Parkinson's disease, Autism, Schizophrenia, alcohol addiction and nicotine addiction. Not surprisingly there are many clinically used drugs targeting nAChR. These drugs are usually administered for months and typically produce long-term changes in receptor properties and/or numbers (Taly et al., 2009). Chronic exposure to nicotine, for example, can cause a two fold up-regulation in the total number of high-affinity receptors (Salette et al., 2005).

nAChR are involved in the pathogenesis or symptomatology of several diseases of the CNS. These diseases are subdivided into two groups: those in which a nAChR subunit gene is mutated and the receptor subtype function is altered (as is the case for autosomal dominant frontal lobe epilepsy); and those involving modification in nAChR expression densities (such as schizophrenia, Tourette's syndrome, attention deficit hyperactivity disorder, autism, depression and anxiety) and neurodegenerative Alzheimer's and Parkinson's disease (Hogg et al., 2003; Gotti and Clementi, 2004; Hogg and Bertrand, 2004).

Mutations in the channel region of the $\alpha 4$ or $\beta 2$ subunits have been found in some families suffering from autosomal dominant frontal lobe epilepsy. The expression of these mutated receptors causes a gain ($\alpha 4$) or loss ($\beta 2$) of function, but in both cases results in functional receptors with a higher ACh sensitivity (Gotti et al., 2006b).

2.13.1 Alzheimer's Disease.

Alzheimer's disease is characterized by progressive cognitive decline and neuronal death. The cholinergic synapses in the basal, forebrain, cerebral cortex and hippocampus were especially reduced (Kasa et al., 1997) as were muscarinic and nicotinic AChR expression (Court et al., 2001). Differences in receptor subtypes have also been observed. In the cerebral cortex, it has been reported that there was a massive reduction in predominantly the $\alpha 4\beta 2$ subtype while the $\alpha 7$ nAChR appears to be spared (Bourin et al., 2003) and in the hippocampus, the expression of $\alpha 7$ nAChR was reduced (Whitehouse and Kalara, 1995; Nordberg et al., 1997; Burghaus et al., 2000; Guan et al., 2000; Nordberg, 2000).

It has been suggested that the $\alpha 7$ nAChR subtype may play a large role in memory. In the hippocampus, a critical region for memory formation, there is a high level of $\alpha 7$ nAChR expression. Gene knockout and antisense RNA studies have indicated a role for $\alpha 7$ nAChR in learning, memory, attention (Wehner et al., 2004; Keller et al., 2005; Curzon et al., 2006) and working-episodic memory (Fernandes et al., 2006; Young et al., 2007). In addition, pharmacological studies have shown that $\alpha 7$ nAChR selective agonists or PAMs improve cognitive deficits associated with AD.

The selective $\alpha 7$ partial agonist, AR-R17779, has been shown to improve scopolamine-elicited deficits in social recognition. AR-R17779 also enhanced the long-term learning and attenuated working-memory deficits in rats (Taly et al., 2009). Two $\alpha 7$ partial agonists, GTS-21 (also a $\alpha 4\beta 2$ antagonist) and MEM-3454 (also a 5HT-3R antagonist) showed precognitive action (Rezvani et al., 2009). In preclinical studies, MEM-3454 enhanced episodic, spatial and working memory. The precognitive effect of MEM-3454 on episodic memory was completely blocked by the $\alpha 7$ specific antagonist methyllycaconitine. In a phase I clinical trial, GTS-21 improved episodic secondary memory tests including word recall and picture and word recognition (Kitagawa et al., 2003). High concentrations of GTS-21 have been shown to reduced cell survival, suggesting a risk of over-stimulation (Meyer et al., 1998).

The toxic peptide A β 1-42 involved in AD has recently been shown to bind to $\alpha 7$ nAChR (Wang et al., 2000). Controversial reports suggest that A β 1-42 may act either as an agonist or as an antagonist on $\alpha 7$ receptors (Dineley et al., 2001; Pettit et al., 2001; Spencer et al., 2006). Other papers have suggested that A β 1-42 does not bind to $\alpha 7$ nAChRs (Lamb et al., 2005; Small et al., 2007).

Currently, partial agonists are receiving more attention as drug development targets than full agonists because of their similar properties and reduced ability to activate the receptors,

possibly leading to a reduced risk of cytotoxicity by Ca^{2+} entry. Allosteric modulators are also being heavily investigated as potential therapeutics due to their ability to alter the amplitude of the receptor response while maintaining the spatial and temporal organization of signal transmission.

Since $\alpha 7$ nAChR play a role in cognitive function (Curzon et al., 1996; Hahn et al., 2003), this subtype has also been a target for drug development. ABT-418, a selective $\alpha 4\beta 2$ full agonist has been shown to have cognitive-enhancing activity in preclinical and Phase II studies (Potter et al., 1999; Arneric et al., 2007). Ispronicline a full agonist on $\alpha 4\beta 2$ nAChR has been tested in clinical trials but failed to demonstrate cognitive improvements.

2.13.2 Autism Spectrum Disorder.

The observation that individuals who suffer from autism spectrum disorder are typically non-smokers suggests that nicotinic receptor expression or function may be altered in autistics (Glennon, 2005). A more recent study has demonstrated that prenatal exposure to nicotine may be linked to infantile autism (Lippiello, 2006). The expression of nAChR appears to be altered in autistics in several brain regions. In the cortical regions, epibatidine binding was shown to be reduced by nearly 30% with little change in α -bungarotoxin binding (Perry et al., 2001). These results indicated that the $\alpha 4\beta 2$ nAChR expression was decreased while expression of $\alpha 7$ nAChRs remained unchanged (Martin-Ruiz et al., 2004).

A possible genetic link also exists. Behavior and linkage analysis studies disclosed that there is an autism susceptibility gene on chromosome 1, which contains the $\beta 2$ nAChR gene (Ferretti and Gianandrea, 1954; Anand and Lindstrom, 1992) as well as chromosomes 6 and 19 (Buxbaum et al., 2004). $\beta 2$ knockout mice provide further evidence for a genetic link through typical autistic behavioral displays, such as a decreased ability for conflict resolution and social interaction (Granon et al., 2003). Larger decreases (> 50%) in epibatidine binding are also observed in the thalamus and striatum while $\alpha 7$ receptors are unaffected (Court et al., 2000; Perry et al., 2001; Martin-Ruiz et al., 2004; Ray et al., 2005). Increases in $\alpha 7$ expression have been shown to occur in cerebellar granule cells (Martin-Ruiz et al., 2004). Chromosome 15 is near another locus thought to be a genetic marker for autism and contains the $\alpha 7$ nAChR gene (Chini et al., 1994; Lamb et al., 2000).

Due to the putative role of nAChR in autism, nicotinic ligands may be useful in treating autistic spectrum disorders (Lichtner et al., 1988; Dani and Bertrand, 2006; Lippiello, 2006; Nicolson et al., 2006) and several nicotinic ligands, such as Galantamine (Razadyne®), are in clinical trials for the treatment of behaviors such as aggression, uncontrollable behavior and inattention (Nicolson et al., 2006). A cholinesterase inhibitor and a non-specific potentiator,

Galantamine enhances nicotinic responses at nicotinic subtypes. Galantamine additionally inhibits nAChRs at concentrations only slightly higher than its peak potentiating concentrations, thus narrowing its therapeutic range. Mecamylamine (Targacept®) is also currently being examined as an autism therapy (Lippiello, 2006). Mecamylamine is a $\alpha 3\beta 4$ nAChR antagonist and has had positive effects in treating Tourette Syndrome and Attention Deficit Disorder (Shytle et al., 2000; Silver et al., 2000).

The current nicotinic treatment ligands are not the ideal treatment strategies for Autism. Non-selective ligands act on all nAChR populations, not just the dysregulated nAChRs. Selective allosteric modulators may be better suited for treating aspects of Autism such as aggression and antisocial behavior. A selective PAM would cause an increase in activity in down-regulated receptors and would only act on the receptors when the endogenous ligand was present maintaining the spatial and temporal relationship within the nicotinic system.

2.13.3 Nicotine Addiction.

nAChR levels in human smokers are higher than nonsmokers as verified by functional magnetic resonance imaging and post mortem measurements (Breese et al., 1997; Perry et al., 1999; Staley et al., 2006; Mamede et al., 2007). The $\alpha 4\beta 2$ nAChR and other subtypes are selectively up-regulated (Nguyen et al., 2003) and active rather than desensitized (Nguyen et al., 2004; Nashmi et al., 2007). The extent of up-regulation appears to be regional and cell sensitive (Nashmi et al., 2007). Up-regulation of highly-sensitive nAChR is partially the biological basis for tolerance, locomotor sensitization and cognitive sensitization associated with chronic nicotine administrations (Buisson and Bertrand, 2002; Gentry and Lukas, 2002; Nashmi et al., 2007; Tapper et al., 2007).

Nicotine's major addictive effects are thought to be mediated through the dopaminergic mesocorticolimbic pathways (Nashmi and Lester, 2006). Dopaminergic neurons originate in the ventral tegmental area and project to the nucleus accumbens and prefrontal cortex. In the ventral tegmental area, the dopaminergic neurons, GABAergic neurons and glutamateric axonal terminals all contain nicotinic receptors (Mansvelder and McGehee, 2000; Mansvelder et al., 2002). Chronic nicotine exposure selectively up-regulates receptor number in the midbrain. Up-regulation occurs in the GABAergic neurons in the ventral tegmental area but not in the somata or the dopaminergic neurons. Dopaminergic neurons are the postsynaptic targets and are inhibited by the GABAergic neurons. As a result, chronic nicotine increases both the basal firing rates and the excitatory effects of nicotine in GABAergic neurons. On dopaminergic neurons chronic nicotine decreases baseline firing rates and attenuates the excitatory effects of nicotine (Nashmi et al., 2007; Lester et al., 2009). It is thought that the balance of excitatory and inhibitory inputs

onto the ventral tegmental area dopaminergic neurons affects dopamine release in the nucleus accumbens and is likely critical for the reinforcing effects of nicotine (Nashmi and Lester, 2006).

Compared to wild-type, $\beta 2$ -knockout mice no longer self-administer nicotine (Picciotto et al., 1998), demonstrating a role for the $\beta 2$ subunit in nicotine addiction. Self-administration of nicotine is also reduced in rats given dihydro- β -erythroidine (DH β E) (a selective $\alpha 4\beta 2$ antagonist) (Watkins et al., 1999). It has been hypothesized that partial agonist may substitute the desired effects of nicotine while also antagonizing nicotine reinforcing properties (Hogg and Bertrand, 2007; Rollema et al., 2007b).

The metabolism of nicotine occurs at a much slower rate than ACh. Nicotine is metabolized only by liver enzymes and has a half-life of about $\sim 120\text{min}^{-1}$ (Matta et al., 2007). In contrast, ACh is hydrolyzed by acetylcholinesterase with a turnover rate of about $\sim 10^4\text{ s}^{-1}$ (Gyermek, 1996). Simulations of synaptic transmission conclude that ACh remains near receptors for $< 1\text{ms}$ (Wathey et al., 1979; Bartol et al., 1991). Due to nicotine's long half-life, it desensitizes receptors and permeates cells. Unlike ACh which has slight membrane permeability ($> 3\text{h}$), nicotine's high permeability allows it to act at the cell surface membrane as well as at the endoplasmic reticulum and Golgi. This process could be a mechanism of up-regulation of nAChR associated with nicotine addiction (Lester et al., 2009). The up-regulation of $\alpha 4\beta 2$ receptors appears to be more geared towards the high-sensitivity stoichiometry $((\alpha 4)_2(\beta 2)_3)$ at the expense of the low-sensitivity channel $((\alpha 4)_3(\beta 2)_2)$ (Lester et al., 2009).

Treatment options for smoking cessation include nicotine and bupropion (a non-competitive antagonists on $\alpha 4\beta 2$ nAChR) (Fiore et al., 2004). These ligands have limited efficacy so the development of more effective therapeutic options is needed. The most recently approved drug for smoking cessation is Varenicline, a $\alpha 4\beta 2$ partial agonist and a full agonist on $\alpha 7$ nAChR (Rollema et al., 2007b). The US Food and Drug Administration and the European Medicines Agency have recently warned of serious side effects including changes in mood and social ideation. It is possible that long-term chronic exposure can lead to modified levels of nAChR densities (Besson et al., 2007).

The National Institute of Health is funding a major effort to find a better solution for nicotine addiction. PAMs are one treatment strategy being explored. The use of PAMs entails a smaller dosage of nicotine needed to satisfy cravings allowing the nicotine addicted individual to gradually reduce their dependence until they no longer need the drug. The major drawback to this approach is that the treatment strategy still targets the reward pathways, which may cause the therapeutic ligand to become an abused drug. Another problem with using PAMs as a possible

nicotine addiction treatment is the ability of some PAMs to reactivate desensitized receptors. Large populations of desensitized receptors are present in the brains of nicotine addicted individuals and the addition of a PAM could cause activation of these desensitized receptors leading to a huge population of activated receptors. The dosage of the therapeutic ligand would aid in the prevention of too many receptors being activated.

2.13.4 Cancer and Angiogenesis.

Genomic studies have shown that chromosome regions 15q24-25 (Hung et al., 2008; Liu et al., 2008a), 15q15.33 (McKay et al., 2008) and 6p21.33 (Wang et al., 2008b) appear to have common sequence variants that may convey a higher risk for developing lung cancer. The 15q24-25 region encompasses the nAChR subunits $\alpha 3$, $\alpha 5$ and $\beta 4$ genes, all of which play a role in nicotine addiction (Spitz et al., 2008; Weiss et al., 2008).

Airway epithelial cells produce and degrade ACh (Proskocil et al., 2004). Human bronchial epithelium (HBE) express $\alpha 3$, $\alpha 5$, $\alpha 7$, $\beta 2$ and $\beta 4$ nAChR subunits (Zia et al., 1997; Maus et al., 1998). The $\alpha 5$ and $\alpha 9$ nAChR have been shown to also express in lung and breast cancers (Lee et al., 2010b). An increase in $\alpha 9$ nAChR expression has been seen in other cancer cells (Lee et al., 2010b).

Nicotine and the tobacco specific nitrosamine 4-(methylnitrosamino)-1-(3-pyridine)-1-butanone (NKK) are agonists for nAChR. In an epithelial cell culture model addition of nicotine derivatives (NKK and *N*-nitrosonornicotine) caused a temporary (1-2.5 hr) up-regulation of the $\alpha 7$ nAChR subunit (Plummer et al., 2005). An increase in proliferation was observed also then reduced by nicotine antagonist (α BTX) (Arredondo et al., 2006a). Nicotine incubation of bronchial epithelial cells caused a production of granulocyte-macrophage colony stimulating factor and stimulated inflammatory cells (Klapproth et al., 1998). In nonmalignant human bronchial epithelial cells, apoptotic effects by damaging agents (such as etoposide, UV irradiation or hydrogen peroxide) were attenuated by nicotine and NKK (West et al., 2003). Thus, in epithelial cells, nicotine and NKK have a stimulatory effect on growth, inflammation and cell survival.

In breast cancer, exposure to nicotine caused an increase in $\alpha 9$ nAChR expression (Shih et al., 2010; Chen et al., 2011). Nicotine itself is not a carcinogen but it does promote the growth of cancer cells and proliferation of endothelial cells. Lee et al., (2010b) indicated that increased expression of $\alpha 9$ nAChR enhances proliferation and colony formation (Lee et al., 2010b).

In small cell lung cancer (SCLC) and non-SCLC (NSCLC) $\alpha 3$, $\alpha 5$, $\alpha 7$ and $\beta 4$ nAChR subunits are expressed (Chini et al., 1992; Tarroni et al., 1992; West et al., 2003). Both NSCLC and SCLC cell lines synthesize and release ACh (Song et al., 2003). In squamous cell carcinoma

(SqCC), the choline acetyltransferase is strongly up-regulated whereas cholinesterase is down-regulated (Martinez-Moreno et al., 2006; Song et al., 2008). This reaction results in an increase in ACh concentration in SqCC compared to normal lung, providing an increased level of endogenous ACh stimuli to nAChR.

In lung cancer, nicotine induces proliferation of tumor cells by binding to the $\alpha 7$ nAChR, leading to the activation of Src and Rb-Raf-1/pERK/p90RSK pathway (Dasgupta et al., 2006b; Carlisle et al., 2007). Stimulation of nAChR by nicotine results in Ca^{2+} influx within seconds. Nicotine additionally induces an increase in fibronectin production (Zheng et al., 2007). Extracellular fibronectin binds to $\alpha 5\beta 1$ integrin which subsequently leads to increased proliferation through ERK, PI3-K and mTOR pathways.

In SCLC and NSCLC cell lines, nicotine diminishes apoptosis (Maneckjee and Minna, 1994; Dasgupta et al., 2006a). The anti-apoptotic effects of nicotine appear to be mediated by the $\alpha 3$ nAChR and required the AKT pathway, leading to an increased recruitment of E2F1 and concomitant dissociation of retinoblastoma tumor suppressor protein. The binding of E2F1 to the promoter of survivin and XIAP genes resulted in the up-regulation of apoptotic inhibitors demonstrating nicotine has a prolonged effect on tumor cell survival by preventing apoptosis.

Individuals diagnosed with smoking-related lung cancer and who continue to smoke have a negative correlation with lung cancer survival (Videtic et al., 2003; Sardari Nia et al., 2005). The lack of survival may be a result of nicotine's positive effects on tumor growth and survival.

Studies have shown that nAChR play a major role in breast and lung cancers. The $\alpha 7$ nAChR are implicated in lung cancer while the $\alpha 9$ nAChR play a major role in breast cancers. nAChR antagonists may decrease the survival of tumor cells and provide a novel avenue for cancer therapy.

The proliferation of tumors involves the formation of new blood vessels, also known as angiogenesis, through the growth factors, intergrins, angioproteins, adhesion and gap junction proteins, transcription factors and other components (Risau, 1997). There are three main steps in angiogenesis. First, vascular endothelial cells (ECs) activation is mediated by hypoxia and/or cytokine release. Second, the basement membrane (BM) is degraded by the matrix metalloproteinases (MMPs). Third, vascular endothelial growth factor (VEGF)- and intergrin-dependent EC migration, proliferation and differentiation. In pathological conditions, endothelial angiogenesis can contribute to neoplastic and non-neoplastic transformations including cancer, atherosclerosis, rheumatoid arthritis and diabetic retinopathy (Folkman, 2006). The initial prompt for pathological angiogenesis may be EC proliferation/dysfunction by VEGF up-regulation and though the release of stored ACh (Parnavelas et al., 1985).

AChRs are involved in angiogenesis, predominantly subtypes $\alpha 7$ and $\alpha 3\beta 4$ nAChR and the subunits $\alpha 3$, $\alpha 5$, $\beta 2$ and $\beta 4$ (West et al., 2003). Bronchial epithelial cells (Carlisle et al., 2004), endothelial cells of blood vessels (Wang et al., 2001), skin keratinocytes (Chernyavsky et al., 2004), lymphocytes, microglial and astrocytes contain neuronal nAChRs containing $\alpha 3$, $\alpha 5$, $\alpha 7$, $\beta 2$ and $\beta 4$ subunits (Conti-Fine et al., 2000; Heeschen et al., 2002).

Angiogenesis and increased vascular permeability are important factors in wound healing, a tightly controlled process involving re-epithelialization, macrophage accumulation, fibroblast infiltration, matrix formation and re-vascularization. Whether nicotine promotes or delays wound healing is a topic of debate (Jacobi et al., 2002; Galiano et al., 2004; Morimoto et al., 2008). In one study non-diabetic mice experienced improved wound healing with the use of topical 100 μ M nicotine (Morimoto et al., 2008) whereas in another study, non-diabetic mouse wounds treated with a lower dosage of nicotine (1-10 nM) displayed no improvement in wound health when compared to phosphate buffered saline (PBS) treated wounds (Jacobi et al., 2002). These results suggest that improvements in wound healing by nicotine may be concentration dependent.

Initial tumor formation requires oxygen and nutrients. Further tumor growth requires communication with the vascular ECs and new blood vessels. Tumor malignancy is dependent on an "angiogenic switch", a combination of an imbalance of pro- and anti-angiogenic factors influenced by hypoxia, low pH, hypoglycemia and inflammatory cytokines (Carmeliet and Jain, 2000; Pandya et al., 2006). A large variety of angiogenic factors are secreted by tumor cells which can overwhelm endogenous angiogenic inhibitors. The ECs migrate towards these angiogenic stimuli, proliferate and form new vessels. In hypoxic microenvironments, tumor ECs proliferate 2-2000 times faster than normal ECs (Griffioen and Molema, 2000).

Nicotine can induce tumor cell proliferation and angiogenesis through nAChRs expressed in cancer cells (Chini et al., 1992; Egleton et al., 2008). The $\alpha 7$ nAChR is the primary receptor subtype that mediates nicotine-mediated tumor cell proliferation. $\alpha 3\beta 4$ containing nAChRs may also play a role in this process (West et al., 2003). Nicotine enhances cell proliferation of cancer cells in small and non-small cell lung carcinomas, pancreatic, colon and bladder cancer cells (Shin et al., 2004; Ye et al., 2004; Wong et al., 2007; Chen et al., 2008).

Nicotine has also been shown to increase the levels of different growth factors such as VEGF, brain derived neurotropic factor (BDNF), epidermal growth factor (EGF), hepatocyte growth factor (HGF), PDGF and transforming growth factor- α (TGF- α) and β (TGF- β) and their respective receptors (Conti-Fine et al., 2000). Alterations in these growth factors influence both the tumor and normal ECs.

One cancer treatment avenue is the use of angiogenesis inhibitors. Heeschen and co-workers demonstrated a decrease in a mouse lung tumor model with the non-specific nAChR antagonist mecamylamine (Heeschen et al., 2002). This decrease in tumor growth included a lower capillary density and a decreased systemic VEGF levels. Mecamylamine is currently in phase II clinical trials. The development of novel inhibiting ligands such as antagonists or NAMs may aid in the inhibition or prevention of tumor growth.

2.14. References.

- Adams CE and Stevens KE (2007) Evidence for a role of nicotinic acetylcholine receptors in schizophrenia. *Front Biosci* 12:4755-4772.
- Adinolfi E, Kim M, Young MT, Di Virgilio F and Surprenant A (2003) Tyrosine phosphorylation of HSP90 within the P2X7 receptor complex negatively regulates P2X7 receptors. *J Biol Chem* 278:37344-37351.
- Akk G, Shu HJ, Wang C, Steinbach JH, Zorumski CF, Covey DF and Mennerick S (2005) Neurosteroid access to the GABAA receptor. *J Neurosci* 25:11605-11613.
- Akk G, Sine S and Auerbach A (1996) Binding sites contribute unequally to the gating of mouse nicotinic alpha D200N acetylcholine receptors. *J Physiol* 496 (Pt 1):185-196.
- Albuquerque EX, Pereira EF, Alkondon M and Rogers SW (2009) Mammalian nicotinic acetylcholine receptors: from structure to function. *Physiol Rev* 89:73-120.
- Albuquerque EX, Pereira EF, Alkondon M, Schratzenholz A and Maelicke A (1997) Nicotinic acetylcholine receptors on hippocampal neurons: distribution on the neuronal surface and modulation of receptor activity. *J Recept Signal Transduct Res* 17:243-266.
- Albuquerque EX, Pereira EF, Mike A, Eisenberg HM, Maelicke A and Alkondon M (2000) Neuronal nicotinic receptors in synaptic functions in humans and rats: physiological and clinical relevance. *Behav Brain Res* 113:131-141.
- Alder NN and Johnson AE (2004) Cotranslational membrane protein biogenesis at the endoplasmic reticulum. *J Biol Chem* 279:22787-22790.
- Alkondon M and Albuquerque EX (2006) Subtype-specific inhibition of nicotinic acetylcholine receptors by choline: a regulatory pathway. *J Pharmacol Exp Ther* 318:268-275.
- Alkondon M, Pereira EF, Barbosa CT and Albuquerque EX (1997) Neuronal nicotinic acetylcholine receptor activation modulates gamma-aminobutyric acid release from CA1 neurons of rat hippocampal slices. *J Pharmacol Exp Ther* 283:1396-1411.
- Alkondon M, Pereira EF, Wonnacott S and Albuquerque EX (1992) Blockade of nicotinic currents in hippocampal neurons defines methyllycaconitine as a potent and specific receptor antagonist. *Mol Pharmacol* 41:802-808.
- American Heart Association I (2011) Nicotine Addiction, in, American Heart Association, Inc.
- Amin J, Brooks-Kayal A and Weiss DS (1997) Two tyrosine residues on the alpha subunit are crucial for benzodiazepine binding and allosteric modulation of gamma-aminobutyric acidA receptors. *Mol Pharmacol* 51:833-841.
- Anand R and Lindstrom J (1992) Chromosomal localization of seven neuronal nicotinic acetylcholine receptor subunit genes in humans. *Genomics* 13:962-967.
- Antolik C, Catino DH, O'Neill AM, Resneck WG, Ursitti JA and Bloch RJ (2007) The actin binding domain of ACF7 binds directly to the tetratricopeptide repeat domains of rapsyn. *Neuroscience* 145:56-65.
- Aramakis VB, Hsieh CY, Leslie FM and Metherate R (2000) A critical period for nicotine-induced disruption of synaptic development in rat auditory cortex. *J Neurosci* 20:6106-6116.
- Araud T, Wonnacott S and Bertrand D (2010) Associated proteins: The universal toolbox controlling ligand gated ion channel function. *Biochem Pharmacol* 80:160-169.

- Arevalo E, Chiara DC, Forman SA, Cohen JB and Miller KW (2005) Gating-enhanced accessibility of hydrophobic sites within the transmembrane region of the nicotinic acetylcholine receptor's δ -subunit. A time-resolved photolabeling study. *J Biol Chem* 280:13631-13640.
- Arias HR, Bhumireddy P, Spitzmaul G, Trudell JR and Bouzat C (2006) Molecular mechanisms and binding site location for the noncompetitive antagonist crystal violet on nicotinic acetylcholine receptors. *Biochemistry* 45:2014-2026.
- Arneric SP, Holladay M and Williams M (2007) Neuronal nicotinic receptors: a perspective on two decades of drug discovery research. *Biochem Pharmacol* 74:1092-1101.
- Arredondo J, Chernyavsky AI and Grando SA (2006a) The nicotinic receptor antagonists abolish pathobiologic effects of tobacco-derived nitrosamines on BEP2D cells. *J Cancer Res Clin Oncol* 132:653-663.
- Arredondo J, Chernyavsky AI, Jolkovsky DL, Webber RJ and Grando SA (2006b) SLURP-2: A novel cholinergic signaling peptide in human mucocutaneous epithelium. *J Cell Physiol* 208:238-245.
- Arroyo-Jimenez MM, Bourgeois JP, Marubio LM, Le Sourd AM, Ottersen OP, Rinvik E, Fairen A and Changeux JP (1999) Ultrastructural localization of the $\alpha 4$ -subunit of the neuronal acetylcholine nicotinic receptor in the rat substantia nigra. *J Neurosci* 19:6475-6487.
- Aubert I, Araujo DM, Cecyre D, Robitaille Y, Gauthier S and Quirion R (1992) Comparative alterations of nicotinic and muscarinic binding sites in Alzheimer's and Parkinson's diseases. *J Neurochem* 58:529-541.
- Auerbach A (2005) Gating of acetylcholine receptor channels: brownian motion across a broad transition state. *Proc Natl Acad Sci U S A* 102:1408-1412.
- Auerbach A and Akk G (1998) Desensitization of mouse nicotinic acetylcholine receptor channels. A two-gate mechanism. *J Gen Physiol* 112:181-197.
- Azam L and McIntosh JM (2009) Alpha-conotoxins as pharmacological probes of nicotinic acetylcholine receptors. *Acta Pharmacol Sin* 30:771-783.
- Baldwin JM (1980) The structure of human carbonmonoxy haemoglobin at 2.7 Å resolution. *J Mol Biol* 136:103-128.
- Banks MI, White JA and Pearce RA (2000) Interactions between distinct GABA(A) circuits in hippocampus. *Neuron* 25:449-457.
- Barik J and Wonnacott S (2006) Indirect modulation by $\alpha 7$ nicotinic acetylcholine receptors of noradrenaline release in rat hippocampal slices: interaction with glutamate and GABA systems and effect of nicotine withdrawal. *Mol Pharmacol* 69:618-628.
- Barlowe C (2003) Signals for COPII-dependent export from the ER: what's the ticket out? *Trends Cell Biol* 13:295-300.
- Barnes NM and Sharp T (1999) A review of central 5-HT receptors and their function. *Neuropharmacology* 38:1083-1152.
- Barry PH and Lynch JW (2005) Ligand-gated channels. *IEEE Trans Nanobioscience* 4:70-80.
- Bartol TM, Jr., Land BR, Salpeter EE and Salpeter MM (1991) Monte Carlo simulation of miniature endplate current generation in the vertebrate neuromuscular junction. *Biophys J* 59:1290-1307.
- Beene DL, Brandt GS, Zhong W, Zacharias NM, Lester HA and Dougherty DA (2002) Cation- π interactions in ligand recognition by serotonergic (5-HT_{3A}) and nicotinic acetylcholine receptors: the anomalous binding properties of nicotine. *Biochemistry* 41:10262-10269.

- Beene DL, Price KL, Lester HA, Dougherty DA and Lummis SC (2004) Tyrosine residues that control binding and gating in the 5-hydroxytryptamine₃ receptor revealed by unnatural amino acid mutagenesis. *J Neurosci* 24:9097-9104.
- Belelli D, Lambert JJ, Peters JA, Wafford K and Whiting PJ (1997) The interaction of the general anesthetic etomidate with the gamma-aminobutyric acid type A receptor is influenced by a single amino acid. *Proc Natl Acad Sci U S A* 94:11031-11036.
- Belelli D, Pau D, Cabras G, Peters JA and Lambert JJ (1999) A single amino acid confers barbiturate sensitivity upon the GABA rho 1 receptor. *Br J Pharmacol* 127:601-604.
- Bencherif M and Lukas RJ (1993) Cytochalasin modulation of nicotinic cholinergic receptor expression and muscarinic receptor function in human TE671/RD cells: a possible functional role of the cytoskeleton. *J Neurochem* 61:852-864.
- Bera AK and Akabas MH (2005) Spontaneous thermal motion of the GABA(A) receptor M2 channel-lining segments. *J Biol Chem* 280:35506-35512.
- Bera AK, Chatav M and Akabas MH (2002) GABA(A) receptor M2-M3 loop secondary structure and changes in accessibility during channel gating. *J Biol Chem* 277:43002-43010.
- Berezhnoy D, Nyfeler Y, Gonthier A, Schwob H, Goeldner M and Sigel E (2004) On the benzodiazepine binding pocket in GABAA receptors. *J Biol Chem* 279:3160-3168.
- Bermudez I and Moroni M (2006) Phosphorylation and function of alpha4beta2 receptor. *J Mol Neurosci* 30:97-98.
- Bertrand D, Bertrand S, Cassar S, Gubbins E, Li J and Gopalakrishnan M (2008) Positive allosteric modulation of the alpha7 nicotinic acetylcholine receptor: ligand interactions with distinct binding sites and evidence for a prominent role of the M2-M3 segment. *Mol Pharmacol* 74:1407-1416.
- Bertrand D and Gopalakrishnan M (2007) Allosteric modulation of nicotinic acetylcholine receptors. *Biochem Pharmacol* 74:1155-1163.
- Besson M, Granon S, Mameli-Engvall M, Cloez-Tayarani I, Maubourguet N, Cormier A, Cazala P, David V, Changeux JP and Faure P (2007) Long-term effects of chronic nicotine exposure on brain nicotinic receptors. *Proc Natl Acad Sci U S A* 104:8155-8160.
- Betz H, Kuhse J, Schmieden V, Laube B, Kirsch J and Harvey RJ (1999) Structure and functions of inhibitory and excitatory glycine receptors. *Ann N Y Acad Sci* 868:667-676.
- Blanton MP, McCardy EA, Huggins A and Parikh D (1998) Probing the structure of the nicotinic acetylcholine receptor with the hydrophobic photoreactive probes [¹²⁵I]TID-BE and [¹²⁵I]TIDPC/16. *Biochemistry* 37:14545-14555.
- Blount P and Merlie JP (1988) Native folding of an acetylcholine receptor alpha subunit expressed in the absence of other receptor subunits. *J Biol Chem* 263:1072-1080.
- Blount P and Merlie JP (1990) Mutational analysis of muscle nicotinic acetylcholine receptor subunit assembly. *J Cell Biol* 111:2613-2622.
- Blount P and Merlie JP (1991) BIP associates with newly synthesized subunits of the mouse muscle nicotinic receptor. *J Cell Biol* 113:1125-1132.
- Blum AP, Lester HA and Dougherty DA (2010) Nicotinic pharmacophore: the pyridine N of nicotine and carbonyl of acetylcholine hydrogen bond across a subunit interface to a backbone NH. *Proc Natl Acad Sci U S A* 107:13206-13211.

- Bocquet N, Nury H, Baaden M, Le Poupon C, Changeux JP, Delarue M and Corringer PJ (2009) X-ray structure of a pentameric ligand-gated ion channel in an apparently open conformation. *Nature* 457:111-114.
- Boess FG, Steward LJ, Steele JA, Liu D, Reid J, Glencorse TA and Martin IL (1997) Analysis of the ligand binding site of the 5-HT₃ receptor using site directed mutagenesis: importance of glutamate 106. *Neuropharmacology* 36:637-647.
- Bourin M, Ripoll N and Dailly E (2003) Nicotinic receptors and Alzheimer's disease. *Curr Med Res Opin* 19:169-177.
- Bourne Y, Talley TT, Hansen SB, Taylor P and Marchot P (2005) Crystal structure of a Cbtx-AChBP complex reveals essential interactions between snake alpha-neurotoxins and nicotinic receptors. *EMBO J* 24:1512-1522.
- Brannigan G, Henin J, Law R, Eckenhoff R and Klein ML (2008) Embedded cholesterol in the nicotinic acetylcholine receptor. *Proc Natl Acad Sci U S A* 105:14418-14423.
- Breese CR, Marks MJ, Logel J, Adams CE, Sullivan B, Collins AC and Leonard S (1997) Effect of smoking history on [³H]nicotine binding in human postmortem brain. *J Pharmacol Exp Ther* 282:7-13.
- Brejci K, van Dijk WJ, Klaassen RV, Schuurmans M, van Der Oost J, Smit AB and Sixma TK (2001) Crystal structure of an ACh-binding protein reveals the ligand-binding domain of nicotinic receptors. *Nature* 411:269-276.
- Briggs CA, Gubbins EJ, Marks MJ, Putman CB, Thimmapaya R, Meyer MD and Surowy CS (2006a) Untranslated region-dependent exclusive expression of high-sensitivity subforms of alpha4beta2 and alpha3beta2 nicotinic acetylcholine receptors. *Mol Pharmacol* 70:227-240.
- Briggs CA, Gubbins EJ, Marks MJ, Putman CB, Thimmapaya R, Meyer MD and Surowy CS (2006b) Untranslated Region Dependent Exclusive Expression of High-Sensitivity Subforms of {alpha}4{beta}2 and {alpha}3{beta}2 Nicotinic Acetylcholine Receptors. *Mol Pharmacol*.
- Brodsky JL, Werner ED, Dubas ME, Goeckeler JL, Kruse KB and McCracken AA (1999) The requirement for molecular chaperones during endoplasmic reticulum-associated protein degradation demonstrates that protein export and import are mechanistically distinct. *J Biol Chem* 274:3453-3460.
- Buhr A, Baur R and Sigel E (1997a) Subtle changes in residue 77 of the gamma subunit of alpha1beta2gamma2 GABA_A receptors drastically alter the affinity for ligands of the benzodiazepine binding site. *J Biol Chem* 272:11799-11804.
- Buhr A, Schaerer MT, Baur R and Sigel E (1997b) Residues at positions 206 and 209 of the alpha1 subunit of gamma-aminobutyric AcidA receptors influence affinities for benzodiazepine binding site ligands. *Mol Pharmacol* 52:676-682.
- Buisson B and Bertrand D (2001) Chronic exposure to nicotine upregulates the human (alpha)4((beta)2 nicotinic acetylcholine receptor function. *J Neurosci* 21:1819-1829.
- Buisson B and Bertrand D (2002) Nicotine addiction: the possible role of functional upregulation. *Trends Pharmacol Sci* 23:130-136.
- Burghaus L, Schutz U, Krempel U, de Vos RA, Jansen Steur EN, Wevers A, Lindstrom J and Schroder H (2000) Quantitative assessment of nicotinic acetylcholine receptor proteins in the cerebral cortex of Alzheimer patients. *Brain Res Mol Brain Res* 76:385-388.
- Buxbaum JD, Silverman J, Keddache M, Smith CJ, Hollander E, Ramoz N and Reichert JG (2004) Linkage analysis for autism in a subset families with obsessive-compulsive behaviors:

- evidence for an autism susceptibility gene on chromosome 1 and further support for susceptibility genes on chromosome 6 and 19. *Mol Psychiatry* 9:144-150.
- Campagna-Slater V and Weaver DF (2007) Anaesthetic binding sites for etomidate and propofol on a GABAA receptor model. *Neurosci Lett* 418:28-33.
- Carlisle DL, Hopkins TM, Gaither-Davis A, Silhanek MJ, Luketich JD, Christie NA and Siegfried JM (2004) Nicotine signals through muscle-type and neuronal nicotinic acetylcholine receptors in both human bronchial epithelial cells and airway fibroblasts. *Respir Res* 5:27.
- Carlisle DL, Liu X, Hopkins TM, Swick MC, Dhir R and Siegfried JM (2007) Nicotine activates cell-signaling pathways through muscle-type and neuronal nicotinic acetylcholine receptors in non-small cell lung cancer cells. *Pulm Pharmacol Ther* 20:629-641.
- Carmeliet P and Jain RK (2000) Angiogenesis in cancer and other diseases. *Nature* 407:249-257.
- Castelan F, Mulet J, Aldea M, Sala S, Sala F and Criado M (2007) Cytoplasmic regions adjacent to the M3 and M4 transmembrane segments influence expression and function of alpha7 nicotinic acetylcholine receptors. A study with single amino acid mutants. *J Neurochem* 100:406-415.
- Castro NG and Albuquerque EX (1995) alpha-Bungarotoxin-sensitive hippocampal nicotinic receptor channel has a high calcium permeability. *Biophys J* 68:516-524.
- Celie PH, Klaassen RV, van Rossum-Fikkert SE, van Elk R, van Nierop P, Smit AB and Sixma TK (2005) Crystal structure of acetylcholine-binding protein from *Bulinus truncatus* reveals the conserved structural scaffold and sites of variation in nicotinic acetylcholine receptors. *J Biol Chem* 280:26457-26466.
- Celie PH, van Rossum-Fikkert SE, van Dijk WJ, Brejc K, Smit AB and Sixma TK (2004) Nicotine and carbamylcholine binding to nicotinic acetylcholine receptors as studied in AChBP crystal structures. *Neuron* 41:907-914.
- Chakrapani S, Bailey TD and Auerbach A (2004) Gating dynamics of the acetylcholine receptor extracellular domain. *J Gen Physiol* 123:341-356.
- Chang CS, Olcese R and Olsen RW (2003) A single M1 residue in the beta2 subunit alters channel gating of GABAA receptor in anesthetic modulation and direct activation. *J Biol Chem* 278:42821-42828.
- Changeux JP (1964) Allosteric Interactions Interpreted in Terms of Quaternary Structure. *Brookhaven Symp Biol* 17:232-249.
- Charpentier E, Wiesner A, Huh KH, Ogier R, Hoda JC, Allaman G, Raggenbass M, Feuerbach D, Bertrand D and Fuhrer C (2005) Alpha7 neuronal nicotinic acetylcholine receptors are negatively regulated by tyrosine phosphorylation and Src-family kinases. *J Neurosci* 25:9836-9849.
- Chen CS, Lee CH, Hsieh CD, Ho CT, Pan MH, Huang CS, Tu SH, Wang YJ, Chen LC, Chang YJ, Wei PL, Yang YY, Wu CH and Ho YS (2011) Nicotine-induced human breast cancer cell proliferation attenuated by garcinol through down-regulation of the nicotinic receptor and cyclin D3 proteins. *Breast Cancer Res Treat* 125:73-87.
- Chen RJ, Ho YS, Guo HR and Wang YJ (2008) Rapid activation of Stat3 and ERK1/2 by nicotine modulates cell proliferation in human bladder cancer cells. *Toxicol Sci* 104:283-293.
- Cheng A, McDonald NA and Connolly CN (2005) Cell surface expression of 5-hydroxytryptamine type 3 receptors is promoted by RIC-3. *J Biol Chem* 280:22502-22507.
- Chernyavsky AI, Arredondo J, Marubio LM and Grando SA (2004) Differential regulation of keratinocyte chemokinesis and chemotaxis through distinct nicotinic receptor subtypes. *J Cell Sci* 117:5665-5679.

Chimienti F, Hogg RC, Plantard L, Lehmann C, Brakch N, Fischer J, Huber M, Bertrand D and Hohl D (2003) Identification of SLURP-1 as an epidermal neuromodulator explains the clinical phenotype of Mal de Meleda. *Hum Mol Genet* 12:3017-3024.

Chini B, Clementi F, Hukovic N and Sher E (1992) Neuronal-type alpha-bungarotoxin receptors and the alpha 5-nicotinic receptor subunit gene are expressed in neuronal and nonneuronal human cell lines. *Proc Natl Acad Sci U S A* 89:1572-1576.

Chini B, Raimond E, Elgoyhen AB, Moralli D, Balzaretto M and Heinemann S (1994) Molecular cloning and chromosomal localization of the human alpha 7-nicotinic receptor subunit gene (CHRNA7). *Genomics* 19:379-381.

Cho CH, Song W, Leitzell K, Teo E, Meleth AD, Quick MW and Lester RA (2005) Rapid upregulation of alpha7 nicotinic acetylcholine receptors by tyrosine dephosphorylation. *J Neurosci* 25:3712-3723.

Clarke PB, Schwartz RD, Paul SM, Pert CB and Pert A (1985) Nicotinic binding in rat brain: autoradiographic comparison of [3H]acetylcholine, [3H]nicotine, and [125I]-alpha-bungarotoxin. *J Neurosci* 5:1307-1315.

Coe JW, Brooks PR, Vetelino MG, Wirtz MC, Arnold EP, Huang J, Sands SB, Davis TI, Lebel LA, Fox CB, Shrikhande A, Heym JH, Schaeffer E, Rollema H, Lu Y, Mansbach RS, Chambers LK, Rovetti CC, Schulz DW, Tingley FD, 3rd and O'Neill BT (2005) Varenicline: an alpha4beta2 nicotinic receptor partial agonist for smoking cessation. *J Med Chem* 48:3474-3477.

Colledge M and Froehner SC (1997) Tyrosine phosphorylation of nicotinic acetylcholine receptor mediates Grb2 binding. *J Neurosci* 17:5038-5045.

Connolly CN, Krishek BJ, McDonald BJ, Smart TG and Moss SJ (1996) Assembly and cell surface expression of heteromeric and homomeric gamma-aminobutyric acid type A receptors. *J Biol Chem* 271:89-96.

Connolly GN, Alpert HR, Wayne GF and Koh H (2007) Trends in nicotine yield in smoke and its relationship with design characteristics among popular US cigarette brands, 1997-2005. *Tob Control* 16:e5.

Conti-Fine BM, Navaneetham D, Lei S and Maus AD (2000) Neuronal nicotinic receptors in non-neuronal cells: new mediators of tobacco toxicity? *Eur J Pharmacol* 393:279-294.

Corringer PJ, Bertrand S, Galzi JL, Devillers-Thierry A, Changeux JP and Bertrand D (1999a) Molecular basis of the charge selectivity of nicotinic acetylcholine receptor and related ligand-gated ion channels. *Novartis Found Symp* 225:215-224; discussion 224-230.

Corringer PJ, Bertrand S, Galzi JL, Devillers-Thierry A, Changeux JP and Bertrand D (1999b) Mutational analysis of the charge selectivity filter of the alpha7 nicotinic acetylcholine receptor. *Neuron* 22:831-843.

Corringer PJ, Galzi JL, Eisele JL, Bertrand S, Changeux JP and Bertrand D (1995) Identification of a new component of the agonist binding site of the nicotinic alpha 7 homooligomeric receptor. *J Biol Chem* 270:11749-11752.

Corringer PJ, Le Novere N and Changeux JP (2000) Nicotinic receptors at the amino acid level. *Annu Rev Pharmacol Toxicol* 40:431-458.

Corsi AK and Schekman R (1997) The luminal domain of Sec63p stimulates the ATPase activity of BiP and mediates BiP recruitment to the translocon in *Saccharomyces cerevisiae*. *J Cell Biol* 137:1483-1493.

Court J, Martin-Ruiz C, Piggott M, Spurden D, Griffiths M and Perry E (2001) Nicotinic receptor abnormalities in Alzheimer's disease. *Biol Psychiatry* 49:175-184.

- Court JA, Martin-Ruiz C, Graham A and Perry E (2000) Nicotinic receptors in human brain: topography and pathology. *J Chem Neuroanat* 20:281-298.
- Curtis L, Buisson B, Bertrand S and Bertrand D (2002) Potentiation of human alpha4beta2 neuronal nicotinic acetylcholine receptor by estradiol. *Mol Pharmacol* 61:127-135.
- Curzon P, Anderson DJ, Nikkei AL, Fox GB, Gopalakrishnan M, Decker MW and Bitner RS (2006) Antisense knockdown of the rat alpha7 nicotinic acetylcholine receptor produces spatial memory impairment. *Neurosci Lett* 410:15-19.
- Curzon P, Brioni JD and Decker MW (1996) Effect of intraventricular injections of dihydro-beta-erythroidine (DH beta E) on spatial memory in the rat. *Brain Res* 714:185-191.
- Cymes GD, Grosman C and Auerbach A (2002) Structure of the transition state of gating in the acetylcholine receptor channel pore: a phi-value analysis. *Biochemistry* 41:5548-5555.
- Dahan DS, Dibas MI, Petersson EJ, Auyeung VC, Chanda B, Bezanilla F, Dougherty DA and Lester HA (2004) A fluorophore attached to nicotinic acetylcholine receptor beta M2 detects productive binding of agonist to the alpha delta site. *Proc Natl Acad Sci U S A* 101:10195-10200.
- Dajas-Bailador F and Wonnacott S (2004) Nicotinic acetylcholine receptors and the regulation of neuronal signalling. *Trends Pharmacol Sci* 25:317-324.
- Daly JW, Garraffo HM, Spande TF, Decker MW, Sullivan JP and Williams M (2000) Alkaloids from frog skin: the discovery of epibatidine and the potential for developing novel non-opioid analgesics. *Nat Prod Rep* 17:131-135.
- Dani JA and Bertrand D (2006) Nicotinic Acetylcholine Receptors and Nicotinic Cholinergic Mechanisms of the Central Nervous System. *Annu Rev Pharmacol Toxicol*.
- Dani JA and Bertrand D (2007) Nicotinic acetylcholine receptors and nicotinic cholinergic mechanisms of the central nervous system. *Annu Rev Pharmacol Toxicol* 47:699-729.
- Dani JA, Radcliffe KA and Pidoplichko VI (2000) Variations in desensitization of nicotinic acetylcholine receptors from hippocampus and midbrain dopamine areas. *Eur J Pharmacol* 393:31-38.
- Dasgupta P, Kinkade R, Joshi B, Decook C, Haura E and Chellappan S (2006a) Nicotine inhibits apoptosis induced by chemotherapeutic drugs by up-regulating XIAP and survivin. *Proc Natl Acad Sci U S A* 103:6332-6337.
- Dasgupta P, Rastogi S, Pillai S, Ordonez-Ercan D, Morris M, Haura E and Chellappan S (2006b) Nicotine induces cell proliferation by beta-arrestin-mediated activation of Src and Rb-Raf-1 pathways. *J Clin Invest* 116:2208-2217.
- Davies PA, Wang W, Hales TG and Kirkness EF (2003) A novel class of ligand-gated ion channel is activated by Zn²⁺. *J Biol Chem* 278:712-717.
- Dellisanti CD, Yao Y, Stroud JC, Wang ZZ and Chen L (2007) Crystal structure of the extracellular domain of nAChR alpha1 bound to alpha-bungarotoxin at 1.94 Å resolution. *Nat Neurosci* 10:953-962.
- Descarries L, Gisiger V and Steriade M (1997) Diffuse transmission by acetylcholine in the CNS. *Prog Neurobiol* 53:603-625.
- Dineley KT, Westerman M, Bui D, Bell K, Ashe KH and Sweatt JD (2001) Beta-amyloid activates the mitogen-activated protein kinase cascade via hippocampal alpha7 nicotinic acetylcholine receptors: In vitro and in vivo mechanisms related to Alzheimer's disease. *J Neurosci* 21:4125-4133.

Dougherty DA (1996) Cation- π interactions in chemistry and biology: a new view of benzene, Phe, Tyr, and Trp. *Science* 271:163-168.

Dougherty DA and Stauffer DA (1990) Acetylcholine binding by a synthetic receptor: implications for biological recognition. *Science* 250:1558-1560.

Doyle DA, Morais Cabral J, Pfuetzner RA, Kuo A, Gulbis JM, Cohen SL, Chait BT and MacKinnon R (1998) The structure of the potassium channel: molecular basis of K⁺ conduction and selectivity. *Science* 280:69-77.

Drisdell RC, Manzana E and Green WN (2004) The role of palmitoylation in functional expression of nicotinic $\alpha 7$ receptors. *J Neurosci* 24:10502-10510.

Dukat M and Glennon RA (2003) Epibatidine: impact on nicotinic receptor research. *Cell Mol Neurobiol* 23:365-378.

Duncalfe LL, Carpenter MR, Smillie LB, Martin IL and Dunn SM (1996) The major site of photoaffinity labeling of the gamma-aminobutyric acid type A receptor by [3H]flunitrazepam is histidine 102 of the alpha subunit. *J Biol Chem* 271:9209-9214.

Dutertre S and Lewis RJ (2006) Toxin insights into nicotinic acetylcholine receptors. *Biochem Pharmacol*.

Dutzler R, Campbell EB and MacKinnon R (2003) Gating the selectivity filter in Cl⁻ chloride channels. *Science* 300:108-112.

Dwoskin LP and Crooks PA (2001) Competitive neuronal nicotinic receptor antagonists: a new direction for drug discovery. *J Pharmacol Exp Ther* 298:395-402.

Eddins D, Sproul AD, Lyford LK, McLaughlin JT and Rosenberg RL (2002) Glutamate 172, essential for modulation of L247T $\alpha 7$ ACh receptors by Ca²⁺, lines the extracellular vestibule. *Am J Physiol Cell Physiol* 283:C1454-1460.

Egleton RD, Brown KC and Dasgupta P (2008) Nicotinic acetylcholine receptors in cancer: multiple roles in proliferation and inhibition of apoptosis. *Trends Pharmacol Sci* 29:151-158.

England PM, Lester HA, Davidson N and Dougherty DA (1997) Site-specific, photochemical proteolysis applied to ion channels in vivo. *Proc Natl Acad Sci U S A* 94:11025-11030.

England PM, Zhang Y, Dougherty DA and Lester HA (1999) Backbone mutations in transmembrane domains of a ligand-gated ion channel: implications for the mechanism of gating. *Cell* 96:89-98.

Faghhi R, Gopalakrishnan M and Briggs CA (2008) Allosteric modulators of the $\alpha 7$ nicotinic acetylcholine receptor. *J Med Chem* 51:701-712.

Fambrough DM (1979) Control of acetylcholine receptors in skeletal muscle. *Physiol Rev* 59:165-227.

Fenster CP, Beckman ML, Parker JC, Sheffield EB, Whitworth TL, Quick MW and Lester RA (1999) Regulation of $\alpha 4\beta 2$ nicotinic receptor desensitization by calcium and protein kinase C. *Mol Pharmacol* 55:432-443.

Fernandes C, Hoyle E, Dempster E, Schalkwyk LC and Collier DA (2006) Performance deficit of $\alpha 7$ nicotinic receptor knockout mice in a delayed matching-to-place task suggests a mild impairment of working/episodic-like memory. *Genes Brain Behav* 5:433-440.

Ferretti R and Gianandrea G (1954) [Edematogenic effect of isoniazid on the tuberculous lung; anatomo-pathological study.]. *Ann Ist Carlo Forlanini* 14:288-292.

Fiore MC, McCarthy DE, Jackson TC, Zehner ME, Jorenby DE, Mielke M, Smith SS, Guiliani TA and Baker TB (2004) Integrating smoking cessation treatment into primary care: an effectiveness study. *Prev Med* 38:412-420.

Fisher JL and Dani JA (2000) Nicotinic receptors on hippocampal cultures can increase synaptic glutamate currents while decreasing the NMDA-receptor component. *Neuropharmacology* 39:2756-2769.

Folkman J (2006) Angiogenesis. *Annu Rev Med* 57:1-18.

Forsayeth JR, Gu Y and Hall ZW (1992) BiP forms stable complexes with unassembled subunits of the acetylcholine receptor in transfected COS cells and in C2 muscle cells. *J Cell Biol* 117:841-847.

Gaddum JH and Picarelli ZP (1957) Two kinds of tryptamine receptor. *Br J Pharmacol Chemother* 12:323-328.

Gahring LC, Vasquez-Opazo GA, Rogers SW. (2010) Choline promotes nicotinic receptor alpha4 + beta2 up-regulation. *J Biol Chem.* 285:19793-801.

Galiano RD, Tepper OM, Pelo CR, Bhatt KA, Callaghan M, Bastidas N, Bunting S, Steinmetz HG and Gurtner GC (2004) Topical vascular endothelial growth factor accelerates diabetic wound healing through increased angiogenesis and by mobilizing and recruiting bone marrow-derived cells. *Am J Pathol* 164:1935-1947.

Galzi JL, Bertrand S, Corringer PJ, Changeux JP and Bertrand D (1996) Identification of calcium binding sites that regulate potentiation of a neuronal nicotinic acetylcholine receptor. *EMBO J* 15:5824-5832.

Galzi JL, Devillers-Thierry A, Hussy N, Bertrand S, Changeux JP and Bertrand D (1992) Mutations in the channel domain of a neuronal nicotinic receptor convert ion selectivity from cationic to anionic. *Nature* 359:500-505.

Gao F, Bren N, Burghardt TP, Hansen S, Henchman RH, Taylor P, McCammon JA and Sine SM (2005) Agonist-mediated conformational changes in acetylcholine-binding protein revealed by simulation and intrinsic tryptophan fluorescence. *J Biol Chem* 280:8443-8451.

Gay EA and Yakel JL (2007) Gating of nicotinic ACh receptors; new insights into structural transitions triggered by agonist binding that induce channel opening. *J Physiol* 584:727-733.

Ge S and Dani JA (2005) Nicotinic acetylcholine receptors at glutamate synapses facilitate long-term depression or potentiation. *J Neurosci* 25:6084-6091.

Gelman MS, Chang W, Thomas DY, Bergeron JJ and Prives JM (1995) Role of the endoplasmic reticulum chaperone calnexin in subunit folding and assembly of nicotinic acetylcholine receptors. *J Biol Chem* 270:15085-15092.

Gentry CL and Lukas RJ (2002) Regulation of nicotinic acetylcholine receptor numbers and function by chronic nicotine exposure. *Curr Drug Targets CNS Neurol Disord* 1:359-385.

Gething MJ (1999) Role and regulation of the ER chaperone BiP. *Semin Cell Dev Biol* 10:465-472.

Giraudat J, Dennis M, Heidmann T, Chang JY and Changeux JP (1986) Structure of the high-affinity binding site for noncompetitive blockers of the acetylcholine receptor: serine-262 of the delta subunit is labeled by [3H]chlorpromazine. *Proc Natl Acad Sci U S A* 83:2719-2723.

Glennon RA (2005) Pharmacophore identification for s1 receptor binding. *Mini-Rev. Med. Chem.* 5:927-940.

- Glennon RA and Dukat M (2000) Central nicotinic receptor ligands and pharmacophores. *Pharm Acta Helv* **74**:103-114.
- Glennon RA, Dukat M and Liao L (2004) Musings on alpha4beta2 nicotinic acetylcholine (nACh) receptor pharmacophore models. *Curr Top Med Chem* **4**:631-644.
- Gotti C and Clementi F (2004) Neuronal nicotinic receptors: from structure to pathology. *Prog Neurobiol* **74**:363-396.
- Gotti C, Moretti M, Clementi F, Riganti L, McIntosh JM, Collins AC, Marks MJ and Whiteaker P (2005) Expression of nigrostriatal alpha 6-containing nicotinic acetylcholine receptors is selectively reduced, but not eliminated, by beta 3 subunit gene deletion. *Mol Pharmacol* **67**:2007-2015.
- Gotti C, Riganti L, Vailati S and Clementi F (2006a) Brain neuronal nicotinic receptors as new targets for drug discovery. *Curr Pharm Des* **12**:407-428.
- Gotti C, Zoli M and Clementi F (2006b) Brain nicotinic acetylcholine receptors: native subtypes and their relevance. *Trends Pharmacol Sci* **27**:482-491.
- Granon S, Faure P and Changeux JP (2003) Executive and social behaviors under nicotinic receptor regulation. *Proc Natl Acad Sci U S A* **100**:9596-9601.
- Gray R, Rajan AS, Radcliffe KA, Yakehiro M and Dani JA (1996) Hippocampal synaptic transmission enhanced by low concentrations of nicotine. *Nature* **383**:713-716.
- Griffioen AW and Molema G (2000) Angiogenesis: potentials for pharmacologic intervention in the treatment of cancer, cardiovascular diseases, and chronic inflammation. *Pharmacol Rev* **52**:237-268.
- Grosman C, Zhou M and Auerbach A (2000) Mapping the conformational wave of acetylcholine receptor channel gating. *Nature* **403**:773-776.
- Gu Y, Forsayeth JR, Verrall S, Yu XM and Hall ZW (1991) Assembly of the mammalian muscle acetylcholine receptor in transfected COS cells. *J Cell Biol* **114**:799-807.
- Guan ZZ, Zhang X, Ravid R and Nordberg A (2000) Decreased protein levels of nicotinic receptor subunits in the hippocampus and temporal cortex of patients with Alzheimer's disease. *J Neurochem* **74**:237-243.
- Gunther U, Benson J, Benke D, Fritschy JM, Reyes G, Knoflach F, Crestani F, Aguzzi A, Arigoni M, Lang Y and et al. (1995) Benzodiazepine-insensitive mice generated by targeted disruption of the gamma 2 subunit gene of gamma-aminobutyric acid type A receptors. *Proc Natl Acad Sci U S A* **92**:7749-7753.
- Gunthorpe MJ and Lummis SC (2001) Conversion of the ion selectivity of the 5-HT(3a) receptor from cationic to anionic reveals a conserved feature of the ligand-gated ion channel superfamily. *J Biol Chem* **276**:10977-10983.
- Guo JZ, Tredway TL and Chiappinelli VA (1998) Glutamate and GABA release are enhanced by different subtypes of presynaptic nicotinic receptors in the lateral geniculate nucleus. *J Neurosci* **18**:1963-1969.
- Gyermek L (1996) New local anesthetic agents. *Anesthesiology* **85**:226-227.
- Hahn B, Shoaib M and Stolerman IP (2003) Involvement of the prefrontal cortex but not the dorsal hippocampus in the attention-enhancing effects of nicotine in rats. *Psychopharmacology (Berl)* **168**:271-279.

- Halevi S, McKay J, Palfreyman M, Yassin L, Eshel M, Jorgensen E and Treinin M (2002) The *C. elegans ric-3* gene is required for maturation of nicotinic acetylcholine receptors. *EMBO J* **21**:1012-1020.
- Halevi S, Yassin L, Eshel M, Sala F, Sala S, Criado M and Treinin M (2003) Conservation within the RIC-3 gene family. Effectors of mammalian nicotinic acetylcholine receptor expression. *J Biol Chem* **278**:34411-34417.
- Hansen SB, Sulzenbacher G, Huxford T, Marchot P, Taylor P and Bourne Y (2005) Structures of *Aplysia* AChBP complexes with nicotinic agonists and antagonists reveal distinctive binding interfaces and conformations. *EMBO J* **24**:3635-3646.
- Hansen SB, Talley TT, Radic Z and Taylor P (2004) Structural and ligand recognition characteristics of an acetylcholine-binding protein from *Aplysia californica*. *J Biol Chem* **279**:24197-24202.
- Hansen SB and Taylor P (2007) Galanthamine and non-competitive inhibitor binding to ACh-binding protein: evidence for a binding site on non-alpha-subunit interfaces of heteromeric neuronal nicotinic receptors. *J Mol Biol* **369**:895-901.
- Hanson SM, Morlock EV, Satyshur KA and Czajkowski C (2008) Structural requirements for eszopiclone and zolpidem binding to the gamma-aminobutyric acid type-A (GABAA) receptor are different. *J Med Chem* **51**:7243-7252.
- Harvey RJ, Thomas P, James CH, Wilderspin A and Smart TG (1999) Identification of an inhibitory Zn²⁺ binding site on the human glycine receptor alpha1 subunit. *J Physiol* **520 Pt 1**:53-64.
- Heeschen C, Weis M, Aicher A, Dimmeler S and Cooke JP (2002) A novel angiogenic pathway mediated by non-neuronal nicotinic acetylcholine receptors. *J Clin Invest* **110**:527-536.
- Hogg RC and Bertrand D (2004) Nicotinic acetylcholine receptors as drug targets. *Curr Drug Targets CNS Neurol Disord* **3**:123-130.
- Hogg RC and Bertrand D (2007) Partial agonists as therapeutic agents at neuronal nicotinic acetylcholine receptors. *Biochem Pharmacol* **73**:459-468.
- Hogg RC, Raggenbass M and Bertrand D (2003) Nicotinic acetylcholine receptors: from structure to brain function. *Rev Physiol Biochem Pharmacol* **147**:1-46.
- Hosie AM, Buckingham SD, Hamon A and Sattelle DB (2006a) Replacement of asparagine with arginine at the extracellular end of the second transmembrane (M2) region of insect GABA receptors increases sensitivity to penicillin G. *Invert Neurosci* **6**:75-79.
- Hosie AM, Clarke L, da Silva H and Smart TG (2009) Conserved site for neurosteroid modulation of GABA A receptors. *Neuropharmacology* **56**:149-154.
- Hosie AM, Wilkins ME, da Silva HM and Smart TG (2006b) Endogenous neurosteroids regulate GABAA receptors through two discrete transmembrane sites. *Nature* **444**:486-489.
- Hosie AM, Wilkins ME and Smart TG (2007) Neurosteroid binding sites on GABA(A) receptors. *Pharmacol Ther* **116**:7-19.
- Hsiao B, Dweck D and Luetje CW (2001) Subunit-dependent modulation of neuronal nicotinic receptors by zinc. *J Neurosci* **21**:1848-1856.
- Hsiao B, Mihalak KB, Magleby KL and Luetje CW (2008) Zinc potentiates neuronal nicotinic receptors by increasing burst duration. *J Neurophysiol* **99**:999-1007.

Hsiao B, Mihalak KB, Repicky SE, Everhart D, Mederos AH, Malhotra A and Luetje CW (2006) Determinants of zinc potentiation on the alpha4 subunit of neuronal nicotinic receptors. *Mol Pharmacol* **69**:27-36.

Hu M, Liu QS, Chang KT and Berg DK (2002) Nicotinic regulation of CREB activation in hippocampal neurons by glutamatergic and nonglutamatergic pathways. *Mol Cell Neurosci* **21**:616-625.

Hu XQ and Lovinger DM (2008) The L293 residue in transmembrane domain 2 of the 5-HT3A receptor is a molecular determinant of allosteric modulation by 5-hydroxyindole. *Neuropharmacology* **54**:1153-1165.

Hu XQ and Peoples RW (2008) Arginine 246 of the pretransmembrane domain 1 region alters 2,2,2-trichloroethanol action in the 5-hydroxytryptamine3A receptor. *J Pharmacol Exp Ther* **324**:1011-1018.

Hu XQ, Zhang L, Stewart RR and Weight FF (2003) Arginine 222 in the pre-transmembrane domain 1 of 5-HT3A receptors links agonist binding to channel gating. *J Biol Chem* **278**:46583-46589.

Huang K and El-Husseini A (2005) Modulation of neuronal protein trafficking and function by palmitoylation. *Curr Opin Neurobiol* **15**:527-535.

Huganir RL, Delcour AH, Greengard P and Hess GP (1986) Phosphorylation of the nicotinic acetylcholine receptor regulates its rate of desensitization. *Nature* **321**:774-776.

Hung RJ, McKay JD, Gaborieau V, Boffetta P, Hashibe M, Zaridze D, Mukeria A, Szeszenia-Dabrowska N, Lissowska J, Rudnai P, Fabianova E, Mates D, Bencko V, Foretova L, Janout V, Chen C, Goodman G, Field JK, Liloglou T, Xinarianos G, Cassidy A, McLaughlin J, Liu G, Narod S, Krokan HE, Skorpén F, Elvestad MB, Hveem K, Vatten L, Linseisen J, Clavel-Chapelon F, Vineis P, Bueno-de-Mesquita HB, Lund E, Martínez C, Bingham S, Rasmuson T, Hainaut P, Riboli E, Ahrens W, Benhamou S, Lagiou P, Trichopoulos D, Holcatova I, Merletti F, Kjaerheim K, Agudo A, Macfarlane G, Talamini R, Simonato L, Lowry R, Conway DI, Znaor A, Healy C, Zelenika D, Boland A, Delepine M, Foglio M, Lechner D, Matsuda F, Blanche H, Gut I, Heath S, Lathrop M and Brennan P (2008) A susceptibility locus for lung cancer maps to nicotinic acetylcholine receptor subunit genes on 15q25. *Nature* **452**:633-637.

Imoto K, Busch C, Sakmann B, Mishina M, Konno T, Nakai J, Bujo H, Mori Y, Fukuda K and Numa S (1988) Rings of negatively charged amino acids determine the acetylcholine receptor channel conductance. *Nature* **335**:645-648.

Jackson MB (1984) Spontaneous openings of the acetylcholine receptor channel. *Proc Natl Acad Sci U S A* **81**:3901-3904.

Jackson MB (1986) Kinetics of unliganded acetylcholine receptor channel gating. *Biophys J* **49**:663-672.

Jacobi J, Jang JJ, Sundram U, Dayoub H, Fajardo LF and Cooke JP (2002) Nicotine accelerates angiogenesis and wound healing in genetically diabetic mice. *Am J Pathol* **161**:97-104.

Jeanclous EM, Lin L, Treuil MW, Rao J, DeCoster MA and Anand R (2001) The chaperone protein 14-3-3eta interacts with the nicotinic acetylcholine receptor alpha 4 subunit. Evidence for a dynamic role in subunit stabilization. *J Biol Chem* **276**:28281-28290.

Jenkins A, Andreasen A, Trudell JR and Harrison NL (2002) Tryptophan scanning mutagenesis in TM4 of the GABA(A) receptor alpha1 subunit: implications for modulation by inhaled anesthetics and ion channel structure. *Neuropharmacology* **43**:669-678.

- Jenkins A, Greenblatt EP, Faulkner HJ, Bertaccini E, Light A, Lin A, Andreasen A, Viner A, Trudell JR and Harrison NL (2001) Evidence for a common binding cavity for three general anesthetics within the GABAA receptor. *J Neurosci* **21**:RC136.
- Ji D, Lape R and Dani JA (2001) Timing and location of nicotinic activity enhances or depresses hippocampal synaptic plasticity. *Neuron* **31**:131-141.
- Johnson AE and van Waes MA (1999) The translocon: a dynamic gateway at the ER membrane. *Annu Rev Cell Dev Biol* **15**:799-842.
- Jones IW, Bolam JP and Wonnacott S (2001) Presynaptic localisation of the nicotinic acetylcholine receptor beta2 subunit immunoreactivity in rat nigrostriatal dopaminergic neurones. *J Comp Neurol* **439**:235-247.
- Jones S, Sudweeks S and Yakel JL (1999) Nicotinic receptors in the brain: correlating physiology with function. *Trends Neurosci* **22**:555-561.
- Karlin A (2004) A touching picture of nicotinic binding. *Neuron* **41**:841-842.
- Kasa P, Rakonczay Z and Gulya K (1997) The cholinergic system in Alzheimer's disease. *Prog Neurobiol* **52**:511-535.
- Kash TL, Jenkins A, Kelley JC, Trudell JR and Harrison NL (2003) Coupling of agonist binding to channel gating in the GABA(A) receptor. *Nature* **421**:272-275.
- Kawaja MD, Flumerfelt BA and Hryciyshyn AW (1990) A comparison of the subnuclear and ultrastructural distribution of acetylcholinesterase and choline acetyltransferase in the rat interpeduncular nucleus. *Brain Res Bull* **24**:517-523.
- Keller JJ, Keller AB, Bowers BJ and Wehner JM (2005) Performance of alpha7 nicotinic receptor null mutants is impaired in appetitive learning measured in a signaled nose poke task. *Behav Brain Res* **162**:143-152.
- Keller SH, Lindstrom J, Ellisman M and Taylor P (2001) Adjacent basic amino acid residues recognized by the COP I complex and ubiquitination govern endoplasmic reticulum to cell surface trafficking of the nicotinic acetylcholine receptor alpha-Subunit. *J Biol Chem* **276**:18384-18391.
- Keller SH, Lindstrom J and Taylor P (1998) Inhibition of glucose trimming with castanospermine reduces calnexin association and promotes proteasome degradation of the alpha-subunit of the nicotinic acetylcholine receptor. *J Biol Chem* **273**:17064-17072.
- Kelley SP, Dunlop JI, Kirkness EF, Lambert JJ and Peters JA (2003) A cytoplasmic region determines single-channel conductance in 5-HT3 receptors. *Nature* **424**:321-324.
- Keramidas A, Moorhouse AJ, Schofield PR and Barry PH (2004) Ligand-gated ion channels: mechanisms underlying ion selectivity. *Prog Biophys Mol Biol* **86**:161-204.
- Kitagawa H, Takenouchi T, Azuma R, Wesnes KA, Kramer WG, Clody DE and Burnett AL (2003) Safety, pharmacokinetics, and effects on cognitive function of multiple doses of GTS-21 in healthy, male volunteers. *Neuropsychopharmacology* **28**:542-551.
- Klapproth H, Racke K and Wessler I (1998) Acetylcholine and nicotine stimulate the release of granulocyte-macrophage colony stimulating factor from cultured human bronchial epithelial cells. *Naunyn Schmiedebergs Arch Pharmacol* **357**:472-475.
- Klink R, de Kerchove d'Exaerde A, Zoli M and Changeux JP (2001) Molecular and physiological diversity of nicotinic acetylcholine receptors in the midbrain dopaminergic nuclei. *J Neurosci* **21**:1452-1463.

- Kooyman AR, van Hooft JA, Vanderheijden PM and Vijverberg HP (1994) Competitive and non-competitive effects of 5-hydroxyindole on 5-HT₃ receptors in N1E-115 neuroblastoma cells. *Br J Pharmacol* **112**:541-546.
- Koshland DE, Jr. (1963) Correlation of Structure and Function in Enzyme Action. *Science* **142**:1533-1541.
- Krasowski MD and Harrison NL (1999) General anaesthetic actions on ligand-gated ion channels. *Cell Mol Life Sci* **55**:1278-1303.
- Krasowski MD, Nishikawa K, Nikolaeva N, Lin A and Harrison NL (2001) Methionine 286 in transmembrane domain 3 of the GABA_A receptor beta subunit controls a binding cavity for propofol and other alkylphenol general anesthetics. *Neuropharmacology* **41**:952-964.
- Kreienkamp HJ, Maeda RK, Sine SM and Taylor P (1995) Intersubunit contacts governing assembly of the mammalian nicotinic acetylcholine receptor. *Neuron* **14**:635-644.
- Krishek BJ, Moss SJ and Smart TG (1998) Interaction of H⁺ and Zn²⁺ on recombinant and native rat neuronal GABA_A receptors. *J Physiol* **507** (Pt 3):639-652.
- Kucken AM, Wagner DA, Ward PR, Teissere JA, Boileau AJ and Czajkowski C (2000) Identification of benzodiazepine binding site residues in the gamma₂ subunit of the gamma-aminobutyric acid(A) receptor. *Mol Pharmacol* **57**:932-939.
- Kuo YP, Xu L, Eaton JB, Zhao L, Wu J and Lukas RJ (2005) Roles for nicotinic acetylcholine receptor subunit large cytoplasmic loop sequences in receptor expression and function. *J Pharmacol Exp Ther* **314**:455-466.
- Kuryatov A, Luo J, Cooper J and Lindstrom J (2005) Nicotine acts as a pharmacological chaperone to up-regulate human alpha₄beta₂ acetylcholine receptors. *Mol Pharmacol* **68**:1839-1851.
- Lamb JA, Moore J, Bailey A and Monaco AP (2000) Autism: recent molecular genetic advances. *Hum Mol Genet* **9**:861-868.
- Lamb PW, Melton MA and Yakel JL (2005) Inhibition of neuronal nicotinic acetylcholine receptor channels expressed in *Xenopus* oocytes by beta-amyloid₁₋₄₂ peptide. *J Mol Neurosci* **27**:13-21.
- Lansdell SJ, Gee VJ, Harkness PC, Doward AI, Baker ER, Gibb AJ and Millar NS (2005) RIC-3 enhances functional expression of multiple nicotinic acetylcholine receptor subtypes in mammalian cells. *Mol Pharmacol* **68**:1431-1438.
- Lape R, Colquhoun D and Sivilotti LG (2008) On the nature of partial agonism in the nicotinic receptor superfamily. *Nature* **454**:722-727.
- Lape R, Krashia P, Colquhoun D and Sivilotti LG (2009) Agonist and blocking actions of choline and tetramethylammonium on human muscle acetylcholine receptors. *J Physiol* **587**:5045-5072.
- Lee BH, Choi SH, Shin TJ, Pyo MK, Hwang SH, Kim BR, Lee SM, Lee JH, Kim HC, Park HY, Rhim H and Nah SY (2010a) Quercetin enhances human alpha₇ nicotinic acetylcholine receptor-mediated ion current through interactions with Ca²⁺ binding sites. *Mol Cells* **30**:245-253.
- Lee CH, Huang CS, Chen CS, Tu SH, Wang YJ, Chang YJ, Tam KW, Wei PL, Cheng TC, Chu JS, Chen LC, Wu CH and Ho YS (2010b) Overexpression and activation of the alpha₉-nicotinic receptor during tumorigenesis in human breast epithelial cells. *J Natl Cancer Inst* **102**:1322-1335.
- Lee Y, Rudell J and Ferns M (2009) Rapsyn interacts with the muscle acetylcholine receptor via alpha-helical domains in the alpha, beta, and epsilon subunit intracellular loops. *Neuroscience* **163**:222-232.

- Leite JF, Blanton MP, Shahgholi M, Dougherty DA and Lester HA (2003) Conformation-dependent hydrophobic photolabeling of the nicotinic receptor: electrophysiology-coordinated photochemistry and mass spectrometry. *Proc Natl Acad Sci U S A* **100**:13054-13059.
- Lena C and Changeux JP (1997) Role of Ca²⁺ ions in nicotinic facilitation of GABA release in mouse thalamus. *J Neurosci* **17**:576-585.
- Lena C, Changeux JP and Mulle C (1993) Evidence for "preterminal" nicotinic receptors on GABAergic axons in the rat interpeduncular nucleus. *J Neurosci* **13**:2680-2688.
- Lester HA, Dibas MI, Dahan DS, Leite JF and Dougherty DA (2004) Cys-loop receptors: new twists and turns. *Trends Neurosci* **27**:329-336.
- Lester HA, Xiao C, Srinivasan R, Son CD, Miwa J, Pantoja R, Banghart MR, Dougherty DA, Goate AM and Wang JC (2009) Nicotine is a selective pharmacological chaperone of acetylcholine receptor number and stoichiometry. Implications for drug discovery. *Aaps J* **11**:167-177.
- Lewis TM, Sivilotti LG, Colquhoun D, Gardiner RM, Schoepfer R and Rees M (1998) Properties of human glycine receptors containing the hyperekplexia mutation alpha1(K276E), expressed in *Xenopus oocytes*. *J Physiol* **507** (Pt 1):25-40.
- Li GD, Chiara DC, Sawyer GW, Husain SS, Olsen RW and Cohen JB (2006) Identification of a GABAA receptor anesthetic binding site at subunit interfaces by photolabeling with an etomidate analog. *J Neurosci* **26**:11599-11605.
- Lichtner RB, Gallick GE and Nicolson GL (1988) Pyrimido-pyrimidine modulation of EGF growth-promoting activity and p21ras expression in rat mammary adenocarcinoma cells. *J Cell Physiol* **137**:285-292.
- Limapichat W, Lester HA and Dougherty DA (2010) Chemical scale studies of the Phe-Pro conserved motif in the cys loop of Cys loop receptors. *J Biol Chem* **285**:8976-8984.
- Lin L, Jeanclos EM, Treuil M, Braunewell KH, Gundelfinger ED and Anand R (2002) The calcium sensor protein visinin-like protein-1 modulates the surface expression and agonist sensitivity of the alpha 4beta 2 nicotinic acetylcholine receptor. *J Biol Chem* **277**:41872-41878.
- Lippiello PM (2006) Nicotinic cholinergic antagonists: a novel approach for the treatment of autism. *Med Hypotheses* **66**:985-990.
- Liu P, Vikis HG, Wang D, Lu Y, Wang Y, Schwartz AG, Pinney SM, Yang P, de Andrade M, Petersen GM, Wiest JS, Fain PR, Gazdar A, Gaba C, Rothschild H, Mandal D, Coons T, Lee J, Kupert E, Seminara D, Minna J, Bailey-Wilson JE, Wu X, Spitz MR, Eisen T, Houlston RS, Amos CI, Anderson MW and You M (2008a) Familial aggregation of common sequence variants on 15q24-25.1 in lung cancer. *J Natl Cancer Inst* **100**:1326-1330.
- Liu Q, Yu KW, Chang YC, Lukas RJ and Wu J (2008b) Agonist-induced hump current production in heterologously-expressed human alpha4beta2-nicotinic acetylcholine receptors. *Acta Pharmacol Sin* **29**:305-319.
- Luetje CW (2004) Getting past the asterisk: the subunit composition of presynaptic nicotinic receptors that modulate striatal dopamine release. *Mol Pharmacol* **65**:1333-1335.
- Lynch JW, Rajendra S, Pierce KD, Handford CA, Barry PH and Schofield PR (1997) Identification of intracellular and extracellular domains mediating signal transduction in the inhibitory glycine receptor chloride channel. *EMBO J* **16**:110-120.
- Lysek N, Rachor E and Lindel T (2002) Isolation and structure elucidation of deformylflustrabromine from the North Sea bryozoan *Flustra foliacea*. *Z Naturforsch C* **57**:1056-1061.

- Maelicke A, Schratzenholz A, Samochocki M, Radina M and Albuquerque EX (2000) Allosterically potentiating ligands of nicotinic receptors as a treatment strategy for Alzheimer's disease. *Behav Brain Res* **113**:199-206.
- Majewska MD, Harrison NL, Schwartz RD, Barker JL and Paul SM (1986) Steroid hormone metabolites are barbiturate-like modulators of the GABA receptor. *Science* **232**:1004-1007.
- Maksay G, Bikadi Z and Simonyi M (2003) Binding interactions of antagonists with 5-hydroxytryptamine_{3A} receptor models. *J Recept Signal Transduct Res* **23**:255-270.
- Mamede M, Ishizu K, Ueda M, Mukai T, Iida Y, Kawashima H, Fukuyama H, Togashi K and Saji H (2007) Temporal change in human nicotinic acetylcholine receptor after smoking cessation: 5IA SPECT study. *J Nucl Med* **48**:1829-1835.
- Maneckjee R and Minna JD (1994) Opioids induce while nicotine suppresses apoptosis in human lung cancer cells. *Cell Growth Differ* **5**:1033-1040.
- Mansvelder HD, Keath JR and McGehee DS (2002) Synaptic mechanisms underlie nicotine-induced excitability of brain reward areas. *Neuron* **33**:905-919.
- Mansvelder HD and McGehee DS (2000) Long-term potentiation of excitatory inputs to brain reward areas by nicotine. *Neuron* **27**:349-357.
- Maricq AV, Peterson AS, Brake AJ, Myers RM and Julius D (1991) Primary structure and functional expression of the 5HT₃ receptor, a serotonin-gated ion channel. *Science* **254**:432-437.
- Marion L and Cockburn WF (1948) The papilionaceous alkaloids; *Baptisia minor*, Lehm. *J Am Chem Soc* **70**:3472-3474.
- Marks MJ, Pauly JR, Gross SD, Deneris ES, Hermans-Borgmeyer I, Heinemann SF and Collins AC (1992) Nicotine binding and nicotinic receptor subunit RNA after chronic nicotine treatment. *J Neurosci* **12**:2765-2784.
- Marritt AM, Cox BC, Yasuda RP, McIntosh JM, Xiao Y, Wolfe BB and Kellar KJ (2005) Nicotinic cholinergic receptors in the rat retina: simple and mixed heteromeric subtypes. *Mol Pharmacol* **68**:1656-1668.
- Martin-Ruiz CM, Lee M, Perry RH, Baumann M, Court JA and Perry EK (2004) Molecular analysis of nicotinic receptor expression in autism. *Brain Res Mol Brain Res* **123**:81-90.
- Martin BR, Onaivi ES and Martin TJ (1989) What is the nature of mecamylamine's antagonism of the central effects of nicotine? *Biochem Pharmacol* **38**:3391-3397.
- Martinez-Moreno P, Nieto-Ceron S, Torres-Lanzas J, Ruiz-Espejo F, Tovar-Zapata I, Martinez-Hernandez P, Rodriguez-Lopez JN, Vidal CJ and Cabezas-Herrera J (2006) Cholinesterase activity of human lung tumours varies according to their histological classification. *Carcinogenesis* **27**:429-436.
- Mascia MP, Trudell JR and Harris RA (2000) Specific binding sites for alcohols and anesthetics on ligand-gated ion channels. *Proc Natl Acad Sci U S A* **97**:9305-9310.
- Matta SG, Balfour DJ, Benowitz NL, Boyd RT, Buccafusco JJ, Caggiula AR, Craig CR, Collins AC, Damaj MI, Donny EC, Gardiner PS, Grady SR, Heberlein U, Leonard SS, Levin ED, Lukas RJ, Markou A, Marks MJ, McCallum SE, Parameswaran N, Perkins KA, Picciotto MR, Quik M, Rose JE, Rothenfluh A, Schafer WR, Stolerman IP, Tyndale RF, Wehner JM and Zirger JM (2007) Guidelines on nicotine dose selection for in vivo research. *Psychopharmacology (Berl)* **190**:269-319.

- Maus AD, Pereira EF, Karachunski PI, Horton RM, Navaneetham D, Macklin K, Cortes WS, Albuquerque EX and Conti-Fine BM (1998) Human and rodent bronchial epithelial cells express functional nicotinic acetylcholine receptors. *Mol Pharmacol* **54**:779-788.
- McClellan AJ, Endres JB, Vogel JP, Palazzi D, Rose MD and Brodsky JL (1998) Specific molecular chaperone interactions and an ATP-dependent conformational change are required during posttranslational protein translocation into the yeast ER. *Mol Biol Cell* **9**:3533-3545.
- McGehee DS, Heath MJ, Gelber S, Devay P and Role LW (1995) Nicotine enhancement of fast excitatory synaptic transmission in CNS by presynaptic receptors. *Science* **269**:1692-1696.
- McGehee DS and Role LW (1995) Physiological diversity of nicotinic acetylcholine receptors expressed by vertebrate neurons. *Annu Rev Physiol* **57**:521-546.
- McKay JD, Hung RJ, Gaborieau V, Boffetta P, Chabrier A, Byrnes G, Zaridze D, Mukeria A, Szeszenia-Dabrowska N, Lissowska J, Rudnai P, Fabianova E, Mates D, Bencko V, Foretova L, Janout V, McLaughlin J, Shepherd F, Montpetit A, Narod S, Krokan HE, Skorpen F, Elvestad MB, Vatten L, Njolstad I, Axelsson T, Chen C, Goodman G, Barnett M, Loomis MM, Lubinski J, Matyjask J, Lener M, Oszutowska D, Field J, Liloglou T, Xinarianos G, Cassidy A, Vineis P, Clavel-Chapelon F, Palli D, Tumino R, Krogh V, Panico S, Gonzalez CA, Ramon Quiros J, Martinez C, Navarro C, Ardanaz E, Larranaga N, Kham KT, Key T, Bueno-de-Mesquita HB, Peeters PH, Trichopoulou A, Linseisen J, Boeing H, Hallmans G, Overvad K, Tjonneland A, Kumle M, Riboli E, Zelenika D, Boland A, Delepine M, Foglio M, Lechner D, Matsuda F, Blanche H, Gut I, Heath S, Lathrop M and Brennan P (2008) Lung cancer susceptibility locus at 5p15.33. *Nat Genet* **40**:1404-1406.
- McKee SA, Harrison EL, O'Malley SS, Krishnan-Sarin S, Shi J, Tetrault JM, Picciotto MR, Petrakis IL, Estevez N, Balchunas E (2009) Varenicline reduces alcohol self-administration in heavy-drinking smokers. *Biol Psychiatry* **66**:185-90.
- McKernan RM, Farrar S, Collins I, Emms F, Asuni A, Quirk K and Broughton H (1998) Photoaffinity labeling of the benzodiazepine binding site of alpha1beta3gamma2 gamma-aminobutyric acidA receptors with flunitrazepam identifies a subset of ligands that interact directly with His102 of the alpha subunit and predicts orientation of these within the benzodiazepine pharmacophore. *Mol Pharmacol* **54**:33-43.
- Mertie JP and Lindstrom J (1983) Assembly in vivo of mouse muscle acetylcholine receptor: identification of an alpha subunit species that may be an assembly intermediate. *Cell* **34**:747-757.
- Mertie JP, Sebbane R, Tzartos S and Lindstrom J (1982) Inhibition of glycosylation with tunicamycin blocks assembly of newly synthesized acetylcholine receptor subunits in muscle cells. *J Biol Chem* **257**:2694-2701.
- Meyer EM, Tay ET, Zoltewicz JA, Meyers C, King MA, Papke RL and De Fiebre CM (1998) Neuroprotective and memory-related actions of novel alpha-7 nicotinic agents with different mixed agonist/antagonist properties. *J Pharmacol Exp Ther* **284**:1026-1032.
- Mihic SJ, Whiting PJ, Klein RL, Wafford KA and Harris RA (1994) A single amino acid of the human gamma-aminobutyric acid type A receptor gamma 2 subunit determines benzodiazepine efficacy. *J Biol Chem* **269**:32768-32773.
- Mihic SJ, Ye Q, Wick MJ, Koltchine VV, Krasowski MD, Finn SE, Mascia MP, Valenzuela CF, Hanson KK, Greenblatt EP, Harris RA and Harrison NL (1997) Sites of alcohol and volatile anaesthetic action on GABA(A) and glycine receptors. *Nature* **389**:385-389.
- Miller C (1989) Genetic manipulation of ion channels: a new approach to structure and mechanism. *Neuron* **2**:1195-1205.
- Miller KW (2002) The nature of sites of general anaesthetic action. *Br J Anaesth* **89**:17-31.

Miller PS and Smart TG (2010) Binding, activation and modulation of Cys-loop receptors. *Trends Pharmacol Sci* **31**:161-174.

Mishina M, Tobimatsu T, Imoto K, Tanaka K, Fujita Y, Fukuda K, Kurasaki M, Takahashi H, Morimoto Y, Hirose T and et al. (1985) Location of functional regions of acetylcholine receptor alpha-subunit by site-directed mutagenesis. *Nature* **313**:364-369.

Miwa JM, Stevens TR, King SL, Caldarone BJ, Ibanez-Tallon I, Xiao C, Fitzsimonds RM, Pavlides C, Lester HA, Picciotto MR and Heintz N (2006) The protoxin lynx1 acts on nicotinic acetylcholine receptors to balance neuronal activity and survival in vivo. *Neuron* **51**:587-600.

Miyazawa A, Fujiyoshi Y, Stowell M and Unwin N (1999) Nicotinic acetylcholine receptor at 4.6 Å resolution: transverse tunnels in the channel wall. *J Mol Biol* **288**:765-786.

Miyazawa A, Fujiyoshi Y and Unwin N (2003) Structure and gating mechanism of the acetylcholine receptor pore. *Nature* **423**:949-955.

Mogg AJ, Whiteaker P, McIntosh JM, Marks M, Collins AC and Wonnacott S (2002) Methyllycaconitine is a potent antagonist of alpha-conotoxin-MII-sensitive presynaptic nicotinic acetylcholine receptors in rat striatum. *J Pharmacol Exp Ther* **302**:197-204.

Monod J, Wyman J and Changeux JP (1965) On the Nature of Allosteric Transitions: A Plausible Model. *J Mol Biol* **12**:88-118.

Moody EJ, Knauer C, Granja R, Strakhova M and Skolnick P (1997) Distinct loci mediate the direct and indirect actions of the anesthetic etomidate at GABA(A) receptors. *J Neurochem* **69**:1310-1313.

Moody EJ, Knauer CS, Granja R, Strakhovava M and Skolnick P (1998) Distinct structural requirements for the direct and indirect actions of the anaesthetic etomidate at GABA(A) receptors. *Toxicol Lett* **100-101**:209-215.

Moretti M, Vailati S, Zoli M, Lippi G, Riganti L, Longhi R, Viegi A, Clementi F and Gotti C (2004) Nicotinic acetylcholine receptor subtypes expression during rat retina development and their regulation by visual experience. *Mol Pharmacol* **66**:85-96.

Morimoto N, Takemoto S, Kawazoe T and Suzuki S (2008) Nicotine at a low concentration promotes wound healing. *J Surg Res* **145**:199-204.

Moriwaki Y, Yoshikawa K, Fukuda H, Fujii YX, Misawa H and Kawashima K (2007) Immune system expression of SLURP-1 and SLURP-2, two endogenous nicotinic acetylcholine receptor ligands. *Life Sci* **80**:2365-2368.

Moroni M and Bermudez I (2006) Stoichiometry and Pharmacology of Two Human alpha4beta2 Nicotinic Receptor Types. *J Mol Neurosci* **30**:95-96.

Moroni M, Vijayan R, Carbone A, Zwart R, Biggin PC and Bermudez I (2008) Non-agonist-binding subunit interfaces confer distinct functional signatures to the alternate stoichiometries of the alpha4beta2 nicotinic receptor: an alpha4-alpha4 interface is required for Zn²⁺ potentiation. *J Neurosci* **28**:6884-6894.

Moroni M, Zwart R, Sher E, Cassels BK and Bermudez I (2006a) alpha4beta2 nicotinic receptors with high and low acetylcholine sensitivity: pharmacology, stoichiometry, and sensitivity to long-term exposure to nicotine. *Mol Pharmacol* **70**:755-768.

Moroni M, Zwart R, Sher E, Cassels BK and Bermudez I (2006b) {alpha}4{beta}2 nicotinic receptors with high and low acetylcholine sensitivity: pharmacology, stoichiometry and sensitivity to chronic exposure to nicotine. *Mol Pharmacol*.

- Morris KD and Amin J (2004) Insight into the mechanism of action of neuroactive steroids. *Mol Pharmacol* **66**:56-69.
- Mrowiec T and Schwappach B (2006) 14-3-3 proteins in membrane protein transport. *Biol Chem* **387**:1227-1236.
- Nashmi R and Lester HA (2006) CNS localization of neuronal nicotinic receptors. *J Mol Neurosci* **30**:181-184.
- Nashmi R, Xiao C, Deshpande P, McKinney S, Grady SR, Whiteaker P, Huang Q, McClure-Begley T, Lindstrom JM, Labarca C, Collins AC, Marks MJ and Lester HA (2007) Chronic nicotine cell specifically upregulates functional alpha 4* nicotinic receptors: basis for both tolerance in midbrain and enhanced long-term potentiation in perforant path. *J Neurosci* **27**:8202-8218.
- Nelson ME, Kuryatov A, Choi CH, Zhou Y and Lindstrom J (2003) Alternate stoichiometries of alpha4beta2 nicotinic acetylcholine receptors. *Mol Pharmacol* **63**:332-341.
- Nguyen HN, Rasmussen BA and Perry DC (2003) Subtype-selective up-regulation by chronic nicotine of high-affinity nicotinic receptors in rat brain demonstrated by receptor autoradiography. *J Pharmacol Exp Ther* **307**:1090-1097.
- Nguyen HN, Rasmussen BA and Perry DC (2004) Binding and functional activity of nicotinic cholinergic receptors in selected rat brain regions are increased following long-term but not short-term nicotine treatment. *J Neurochem* **90**:40-49.
- Nicolson R, Craven-Thuss B and Smith J (2006) A prospective, open-label trial of galantamine in autistic disorder. *J Child Adolesc Psychopharmacol* **16**:621-629.
- Nishimura N and Balch WE (1997) A di-acidic signal required for selective export from the endoplasmic reticulum. *Science* **277**:556-558.
- Nordberg A (2000) Neuroprotection in Alzheimer's disease - new strategies for treatment. *Neurotox Res* **2**:157-165.
- Nordberg A (2001) Nicotinic receptor abnormalities of Alzheimer's disease: therapeutic implications. *Biol Psychiatry* **49**:200-210.
- Nordberg A, Lundqvist H, Hartvig P, Andersson J, Johansson M, Hellstrom-Lindahi E and Langstrom B (1997) Imaging of nicotinic and muscarinic receptors in Alzheimer's disease: effect of tacrine treatment. *Dement Geriatr Cogn Disord* **8**:78-84.
- Olsen RW and Sieghart W (2008) International Union of Pharmacology. LXX. Subtypes of gamma-aminobutyric acid(A) receptors: classification on the basis of subunit composition, pharmacology, and function. Update. *Pharmacol Rev* **60**:243-260.
- Oshikawa J, Toya Y, Fujita T, Egawa M, Kawabe J, Umemura S and Ishikawa Y (2003) Nicotinic acetylcholine receptor alpha 7 regulates cAMP signal within lipid rafts. *Am J Physiol Cell Physiol* **285**:C567-574.
- Ostromov K, Shaikhutdinova A and Skorinkin A (2008) Modeling study of mecamylamine block of muscle type acetylcholine receptors. *Eur Biophys J* **37**:393-402.
- Pacheco MA, Pastoor TE and Wecker L (2003) Phosphorylation of the alpha4 subunit of human alpha4beta2 nicotinic receptors: role of cAMP-dependent protein kinase (PKA) and protein kinase C (PKC). *Brain Res Mol Brain Res* **114**:65-72.
- Pandya NM, Dhalla NS and Santani DD (2006) Angiogenesis--a new target for future therapy. *Vascul Pharmacol* **44**:265-274.

- Papke RL, Bencherif M and Lippiello P (1996) An evaluation of neuronal nicotinic acetylcholine receptor activation by quaternary nitrogen compounds indicates that choline is selective for the alpha 7 subtype. *Neurosci Lett* **213**:201-204.
- Paradiso K, Sabey K, Evers AS, Zorumski CF, Covey DF and Steinbach JH (2000) Steroid inhibition of rat neuronal nicotinic alpha4beta2 receptors expressed in HEK 293 cells. *Mol Pharmacol* **58**:341-351.
- Paradiso K, Zhang J and Steinbach JH (2001) The C terminus of the human nicotinic alpha4beta2 receptor forms a binding site required for potentiation by an estrogenic steroid. *J Neurosci* **21**:6561-6568.
- Parnavelas JG, Kelly W and Burnstock G (1985) Ultrastructural localization of choline acetyltransferase in vascular endothelial cells in rat brain. *Nature* **316**:724-725.
- Paulson HL, Ross AF, Green WN and Claudio T (1991) Analysis of early events in acetylcholine receptor assembly. *J Cell Biol* **113**:1371-1384.
- Peng X, Gerzanich V, Anand R, Whiting PJ and Lindstrom J (1994) Nicotine-induced increase in neuronal nicotinic receptors results from a decrease in the rate of receptor turnover. *Mol Pharmacol* **46**:523-530.
- Pereira EF, Alkondon M, Tano T, Castro NG, Froes-Ferrao MM, Rozental R, Aronstam RS, Schrattenholz A, Maelicke A and Albuquerque EX (1993) A novel agonist binding site on nicotinic acetylcholine receptors. *J Recept Res* **13**:413-436.
- Perry DC, Davila-Garcia MI, Stockmeier CA and Kellar KJ (1999) Increased nicotinic receptors in brains from smokers: membrane binding and autoradiography studies. *J Pharmacol Exp Ther* **289**:1545-1552.
- Perry EK, Lee ML, Martin-Ruiz CM, Court JA, Volsen SG, Merrit J, Folly E, Iversen PE, Bauman ML, Perry RH and Wenk GL (2001) Cholinergic activity in autism: abnormalities in the cerebral cortex and basal forebrain. *Am J Psychiatry* **158**:1058-1066.
- Peters L, Konig GM, Wright AD, Pukall R, Stackebrandt E, Eberl L and Riedel K (2003) Secondary metabolites of *Flustra foliacea* and their influence on bacteria. *Appl Environ Microbiol* **69**:3469-3475.
- Peters L, Wright AD, Kehraus S, Gundisch D, Tilotta MC and Konig GM (2004) Prenylated indole alkaloids from *Flustra foliacea* with subtype specific binding on NACHRs. *Planta Med* **70**:883-886.
- Pettit DL, Shao Z and Yakel JL (2001) beta-Amyloid(1-42) peptide directly modulates nicotinic receptors in the rat hippocampal slice. *J Neurosci* **21**:RC120.
- Pfister JA, Gardner DR, Panter KE, Manners GD, Ralphs MH, Stegelmeier BL and Schoch TK (1999) Larkspur (*Delphinium* spp.) poisoning in livestock. *J Nat Toxins* **8**:81-94.
- Picciotto MR, Caldarone BJ, Brunzell DH, Zachariou V, Stevens TR and King SL (2001) Neuronal nicotinic acetylcholine receptor subunit knockout mice: physiological and behavioral phenotypes and possible clinical implications. *Pharmacol Ther* **92**:89-108.
- Picciotto MR and Zoli M (2002) Nicotinic receptors in aging and dementia. *J Neurobiol* **53**:641-655.
- Picciotto MR, Zoli M, Rimondini R, Lena C, Marubio LM, Pich EM, Fuxe K and Changeux JP (1998) Acetylcholine receptors containing the beta2 subunit are involved in the reinforcing properties of nicotine. *Nature* **391**:173-177.
- Plempner RK, Bohmler S, Bordallo J, Sommer T and Wolf DH (1997) Mutant analysis links the translocon and BiP to retrograde protein transport for ER degradation. *Nature* **388**:891-895.

Plummer HK, Dhar M and Schuller HM (2005) Expression of the alpha7 nicotinic acetylcholine receptor in human lung cells. *Respir Res* **6**:29.

Potter A, Corwin J, Lang J, Piasecki M, Lenox R and Newhouse PA (1999) Acute effects of the selective cholinergic channel activator (nicotinic agonist) ABT-418 in Alzheimer's disease. *Psychopharmacology (Berl)* **142**:334-342.

Price KL, Bower KS, Thompson AJ, Lester HA, Dougherty DA and Lummis SC (2008) A hydrogen bond in loop A is critical for the binding and function of the 5-HT3 receptor. *Biochemistry* **47**:6370-6377.

Price KL and Lummis SC (2004) The role of tyrosine residues in the extracellular domain of the 5-hydroxytryptamine3 receptor. *J Biol Chem* **279**:23294-23301.

Proskocil BJ, Sekhon HS, Jia Y, Savchenko V, Blakely RD, Lindstrom J and Spindel ER (2004) Acetylcholine is an autocrine or paracrine hormone synthesized and secreted by airway bronchial epithelial cells. *Endocrinology* **145**:2498-2506.

Purohit P, Mitra A and Auerbach A (2007) A stepwise mechanism for acetylcholine receptor channel gating. *Nature* **446**:930-933.

Purves DA, G.J.; Fitzpatrick, D.; Hall, W.C.; LaMantia, A.S.; MsNamara, J.O.; Williams, S.M. (2004) *Neuroscience, Third Edition*. Sinauer Associates, Inc., Sunderland, Massachusetts.

Puskar NL, Xiu X, Lester HA and Dougherty DA (2011) Two neuronal nicotinic Acetylcholine receptors - alpha4beta4 and alpha7 - show differential agonist binding modes. *J Biol Chem*.

Quick MW and Lester RA (2002) Desensitization of neuronal nicotinic receptors. *J Neurobiol* **53**:457-478.

Rabenstein RL, Caldarone BJ and Picciotto MR (2006) The nicotinic antagonist mecamylamine has antidepressant-like effects in wild-type but not beta2- or alpha7-nicotinic acetylcholine receptor subunit knockout mice. *Psychopharmacology (Berl)* **189**:395-401.

Radcliffe KA and Dani JA (1998) Nicotinic stimulation produces multiple forms of increased glutamatergic synaptic transmission. *J Neurosci* **18**:7075-7083.

Ray MA, Graham AJ, Lee M, Perry RH, Court JA and Perry EK (2005) Neuronal nicotinic acetylcholine receptor subunits in autism: an immunohistochemical investigation in the thalamus. *Neurobiol Dis* **19**:366-377.

Ren XQ, Cheng SB, Treuil MW, Mukherjee J, Rao J, Braunewell KH, Lindstrom JM and Anand R (2005) Structural determinants of alpha4beta2 nicotinic acetylcholine receptor trafficking. *J Neurosci* **25**:6676-6686.

Rezvani AH, Kholdebarin E, Brucato FH, Callahan PM, Lowe DA and Levin ED (2009) Effect of R3487/MEM3454, a novel nicotinic alpha7 receptor partial agonist and 5-HT3 antagonist on sustained attention in rats. *Prog Neuropsychopharmacol Biol Psychiatry* **33**:269-275.

Risau W (1997) Mechanisms of angiogenesis. *Nature* **386**:671-674.

Robinson MS (2004) Adaptable adaptors for coated vesicles. *Trends Cell Biol* **14**:167-174.

Roccamo AM and Barrantes FJ (2007) Charged amino acid motifs flanking each extreme of the alphaM4 transmembrane domain are involved in assembly and cell-surface targeting of the muscle nicotinic acetylcholine receptor. *J Neurosci Res* **85**:285-293.

Role LW and Berg DK (1996) Nicotinic receptors in the development and modulation of CNS synapses. *Neuron* **16**:1077-1085.

Rollema H, Chambers LK, Coe JW, Glowa J, Hurst RS, Lebel LA, Lu Y, Mansbach RS, Mather RJ, Rovetti CC, Sands SB, Schaeffer E, Schulz DW, Tingley FD, 3rd and Williams KE (2007a) Pharmacological profile of the alpha4beta2 nicotinic acetylcholine receptor partial agonist varenicline, an effective smoking cessation aid. *Neuropharmacology* **52**:985-994.

Rollema H, Coe JW, Chambers LK, Hurst RS, Stahl SM and Williams KE (2007b) Rationale, pharmacology and clinical efficacy of partial agonists of alpha(4)beta(2) nACh receptors for smoking cessation. *Trends Pharmacol Sci.* **28**:316-25.

Rosenberg MM, Yang F, Giovanni M, Mohn JL, Temburni MK and Jacob MH (2008) Adenomatous polyposis coli plays a key role, in vivo, in coordinating assembly of the neuronal nicotinic postsynaptic complex. *Mol Cell Neurosci* **38**:138-152.

Sala F, Mulet J, Reddy KP, Bernal JA, Wikman P, Valor LM, Peters L, Konig GM, Criado M and Sala S (2005) Potentiation of human alpha4beta2 neuronal nicotinic receptors by a *Flustra foliacea* metabolite. *Neurosci Lett* **373**:144-149.

Salette J, Pons S, Devillers-Thiery A, Soudant M, Prado de Carvalho L, Changeux JP and Corringer PJ (2005) Nicotine upregulates its own receptors through enhanced intracellular maturation. *Neuron* **46**:595-607.

Samochocki M, Hoffle A, Fehrenbacher A, Jostock R, Ludwig J, Christner C, Radina M, Zerlin M, Ullmer C, Pereira EF, Lubbert H, Albuquerque EX and Maelicke A (2003) Galantamine is an allosterically potentiating ligand of neuronal nicotinic but not of muscarinic acetylcholine receptors. *J Pharmacol Exp Ther* **305**:1024-1036.

Sardari Nia P, Weyler J, Colpaert C, Vermeulen P, Van Marck E and Van Schil P (2005) Prognostic value of smoking status in operated non-small cell lung cancer. *Lung Cancer* **47**:351-359.

Schaerer MT, Buhr A, Baur R and Sigel E (1998) Amino acid residue 200 on the alpha1 subunit of GABA(A) receptors affects the interaction with selected benzodiazepine binding site ligands. *Eur J Pharmacol* **354**:283-287.

Schrattenholz A, Godovac-Zimmermann J, Schafer HJ, Albuquerque EX and Maelicke A (1993) Photoaffinity labeling of Torpedo acetylcholine receptor by physostigmine. *Eur J Biochem* **216**:671-677.

Schreiter C, Hovius R, Costioli M, Pick H, Kellenberger S, Schild L and Vogel H (2003) Characterization of the ligand-binding site of the serotonin 5-HT3 receptor: the role of glutamate residues 97, 224, AND 235. *J Biol Chem* **278**:22709-22716.

Schulte MK, Hill, R.A., Bikadi, Z., Maksay G., Parihar, H.S., Joshi, P. and Suryanarayanan, A. (2006) The Structural Basis of Ligand Interactions in the 5-HT3R, in *Biological and Biophysical Aspects of Ligand-Gated Ion Channel Receptor Superfamilies* (Arias H ed) pp 127-154, Research Signpost.

Scott LJ and Goa KL (2000) Galantamine: a review of its use in Alzheimer's disease. *Drugs* **60**:1095-1122.

Seguela P, Wadiche J, Dineley-Miller K, Dani JA and Patrick JW (1993) Molecular cloning, functional properties, and distribution of rat brain alpha 7: a nicotinic cation channel highly permeable to calcium. *J Neurosci* **13**:596-604.

Shan Q, Nevin ST, Hadrill JL and Lynch JW (2003) Asymmetric contribution of alpha and beta subunits to the activation of alphabeta heteromeric glycine receptors. *J Neurochem* **86**:498-507.

Sharma G and Vijayaraghavan S (2003) Modulation of presynaptic store calcium induces release of glutamate and postsynaptic firing. *Neuron* **38**:929-939.

Sher E, Chen Y, Sharpies TJ, Broad LM, Benedetti G, Zwart R, McPhie GI, Pearson KH, Baldwinson T and De Filippi G (2004) Physiological roles of neuronal nicotinic receptor subtypes: new insights on the nicotinic modulation of neurotransmitter release, synaptic transmission and plasticity. *Curr Top Med Chem* **4**:283-297.

Shih YL, Liu HC, Chen CS, Hsu CH, Pan MH, Chang HW, Chang CH, Chen FC, Ho CT, Yang YY and Ho YS (2010) Combination treatment with luteolin and quercetin enhances antiproliferative effects in nicotine-treated MDA-MB-231 cells by down-regulating nicotinic acetylcholine receptors. *J Agric Food Chem* **58**:235-241.

Shin VY, Wu WK, Ye YN, So WH, Koo MW, Liu ES, Luo JC and Cho CH (2004) Nicotine promotes gastric tumor growth and neovascularization by activating extracellular signal-regulated kinase and cyclooxygenase-2. *Carcinogenesis* **25**:2487-2495.

Shoop RD, Yamada N and Berg DK (2000) Cytoskeletal links of neuronal acetylcholine receptors containing alpha 7 subunits. *J Neurosci* **20**:4021-4029.

Shytle RD, Silver AA and Sanberg PR (2000) Comorbid bipolar disorder in Tourette's syndrome responds to the nicotinic receptor antagonist mecamylamine (Inversine). *Biol Psychiatry* **48**:1028-1031.

Sigel E (2002) Mapping of the benzodiazepine recognition site on GABA(A) receptors. *Curr Top Med Chem* **2**:833-839.

Sigel E and Buhr A (1997) The benzodiazepine binding site of GABAA receptors. *Trends Pharmacol Sci* **18**:425-429.

Sigel E, Schaerer MT, Buhr A and Baur R (1998) The benzodiazepine binding pocket of recombinant alpha1beta2gamma2 gamma-aminobutyric acidA receptors: relative orientation of ligands and amino acid side chains. *Mol Pharmacol* **54**:1097-1105.

Silver AA, Shytle RD and Sanberg PR (2000) Mecamylamine in Tourette's syndrome: a two-year retrospective case study. *J Child Adolesc Psychopharmacol* **10**:59-68.

Sine SM, Wang HL, Hansen S and Taylor P (2010) On the origin of ion selectivity in the Cys-loop receptor family. *J Mol Neurosci* **40**:70-76.

Sjoblom T, Bohlin L and Christophersen C (1983) Studies of Swedish marine organisms. II. Muscle-relaxant alkaloids from the marine bryozoan *Flustra foliacea*. *Acta Pharm Suec* **20**:415-418.

Small DH, Maksel D, Kerr ML, Ng J, Hou X, Chu C, Mehrani H, Unabia S, Azari MF, Loiacono R, Aguilar MI and Chebib M (2007) The beta-amyloid protein of Alzheimer's disease binds to membrane lipids but does not bind to the alpha7 nicotinic acetylcholine receptor. *J Neurochem* **101**:1527-1538.

Smit AB, Syed NI, Schaap D, van Minnen J, Klumperman J, Kits KS, Lodder H, van der Schors RC, van Elk R, Sorgedraeger B, Brejc K, Sixma TK and Geraerts WP (2001) A glia-derived acetylcholine-binding protein that modulates synaptic transmission. *Nature* **411**:261-268.

Smith MM, Lindstrom J and Merlie JP (1987) Formation of the alpha-bungarotoxin binding site and assembly of the nicotinic acetylcholine receptor subunits occur in the endoplasmic reticulum. *J Biol Chem* **262**:4367-4376.

Smulders CJ, Zwart R, Bermudez I, van Kleef RG, Groot-Kormelink PJ and Vijverberg HP (2005) Cholinergic drugs potentiate human nicotinic alpha4beta2 acetylcholine receptors by a competitive mechanism. *Eur J Pharmacol* **509**:97-108.

Song P, Sekhon HS, Fu XW, Maier M, Jia Y, Duan J, Proskosil BJ, Gravett C, Lindstrom J, Mark GP, Saha S and Spindel ER (2008) Activated cholinergic signaling provides a target in squamous cell lung carcinoma. *Cancer Res* **68**:4693-4700.

Song P, Sekhon HS, Jia Y, Keller JA, Blusztajn JK, Mark GP and Spindel ER (2003) Acetylcholine is synthesized by and acts as an autocrine growth factor for small cell lung carcinoma. *Cancer Res* **63**:214-221.

Spencer JP, Weil A, Hill K, Hussain I, Richardson JC, Cusdin FS, Chen YH and Randall AD (2006) Transgenic mice over-expressing human beta-amyloid have functional nicotinic alpha 7 receptors. *Neuroscience* **137**:795-805.

Spier AD and Lummis SC (2000) The role of tryptophan residues in the 5-Hydroxytryptamine(3) receptor ligand binding domain. *J Biol Chem* **275**:5620-5625.

Spitz MR, Amos CI, Dong Q, Lin J and Wu X (2008) The CHRNA5-A3 region on chromosome 15q24-25.1 is a risk factor both for nicotine dependence and for lung cancer. *J Natl Cancer Inst* **100**:1552-1556.

St John PA (2009) Cellular trafficking of nicotinic acetylcholine receptors. *Acta Pharmacol Sin* **30**:656-662.

Staley JK, Krishnan-Sarin S, Cosgrove KP, Krantzler E, Frohlich E, Perry E, Dubin JA, Estok K, Brenner E, Baldwin RM, Tamagnan GD, Seibyl JP, Jatlow P, Picciotto MR, London ED, O'Malley S and van Dyck CH (2006) Human tobacco smokers in early abstinence have higher levels of beta2* nicotinic acetylcholine receptors than nonsmokers. *J Neurosci* **26**:8707-8714.

Stell BM, Brickley SG, Tang CY, Farrant M and Mody I (2003) Neuroactive steroids reduce neuronal excitability by selectively enhancing tonic inhibition mediated by delta subunit-containing GABAA receptors. *Proc Natl Acad Sci U S A* **100**:14439-14444.

Steward LJ, Boess FG, Steele JA, Liu D, Wong N and Martin IL (2000) Importance of phenylalanine 107 in agonist recognition by the 5-hydroxytryptamine(3A) receptor. *Mol Pharmacol* **57**:1249-1255.

Sunesen M, de Carvalho LP, Dufresne V, Grailhe R, Savatier-Duclert N, Gibor G, Peretz A, Attali B, Changeux JP and Paas Y (2006) Mechanism of Cl⁻ selection by a glutamate-gated chloride (GluCl) receptor revealed through mutations in the selectivity filter. *J Biol Chem* **281**:14875-14881.

Suryanarayanan A, Joshi PR, Bikadi Z, Mani M, Kulkarni TR, Gaines C and Schulte MK (2005) The loop C region of the murine 5-HT3A receptor contributes to the differential actions of 5-hydroxytryptamine and m-chlorophenylbiguanide. *Biochemistry* **44**:9140-9149.

Swanson LW, Simmons DM, Whiting PJ and Lindstrom J (1987) Immunohistochemical localization of neuronal nicotinic receptors in the rodent central nervous system. *J Neurosci* **7**:3334-3342.

Taly A, Corringer PJ, Guedin D, Lestage P and Changeux JP (2009) Nicotinic receptors: allosteric transitions and therapeutic targets in the nervous system. *Nat Rev Drug Discov* **8**:733-750.

Taly A, Delarue M, Grutter T, Nilges M, Le Novere N, Corringer PJ and Changeux JP (2005) Normal mode analysis suggests a quaternary twist model for the nicotinic receptor gating mechanism. *Biophys J* **88**:3954-3965.

Tapia L, Kuryatov A and Lindstrom J (2007) Ca²⁺ permeability of the (alpha4)₃(beta2)₂ stoichiometry greatly exceeds that of (alpha4)₂(beta2)₃ human acetylcholine receptors. *Mol Pharmacol* **71**:769-776.

Tapper AR, McKinney SL, Marks MJ and Lester HA (2007) Nicotine responses in hypersensitive and knockout alpha 4 mice account for tolerance to both hypothermia and locomotor suppression in wild-type mice. *Physiol Genomics* **31**:422-428.

Tarroni P, Rubboli F, Chini B, Zwart R, Oortgiesen M, Sher E and Clementi F (1992) Neuronal-type nicotinic receptors in human neuroblastoma and small-cell lung carcinoma cell lines. *FEBS Lett* **312**:66-70.

Teissere JA and Czajkowski C (2001) A (beta)-strand in the (gamma)2 subunit lines the benzodiazepine binding site of the GABA A receptor: structural rearrangements detected during channel gating. *J Neurosci* **21**:4977-4986.

Ternburni MK, Blitzblau RC and Jacob MH (2000) Receptor targeting and heterogeneity at interneuronal nicotinic cholinergic synapses in vivo. *J Physiol* **525 Pt 1**:21-29.

Thompson AJ, Padgett CL and Lummis SC (2006) Mutagenesis and molecular modeling reveal the importance of the 5-HT3 receptor F-loop. *J Biol Chem* **281**:16576-16582.

Thompson AJ, Price KL, Reeves DC, Chan SL, Chau PL and Lummis SC (2005) Locating an antagonist in the 5-HT3 receptor binding site using modeling and radioligand binding. *J Biol Chem* **280**:20476-20482.

Thomsen T, Kaden B, Fischer JP, Bickel U, Barz H, Gusztony G, Cervos-Navarro J and Kewitz H (1991) Inhibition of acetylcholinesterase activity in human brain tissue and erythrocytes by galanthamine, physostigmine and tacrine. *Eur J Clin Chem Clin Biochem* **29**:487-492.

Tredway TL, Guo JZ and Chiappinelli VA (1999) N-type voltage-dependent calcium channels mediate the nicotinic enhancement of GABA release in chick brain. *J Neurophysiol* **81**:447-454.

Treinin M (2008) RIC-3 and nicotinic acetylcholine receptors: biogenesis, properties, and diversity. *Biotechnol J* **3**:1539-1547.

Tsai CJ, del Sol A and Nussinov R (2008) Allostery: absence of a change in shape does not imply that allostery is not at play. *J Mol Biol* **378**:1-11.

Turner JR and Kellar KJ (2005) Nicotinic cholinergic receptors in the rat cerebellum: multiple heteromeric subtypes. *J Neurosci* **25**:9258-9265.

Tutka P and Zatonski W (2006) Cytisine for the treatment of nicotine addiction: from a molecule to therapeutic efficacy. *Pharmacol Rep* **58**:777-798.

Umbriaco D, Watkins KC, Descarries L, Cozzari C and Hartman BK (1994) Ultrastructural and morphometric features of the acetylcholine innervation in adult rat parietal cortex: an electron microscopic study in serial sections. *J Comp Neurol* **348**:351-373.

Unwin N (1995) Acetylcholine receptor channel imaged in the open state. *Nature* **373**:37-43.

Unwin N (2005) Refined structure of the nicotinic acetylcholine receptor at 4Å resolution. *J Mol Biol* **346**:967-989.

Unwin N, Miyazawa A, Li J and Fujiyoshi Y (2002) Activation of the nicotinic acetylcholine receptor involves a switch in conformation of the alpha subunits. *J Mol Biol* **319**:1165-1176.

Valor LM, Mulet J, Sala F, Sala S, Ballesta JJ and Criado M (2002) Role of the large cytoplasmic loop of the alpha 7 neuronal nicotinic acetylcholine receptor subunit in receptor expression and function. *Biochemistry* **41**:7931-7938.

Venkataraman P, Joshi P, Venkatachalan SP, Muthalagi M, Parihar HS, Kirschbaum KS and Schulte MK (2002a) Functional group interactions of a 5-HT3R antagonist. *BMC Biochem* **3**:16.

- Venkataraman P, Venkatachalan SP, Joshi PR, Muthalagi M and Schulte MK (2002b) Identification of critical residues in loop E in the 5-HT₃ASR binding site. *BMC Biochem* **3**:15.
- Vernino S, Amador M, Luetje CW, Patrick J and Dani JA (1992) Calcium modulation and high calcium permeability of neuronal nicotinic acetylcholine receptors. *Neuron* **8**:127-134.
- Vernino S, Rogers M, Radcliffe KA and Dani JA (1994) Quantitative measurement of calcium flux through muscle and neuronal nicotinic acetylcholine receptors. *J Neurosci* **14**:5514-5524.
- Videtic GM, Stitt LW, Dar AR, Kocha WI, Tomiak AT, Truong PT, Vincent MD and Yu EW (2003) Continued cigarette smoking by patients receiving concurrent chemoradiotherapy for limited-stage small-cell lung cancer is associated with decreased survival. *J Clin Oncol* **21**:1544-1549.
- Vizi ES (2000) Role of high-affinity receptors and membrane transporters in nonsynaptic communication and drug action in the central nervous system. *Pharmacol Rev* **52**:63-89.
- Wada E, Wada K, Boulter J, Deneris E, Heinemann S, Patrick J and Swanson LW (1989) Distribution of alpha 2, alpha 3, alpha 4, and beta 2 neuronal nicotinic receptor subunit mRNAs in the central nervous system: a hybridization histochemical study in the rat. *J Comp Neurol* **284**:314-335.
- Wagner DA and Czajkowski C (2001) Structure and dynamics of the GABA binding pocket: A narrowing cleft that constricts during activation. *J Neurosci* **21**:67-74.
- Wanamaker CP, Christianson JC and Green WN (2003) Regulation of nicotinic acetylcholine receptor assembly. *Ann N Y Acad Sci* **998**:66-80.
- Wang F, Nelson ME, Kuryatov A, Olale F, Cooper J, Keyser K and Lindstrom J (1998) Chronic nicotine treatment up-regulates human alpha3 beta2 but not alpha3 beta4 acetylcholine receptors stably transfected in human embryonic kidney cells. *J Biol Chem* **273**:28721-28732.
- Wang HL, Cheng X, Taylor P, McCammon JA and Sine SM (2008a) Control of cation permeation through the nicotinic receptor channel. *PLoS Comput Biol* **4**:e41.
- Wang HY, Lee DH, Davis CB and Shank RP (2000) Amyloid peptide Abeta(1-42) binds selectively and with picomolar affinity to alpha7 nicotinic acetylcholine receptors. *J Neurochem* **75**:1155-1161.
- Wang JM, Zhang L, Yao Y, Viroonchatapan N, Rothe E and Wang ZZ (2002) A transmembrane motif governs the surface trafficking of nicotinic acetylcholine receptors. *Nat Neurosci* **5**:963-970.
- Wang K, Hackett JT, Cox ME, Van Hoek M, Lindstrom JM and Parsons SJ (2004) Regulation of the neuronal nicotinic acetylcholine receptor by SRC family tyrosine kinases. *J Biol Chem* **279**:8779-8786.
- Wang Y, Broderick P, Webb E, Wu X, Vijayakrishnan J, Matakidou A, Qureshi M, Dong Q, Gu X, Chen WV, Spitz MR, Eisen T, Amos CI and Houlston RS (2008b) Common 5p15.33 and 6p21.33 variants influence lung cancer risk. *Nat Genet* **40**:1407-1409.
- Wang Y, Pereira EF, Maus AD, Ostlie NS, Navaneetham D, Lei S, Albuquerque EX and Conti-Fine BM (2001) Human bronchial epithelial and endothelial cells express alpha7 nicotinic acetylcholine receptors. *Mol Pharmacol* **60**:1201-1209.
- Ward JM, Cockcroft VB, Lunt GG, Smillie FS and Wonnacott S (1990) Methyllycaconitine: a selective probe for neuronal alpha-bungarotoxin binding sites. *FEBS Lett* **270**:45-48.
- Wathey JC, Nass MM and Lester HA (1979) Numerical reconstruction of the quantal event at nicotinic synapses. *Biophys J* **27**:145-164.
- Watkins SS, Epping-Jordan MP, Koob GF and Markou A (1999) Blockade of nicotine self-administration with nicotinic antagonists in rats. *Pharmacol Biochem Behav* **62**:743-751.

- Wehner JM, Keller JJ, Keller AB, Picciotto MR, Paylor R, Booker TK, Beaudet A, Heinemann SF and Balogh SA (2004) Role of neuronal nicotinic receptors in the effects of nicotine and ethanol on contextual fear conditioning. *Neuroscience* **129**:11-24.
- Weiss RB, Baker TB, Cannon DS, von Niederhausern A, Dunn DM, Matsunami N, Singh NA, Baird L, Coon H, McMahon WM, Piper ME, Fiore MC, Scholand MB, Connett JE, Kanner RE, Gahring LC, Rogers SW, Hoidal JR and Leppert MF (2008) A candidate gene approach identifies the CHRNA5-A3-B4 region as a risk factor for age-dependent nicotine addiction. *PLoS Genet* **4**:e1000125.
- Wells GB (2008) Structural answers and persistent questions about how nicotinic receptors work. *Front Biosci* **13**:5479-5510.
- Weltzin MM and Schulte MK (2010) Pharmacological characterization of the allosteric modulator desformylflustrabromine and its interaction with alpha4beta2 neuronal nicotinic acetylcholine receptor orthosteric ligands. *J Pharmacol Exp Ther* **334**:917-926.
- West KA, Brognard J, Clark AS, Linnoila IR, Yang X, Swain SM, Harris C, Belinsky S and Dennis PA (2003) Rapid Akt activation by nicotine and a tobacco carcinogen modulates the phenotype of normal human airway epithelial cells. *J Clin Invest* **111**:81-90.
- White BH and Cohen JB (1992) Agonist-induced changes in the structure of the acetylcholine receptor M2 regions revealed by photoincorporation of an uncharged nicotinic noncompetitive antagonist. *J Biol Chem* **267**:15770-15783.
- Whitehouse PJ and Kalaria RN (1995) Nicotinic receptors and neurodegenerative dementing diseases: basic research and clinical implications. *Alzheimer Dis Assoc Disord* **9 Suppl 2**:3-5.
- Wick MJ, Mihic SJ, Ueno S, Mascia MP, Trudell JR, Brozowski SJ, Ye Q, Harrison NL and Harris RA (1998) Mutations of gamma-aminobutyric acid and glycine receptors change alcohol cutoff: evidence for an alcohol receptor? *Proc Natl Acad Sci U S A* **95**:6504-6509.
- Wiesner A and Fuhrer C (2006) Regulation of nicotinic acetylcholine receptors by tyrosine kinases in the peripheral and central nervous system: same players, different roles. *Cell Mol Life Sci* **63**:2818-2828.
- Williams BM, Temburni MK, Levey MS, Bertrand S, Bertrand D and Jacob MH (1998) The long internal loop of the alpha 3 subunit targets nAChRs to subdomains within individual synapses on neurons in vivo. *Nat Neurosci* **1**:557-562.
- Wingrove PB, Thompson SA, Wafford KA and Whiting PJ (1997) Key amino acids in the gamma subunit of the gamma-aminobutyric acidA receptor that determine ligand binding and modulation at the benzodiazepine site. *Mol Pharmacol* **52**:874-881.
- Wong HP, Yu L, Lam EK, Tai EK, Wu WK and Cho CH (2007) Nicotine promotes cell proliferation via alpha7-nicotinic acetylcholine receptor and catecholamine-synthesizing enzymes-mediated pathway in human colon adenocarcinoma HT-29 cells. *Toxicol Appl Pharmacol* **221**:261-267.
- Wonnacott S (1997) Presynaptic nicotinic ACh receptors. *Trends Neurosci* **20**:92-98.
- Wolf NJ (1991) Cholinergic systems in mammalian brain and spinal cord. *Prog Neurobiol* **37**:475-524.
- Wooltorton JR, Pidoplichko VI, Broide RS and Dani JA (2003) Differential desensitization and distribution of nicotinic acetylcholine receptor subtypes in midbrain dopamine areas. *J Neurosci* **23**:3176-3185.
- Wotring VE and Weiss DS (2008) Charge scan reveals an extended region at the intracellular end of the GABA receptor pore that can influence ion selectivity. *J Gen Physiol* **131**:87-97.

- Xiao Y, Baydyuk M, Wang HP, Davis HE and Kellar KJ (2004) Pharmacology of the agonist binding sites of rat neuronal nicotinic receptor subtypes expressed in HEK 293 cells. *Bioorg Med Chem Lett* **14**:1845-1848.
- Xu J, Zhu Y and Heinemann SF (2006) Identification of sequence motifs that target neuronal nicotinic receptors to dendrites and axons. *J Neurosci* **26**:9780-9793.
- Yan D, Schulte MK, Bloom KE and White MM (1999) Structural features of the ligand-binding domain of the serotonin 5HT₃ receptor. *J Biol Chem* **274**:5537-5541.
- Yan D and White MM (2002) Interaction of d-tubocurarine analogs with mutant 5-HT₃ receptors. *Neuropharmacology* **43**:367-373.
- Yan D and White MM (2005) Spatial orientation of the antagonist granisetron in the ligand-binding site of the 5-HT₃ receptor. *Mol Pharmacol* **68**:365-371.
- Ye YN, Liu ES, Shin VY, Wu WK, Luo JC and Cho CH (2004) Nicotine promoted colon cancer growth via epidermal growth factor receptor, c-Src, and 5-lipoxygenase-mediated signal pathway. *J Pharmacol Exp Ther* **308**:66-72.
- You H, Kozuska JL, Paulsen IM and Dunn SM (2010) Benzodiazepine modulation of the rat GABA_A receptor alpha4beta3gamma2L subtype expressed in *Xenopus* oocytes. *Neuropharmacology* **59**:527-533.
- Young GT, Zwart R, Walker AS, Sher E and Millar NS (2008) Potentiation of alpha7 nicotinic acetylcholine receptors via an allosteric transmembrane site. *Proc Natl Acad Sci U S A* **105**:14686-14691.
- Young JW, Crawford N, Kelly JS, Kerr LE, Marston HM, Spratt C, Finlayson K and Sharkey J (2007) Impaired attention is central to the cognitive deficits observed in alpha 7 deficient mice. *Eur Neuropsychopharmacol* **17**:145-155.
- Yu XM and Hall ZW (1994a) The role of the cytoplasmic domains of individual subunits of the acetylcholine receptor in 43 kDa protein-induced clustering in COS cells. *J Neurosci* **14**:785-795.
- Yu XM and Hall ZW (1994b) A sequence in the main cytoplasmic loop of the alpha subunit is required for assembly of mouse muscle nicotinic acetylcholine receptor. *Neuron* **13**:247-255.
- Zarei MM, Radcliffe KA, Chen D, Patrick JW and Dani JA (1999) Distributions of nicotinic acetylcholine receptor alpha7 and beta2 subunits on cultured hippocampal neurons. *Neuroscience* **88**:755-764.
- Zheng Y, Ritzenthaler JD, Roman J and Han S (2007) Nicotine Stimulates Human Lung Cancer Cell Growth by Inducing Fibronectin Expression. *Am J Respir Cell Mol Biol*.
- Zhong W, Gallivan JP, Zhang Y, Li L, Lester HA and Dougherty DA (1998) From ab initio quantum mechanics to molecular neurobiology: a cation-pi binding site in the nicotinic receptor. *Proc Natl Acad Sci U S A* **95**:12088-12093.
- Zhou FM, Wilson CJ and Dani JA (2002) Cholinergic interneuron characteristics and nicotinic properties in the striatum. *J Neurobiol* **53**:590-605.
- Zhou Y, Morais-Cabral JH, Kaufman A and MacKinnon R (2001) Chemistry of ion coordination and hydration revealed by a K⁺ channel-Fab complex at 2.0 Å resolution. *Nature* **414**:43-48.
- Zhou Y, Nelson ME, Kuryatov A, Choi C, Cooper J and Lindstrom J (2003) Human alpha4beta2 acetylcholine receptors formed from linked subunits. *J Neurosci* **23**:9004-9015.
- Zhou Y, Pearson JE and Auerbach A (2005) Phi-value analysis of a linear, sequential reaction mechanism: theory and application to ion channel gating. *Biophys J* **89**:3680-3685.

Zia S, Ndoye A, Nguyen VT and Grando SA (1997) Nicotine enhances expression of the alpha 3, alpha 4, alpha 5, and alpha 7 nicotinic receptors modulating calcium metabolism and regulating adhesion and motility of respiratory epithelial cells. *Res Commun Mol Pathol Pharmacol* **97**:243-262.

Zoli M, Le Novere N, Hill JA, Jr. and Changeux JP (1995) Developmental regulation of nicotinic ACh receptor subunit mRNAs in the rat central and peripheral nervous systems. *J Neurosci* **15**:1912-1939.

Zwart R, Broad LM, Xi Q, Lee M, Moroni M, Bermudez I and Sher E (2006a) 5-I A-85380 and TC-2559 differentially activate heterologously expressed alpha4beta2 nicotinic receptors. *Eur J Pharmacol*.

Zwart R, Broad LM, Xi Q, Lee M, Moroni M, Bermudez I and Sher E (2006b) 5-I A-85380 and TC-2559 differentially activate heterologously expressed alpha4beta2 nicotinic receptors. *Eur J Pharmacol* **539**:10-17.

Zwart R and Vijverberg HP (1998) Four pharmacologically distinct subtypes of alpha4beta2 nicotinic acetylcholine receptor expressed in *Xenopus laevis* oocytes. *Mol Pharmacol* **54**:1124-1131.

CHAPTER 3: Pharmacological Characterization of the Allosteric Modulator Desformylflustrabromine and its Interaction with $\alpha 4\beta 2$ nAChR Orthosteric Ligands¹

3.1 Abstract.

Neuronal nicotinic acetylcholine receptors (nAChRs) are members of the Cys-loop superfamily of ligand-gated ion channels. nAChRs are involved in modulating nicotinic based signal transmission in the CNS and are implicated in a range of CNS disorders. Desformylflustrabromine (dFBr) is a positive allosteric modulator which potentiates $\alpha 4\beta 2$ nAChRs. Sala et al. report that dFBr is selective for the $\alpha 4\beta 2$ receptor relative to other common nAChR subtypes (Sala et al., 2005). Co-application of dFBr with acetylcholine produces a bell-shaped dose response curve with a peak potentiation of over 265% (Kim et al., 2007) at dFBr concentrations $< 10 \mu\text{M}$ and inhibition of responses at concentrations $> 10 \mu\text{M}$. The potentiation and inhibition components of dFBr modulated responses were examined using two-electrode voltage clamp and human $\alpha 4\beta 2$ nAChRs expressed in *Xenopus laevis* oocytes. Currents to both partial and full agonists were potentiated by dFBr. Responses to low efficacy agonists were potentiated significantly more than responses to high efficacy agonists. Antagonist pIC_{50} values were unaffected by co-application of dFBr. In addition to its potentiating effects, dFBr was also able to induce current spikes when applied to desensitized receptors suggestive of a shift in equilibrium from the desensitized to open conformation. In contrast to potentiation, inhibition of ACh responses by dFBr is dependent on membrane potential and is likely the result of open-channel block by dFBr and acetylcholine. Our data indicate distinct mechanisms for the potentiation and inhibition components of dFBr action. dFBr could prove useful for therapeutic enhancement of responses at $\alpha 4\beta 2$ containing synapses.

¹ Weltzin, M. M. and Schulte, M. K. 2010. Pharmacological Characterization of the Allosteric Modulator Desformylflustrabromine and its Interaction with $\alpha 4\beta 2$ nAChR Orthosteric Ligands. *J Pharmacol Exp Ther.* Sep 1;334(3):917-26.

3.2 Introduction.

The CNS expression of neuronal nicotinic acetylcholine receptor (nAChR) subtypes are altered in many neurological disorders including Alzheimer's disease (Court et al., 2001; Nordberg, 2001), Autism (Martin-Ruiz et al., 2004; Lippiello, 2006), Parkinson's disease (Aubert et al., 1992) and Schizophrenia (Woodruff-Pak and Gould, 2002; Friedman, 2004; Adams and Stevens, 2007). In Alzheimer's disease, multiple subtypes of nAChRs decline producing a decrease in cholinergic tone (Court et al., 2001; Nordberg, 2001). Post-mortem studies of Autistics have shown both decreases and increases in nAChR subtypes (Court et al., 2001; Nordberg, 2001; Martin-Ruiz et al., 2004; Lippiello, 2006). Increases in receptor populations should be amenable to remediation with antagonists but treatment of disorders involving decreases in receptor number are more difficult. Treatment strategies aimed at increasing activity of cholinergic systems have focused on acetylcholinesterase inhibitors and partial agonists (Corey-Bloom, 2003; Nicolson et al., 2006). While agonists are potentially useful therapeutically, the rapid desensitization of nAChRs produced by chronic exposure to agonists limits their usefulness.

Positive allosteric modulators (PAM) represent an alternative treatment strategy. Since PAMs typically enhance agonist responses without activating receptors, synaptic currents remain linked to endogenous neurotransmitter release. In disorders where differential changes in nAChR densities occur, non-selective compounds may improve some symptoms while exacerbating others. The development of subtype selective PAMs is an important step in developing therapeutic treatments for neurological disorders involving alterations in nicotinic tone.

Desformylflustrabromine (dFBr) is a novel PAM that potentiates ACh induced whole cell responses of the $\alpha 4\beta 2$ nAChR subtype by greater than 265% (3 μ M dFBr co-applied with 100 μ M ACh). Previous studies have shown no apparent potentiation of other subtypes including $\alpha 7$ and $\alpha 3\beta 4$ (Sala et al., 2005; Kim et al., 2007). On $\alpha 4\beta 2$ receptors, co-application of increasing concentrations of dFBr with a fixed concentration of ACh produces a bell-shaped dose response curve containing both stimulatory (<10 μ M dFBr) and inhibitory components (>10 μ M dFBr) (Kim et al., 2007). On $\alpha 7$ receptors, only the inhibitory component is present. Previous studies using dFBr extracted from *Flustra foliacea* suggested potentiation may be a result of altered channel gating kinetics (Sala et al., 2005). At inhibitory concentrations of dFBr "rebound" or "hump currents" have been observed suggesting dFBr inhibition may be attributable to open-channel block (Kim et al., 2007).

The current study aims to better understand the mechanisms of dFBr potentiation and inhibition. We investigated both the inhibitory and potentiating actions of dFBr using a series of

full agonists, partial agonists and antagonists. Our data suggest that inhibition and potentiation are mediated by distinct mechanisms at different binding sites. Inhibition appears to be the result of channel block by both dFBr and the stimulating agonist. dFBr was determined to potentiate low efficacy agonists greater than high efficacy agonists and was capable of recovering receptors from desensitization. This supports the hypothesis that dFBr inhibition is caused by open-channel block while potentiation is due to a change in the equilibrium between open and desensitized conformations.

3.3 Methods.

3.3.1 Receptors and RNA.

The cDNA for human $\alpha 4$ and $\beta 2$ nAChR subunits was generously provided by Dr. Jon Lindstrom (University of Pennsylvania). This cDNA was inserted into a pcDNA3.1/Zeo (Invitrogen, Carlsbad, CA) mammalian expression vector to produce mRNA for receptor expression in *Xenopus laevis* oocytes. *Xenopus laevis* frogs and frog food were purchased from *Xenopus* Express (Homosassa, FL). Ovarian lobes were surgically removed from Finquel anesthetized *Xenopus laevis* frogs and washed twice in Ca^{+2} -free Barth's buffer (82.5 mM NaCl; 2.5 mM KCl; 1 mM MgCl_2 ; 5 mM HEPES, pH 7.4) then gently shaken with 1.5 mg/mL collagenase (Sigma type II, Sigma-Aldrich, MO) for 20min at 20–25°C. Stage V and VI oocytes were selected for microinjection (University of Alaska Institutional Animal Care and Use Committee: 08-71). No more than four surgeries were conducted on each frog. A recovery period greater than six weeks was allowed between repeat surgeries on the same animal. Synthetic cRNA transcripts for human $\alpha 4\beta 2$ were prepared using the T7 mMACHINE™ High Yield Capped RNA Transcription Kit (Ambion, Austin, TX). Oocytes were injected with a total of 50 nL cRNA at a concentration of 300 ng/ μL and incubated at 19°C for 24-72h prior to their use in voltage clamp experiments. At least two different batches of oocytes were used per experiment. dFBr·HCl was synthesized by Dr. Richard Glennon (Virginia Commonwealth University) (Kim et al., 2007) and dissolved in ND-96 buffer prior to use.

3.3.2 Two-Electrode Voltage Clamp.

Recordings were performed using an automated two-electrode voltage-clamp system incorporating an OC-725C oocyte clamp amplifier (Warner Instruments, Hamden, CT) coupled to a computerized data acquisition (Datapac 2000, RUN technologies, Mission Viejo, CA) and autoinjection system (Gilson, Middleton, WI). Recording and current electrodes with resistance 1–4 M Ω were filled with 3 M KCl. Details of the chambers and methodology employed for

electrophysiological recordings have been described earlier (Joshi et al., 2004). Oocytes were held in a vertical flow chamber of 200 μ L volume, clamped at a holding potential of -60 mV and perfused with ND-96 recording buffer (96 mM NaCl; 2 mM KCl; 1.8 mM CaCl₂; 1 mM MgCl₂; 5 mM HEPES; pH 7.4) at a rate of 20 mL/min. For voltage step experiments, the holding potential was varied from -100 mV to +20 mV. Test compounds (Sigma-Aldrich, Natick, MO and Tocris, Ellisville, MO) were dissolved in ND-96 buffer and injected into the chamber at a rate of 20 mL/min using a Gilson auto-sampler injection system.

3.3.3 Electrophysiology Dose/Response Experiments.

Dose/response curves for the full agonist (Acetylcholine·Cl, (ACh) [Sigma-Aldrich]) and the partial agonists ((-)-nicotine [Riedel-de-Haën, Germany], choline·Cl [Sigma-Aldrich] and cytosine [Sigma-Aldrich]) were evaluated at concentrations ranging from 0.01 μ M-300 μ M for ACh, nicotine and cytosine and 0.1 μ M-30 mM for choline. The effects of dFBr on agonist efficacies were determined by co-exposure of varied concentrations of agonist with 1 μ M dFBr.

The competitive antagonists (Dihydro- β -erythroidine·HBr [Tocris], DMAB-anabaseine·2HCl [Tocris] and tropisetron·HCl [Tocris]) were evaluated for their ability to inhibit responses to 1 mM ACh at antagonist concentrations ranging from 0.001 μ M-100 μ M. The effect of dFBr on antagonist inhibition was determined by co-exposing receptors to antagonist, 1 mM ACh and 1 μ M dFBr.

In order to permit comparison of responses from different oocytes, individual responses to drug application were normalized to control responses elicited using 1 mM ACh. Data were collected from at least four replicate experiments using oocytes obtained from at least two different frogs.

3.3.4 Exposure of dFBr Prior to Agonist Activation and During Agonist Induced Desensitization.

To study the effects of dFBr prior to agonist activation (pre-exposure) on α 4 β 2 nAChR, 1 μ M dFBr was bath applied at a rate of 4 mL/min 30s prior to application of agonist. Following pre-exposure to dFBr, 1 mM ACh, was applied at a 20 mL/min perfusion rate for 3s. The slope of the rising phase of the response was determined from current data during the linear portion of the response prior to the peak current. Slopes for pre- and co-exposure experiments were compared using these data and p values were calculated based on the null hypothesis using an unpaired t-test.

dFBr was also applied during the desensitization refractory phase of the agonist response. In these "post-exposure" experiments, saturating concentrations of agonists (1 mM ACh, 10 mM ACh or 100 μ M cytisine) were bath applied at a rate of 4 mL/min prior to exposure to dFBr. One μ M dFBr was applied at a rate of 20 mL/min in repeated 3s pulses once the agonist response entered the refractory desensitized phase of the response. Responses were normalized to currents obtained by using the appropriate ACh concentration in the absence of dFBr. The slope of the rising phase of the response was determined from current data during the linear portion of the response prior to the peak current. The agonist and dFBr induced currents were compared using p values calculated based on the null hypothesis using an unpaired t-test.

The effects of long-term exposure to 1 μ M dFBr on activated receptors were also investigated. One mM ACh or 100 μ M cytisine were bath applied at a rate of 4 mL/min. Eight mL of 1 μ M dFBr with and without agonist was perfused at a rate of 10 mL/min for 48s to desensitized receptors. As a control, 1 mM ACh was bath applied while 1 mM ACh was perfused for 48s at the onset of the maximum induced response. Alterations in the response currents were examined.

3.3.5 Voltage Step Experiments.

The voltage dependence of both dFBr potentiation and inhibition was determined by using α 4 β 2 expressing *Xenopus laevis* oocytes and two-electrode voltage clamp. The membrane potential was incrementally increased in 10 mV steps ranging from -100 mV to +20 mV. Cytisine was chosen as the stimulating ligand for these experiments since it has been previously shown to not induce channel block of nAChRs at 100 μ M (Liu et al., 2008). dFBr at either 10 μ M (potentiating concentration) or 30 μ M (inhibitory concentration) was co-applied with a fixed concentration of 100 μ M cytisine (saturating concentration) at each voltage step. Responses were normalized to the response obtained at a membrane potential of -60 mV and 1 mM acetylcholine applied alone. The membrane potential (V_m) was plotted against the normalized current. The slope of the V_m vs I plot was determined using linear regression.

3.3.6 Data Analysis.

Concentration/response curves were fit using non-linear curve fitting and GraphPad Prism Software (San Diego, CA) with standard built-in algorithms. Values for the log EC_{50} and nH were determined by fitting the concentration response data to a single site binding model:

$$I = \frac{b + (I_{\max} - b)}{1 + 10^{(\text{Log}EC_{50} - \text{Log}[L]) * nH}} \quad (1)$$

Where I is the current elicited on application of agonist, b is the baseline current in the absence of ligand, L is the ligand concentration and nH is the Hill slope. The EC_{50} value is the concentration of agonist producing currents equal to one half the maximal current (I_{max}). The pEC_{50} values reported in the data tables reflect the negative log of the EC_{50} . EC_{50} values were also calculated from the $\log EC_{50}$ and are included in the tables for convenience. I_{max} values for different partial and full agonists were compared to evaluate relative apparent efficacies and apparent efficacy changes as a result of dFBr co-application. In order to permit comparison of full and partial agonist data from different oocytes, responses for all test compounds were normalized to the currents obtained with 1 mM ACh in the absence of dFBr.

For inhibition experiments, pIC_{50} ($-\log IC_{50}$) and IC_{50} values were determined by fitting concentration/response data to a single site competition model:

$$I = \frac{b + (I_{max} - b)}{1 + 10^{(\log[L] - \log IC_{50})}} \quad (2)$$

Where I is the current at a specific inhibitor/agonist concentrations, b is the baseline current in the absence of agonist and L is the ligand concentration. The IC_{50} value is the concentration of antagonist that reduces the current to one half that obtained by the identical concentration of agonist alone. The pIC_{50} values reported in the data tables reflect the negative log of the IC_{50} . pIC_{50} values were typically determined at agonist concentrations equal to the EC_{50} for the agonist used. In order to compare data from different oocytes, currents were normalized to those obtained from application of 1 mM ACh alone. For experiments involving co-perfusions of both an antagonist and agonist with dFBr responses were normalized to those obtained by co-perfusion of 1 μ M dFBr with 1 mM ACh.

Comparisons of pEC_{50} or pIC_{50} values were conducted using an unpaired t-test and p values calculated based on the null hypothesis.

3.4 Results.

3.4.1 dFBr Inhibition Involves Open-Channel Block.

Understanding the nature of dFBr inhibition is essential to correctly interpreting overall response kinetics. Clues to the mechanism of dFBr inhibition come from previous studies of dFBr that show the presence of hump currents during washout of dFBr and agonist (Kim et al., 2007). Hump currents, also known as rebound currents, are inward currents which occur during the desensitized phase of the response on washout of the ligand. Hump currents have been previously linked to open-channel block (Liu et al., 2008) and are thought to be induced when an agonist binds with high affinity to the orthosteric site and with lower affinity in the channel. During washout of the ligand, the ligand bound to the channel dissociates more rapidly thus removing the channel block and producing transient increases in the observed response. The observation of hump currents suggests dFBr inhibition may involve channel block. To explore this possibility, we evaluated the inhibition of cytosine induced currents at a series of different membrane potentials. Cytosine was chosen for these experiments since it's a known partial agonist that does not appear to act as a channel blocker (Liu et al., 2008) (Figure 3.1). While other more efficacious agonists could have been used for these experiments, the ability of these agonists to channel block would have complicated analysis of the results making it difficult to determine if any observed channel block is due to the stimulating agonist or dFBr. Increased membrane potential will typically reduce channel block thus increasing conductance at higher potentials as indicated by increased slopes in plots of voltage vs current (V/I). Figure 3.1 shows a V/I plot obtained by co-application of dFBr with 100 μM cytosine at both potentiating and inhibiting dFBr concentrations. At concentrations of dFBr that are potentiating rather than inhibiting (10 μM) co-exposure of 100 μM cytosine (saturating concentration of cytosine) produces a V/I plot that is linear over the entire range of membrane potentials tested. This verifies the lack of channel block by cytosine. In contrast, co-application of a higher, inhibitory concentration of dFBr (30 μM) with 100 μM cytosine produces a V/I plot that is non-linear over the range of membrane potentials tested.

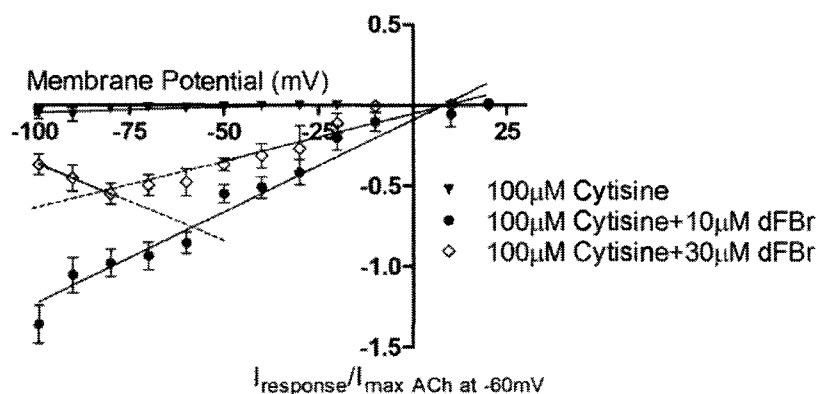


Figure 3.1 Voltage dependence of potentiation and inhibition by dFBr.

Membrane potential was increased in 10 mV steps from -100 mV to +20 mV using two-electrode voltage clamp on $\alpha 4\beta 2$ nAChR expressing oocytes. Responses were obtained as discussed in the methods section and were normalized to those elicited by application of 1 mM ACh at -60 mV from the same oocyte. At least two batches of oocytes from different frogs were harvested for the experiments. Each data point represents at least $n \geq 4$ replicates with error bars shown as \pm SEM. For the control group (100 μ M cytisine) the relationship between the induced response and the applied membrane potential is linear over the entire range of membrane potentials. Potentiating concentrations of dFBr (10 μ M) co-applied with 100 μ M cytisine show a similar linear relationship. Co-application of 30 μ M dFBr (inhibitory concentration) with 100 μ M cytisine shows a nonlinear relationship between membrane potential and the induced response.

3.4.2 dFBr Potentiates Low Efficacious Agonists More Than Full Agonists.

Partial agonists are useful tools in studying mechanisms of allosteric modulators. Changes in response profiles, I_{max} and pEC_{50} values for partial agonists that result from the addition of a modulator, such as dFBr, can provide clues to the mechanism underlying the actions of the modulator. We investigated dFBr's influence on the full agonist ACh and the partial agonists nicotine, choline and cytisine. ACh and choline were examined to explore possible physiological effects of dFBr within the synapse. While choline has not previously been considered a partial agonist at $\alpha 4\beta 2$ receptors, the observed effects of dFBr on agonist efficacies led us to consider whether choline might be revealed as an agonist for $\alpha 4\beta 2$ receptors in the presence of dFBr. Nicotine, a common substance of abuse, was selected because of its pathological significance in drug addiction. Cytisine was chosen because it is a $\alpha 4\beta 2$ partial agonist that does not induce channel block (Liu et al., 2008). In addition, the smoking cessation drug varenicline is a derivative of cytisine allowing us to explore dFBr's potential influence on this therapeutic treatment (Coe et al., 2005). dFBr's alterations of response profiles, pEC_{50} ($-\log EC_{50}$), I_{max} and Hill coefficients (n_H) for full and partial agonists are shown in Figure 3.2, Figure 3.3 and Table 3.1 respectively.

Figure 3.2 shows responses of $\alpha 4\beta 2$ receptors to different concentrations of agonist applied alone (left series of traces) or with increasing concentrations of dFBr at a fixed (EC_{75}) concentration of agonist or partial agonist (right series of traces). Agonist control responses show increases in the rise time and peak responses with increasing agonist concentrations (Figure 3.2). The desensitization profiles remain unaltered, although this is difficult to determine from responses obtained using the weak partial agonists choline and cytosine. Co-application of increasing concentrations of dFBr altered the profile of responses induced by agonists and partial agonists (Figure 3.2). As dFBr concentration is increased responses to ACh, nicotine, choline and cytosine show marked increases in the rise time of the response and peak currents. Desensitization rates are initially unchanged at low dFBr concentrations but increase as the concentration of dFBr is increased. This increase in the desensitization rate does not appear to occur with cytosine. Changes in responses resulting from application of dFBr were identical whether dFBr was co-applied or applied before addition of ACh (results not shown).

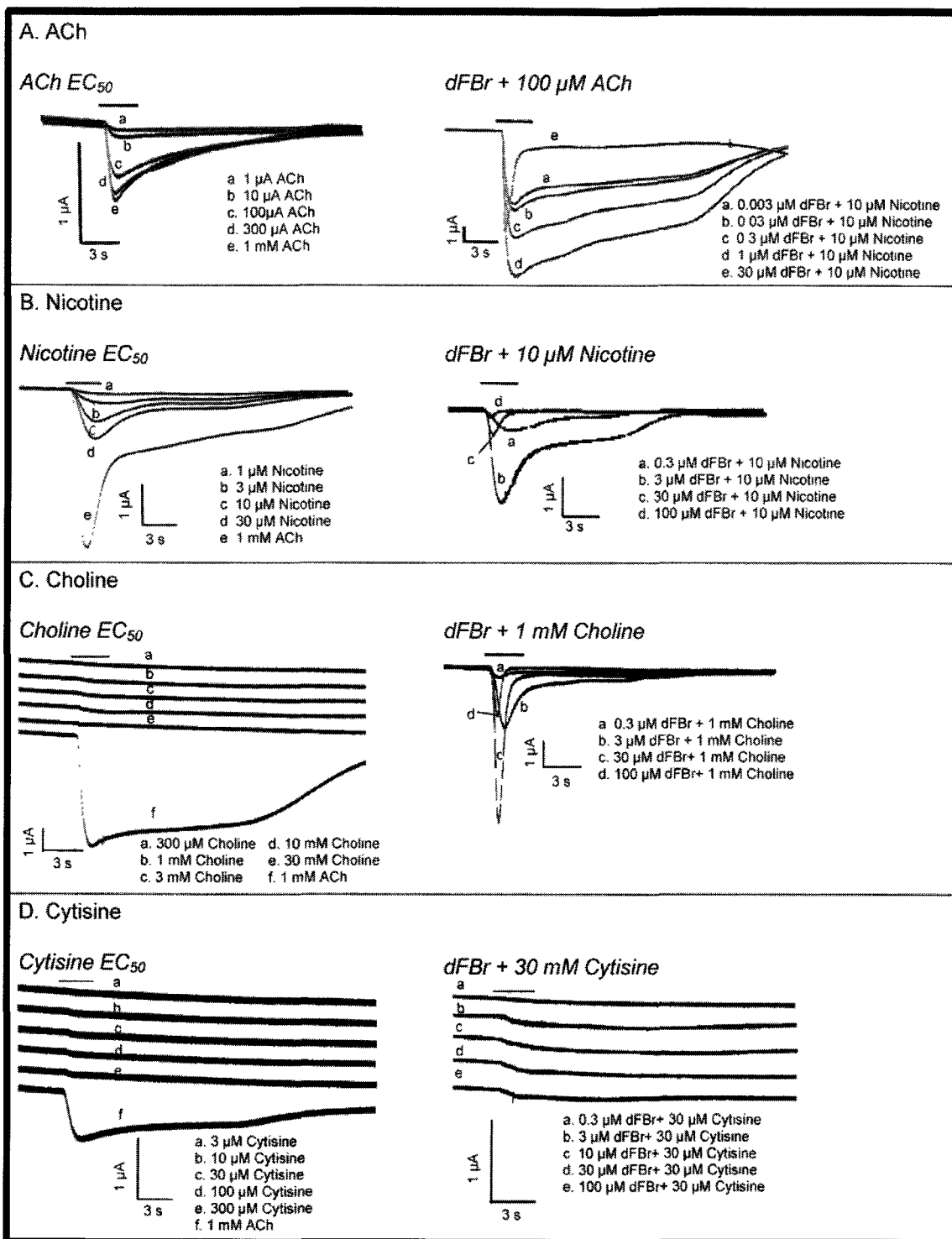


Figure 3.2 dFBr modulated responses to nAChR agonists and partial agonists.

Responses were obtained from *Xenopus* oocytes under voltage clamp conditions ($V_m = -60$ mV). Responses to agonists alone are shown in the **left** column. The **right** column show traces obtained at increasing concentrations of dFBr co-applied with fixed concentrations of either **A.** acetylcholine, **B.** nicotine, **C.** choline or **D.** cytisine. The legend for each panel shows the concentration of agonist applied alone (left) or the concentration of dFBr and co-applied (right). The solid bar above the response traces indicates the time the oocyte was exposed to the agonist and/or dFBr. All traces for each set of responses (left, right, A, B, C or D) were recorded from a single oocyte expressing $\alpha 4\beta 2$ receptors (mRNA injected at a ratio of 1 α :1 β). Similar data obtained at varied agonist concentrations were pooled and the data plotted to produce the dose response curves shown in Figure 3.3 and the data shown in Table 3.1.

The apparent pEC_{50} , efficacy and Hill coefficients (n_H) for each agonist were determined from concentration response data and are showed in Figure 3.3 and Table 3.1. The pEC_{50} values for the tested agonist were not altered by co-application of 1 μ M dFBr. Choline invoked extremely small currents making determination of pEC_{50} values in the absence of dFBr difficult; thus making it impossible to determine if the pEC_{50} changed as a result of dFBr application.

I_{max} values increased significantly in all cases and appeared to increase more substantially for weak partial agonists compared to the stronger partial agonist nicotine and the full agonist ACh (Table 3.1, Figure 3.3). A 2.70 fold increase in the I_{max} was observed for ACh in the presence of 1 μ M dFBr ($p < 0.0001$) while an increase of over 9.0 fold was observed for the weak partial agonists choline and cytosine ($p < 0.0001$). Increases in I_{max} for ACh are consistent with previously reported data for ACh (Sala et al., 2005; Kim et al., 2007). I_{max} values obtained for nicotine indicate a non-significant increase of 7.6 fold in the presence of 1 μ M dFBr ($p = 0.0069$) compared to nicotine alone. The maximum potentiated responses to weak partial agonists failed to reach similar amplitudes to potentiated responses of the full agonist ACh (Table 3.1). Hill slopes were not significantly altered for any of the four agonists tested.

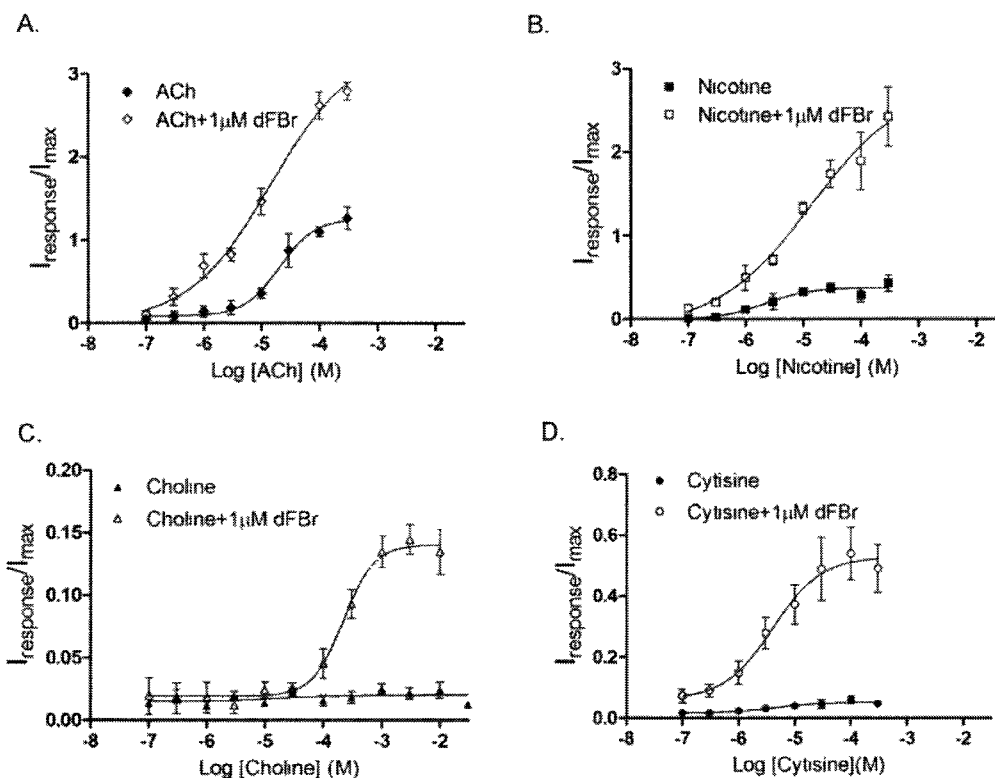


Figure 3.3 Dose response curves for agonists and partial agonists in the presence and absence of 1 μM dFBr.

dFBr and the appropriate concentration of agonist or partial agonist were co-applied to *Xenopus* oocytes expressing $\alpha 4\beta 2$ receptors (mRNA injected at a ratio of 1 α :1 β). The peak current was measured and responses normalized to currents elicited by 1mM ACh applied alone to the same oocyte. Each data point represents the combined data from at least four different experiments from a minimum of two different oocytes harvested from different frogs. Error bars indicate \pm SEM. pEC_{50} , I_{max} and Hill slope (n_H) were calculated using non-linear curve fitting algorithms and are shown in Table 3.1.

Table 3.1. dFBr induced effects on response kinetics for agonists and partial agonists.

The data were obtained using non-linear curve fitting algorithms from the dose response curves shown in Figure 3.3. Since individual responses were normalized to the response elicited by 1mM ACh alone, the I_{max} value shown represents the maximum current elicited relative to that obtained with 1mM ACh in the absence of dFBr. Values in brackets indicate the fractional change in the value resulting from co-application of 1 μ M dFBr. The statistical significance of observed differences in pEC_{50} , I_{max} and n_H as a result of 1 μ M dFBr co-application were evaluated using a paired student t-test. p -values are given in parentheses under the fold change. Values were considered statistically different at $p < 0.0001$.

Ligand	$pEC_{50} \pm SEM$ EC_{50} [μ M]		$I_{max} \pm SEM$		$n_H \pm SEM$	
	0 μ M dFBr	1 μ M dFBr [Fold Change]	0 μ M dFBr	1 μ M dFBr [Fold Change]	0 μ M dFBr	1 μ M dFBr [Fold Change]
ACh	4.7 \pm 0.1 (21)	4.8 \pm 0.3 (15) [1.0] ($p = 0.58$)	1.3 \pm 0.10	3.3 \pm 0.6 [2.7] ($p < 0.0001$)	1.4 \pm 0.5	0.6 \pm 0.2 [0.43] ($p = 0.21$)
Nicotine	5.7 \pm 0.3 (2.1)	4.9 \pm 0.5 (14) [0.9] ($p = 0.15$)	0.38 \pm .05	2.9 \pm 1.0 [7.6] ($p = 0.0069$)	1.1 \pm 0.8	0.5 \pm 0.4 [0.45] ($p = 0.55$)
Choline	N.D.*	3.7 \pm 0.1 (220) ($p = N.D.$)	0.015 \pm 0.003	0.14 \pm 0.008 [9.3] ($p < 0.0001$)	N.D.*	1.7 \pm 0.5 ($p = N.D.$)
Cytisine	5.3 \pm 0.5 (4.6)	5.4 \pm 0.3 (4.0) [1.0] ($p = 0.91$)	0.053 \pm 0.01	0.53 \pm 0.06 [9.9] ($p < 0.0001$)	0.94 \pm 0.98	1.0 \pm 0.6 [1.1] ($p = 0.95$)

*Value could not be accurately determined due to low efficacy of choline.

3.4.3 dFBr Does Not Appear to Alter Inhibition by Antagonists.

Since antagonists are typically thought to bind to the closed state of the receptor and do not stabilize the open conformation, they can be used to determine if application of dFBr produces a conformational change in the orthosteric binding site of the antagonist bound conformation. It is also possible that known antagonists might only weakly stabilize the open state and act as very poor partial agonists (similar to choline). These compounds might reveal themselves as agonists in the presence of modulators such as dFBr. We evaluated the effects of dFBr on three different nAChR antagonists Dihydro- β -erythroidine (DH β E), DMAB-anabaseine and Tropicsetron. Compounds with diverse actions, selectivity and structures were chosen. DMAB-

anabaseine is a partial agonist on $\alpha 7$ nAChRs but a competitive antagonist on other nAChRs including the $\alpha 4\beta 2$ subtype (Stevens et al., 1998). DH β E is a neuronal nAChR $\alpha 4$ selective competitive antagonist (Harvey et al., 1996), and tropisetron is a 5-HT $_3$ and $\alpha 4\beta 2$ nAChR receptor competitive antagonist (Middlemiss and Tricklebank, 1992).

Antagonists were evaluated for their ability to inhibit responses to 1 mM ACh on $\alpha 4\beta 2$ nAChR expressing oocytes in the presence and absence of 1 μ M dFBr (Figure 3.4). pIC $_{50}$ (-log IC $_{50}$) values were determined from these data and compared (inset, Figure 3.4). No significant change in pIC $_{50}$ was observed for DH β E or tropisetron (Figure 3.4, table insert). In the presence of dFBr, the DMAB-anabaseine pIC $_{50}$ was increased significantly ($p < 0.0001$). The dose-response curve of co-application of dFBr and DMAB appears biphasic, however; fitting the data to a two site model did not produce any improvement compared to the single site model (single site, $r^2 = 0.77$; two site, $r^2 = 0.77$). It is possible that a biphasic curve could be produced as a result of expression of both high and low affinity $\alpha 4\beta 2$ stoichiometries. It has been shown that DH β E has different inhibitory effects on the two different receptor stoichiometries (Moroni et al., 2006). DMAB-anabaseine may have similar effects, but to our knowledge this ligand has not been tested on high and low affinity $\alpha 4\beta 2$ nAChRs.

To determine if dFBr could stimulate an agonist-like response with antagonists, 1 μ M dFBr was co-applied in the absence of ACh at antagonist concentrations up to 100 μ M. No currents were observed under these conditions.

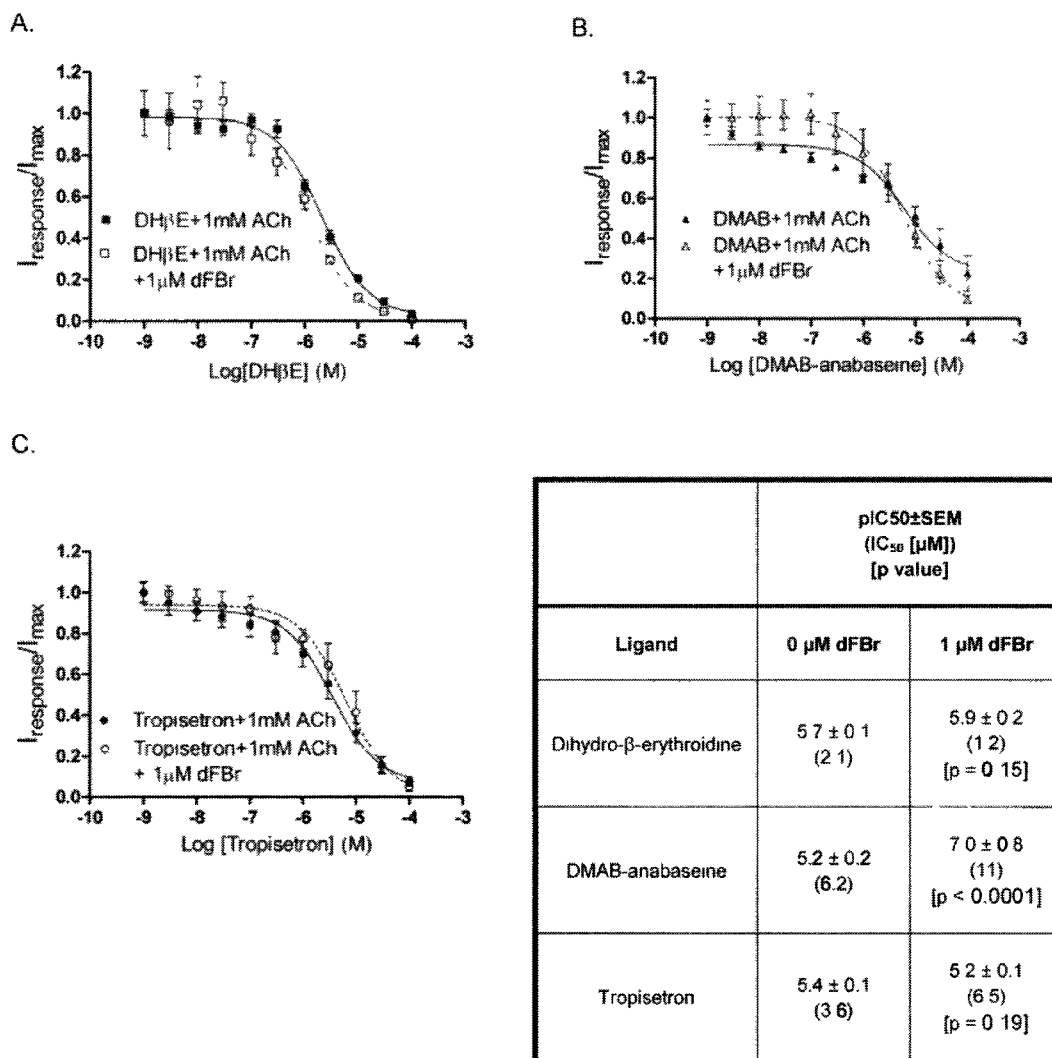


Figure 3.4 Co-application of dFBr with nAChR antagonists.

Xenopus oocytes expressing $\alpha 4\beta 2$ receptors (mRNA injected at a ratio of 1 α :1 β) were exposed to 1 mM ACh and responses inhibited by co-application of increasing concentrations of **A.** DH β E, **B.** DMAB-anabaseine or **C.** tropisetron. Since individual peak amplitudes were normalized to those elicited by 1 mM ACh applied alone on the same oocyte, I_{max} values express peak currents relative to those obtained with 1 mM ACh. pIC₅₀ values (inset table) were determined using non-linear curve fitting as described in the methods. Data points represent at least 4 replicate values obtained from a minimum of two oocytes harvested from different frogs. Error bars indicate \pm SEM.

3.4.4 dFBr Can Reactivate Desensitized Receptors.

To examine the effect of dFBr on desensitized receptors, dFBr was applied to $\alpha 4\beta 2$ receptors desensitized with saturating concentrations of ACh (Figure 3.5). In the absence of dFBr, repeated application of 10 mM ACh during the desensitization period of the response elicits no additional current (Figure 3.5A Top). This is consistent with the presence of a large number of desensitized receptors in the preparation that are resistant to reactivation by ACh. Application of 3s pulses of dFBr applied during the desensitized phase produced large inward currents (Figure 3.5A Bottom). Repeated 3s applications of dFBr produced a series of responses with progressively decreasing peak currents (Figure 3.5B and C). When responses were elicited using 1 mM ACh (Figure 3.5B), rather than 10 mM ACh, activation with 1 μ M dFBr produced hump currents immediately following the 3s dFBr pulse. The activation slope for the first dFBr pulse obtained during the desensitization period was -190 ± 9 nA/s for 1 mM ACh induced responses and -1020 ± 130 nA/s for 10 mM ACh induced responses. Activation slopes for responses in which dFBr and ACh were co-applied to non-desensitized receptors as shown in Figure 3.2 were also determined: 1mM ACh + 1 μ M dFBr, -13 ± 2 nA/s and 10 mM ACh + 1 μ M dFBr, -66 ± 6 nA/s. Thus, the activation slope of the response to a dFBr pulse applied during desensitization is 15 times faster than co-application of ACh and dFBr to non-desensitized receptors. This is a significant change in the activation slope ($p < 0.001$). When 100 μ M cytosine was used as the stimulating agonist and dFBr was applied during the desensitizing phase, a similar effect was observed (Figure 3.5C). Repeated 3s applications of 1 μ M dFBr along with continuous application of 100 μ M cytosine produced repeated responses that decline only slightly in amplitude with each repetition. The activation slope for the first dFBr pulse applied during the desensitization phase of responses to 100 μ M cytosine was -66 ± 26 nA/s compared to -0.66 ± 0.18 nA/s for co-application of 1 μ M dFBr and 100 μ M cytosine to non-desensitized receptors. This is a significant increase ($p < 0.01$) in the activation slope of approximately 100 fold.

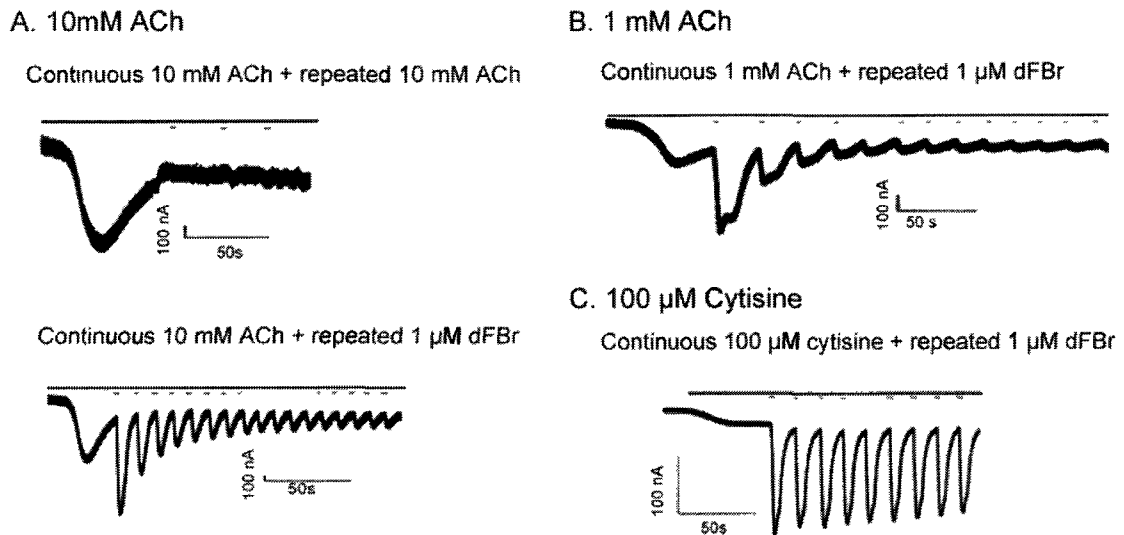


Figure 3.5 dFBr reactivates desensitized receptors.

Acetylcholine or cytosine were bath applied to *Xenopus* oocytes expressing $\alpha 4\beta 2$ receptors at a rate of 3 ml/min for 30s. During the desensitized portion of the response, 3s pulses of either acetylcholine (A) or dFBr (B and C) were repeatedly applied at a perfusion rate of 20 ml/min in the continued presence of agonist. Solid bars above the traces show the application of ACh or cytosine (continuous bar) and the repeated pulsed application of 1 μ M dFBr (short lines on B and C plots). **A Top.** Control trace showing repeated pulses of 10 mM acetylcholine applied during the desensitization period of a response to bath applied 10 mM ACh. Minimal current was observed under these conditions. **A Bottom.** Application of 3s pulses of 1 μ M dFBr during the desensitization period produces large currents that decline back to baseline with repeated pulses of dFBr. **B.** Application of 3s pulses of 1 μ M dFBr during the desensitization period of responses to 1 mM ACh produces similar effects to A Bottom except pulses are broadened and show possible hump currents. **C.** Application of 3s pulses of 1 μ M dFBr during the desensitization period of responses to 100 μ M cytosine. Large currents were observed similar to those shown in A Bottom but with a slower rate of decline. Each experiment (A-C) was repeated at least four times on different oocytes harvested from at least two different frogs. The slope of the rising phase of the first peak generated by application of dFBr during the desensitizing period in each case was determined (activation slope): **A Bottom.** -1020 ± 130 nA/s, **B.** -190 ± 9 nA/s and **C.** -66 ± 26 nA/s.

3.4.5 dFBr Induced Currents Elicited on Desensitized Receptors Decline with Continuous Exposure to dFBr.

The data shown in Figure 3.5 demonstrate the effect of a quick pulse of dFBr applied during the desensitization phase of the response. It was unclear from these experiments whether dFBr elicited responses on desensitized receptors would show typical desensitizing kinetics during longer exposures to dFBr. To determine if receptors desensitize in the continued presence of dFBr, we conducted experiments in which desensitized nAChR preparations were exposed to dFBr for longer time periods. Figure 3.6 shows the effects of application of 1 μ M dFBr for 48s to receptors pre-exposed to ACh. Co-exposure of oocytes to 1 mM ACh and 1 μ M dFBr for 48s produces a typical dFBr potentiated response (Figure 3.6A). As in Figure 3.5A, bath application of a control pulse of 1 mM ACh for 48s after the response peak produces no additional current (Figure 3.6B). Application of 1 μ M dFBr for 48s immediately after the ACh response peak and in the continued presence of 1 mM ACh (Figure 3.6C) produces a response similar in shape and amplitude to that resulting from co-exposure to ACh and dFBr (Figure 3.6A). A similar experiment in which 1 μ M dFBr was applied concurrent with termination of the ACh perfusion produced a different response (Figure 3.6D). When 1 mM ACh was replaced rapidly by 1 μ M dFBr after the response peak, a more rapidly desensitizing and sharper response peak was observed. When 1 μ M dFBr was again replaced with 1 mM ACh a similar sharp peak was observed although with an apparently slower rate of desensitization. In all cases, where 1 μ M dFBr was applied, either in conjunction with 1 mM ACh or after the 1 mM ACh peak (Figures 3.6 A, C and D) removal of dFBr returned the response to its appropriate non-potentiated level. Thus, application of 1 μ M dFBr produces peak responses that appear superimposed on the 1 mM ACh response.

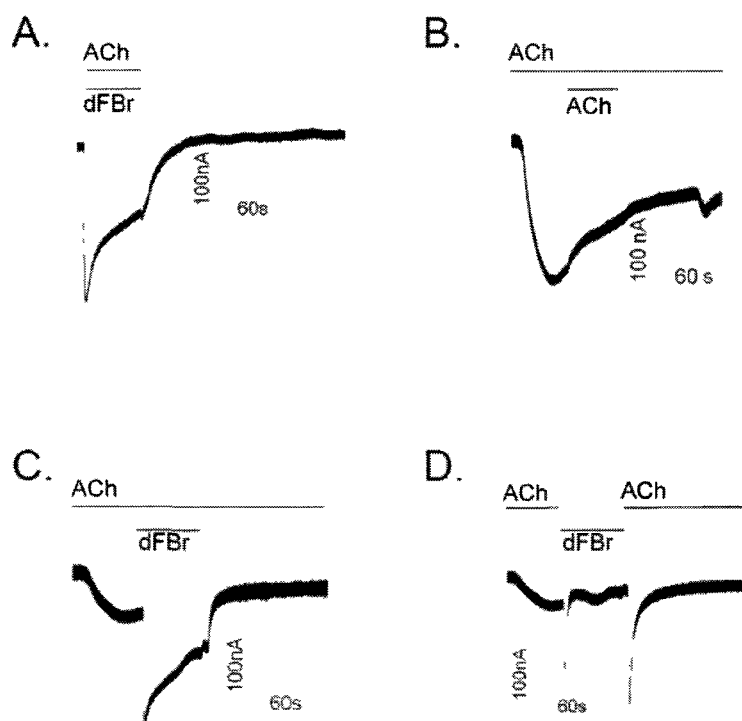


Figure 3.6 The amplitude of dFBr induced currents on desensitized receptors decline during long exposures to dFBr.

Responses in each panel were elicited by bath application of 1 mM ACh on *Xenopus* oocytes expressing $\alpha 4\beta 2$ receptors. The top solid line above each trace indicates the time period during which the oocyte was exposed to ACh. The bottom line above the trace indicates the period of application of either ACh (A) or dFBr (B, C, or D). **A.** Co-application of 1 mM ACh and 1 μ M dFBr for 48s at a flow rate of 8 ml/min (No pre-exposure to ACh). **B.** Control trace resulting from exposure to 1 mM ACh at a rate of 4 ml/min with 1 mM ACh applied during the desensitization period for 48 s at 8 ml/min. **C.** Application of 1 μ M dFBr at the peak of a response elicited by exposure to 1 mM ACh. ACh was present before, during and after application of dFBr. **D.** Application of 1 μ M dFBr at the peak of a response elicited by exposure to 1 mM ACh. Unlike the experiment shown in C, perfusion of 1 mM ACh was discontinued during the application of 1 mM dFBr then restored at the end of the 48s dFBr exposure. The responses shown were obtained from different oocytes. Due to different levels of receptor expression, no comparison of peak amplitudes was possible under these conditions.

3.5 Discussion.

Previous studies demonstrate that the potentiating effects of dFBr and its apparent selectivity (based on previous studies) for the $\alpha 4\beta 2$ subtype of nAChRs make it an ideal candidate for the development of novel positive allosteric modulators (PAMs) for $\alpha 4\beta 2$ nAChRs (Sala et al., 2005; Kim et al., 2007). The work described here addresses three elements of dFBr modulation on $\alpha 4\beta 2$ nAChR important to its ultimate development as a therapeutic agent: a. The nature of its bell-shaped response profile; b. Its effect on the action of $\alpha 4\beta 2$ nicotinic full agonists, partial agonists and antagonists; and c. Its effects on receptor kinetics.

3.5.1 The Bell-Shaped Dose/Response of dFBr.

We have previously demonstrated the ability of synthetic dFBr to potentiate ACh induced responses at concentrations less than 10 μM and inhibit responses at concentrations greater than 10 μM dFBr (Kim et al., 2007). The observation of rebound currents on washout of dFBr/agonist led us to hypothesize that dFBr produced inhibition of ACh responses through a mechanism involving open-channel block (Kim et al., 2007; Liu et al., 2008). The non-linear V/I relationship of dFBr inhibition observed in voltage step experiments strongly supports our hypothesis that dFBr inhibition results from open-channel block.

ACh has been previously demonstrated to inhibit its own responses by blocking the ion channel at high concentrations. To determine if dFBr could also block the channel, we conducted experiments with the non-channel blocking partial agonist cytisine as the stimulating agonist (Liu et al., 2008). The non-linear V/I relationship at dFBr concentrations $> 10 \mu\text{M}$ suggests that dFBr itself is capable of channel block. The linear V/I relationship at dFBr concentrations $< 10 \mu\text{M}$ supports our hypothesis that potentiation and inhibition are mediated by different mechanisms. This suggests that future analogs of dFBr could be developed that do not inhibit $\alpha 4\beta 2$ nAChRs and are better able to potentiate agonist responses with less effect on the apparent desensitization kinetics.

3.5.2 The Effect of dFBr on the Action of Nicotinic Agonists and Partial Agonists.

We examined the ability of dFBr to enhance the action of other compounds involved in nAChR signaling including choline, nicotine and cytisine. Both nicotine and varenicline (a derivative of cytisine) are being explored and/or utilized as therapeutic agents. dFBr did not alter the pEC_{50} of ACh, choline, nicotine and cytisine. I_{max} values for all three partial agonists were increased with a much more substantial enhancement obtained for the low efficacy partial agonists choline (9.3X) and cytisine (9.9X) then for the higher efficacy agonist nicotine (7.6X).

dFBr co-applied with choline produced a response of approximately 12% of the non-potentiated ACh response. While it is difficult to extrapolate the effects on synaptic function from receptors expressed in *Xenopus* oocytes, it is likely that increased activation by choline would alter the time course for synaptic currents. The nicotine response during dFBr co-application was equivalent to a non-potentiated response to ACh. This raises the possibility of future therapies combining a lower nicotine dose with a dFBr class compound.

dFBr co-application did not alter the pEC₅₀ values for ACh, nicotine or cytisine. These observations, along with the enhanced affinity for the antagonist DMAB-anabaseine lead us to conclude that dFBr may alter relative stabilities of receptor conformations involved in channel gating (channel opening and desensitization).

3.5.3 The Effect of dFBr on Inhibition of Responses by Nicotinic Antagonists.

We evaluated the ability of three structurally different competitive antagonists (DH β E, DMAB-anabaseine and tropisetron) to inhibit responses to ACh in the presence and absence of dFBr. No significant changes in inhibition kinetics were observed for the DH β E and tropisetron. DMAB-anabaseine, a α 7 partial agonist, produced a 1.4 fold increase in its pIC₅₀ value with the application of 1 μ M dFBr. The effect of dFBr on antagonist pIC₅₀ values appears to be minimal.

Conformational changes induced by allosteric modulators could alter the orthosteric binding site causing an antagonist (or poor agonist) to become a functional agonist. The benzodiazepine (BZD) flurazepam induces conformational rearrangements in the GABA binding site on GABA_AR, demonstrating shared allosteric interactions between the GABA and BZD binding sites (Kloda and Czajkowski, 2007). To determine if a similar action might occur with nicotinic antagonists, we examined the effects of dFBr co-application with antagonists in the absence of stimulating ACh. We did not observe any currents for any antagonist tested; including the α 7 partial agonist DMAB-anabaseine. The lack of any change in antagonist action suggests that dFBr does not produce its effects through alteration of the unbound, closed receptor conformation. This further supports our hypothesis that dFBr potentiation is the result of alterations in gating rather than ligand binding.

3.5.4 Recovery of Desensitized Receptors by dFBr.

Several possible mechanisms could produce the observed changes in partial agonist apparent efficacies. Agonist efficacy has been correlated to varying degrees of C-loop closure over the ligand seated within the orthosteric binding pocket in ionotropic glutamate (iGluR),

glycine receptors and AChBP (Armstrong and Gouaux, 2000; Hogner et al., 2002; Armstrong et al., 2003; Furukawa and Gouaux, 2003; Jin et al., 2003; Celie et al., 2004; Han et al., 2004; Hansen et al., 2005). Further studies suggest that efficacy of agonists at both iGlu and glycine receptors are determined by the ability of the agonist to stabilize the active receptor conformation (Furukawa and Gouaux, 2003; Han et al., 2004; Inanobe et al., 2005; Robert et al., 2005; Mayer, 2006). In a model for glycine and nAChRs, agonist efficacy differences are suggested to originate in the agonist affinity for a hypothesized flipped state relative to the closed state (Lape et al., 2008). Stabilization of the open conformation could also shift the equilibrium from the desensitized to the open state. One implication of the latter mechanism would be the possibility that application of dFBr to a desensitized receptor population would elicit currents by reactivating desensitized receptors. This ability has previously been reported for type II PAMs including PNU-120596 and TQS (Hurst et al., 2005; Bertrand and Gopalakrishnan, 2007; Gronlien et al., 2007) but not for dFBr.

To determine if dFBr could reactivate desensitized receptors, dFBr was applied during the desensitization period of a 1 mM ACh elicited response. Large currents were observed in response to dFBr application that were similar in magnitude to those obtained for a control exposure of ACh to non-desensitized receptors. These responses decline rapidly on removal of dFBr. With longer exposures, responses desensitized in the continuous presence of dFBr and ACh; returning to the pre-dFBr level on removal of the modulator. The decline in the dFBr elicited response over time could be the result of open channel block by both ACh and dFBr as described earlier but could also reflect the existence of a desensitized-open conformation that relaxes to a new desensitized state in the continued presence of dFBr as has been proposed for ivermectin (Krause et al., 1998; Gronlien et al., 2007). The observed decline in the response is similar to that observed when dFBr is co-applied with ACh to non-desensitized receptors but the time to peak is significantly shortened. This would be consistent with either independent binding of ACh and dFBr or a requirement for ACh to bind first.

When dFBr is applied to desensitized receptors with the simultaneous removal of ACh, a large peak is elicited that quickly returns to the pre-dFBr amplitude. A second switch from perfusion with dFBr back to ACh produces an ACh elicited peak in the absence of dFBr that also desensitizes rapidly back to the baseline response amplitude. These data suggest that ACh and dFBr bind independently with no requirement for ACh to bind before dFBr or vice versa. The rapid rise of the response peaks in Figure 3.6D appears to be the result of either ACh bound first followed by dFBr (first peak) or dFBr bound followed by ACh activation (second peak). The rapid decline of the first peak (Figure 3.6D) is likely the result of ACh dissociation from the receptor during dFBr application and the decline of the second peak represents dissociation of dFBr from

the receptor. Thus the rate of decline in Figure 3.6D may be reflective of the dissociation rates for either ACh (left trace) or dFBr (right peak).

It has been postulated that the ability to re-open desensitized receptors could be a common feature of type II modulators (Galzi et al., 1992; Briggs et al., 1999). Thus, dFBr could be classified as a $\alpha 4\beta 2$ type II PAM. Some concern has been expressed regarding alterations in desensitization rates by type II PAMs since such changes might adversely affect cell viability due to increased Ca^{2+} permeability. This remains a concern with dFBr, particularly due to its ability to reopen desensitized receptors. The balance between potentiation and channel block may be an important consideration therapeutically since channel block could reduce the problem of Ca^{2+} entry through the channel. The combined channel block and potentiation with dFBr produces sharper, more rapidly desensitizing responses rather than prolonged openings as have been observed in type II PAMs. The enhancement of partial agonist activities presents the possibility for combination therapies between dFBr like compounds and therapeutic partial agonists.

3.6 References.

- Adams CE and Stevens KE (2007) Evidence for a role of nicotinic acetylcholine receptors in schizophrenia. *Front Biosci* 12:4755-4772.
- Armstrong N and Gouaux E (2000) Mechanisms for activation and antagonism of an AMPA-sensitive glutamate receptor: crystal structures of the GluR2 ligand binding core. *Neuron* 28:165-181.
- Armstrong N, Mayer M and Gouaux E (2003) Tuning activation of the AMPA-sensitive GluR2 ion channel by genetic adjustment of agonist-induced conformational changes. *Proc Natl Acad Sci U S A* 100:5736-5741.
- Aubert I, Araujo DM, Cecyre D, Robitaille Y, Gauthier S and Quirion R (1992) Comparative alterations of nicotinic and muscarinic binding sites in Alzheimer's and Parkinson's diseases. *J Neurochem* 58:529-541.
- Bertrand D and Gopalakrishnan M (2007) Allosteric modulation of nicotinic acetylcholine receptors. *Biochem Pharmacol* 74:1155-1163.
- Briggs CA, McKenna DG, Monteggia LM, Touma E, Roch JM, Arneric SP, Gopalakrishnan M and Sullivan JP (1999) Gain of function mutation of the alpha7 nicotinic receptor: distinct pharmacology of the human alpha7V274T variant. *Eur J Pharmacol* 366:301-308.
- Celie PH, van Rossum-Fikkert SE, van Dijk WJ, Brejc K, Smit AB and Sixma TK (2004) Nicotine and carbamylcholine binding to nicotinic acetylcholine receptors as studied in AChBP crystal structures. *Neuron* 41:907-914.
- Coe JW, Brooks PR, Vetelino MG, Wirtz MC, Arnold EP, Huang J, Sands SB, Davis TI, Lebel LA, Fox CB, Shrikhande A, Heym JH, Schaeffer E, Rollema H, Lu Y, Mansbach RS, Chambers LK, Rovetti CC, Schulz DW, Tingley FD, 3rd and O'Neill BT (2005) Varenicline: an alpha4beta2 nicotinic receptor partial agonist for smoking cessation. *J Med Chem* 48:3474-3477.
- Corey-Bloom J (2003) Galantamine: a review of its use in Alzheimer's disease and vascular dementia. *Int J Clin Pract* 57:219-223.
- Court J, Martin-Ruiz C, Piggott M, Spurden D, Griffiths M and Perry E (2001) Nicotinic receptor abnormalities in Alzheimer's disease. *Biol Psychiatry* 49:175-184.
- Friedman JI (2004) Cholinergic targets for cognitive enhancement in schizophrenia: focus on cholinesterase inhibitors and muscarinic agonists. *Psychopharmacology (Berl)* 174:45-53.
- Furukawa H and Gouaux E (2003) Mechanisms of activation, inhibition and specificity: crystal structures of the NMDA receptor NR1 ligand-binding core. *Embo J* 22:2873-2885.
- Galzi JL, Devillers-Thiery A, Hussy N, Bertrand S, Changeux JP and Bertrand D (1992) Mutations in the channel domain of a neuronal nicotinic receptor convert ion selectivity from cationic to anionic. *Nature* 359:500-505.
- Gronlien JH, Haakerud M, Ween H, Thorin-Hagene K, Briggs CA, Gopalakrishnan M and Malysz J (2007) Distinct profiles of alpha7 nAChR positive allosteric modulation revealed by structurally diverse chemotypes. *Mol Pharmacol*.
- Han NL, Clements JD and Lynch JW (2004) Comparison of taurine- and glycine-induced conformational changes in the M2-M3 domain of the glycine receptor. *J Biol Chem* 279:19559-19565.
- Hansen SB, Sulzenbacher G, Huxford T, Marchot P, Taylor P and Bourne Y (2005) Structures of Aplysia AChBP complexes with nicotinic agonists and antagonists reveal distinctive binding interfaces and conformations. *EMBO J* 24:3635-3646.

- Harvey SC, Maddox FN and Luetje CW (1996) Multiple determinants of dihydro-beta-erythroidine sensitivity on rat neuronal nicotinic receptor alpha subunits. *J Neurochem* 67:1953-1959.
- Hogner A, Kastrup JS, Jin R, Liljefors T, Mayer ML, Egebjerg J, Larsen IK and Gouaux E (2002) Structural basis for AMPA receptor activation and ligand selectivity: crystal structures of five agonist complexes with the GluR2 ligand-binding core. *J Mol Biol* 322:93-109.
- Hurst RS, Hajos M, Raggenbass M, Wall TM, Higdon NR, Lawson JA, Rutherford-Root KL, Berkenpas MB, Hoffmann WE, Piotrowski DW, Groppi VE, Allaman G, Ogier R, Bertrand S, Bertrand D and Arneric SP (2005) A novel positive allosteric modulator of the alpha7 neuronal nicotinic acetylcholine receptor: in vitro and in vivo characterization. *J Neurosci* 25:4396-4405.
- Inanobe A, Furukawa H and Gouaux E (2005) Mechanism of partial agonist action at the NR1 subunit of NMDA receptors. *Neuron* 47:71-84.
- Jin R, Banke TG, Mayer ML, Traynelis SF and Gouaux E (2003) Structural basis for partial agonist action at ionotropic glutamate receptors. *Nat Neurosci* 6:803-810.
- Joshi PR, Suryanarayanan A and Schulte MK (2004) A vertical flow chamber for *Xenopus* oocyte electrophysiology and automated drug screening. *J Neurosci Methods* 132:69-79.
- Kim JS, Padnya A, Weltzin M, Edmonds BW, Schulte MK and Glennon RA (2007) Synthesis of desformylflustrabromine and its evaluation as an alpha4beta2 and alpha7 nACh receptor modulator. *Bioorg Med Chem Lett* 17:4855-4860.
- Kloda JH and Czajkowski C (2007) Agonist-, antagonist-, and benzodiazepine-induced structural changes in the alpha1 Met113-Leu132 region of the GABAA receptor. *Mol Pharmacol* 71:483-493.
- Krause RM, Buisson B, Bertrand S, Corringer PJ, Galzi JL, Changeux JP and Bertrand D (1998) Ivermectin: a positive allosteric effector of the alpha7 neuronal nicotinic acetylcholine receptor. *Mol Pharmacol* 53:283-294.
- Lape R, Colquhoun D and Sivilotti LG (2008) On the nature of partial agonism in the nicotinic receptor superfamily. *Nature* 454:722-727.
- Lippiello PM (2006) Nicotinic cholinergic antagonists: a novel approach for the treatment of autism. *Med Hypotheses* 66:985-990.
- Liu Q, Yu KW, Chang YC, Lukas RJ and Wu J (2008) Agonist-induced hump current production in heterologously-expressed human alpha4beta2-nicotinic acetylcholine receptors. *Acta Pharmacol Sin* 29:305-319.
- Martin-Ruiz CM, Lee M, Perry RH, Baumann M, Court JA and Perry EK (2004) Molecular analysis of nicotinic receptor expression in autism. *Brain Res Mol Brain Res* 123:81-90.
- Mayer ML (2006) Glutamate receptors at atomic resolution. *Nature* 440:456-462.
- Middlemiss DN and Tricklebank MD (1992) Centrally active 5-HT receptor agonists and antagonists. *Neurosci Biobehav Rev* 16:75-82.
- Moroni M and Bermudez I (2006) Stoichiometry and Pharmacology of Two Human alpha4beta2 Nicotinic Receptor Types. *J Mol Neurosci* 30:95-96.
- Nicolson R, Craven-Thuss B and Smith J (2006) A prospective, open-label trial of galantamine in autistic disorder. *J Child Adolesc Psychopharmacol* 16:621-629.
- Nordberg A (2001) Nicotinic receptor abnormalities of Alzheimer's disease: therapeutic implications. *Biol Psychiatry* 49:200-210.

Robert A, Armstrong N, Gouaux JE and Howe JR (2005) AMPA receptor binding cleft mutations that alter affinity, efficacy, and recovery from desensitization. *J Neurosci* 25:3752-3762.

Sala F, Mulet J, Reddy KP, Bernal JA, Wikman P, Valor LM, Peters L, Konig GM, Criado M and Sala S (2005) Potentiation of human alpha4beta2 neuronal nicotinic receptors by a *Flustra foliacea* metabolite. *Neurosci Lett* 373:144-149.

Stevens KE, Kem WR, Mahnir VM and Freedman R (1998) Selective alpha7-nicotinic agonists normalize inhibition of auditory response in DBA mice. *Psychopharmacology (Berl)* 136:320-327.

Weltzin MM and Schulte MK (2010) Pharmacological characterization of the allosteric modulator desformylflustrabromine and its interaction with alpha4beta2 neuronal nicotinic acetylcholine receptor orthosteric ligands. *J Pharmacol Exp Ther* 334:917-926.

Woodruff-Pak DS and Gould TJ (2002) Neuronal nicotinic acetylcholine receptors: involvement in Alzheimer's disease and schizophrenia. *Behav Cogn Neurosci Rev* 1:5-20.

CHAPTER 4: Non-orthosteric Subunit Faces are Involved in $\alpha 4\beta 2$ nAChR Responses to Acetylcholine and Desformylflustrabromine in High- and Low-sensitivity Receptor Preparations.

4.1 Abstract.

Alterations in expression patterns of $\alpha 4\beta 2$ nicotinic acetylcholine receptors (nAChR) have been demonstrated to alter nicotinic neurotransmission and have been implicated in neurological disorders including Autism, nicotine addiction, Alzheimer's and Parkinson's disease. Positive allosteric modulators (PAMs) represent promising new leads for the development of therapeutic agents for the treatment of these disorders. This study investigates the involvement of non-orthosteric subunit interfaces of $\alpha 4\beta 2$ receptors in the potentiation of acetylcholine (ACh) induced responses by the PAM desformylflustrabromine (dFBr). Amino acids on the non-orthosteric $\beta 2+$ and $\alpha 4-$ subunit faces were mutated to alanine and receptors expressed in *Xenopus laevis* oocytes. Acetylcholine induced responses in the presence and absence of dFBr were recorded with two-electrode voltage clamp techniques. Three fundamentally different results were observed. Several mutations altered the ACh dose-response curves, supporting a role for these amino acids in mediating agonist induced conformational changes in $\alpha 4\beta 2$ nAChRs. A second group of mutations selectively altered the ability of dFBr to potentiate ACh induced responses but had minimal effect on responses to ACh alone (low-sensitivity preparation: $\beta 2W176A$, $\beta 2T177A$, $\beta 2D179A$, $\beta 2D217A$ and $\alpha 4W88A$; high-sensitivity preparation $\beta 2T177A$, $\beta 2D116A$ and $\beta 2Y120A$). The remaining mutations had no effect on either dFBr or ACh effects. Our data supports our hypothesis that allosteric modulation by dFBr involves its interaction within the $\beta 2+/\alpha 4-$ cleft and suggests that its effects may involve alterations in subunit interactions involving $\beta 2+$ and $\alpha 4-$. In addition to supporting a putative binding site for dFBr, these data also demonstrate the importance of this region in normal receptor kinetics.

4.2 Introduction.

Nicotinic acetylcholine (nAChR), GABA_A, 5HT₃ and glycine receptors are members of the Cys-loop super family of ligand gated ion channels (LGIC). nAChRs are integral membrane proteins involved in cholinergic transmission in the central and peripheral nervous systems (Taly et al., 2009). Dysregulation of nAChRs has been postulated to be involved in neurological disorders including Alzheimer's disease (Court et al., 2001; Nordberg, 2001), Schizophrenia (Adams and Stevens, 2007), Parkinson's disease (Aubert et al., 1992), Autism (Martin-Ruiz et al., 2004; Lippiello, 2006) and nicotine addiction (Picciotto et al., 2001).

The predominant nAChRs subtypes found in brain are the homomeric $\alpha 7$ and the heteromeric $\alpha 4\beta 2$ receptors (Mudo et al., 2007). Recent studies have suggested that $\alpha 4\beta 2$ nAChRs can form high- (HS) and low- (LS) ACh sensitivity receptors (Nelson et al., 2003; Zhou et al., 2003; Briggs et al., 2006; Moroni et al., 2006; Zwart et al., 2006; Tapia et al., 2007). Altering the $\alpha:\beta$ subunit injection ratio in *Xenopus* oocytes has been demonstrated to alter the relative ratios of a HS to LS $\alpha 4\beta 2$ receptors expressed, presumably a result of different $\alpha 4\beta 2$ stoichiometries. Studies have provided suggestive evidence that similar HS and LS $\alpha 4\beta 2$ nAChR stoichiometries are expressed in the mammalian brain (Marks et al., 2000; Butt et al., 2002; Gotti et al., 2008) and can be altered by chronic exposure to nicotine (Moretti et al., 2010). The precise arrangement of the $\alpha 4$ and $\beta 2$ subunits within the different $\alpha 4\beta 2$ receptors is unknown.

Ligands, such as Positive Allosteric Modulators (PAMs) that selectively target nAChRs are potentially important therapeutic agents that could prove useful for the treatment of pathologies involving alterations in nAChR expression. PAMs are ligands which bind at allosteric sites and alter responses to agonists such as the endogenous agonist ACh although they have no agonist properties of their own and have different effects on agonist responses. PAMs have been identified that modify peak currents of the agonist induced responses (Type I profile) or alter both the peak current and time course of the agonist evoked response (Type II profile) (Bertrand and Gopalakrishnan, 2007). The development of PAMs that are selective for specific receptor subtypes and stoichiometries would be potentially beneficial for the treatment of pathological conditions where only one receptor subtype or stoichiometry is deregulated and would provide useful pharmacological probes for identification of specific subtypes in CNS function. The design and development of different classes of PAMs will be facilitated by identification and modeling of the respective allosteric binding sites.

Desformylflustrabromine (dFBr) is a recently discovered PAM that potentiates ACh evoked currents on $\alpha 4\beta 2$ nAChRs and inhibits ACh induced currents on other common nAChR subtypes (Sala et al., 2005; Kim et al., 2007; Weltzin and Schulte, 2010b). The synthetic form of

this natural compound has been shown to increase maximal currents induced by ACh on $\alpha 4\beta 2$ nAChRs by 265% without altering the EC_{50} for ACh. Similar effects are observed when dFBr is co-applied with partial agonists although increases in efficacy are greater for partial agonists compared to ACh (Kim et al., 2007; Weltzin and Schulte, 2010). In addition, dFBr has been shown to induce currents when applied to desensitized receptors continuously exposed to ACh. While the mechanism of dFBr potentiation is unknown it has been proposed that dFBr potentiates $\alpha 4\beta 2$ nAChRs and “rescues” receptors from desensitization by altering the equilibrium between open and desensitized receptor conformations (Sala et al., 2005; Weltzin and Schulte, 2010b). Inhibition of agonist induced responses by high concentrations of dFBr ($> 10 \mu\text{M}$) appears to involve open channel block by dFBr (Weltzin and Schulte, 2010).

The current study investigates the mechanistic role of the $\beta 2+$ and $\alpha 4-$ subunit faces in the potentiation of ACh induced responses by dFBr. Using site-directed mutagenesis, amino acids within the $\beta 2+/ \alpha 4-$ subunit interface were mutated to alanine and mutant receptors were expressed in *Xenopus laevis* oocytes. The effects of each mutation were evaluated using two-electrode voltage clamp techniques on both HS and LS $\alpha 4\beta 2$ receptors. HS and LS receptors were expressed by altering the injection ratios of $\alpha 4$ and $\beta 2$ as described previously by Nelson et al. (2003). The putative binding site for dFBr at the $\beta 2+/ \alpha 4-$ subunit interface relative to the orthosteric binding site on $\alpha 4\beta 2$ receptor is similar to the position of the benzodiazepine binding site on GABA_A receptors relative to the GABA orthosteric binding site. We thus used homology between the $\beta 2+/ \alpha 4-$ subunit interface and the GABA_A benzodiazepine as a guide for mutagenesis. Eight $\beta 2+$ amino acids and two $\alpha-$ face amino acids were selected and are shown in Figure 4.1. The data suggest that non-orthosteric subunit faces are involved in receptor conformational changes in response to ACh in the absence of allosteric modulation and data obtained in the presence of dFBr support the conclusion that the dFBr binding site is located on the $\beta 2+$ face. Binding of dFBr to the allosteric binding site appears to utilize amino acid interactions in this region equivalent to binding loops A, B and C previously described for the orthosteric binding site (Sigel 2002; Lester et al., 2004).

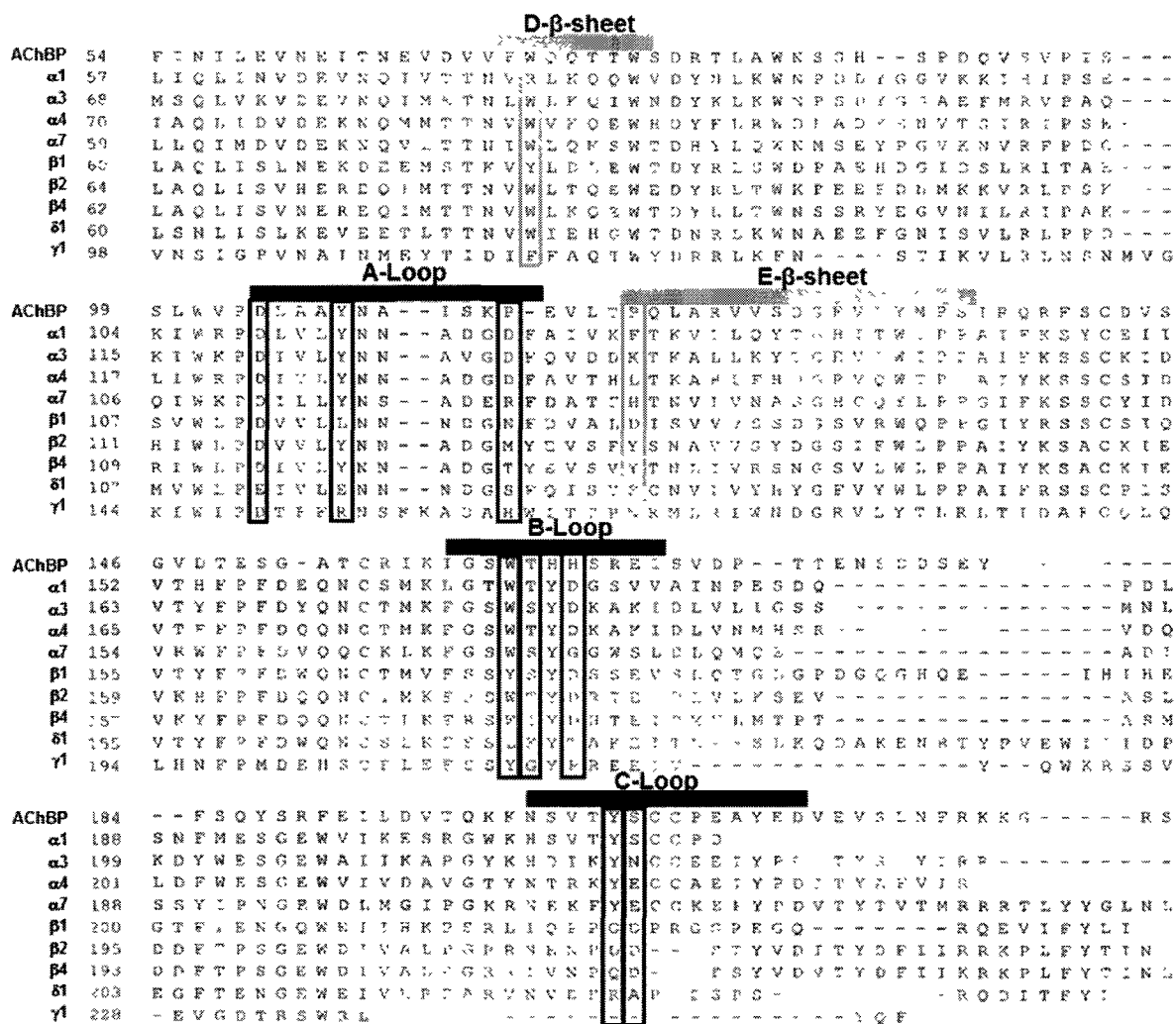


Figure 4.1. DNA sequence alignments for AChBP and nAChR subtypes.

Alanine mutations are made on amino acids on the loops A (β 2D116, β 2Y120 and β 2Y127), B (β 2W176, β 2T177 and β 2D179) and C (β 2D217 and β 2D218) located on the β 2+ face (black boxes) and on the β -sheets D (α 4W88) and E (α 4K140) of the α 4- face (grey boxes).

4.3 Materials and Methods.

4.3.1 Receptors and mRNA.

The cDNA sequences for human $\alpha 4$ (NCBI Reference Sequence: NM_000744.5), $\beta 2$ (NCBI Reference Sequence: NM_000748.2) and $\alpha 7$ (NCBI Reference Sequence: NM_000746.3) nAChR subunits were used to synthesize a full length cDNA for each subunit. cDNA synthesis was conducted by GeneArt Inc. (Burlingame, CA). The $\beta 2$ cDNA was inserted into the pcDNA3.1/Zeo(+) mammalian expression vector with restriction enzymes Not I and Xho I and the $\alpha 4$ cDNA was inserted into the pcDNA3.1/hygromycin mammalian expression vector with restriction enzymes Hind III and BamHI (vectors procured from Invitrogen, Carlsbad, CA; restriction enzymes purchased from New England Biolabs). The cDNA for $\alpha 7$ nAChR subunit was inserted into the pBudCE4.1 expression vector (Invitrogen) with restriction enzymes Sai I and Xba. All constructs were fully sequenced and confirmed to be identical to the published sequences for each subunit. Synthetic DNA was used to transform AG1 super-competent cells (Stratagene) for production of cDNA. Synthetic cRNA transcripts for wild-type and mutant subunits were prepared using the T7 mMESSAGE mMACHINE™ High Yield Capped RNA Transcription Kit (Ambion, Austin, TX).

Mutant cDNA was created using commercial mutagenesis services (DNA 2.0, Menlo Park, CA). All mutations were confirmed by DNA sequencing. The resulting DNA was inserted into the pcDNA3.1/Hygromycin vector (Invitrogen, Carlsbad, CA) and used to transform NEB 10-beta *E. coli* (DNA 2.0) cells.

4.3.2 Experimental Chemicals and Test Compounds.

Acetylcholine (ACh), other salts and buffering agents were obtained from Sigma-Aldrich, Inc (MO). Desformylflustrabromine·HCl (dFBr) was synthesized by Dr. Richard Glennon (Virginia Commonwealth University) according to a previously published procedure (Kim et al., 2007).

4.3.3 *Xenopus laevis* Oocytes and Receptor Expression.

Xenopus laevis frogs and frog food were purchased from Nacso (Fort Atkinson, WI). Ovarian lobes were surgically removed from Finquel anesthetized *Xenopus laevis* frogs and washed twice in Ca²⁺-free Barth's buffer (82.5 mM NaCl; 2.5 mM KCl; 1 mM MgCl₂; 5 mM HEPES, pH 7.4) then gently shaken with 1.5 mg/mL collagenase (Sigma type II, Sigma-Aldrich Inc., MO) for 20min at 20–25°C. Stage V and VI oocytes were selected for microinjection. No more than four surgeries were conducted on each frog. A recovery period greater than six weeks was allowed in between surgeries (*Xenopus* protocols conform to those approved by the

University of Alaska Fairbanks Institutional Animal Care and Use Committee; approval number 08-71).

For expression of $\alpha 4\beta 2$ nAChRs, oocytes were injected with 50 nL cRNA. Injected oocytes were incubated at 19°C for 24-72h prior to their use in voltage clamp experiments. For the high-sensitivity receptor preparations (HS), oocytes were injected with 50 nL of a mixture containing 250 ng/ μ L of $\alpha 4$ cRNA and 50 ng/ μ L of $\beta 2$ cRNA (5:1 ratio of $\alpha 4$ to $\beta 2$). For the low-sensitivity receptor preparation (LS) oocytes were injected with 50 nL of a mixture of 50 ng/ μ L $\alpha 4$ cRNA and 250 ng/ μ L $\beta 2$ cRNA (1:5 ratio of $\alpha 4$ to $\beta 2$). The EC_{50} values obtained for ACh induced currents on the HS and LS receptor preparations obtained from these injection ratios were verified by electrophysiology assays as described below and found to compare well with published values for the high ACh-sensitive and low ACh-sensitive receptors (Zwart and Vijverberg, 1998; Moroni et al., 2006). EC_{50} values and response profiles indicated the expression of predominantly the HS or LS subtypes although it is likely that both are present in each experiment.

4.3.4 Two-Electrode Voltage Clamp.

Current recordings were performed using an automated two-electrode voltage-clamp system incorporating an OC-725C oocyte clamp amplifier (Warner Instruments, Hamden, CT) coupled to a computerized data acquisition (Datapac 2000, RUN technologies, Mission Viejo, CA) and autoinjection system (Gilson, Middleton, WI). Recording and current electrodes with resistance 1–4 M Ω were filled with 3 M KCl. Details of the chambers and methodology employed for electrophysiological recordings have been described earlier (Joshi et al., 2004). Oocytes were held in a vertical flow chamber of 200 μ L volume, clamped at a holding potential of -60 mV and perfused with various ND-96 recording buffers. A phosphate ND-96 recording buffers was used in these experiments due to the findings that HEPES modulates the HS receptors (Weltzin, 2010). The phosphate ND-96 recording solution is similar to HEPES in all regards except with the omission of HEPES and the addition of phosphate (96 mM NaCl, 2 mM KCl, 1.8 mM CaCl₂, 1 mM MgCl₂, 2 mM phosphate). Test compounds were dissolved in buffer and injected into the chamber at 20 mL/min using a Gilson auto-sampler injection system (Joshi et al., 2004).

4.3.5 Electrophysiology Dose-Response Experiments.

Dose-response curves for the endogenous nAChR agonist Acetylcholine·Cl, (ACh) (Sigma-Aldrich) were determined for both wild-type and mutant receptors expressed in HS and LS receptor preparations at ACh concentrations ranging from 0.1 μ M - 3 mM. Broader concentration ranges were used when necessary to fully define the ACh dose/response curves.

For wild-type and mutant receptors expressed in the LS preparation, dose-response curves for dFBr were determined by co-application of 100 μM ACh (EC_{75}) with varying concentrations of dFBr (0.001 – 100 μM). For wild-type and mutant receptors expressed in the HS preparation, dFBr dose-response curves were determined by co-application of 10 μM ACh (EC_{75}) with varying concentrations of dFBr (0.001 – 100 μM).

In order to compare responses from different oocytes, individual responses to drug application were normalized to control responses elicited using 10 μM ACh for receptors expressed by the HS receptor technique for both wild-type and mutated receptors. For wild-type and mutant receptors in the LS preparation responses were normalized to those obtained using 100 μM ACh. Data were collected from at least four replicate experiments using oocytes obtained from at least two different frogs.

4.3.6 Data Analysis and Statistics.

Dose-response curves were fit using non-linear curve fitting and GraphPad Prism Software (San Diego, CA) with standard built-in algorithms. pEC_{50} ($-\log \text{EC}_{50}$) and EC_{50} values were determined by fitting concentration/response data to a single site binding model:

$$I = \frac{b + (I_{\max} - b)}{1 + 10^{(\text{LogEC}_{50} - \text{Log}[L]) * nH}} \quad (1)$$

Where I is the current elicited on application of agonist, b is the baseline current in the absence of ligand, L is the ligand concentration and nH is the Hill slope. The EC_{50} value is the concentration of agonist producing currents equal to one half the maximal current (I_{\max}).

Mutant $\beta 2\text{D}179\text{A}$ and $\alpha 4\text{W}88\text{A}$ receptors which displayed dFBr potentiation with no inhibition at higher dFBr concentrations were also fit to equation 1 rather than equation 2 (bell shaped dose/response). For consistency with the bell-shaped dose response curves used for other dFBr experiments, the Hill slope (nH) was constrained to 1 in these experiments.

PAMs often produce bell shaped dose-response curves with both potentiating and inhibiting phases. dFBr displayed this typical dose-response profile on wild-type and some mutant receptors. The pEC_{50} ($-\log \text{EC}_{50}$) and pIC_{50} ($-\log \text{IC}_{50}$) values were determined in these cases by simultaneously fitting both the potentiation and inhibition phases using equation 2 and GraphPad Prism Software (San Diego, CA). Similar equations have been used previously to examine bell-shaped PAM data (Harvey et al., 1999; Hsiao et al., 2001; Hsiao et al., 2006; Kim et al., 2007; Weltzin and Schulte, 2010a). Mutant receptors that did not display a bell shaped response to dFBr were fit with other algorithms (see equation 1 and equation 3).

$$I = I_{maxcalc} + \left(\frac{(Plateau1 - I_{maxcalc})}{1 + 10^{((LogEC_{50} - LogX) * n_{H1})}} \right) + \left(\frac{(Plateau2 - I_{maxcalc})}{1 + 10^{((LogX - LogIC_{50}) * n_{H2})}} \right) \quad (2)$$

I is the current elicited on application of agonist, $I_{maxcalc}$ is the calculated maximum induced current of both the potentiation and inhibition curves. *Plateau 1* is the initial current prior to addition of the modulator and *Plateau 2* is the plateau after the inhibition of the agonist response at high concentrations of the modulator. The EC_{50} value is the concentration of modulator producing currents equal to one half the calculated maximum current ($I_{maxcalc}$) during co-application with agonist. The IC_{50} is the concentration of modulator required to inhibit the response to $1/2 I_{maxcalc}$. The responses elicited from different oocytes and different concentrations of potentiator are typically normalized to the response to a control concentration of ACh to account for differences in expression between preparations. In potentiation experiments the current elicited by a specific concentration of the potentiating ligand + ACh ($I_{response}$) is divided by the current elicited by an identical concentration of ACh in the absence of the potentiating ligand. Thus, in the absence of a potentiator the response amplitude is equal to 1.0. Potentiation is typically referred to in the text as a percentage of the unpotentiated response. This percentage is calculated as the peak of the bell shaped dose-response curve X 100. Since the unpotentiated response is defined as 1.0, a 180% potentiation would, for example, represent an observed potentiation of 1.8 X the observed unpotentiated peak response. This peak response is typically less than the $I_{maxcalc}$ due to simultaneous inhibition by the ligand that produces the bell shaped dose-response curve.

Simultaneous fitting of two Hill equations can prove difficult if the EC_{50} and IC_{50} values are close together due to the inability to collect data near the value of $I_{maxcalc}$. In these cases, insufficient data is present to fully define the curve and some constants must be approximated for the fit to converge and the appropriate EC_{50} and IC_{50} values determined. In order to overcome these limitations, Hill slopes for potentiation and inhibition were typically fixed at +1 and -1 respectively. The $I_{maxcalc}$ was constrained to < 6. The constraints for the mutant $\beta 2Y127A$ expressed using the LS receptor preparation are as follows: Plateau 1 = 1, $I_{maxcalc}$ < 21 (due to dFBr having a greater $I_{maxcalc}$ on $\beta 2Y127A$), Plateau 2 = 2.75 (the I_{max} value of the highest dFBr concentration tested), $n_{H1} = -4$ and $n_{H2} = -2$ (n_H values which allowed for the best curve fit of the data). The $I_{maxcalc}$ of mutants $\alpha 4W88A$ expressed using the LS receptor preparation were constrained to < 25 rather than < 6 due to dFBr having a greater $I_{maxcalc}$ on $\alpha 4W88A$ compared to the other examined mutations.

Some mutants displayed no potentiation on exposure to dFBr although inhibition was still observed. These inhibition curves were fit using non-linear curve fitting and GraphPad Prism

Software (San Diego, CA) with standard built-in algorithms (equation 3). pIC_{50} ($-\log EC_{50}$) values were determined by fitting concentration/response data to a log (inhibitor) versus response binding model:

$$I = Plateau2 + \left(\frac{Plateau1 - Plateau2}{1 + 10^{(LogX - LogIC_{50}) * n_H}} \right) \quad (3)$$

Where I is the current elicited on application of agonist and modulator, $Plateau 1$ is the current elicited by the agonist prior to addition of the inhibitor. $Plateau 2$ is the current at saturating concentrations of inhibitor. The IC_{50} is the concentration of modulator that inhibits the current by $1/2 I_{max}$. In order to permit comparison of data from different oocytes, responses for all test compounds were normalized to the currents obtained with $10 \mu M$ ACh for receptors expressed by the HS receptor preparation and $100 \mu M$ ACh for receptors expressed via the LS receptor preparations. The n_H was constrained to -1 to allow for better comparison to results obtained for wild-type receptors.

The degree of change resulting from individual mutations was calculated as a ratio of the mutant value by the wild-type value. For values where a decrease was seen with the mutation, one was divided by the calculated fold change.

Statistical comparisons of pEC_{50} or pIC_{50} values used an unpaired t-test with p values calculated based on the null hypothesis.

4.4 Results.

A series of amino acids were mutated to alanine to investigate the role the $\beta 2+$ and $\alpha 4-$ faces of the $\alpha 4\beta 2$ nAChR in mediating the effects of ACh and dFBr. Residues to be mutated were selected based on homology with other LGIC subunits and were at equivalent positions to those previously identified in the binding pocket for benzodiazepines on GABA_A receptors (GABA_A $\alpha 1H101$, $\alpha 1Y159$, $\alpha 1S205$, $\alpha 1T206$, $\gamma 1M130$ and $\gamma F77$) (Wieland et al., 1992; Amin et al., 1997; Buhr et al., 1997a; Buhr et al., 1997b; Buhr and Sigel, 1997; Wagner and Czajkowski, 2001). Figure 4.2 displays the alignments between nAChRs and GABA_AR subunits involved in the putative dFBr binding site and the benzodiazepine binding site. Residues mutated on the $\beta 2+$ face include W176 (GABA_A $\alpha Y159$), T177 and D179 on the B-loop; D217 and D218 (GABA_A $\alpha 1S205$ and $\alpha 1T206$) on the C-loop; and D116, Y120 (GABA_A $\alpha 1H101$) and Y127 on the A-loop. Residues mutated on the $\alpha 4-$ face include K140 (E- β strand) (GABA_A $\gamma 1M130$) and W88 (D- β strand) (GABA_A $\gamma 1F77$). Each mutant receptor was characterized using two-electrode voltage clamp recording. Dose-response curves were obtained for ACh stimulation in the absence of dFBr and for co-application of dFBr and ACh using oocytes expressing both low- (LS) and high- (HS) ACh sensitivity receptor populations.

B-Loop	
nAChR α 4	F G S W T Y D K A I
nAChR β 2	F R S W T Y D R T E
GABA $_A$ R α 1	F G S Y A Y T R A E
GABA $_A$ R γ 1	F S S Y G Y P R E E

C-Loop	
nAChR α 4	K Y K C - C E E I Y P D
nAChR β 2	- - - - - D D S T Y V D
GABA $_A$ R α 1	S S - - - - - T G E Y V V
GABA $_A$ R γ 1	- - - - - - - - - - -

A-Loop	
nAChR α 4	P D I V L Y N N A D G D F A
nAChR β 2	P D I V L Y N N A D G M Y E
GABA $_A$ R α 1	P D T F F H N G K K S V A H
GABA $_A$ R γ 1	P D T F F R N S K K A D A H

E-β-sheet	D-β-sheet		
nAChR α 4	L T K A H L	nAChR α 4	T N V W V K Q
nAChR β 2	Y S N A V V	nAChR β 2	T N V W L T Q
GABA $_A$ R α 1	M P N K L L	GABA $_A$ R α 1	I D V F F R Q
GABA $_A$ R γ 1	N R M L R I	GABA $_A$ R γ 1	I D I F F A Q

Figure 4.2. DNA sequences for the binding- loops and - β -sheets for the nAChR subunits α 4 and β 2 and GABA $_A$ R subunits α 1 and γ .

The residues in the α 4 and β 2 subunits that were mutated in the current study are emphasized in back boxes. Key amino acids that are involved in the binding of benzodiazepines in the GABA $_A$ R residues are accentuated in grey boxes.

4.4.1. High- and Low- Sensitivity Wild-type $\alpha 4\beta 2$ Receptor Preparations.

4.4.1.1. ACh Dose-Response on High- and Low- ACh Sensitivity $\alpha 4\beta 2$ Receptors.

ACh concentration-response curves were obtained for wild-type receptors using the LS (injection ratio 5:1 α : β) and HS (injection ratio 1:5 α : β) receptor preparations and by applying varying concentrations of ACh (0.1 – 3000 μ M). The dose-response curves were sigmoidal in shape (Figure 4.3A). Receptors expressed using the LS receptor preparation had a significantly different ACh pEC₅₀ value 4.5 ± 0.1 (EC₅₀ = 34 μ M) compared to receptors expressed using the HS receptor preparation (ACh pEC₅₀ value of 5.2 ± 0.1 (EC₅₀ = 5.8 μ M)) ($p < 0.0001$) (Table 4.1 and 4.2). The Hill slope (n_H) for receptors expressed using the LS receptor preparation ($n_H = 1.4 \pm 0.3$) were not significantly different from receptors expressed using the HS preparation ($n_H = 1.9 \pm 0.3$) ($p = 0.2893$).

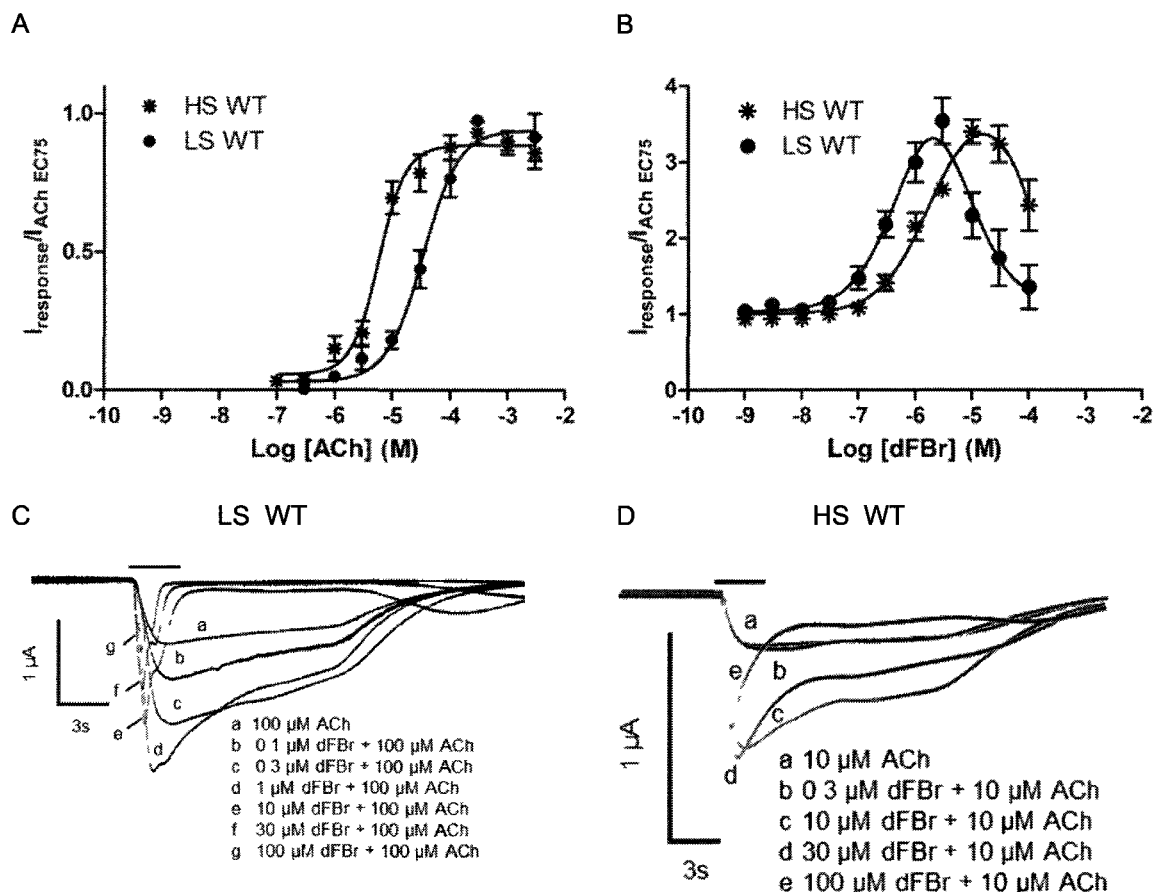


Figure 4.3. ACh and dFBr dose-response curves for wild-type (WT) receptors expressed using the high-sensitivity (HS) and low-sensitivity (LS) receptor preparations.

Xenopus oocytes are prepared using the high and low-sensitivity receptor preparations (HS mRNA injected at a ratio of 1 α :5 β ; LS mRNA injection at a ratio of 5 α :1 β). Expressing oocytes were exposed to increasing concentrations of ACh and dFBr. **A)** ACh dose-response curves for wild-type receptors. Individual peak amplitudes were normalized to the I_{max} on the same oocyte. **B)** Dose-response curves for co-application of varying concentrations of dFBr and the ACh EC75 for wild-type receptors. **C)** Co-application of dFBr and ACh response traces for wild-type receptors expressed via the LS receptor preparation. **D)** Co-application of dFBr and ACh response profiles for wild-type receptors expressed by the HS receptor preparation. Response traces were recorded from a single oocyte. The solid bar above the response trace indicates the time the oocyte was exposed to co-application of varying concentrations of dFBr and the ACh EC75. The ACh and dFBr dose-response values were determined using non-linear curve fitting as described in the methods and are reported in Table 4.1 and 4.2. Data points represent at least 4 replicate values obtained from a minimum of two oocytes harvested from different frogs. Error bars indicate \pm SEM.

Table 4.1 Summary of the calculated results determined from ACh and dFBr potentiation of ACh dose-response results from wild-type (WT) and mutant $\alpha 4\beta 2$ receptors expressed using the low-sensitivity (LS) receptor preparation.

		ACh Dose Response		dFBr Potentiation of ACh Induced Responses		
Mutation	Mutation Location	$pEC_{50} \pm SEM$ ($EC_{50}, \mu M$)	n_H	$pEC_{50} \pm SEM$ ($EC_{50}, \mu M$)	$pIC_{50} \pm SEM$ ($IC_{50}, \mu M$)	$I_{max} \pm SEM$
LS WT	WT	4.5 ± 0.1 (34)	1.4 ± 0.3	6.1 ± 0.4 (0.79)	5.3 ± 0.4 (5.0)	3.4 ± 0.4
LS $\beta 2W176A$	$\beta 2$, B-Loop	5.3 ± 0.3 (5.1)	$0.4 \pm 0.1^{***}$	6.6 ± 0.6 (0.25)	5.1 ± 0.6 (7.9)	2.1 ± 0.3
LS $\beta 2T177A$	$\beta 2$, B-Loop	3.6 ± 0.7 (226)	0.5 ± 0.2	6.7 ± 0.5 (0.20)	4.7 ± 0.5 (20)	$2.0 \pm 0.2^{**}$
LS $\beta 2D179A$	$\beta 2$, B-Loop	4.1 ± 0.3 (76)	1.2 ± 0.1	5.5 ± 0.2 (3.1)	N.D.	3.7 ± 0.4
LS $\beta 2D217A$	$\beta 2$, C-Loop	4.6 ± 0.2 (25)	1.3 ± 0.2	6.6 ± 0.5 (0.25)	5.4 ± 0.6 (4.0)	2.2 ± 0.2
LS $\beta 2D218A$	$\beta 2$, C-Loop	4.4 ± 0.1 (41)	0.8 ± 0.2	6.0 ± 0.3 (1.0)	4.8 ± 0.4 (16)	2.7 ± 0.4
LS $\beta 2D116A$	$\beta 2$, A-Loop	4.2 ± 0.1 (59)	1.1 ± 0.1	6.1 ± 0.3 (0.79)	5.3 ± 0.4 (5.0)	3.0 ± 0.3
LS $\beta 2Y120A$	$\beta 2$, A-Loop	$4.0 \pm 0.1^{**}$ (111)	1.3 ± 0.2	8.5 ± 1.4 (0.0032)	N.D.	$1.6 \pm 0.2^{**}$
LS $\beta 2Y127A$	$\beta 2$, A-Loop	$3.3 \pm 1.1^{**}$ (559)	$0.4 \pm 0.2^{**}$	5.9 ± 0.6 (1.3)	5.0 ± 0.6 (10)	$20 \pm 3^{**}$
LS $\alpha 4K140A$	$\alpha 4$, E-Loop	$7.0 \pm 0.1^{***}$ (0.099)	$0.8 \pm 0.1^*$	N.D.	4.1 ± 1.1 (79)	N.D.
LS $\alpha 4W88A$	$\alpha 4$, D-Loop	4.9 ± 0.2 (14)	0.7 ± 0.3	5.5 ± 0.2 (3.2)	N.D.	$21.0 \pm 4^{***}$

Data represent mean \pm SEM. Data points represent at least 4 replicate values obtained from a minimum of two oocytes harvested from different frogs. pEC_{50} is the $-\log$ of the EC_{50} value; pIC_{50} is the $-\log$ of the IC_{50} value; I_{max} observed is the maximum induced current observed n_H . ** and *** Indicate values significantly different from wild-type receptors with $p < 0.01$ and $p < 0.0001$, respectively.

Table 4.2 Summary of the calculated results determined from ACh and dFBr potentiation of ACh dose-response results from wild-type (WT) and mutant $\alpha\beta 2$ receptors expressed using the high-sensitivity (HS) receptor preparation.

		ACh Dose Response		dFBr Potentiation of ACh Induced Responses		
Mutation	Mutation Location	$pEC_{50} \pm SEM$ (EC_{50} , μM)	n_H	$pEC_{50} \pm SEM$ (EC_{50} , μM)	$pIC_{50} \pm SEM$ (iC_{50} μM)	$I_{max} \pm SEM$
HS WT	WT	5.2 ± 0.1 (5.8)	1.9 ± 0.3	5.7 ± 0.1 (2.0)	3.5 ± 1.9 (316)	3.6 ± 0.3
HS $\beta 2W176A$	$\beta 2$, B-Loop	$6.0 \pm 0.1^{***}$ (0.91)	0.8 ± 0.1	N.D.	7.9 ± 0.3 (0.013)	N.D.
HS $\beta 2T177A$	$\beta 2$, B-Loop	5.7 ± 0.2 (1.9)	0.9 ± 0.3	5.9 ± 0.9 (1.3)	5.4 ± 1.0 (4.0)	$2.4 \pm 0.3^{**}$
HS $\beta 2D179A$	$\beta 2$, B-Loop	$6.0 \pm 0.1^{***}$ (0.98)	$0.7 \pm 0.1^{**}$	5.8 ± 0.6 (25)	3.7 ± 3.0 (200)	$1.8 \pm 0.2^{***}$
HS $\beta 2D217A$	$\beta 2$, C-Loop	$5.8 \pm 0.1^{***}$ (1.5)	1.1 ± 0.3	5.2 ± 0.4 (6.3)	4.4 ± 1.0 (40)	3.2 ± 0.1
HS $\beta 2D218A$	$\beta 2$, C-Loop	5.5 ± 0.1 (2.9)	1.2 ± 0.2	5.5 ± 0.3 (3.2)	3.7 ± 1.3 (200)	3.4 ± 0.3
HS $\beta 2D116A$	$\beta 2$, A-Loop	5.2 ± 0.1 (6.2)	0.9 ± 0.2	5.8 ± 0.3 (1.6)	4.8 ± 0.4 (17)	$2.6 \pm 0.2^{**}$
HS $\beta 2Y120A$	$\beta 2$, A-Loop	5.7 ± 0.2 (2.2)	$0.4 \pm 0.1^{***}$	6.4 ± 0.7 (0.40)	4.7 ± 1.7 (20)	$1.3 \pm 0.1^{***}$
HS $\beta 2Y127A$	$\beta 2$, A-Loop	$6.4 \pm 0.1^{***}$ (0.40)	$0.5 \pm 0.1^{**}$	5.7 ± 0.3 (2.0)	4.1 ± 0.8 (70)	$2.4 \pm 0.1^{**}$
HS $\alpha 4K140A$	$\alpha 4$, E-Loop	$7.2 \pm 0.1^{***}$ (0.058)	2.5 ± 0.8	N.D.	5.9 ± 0.3 (1.3)	N.D.
HS $\alpha 4W88A$	$\alpha 4$, D-Loop	$6.2 \pm 0.2^{**}$ (0.57)	1.1 ± 0.5	5.7 ± 0.3 (2.0)	4.3 ± 0.6 (50)	3.9 ± 0.3

Data represent mean \pm SEM. Data points represent at least 4 replicate values obtained from a minimum of two oocytes harvested from different frogs. pEC_{50} is the $-\log$ of the EC_{50} value; pIC_{50} is the $-\log$ of the IC_{50} value; I_{max} observed is the maximum induced current observed n_H . ** and *** Indicate values significantly different from wild-type receptors with $p < 0.01$ and $p < 0.0001$, respectively.

4.4.1.2. Effects of dFBr on Wild-Type Low- and High- ACh Sensitivity Receptors.

dFBr is a positive allosteric modulator (PAM) of $\alpha 4\beta 2$ nAChRs (Kim et al., 2007; Weltzin and Schulte, 2010b). One of the goals of this study was to locate the putative dFBr binding site. Here we examined the effects of dFBr on the LS and HS receptor preparations using both wild-type and mutant receptors. dFBr did not induce activation of wild-type or mutant channels expressed in either the HS and LS receptor preparations without co-application of ACh.

Wild-type and mutant dose-response curves for dFBr potentiation were determined by co-application of dFBr at concentrations ranging from 0.001 – 100 μM dFBr and a fixed ACh concentration equal to the EC_{75} for ACh (10 μM for HS and 100 μM for LS receptor preparations) to *Xenopus laevis* oocytes injected using the LS or HS injection ratios and evaluated via two-electrode voltage clamp. ACh (100 μM) induced responses of wild-type receptors prepared using the LS receptor preparation were potentiated by co-applications of 0.001 - 3 μM concentrations of dFBr (Figure 4.3B, Table 4.1). The pEC_{50} determined for dFBr on the LS receptors is 6.1 ± 0.3 ($\text{EC}_{50} = 0.79 \mu\text{M}$). Responses were maximally potentiated 280% by application of approximately 3 μM dFBr co-applied with 100 μM ACh. dFBr concentrations in excess of 10 μM produced inhibition of dFBr potentiated ACh induced responses (Figure 4.3B, Table 4.1). The pIC_{50} value for dFBr inhibition was 5.3 ± 0.4 ($\text{IC}_{50} = 5.0 \mu\text{M}$).

In the HS preparation, co-application of varying concentrations of dFBr with 10 μM ACh produced a similar bell shaped dose-response curve to the LS preparation but appeared displaced slightly to the right (Figure 4.3B). The pEC_{50} value determined for the potentiation phase of the dose response curve was 5.7 ± 0.1 ($\text{EC}_{50} = 2.0 \mu\text{M}$) (Table 4.2). Co-application of 10 μM dFBr and 10 μM ACh enhanced ACh induced currents maximally by approximately 360%. Concentrations of dFBr less than 30 μM potentiate ACh induced currents while those greater than 10 μM dFBr inhibit the dFBr potentiated response (Figure 4.3B). The pIC_{50} value was estimated to be approximately 3.5 ± 1.9 ($\text{IC}_{50} = 316 \mu\text{M}$) (Table 4.2).

Comparisons of the HS and LS preparations show minimal statistically significant differences in the dFBr dose-response results. No significant differences were observed when we compare pEC_{50} , $I_{\text{max observed}}$ and pIC_{50} values for dFBr between the HS and LS receptor preparations (Table 4.1 and 4.2). Although visual inspection of Figure 4.3B suggested that the LS preparation dFBr dose-response curve was shifted to the left compared dFBr dose-response curve collected using the HS receptor preparation.

Typical responses to dFBr potentiation of ACh induced responses are shown in the lower panel in Figure 4.3. While the HS preparation appeared to produce smaller responses in this figure the difference is likely due to different in receptor expression levels between the two

experiments and differences in cation conductances between the two receptor populations (Tapia et al., 2007). The overall effects of dFBr appeared to be similar in both cases with amplification of the overall response at lower concentrations followed by a sharpening of the response peak with an increase in the desensitizing phase at concentrations that produce the maximum potentiation ($\sim 3 \mu\text{M} - 10 \mu\text{M}$) then a decrease in the sharpened peak amplitude at high dFBr concentrations. The presence of tail currents or hump currents in some traces (see trace e for both HS and LS preparations) suggested the presence of open channel block as previously determined for the mixed HS and LS preparations using a 1:1 $\alpha 4:\beta 2$ mRNA injection ratio.

4.4.2. $\beta 2$ B-Loop Mutations.

The B-loop region of the orthosteric binding site of nAChRs and other LGICs is thought to form a major component of the ligand binding pocket and are present on the plus face of one receptor subunit. In particular, a conserved W aromatic residue ($\beta 2\text{W}176$, $\alpha 4\text{W}149$) in this region (see Figure 4.1) has been shown to interact with ligands in the orthosteric site (for review see (Lester et al., 2004)). $\alpha 1\text{Y}159$ is the equivalent residue in the GABA_ARs allosteric benzodiazepine binding site that has been shown to reduce benzodiazepine modulation when mutated (Amin et al., 1997). The $\beta 2\text{T}177$ and $\beta 2\text{D}179$ are only conserved in nAChR subunits which form heteromeric receptors. These two residues were chosen for their potential to interact with functional groups on the dFBr molecule and to aid in our understanding of ligand selectivity. To evaluate the potential involvement of these amino acids in normal receptor function and/or the action of dFBr, these residues were individually mutated to alanine. The effects of these mutations are summarized in Table 4.1 for the LS preparation and Table 4.2 for the HS preparation.

4.4.2.1. Effects of $\beta 2$ B-loop Mutations on ACh Induced Responses.

Figure 4.4A shows concentration-response data obtained at increasing concentrations of ACh concentrations (0.1 – 3000 μM) for B-loop mutant receptors using the 5:1 $\alpha 4:\beta 2$ mRNA injection ratio (LS preparation). The pEC_{50} values determined for the B-loop mutations were not significantly different from wild-type receptors ($\beta 2\text{T}177\text{A}$ $p = 0.0624$; $\beta 2\text{W}176\text{A}$ $p = 0.0203$; $\beta 2\text{D}179\text{A}$ $p=0.0144$) (Figure 4.4A, Table 4.1). Thus alanine mutations of $\beta 2\text{W}176$, $\beta 2\text{T}177$ and $\beta 2\text{D}179$ did not significantly alter the pEC_{50} for ACh stimulation of the LS $\alpha 4\beta 2$ nAChR preparation.

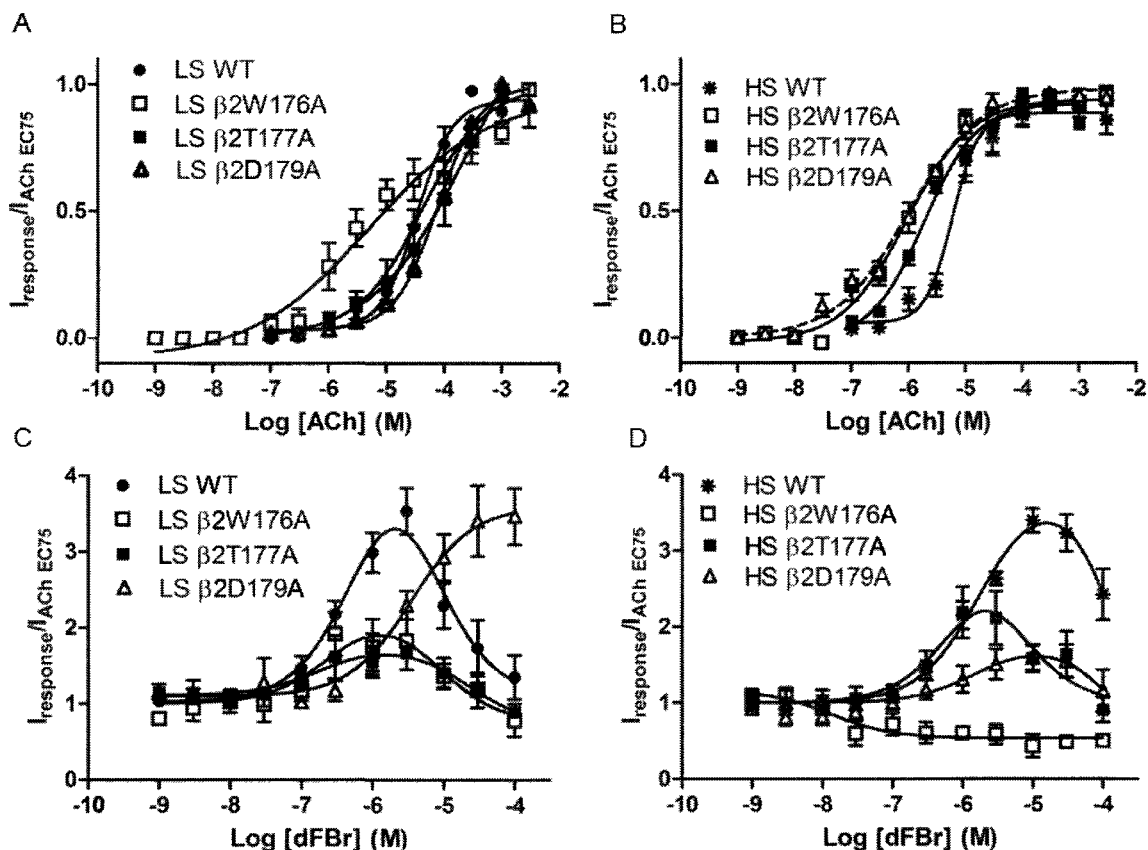


Figure 4.4. ACh and dFBr dose-response curves for $\beta 2+$ face B-loop mutants and wild-type (WT) receptors expressed using the low- (LS) and high- (HS) sensitivity receptor preparation.

Xenopus oocytes were prepared using the HS and LS receptor preparations (HS mRNA injected at a ratio of $1\alpha:5\beta$; LS mRNA injection at a ratio of $5\alpha:1\beta$). Expressing oocytes were exposed to increasing concentrations of ACh and dFBr. **A and B)** ACh dose-response curves for wild-type and $\beta 2+$ face B-loop mutant receptors expressed using the LS and HS receptor preparations. Individual peak amplitudes were normalized to the I_{\max} on the same oocyte. **C and D)** Dose-response curves for co-application of varying concentrations of dFBr and the EC_{75} ACh for wild-type and $\beta 2+$ face B-loop mutant receptors expressed using the LS and HS receptor preparations. The ACh and dFBr dose-response values were determined using non-linear curve fitting as described in the methods and are reported in Table 4.1 and 4.2. Data points represent at least 4 replicate values obtained from a minimum of two oocytes harvested from different frogs. Error bars indicate \pm SEM.

Analysis of n_H values on the wild-type and mutants expressed using the LS preparation revealed no significant differences compared to wild-type, except in the cases of the $\beta 2W176A$ receptor ($p = 0.0001$) (Figure 4.4A, Table 4.1). Mutation of $\beta 2W176$ to alanine produced a

significant decrease in n_H to 0.4 (compared to 1.4 for wild-type receptors). This indicates a potential decrease in cooperativity between the ACh binding sites in this preparation or some other currently unknown effect on receptor kinetics.

The effects of B-loop mutations on ACh stimulation of HS receptors were slightly different from those described above for the LS preparation (Figure 4.4B and Table 4.2). $\beta 2T177A$ had no significant effect on its ACh pEC_{50} value. $\beta 2W176A$ and $\beta 2D179A$ receptors in the HS preparation produced pEC_{50} values that were significantly decreased compared to wild-type ($p < 0.0001$). Increases in pEC_{50} ranged from 1.1-1.2 fold compared to wild-type receptors (corresponding to approximate EC_{50} decrease of 3.1 to 5.7 fold). The n_H was significantly decreased only for the $\beta 2D179A$ mutant (0.7 for the mutant receptor, $p = 0.0097$) (Table 4.2). These results suggest that residues $\beta 2W176$ and $\beta 2D179$ may be involved in ACh conformational change of the protein.

4.4.2.2. Effects of $\beta 2$ B-loop Mutations on dFBr Potentiation.

In contrast to the slight effects observed for B-loop mutations on ACh dose response curves, the alteration in dFBr potentiation were more profound. Co-application of dFBr at concentrations ranging from 0.001 – 100 μM in the presence of 100 μM ACh (Figure 4.4C, Table 4.1) produced curves with differences in dFBr efficacy (I_{max}) as well as potency (pEC_{50}) on the LS preparation. dFBr produced similar effects to wild-type on the $\beta 2W176A$ and $\beta 2T177A$ mutant receptors compared to wild-type receptors with only a slight decrease in pEC_{50} (decreased EC_{50} values of 3.2 and 4.0 fold respectively) and a significant decrease in $\beta 2T177A$ observed I_{max} ($p = 0.0050$) (Table 4.1). $\beta 2D179A$ receptors expressed in the LS preparation did not produce bell-shaped dose-response curves. The concentration-response data for dFBr appeared shifted to the right, although this decrease in the pEC_{50} was not statistically significant (Figure 4.4C, Table 4.1). Slight or perhaps no inhibitory component was observed, possibly reflecting a rightward shift in the inhibitory component of the curve that prevents the observation of inhibition in the concentration range of dFBr utilized in these experiments. The magnitude of the observed I_{max} for peak dFBr potentiation is similar to wild-type receptors (Figure 4.4C, Table 4.1).

$\beta 2W176A$ receptors expressed in the LS receptor preparation appeared to reduce the level of potentiation achieved by dFBr co-application while in the HS preparation, potentiation was completely eliminated (Figure 4.4D, Table 4.2). Partial inhibition of the ACh response (40-50%) was also observed and the pIC_{50} of dFBr appeared to be enhanced compared to wild-type receptors but the values were not significantly different ($p = 0.0419$). As with the LS preparation, the $\beta 2T177A$ mutation produced a bell-shaped dose-response curve for dFBr but with a significantly reduced level of potentiation ($p = 0.0062$).

The effects of the β 2D179A mutation expressed in the HS preparation differed substantially from the LS preparation. While the LS preparation of the β 2D179A mutation produced an apparent rightward shift in the dose-response curve and a decrease in the observed potentiation, in the HS preparation this mutation produced little effect on the pEC_{50} and pIC_{50} but produced a 2 fold decrease in potentiation ($p < 0.0001$) (Figure 4.4D, Table 4.2).

These results suggest that β 2T177 may be involved in the putative dFBr binding site. The alanine mutation of β 2T177 did not alter the ACh concentration-response curve for either receptor preparation. Residues β 2W176 and β 2D179 could be involved in the dFBr binding site but due to the alanine mutations affecting the ACh dose-response curves, unquestionable conclusions cannot be made.

4.4.2.3. Response Profiles Obtained With Co-application of dFBr and ACh on B-loop Mutant Receptors.

The LS preparation response profiles appeared to be similar for the B-loop mutant receptors, β 2W176A and β 2T177A, compared to wild-type receptors. That is at increasing low concentrations of dFBr the overall response appeared augmented. At the peak dFBr potentiating concentrations the response peak appeared sharper and an increase in desensitization lagging phase was observed. Application of dFBr inhibitory concentrations, the response peak remained sharp and the desensitization lagging phase quickly returned to the baseline current. The β 2D179A also followed this trend in response profiles with the exception that at low dFBr concentrations, the responses returned slower to the baseline current when compared to wild-type receptors (Figure 4.5A).

The response profiles of mutant receptors expressed using the HS preparation appeared to be similar to wild-type receptors in the LS and HS preparations (see appendix A). Differences were seen in the β 2W176A receptor where only decreases in peak responses were observed (see appendix A). The β 2T177A mutation appeared to have a prolonged return to the baseline compared to wild-type receptors (Figure 4.5B, traces a-c).

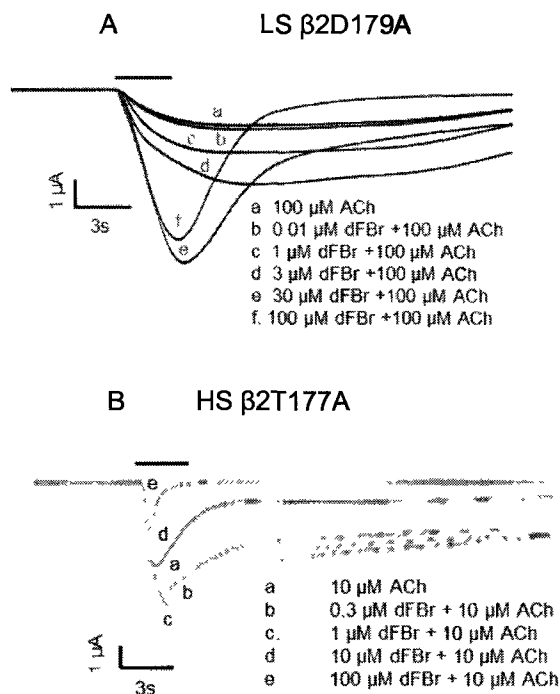


Figure 4.5. Response profiles that appeared different from wild-type receptors for co-application of varying concentrations of dFBr and ACh for β 2+ face B-loop mutant receptors expressed using the low- (LS) and high- (HS) sensitivity receptor preparations.

Xenopus oocytes were prepared using the high- and low-sensitivity receptor preparations (HS mRNA injected at a ratio of 1 α :5 β ; LS mRNA injected at a ratio of 5 α :1 β). Expressing oocytes are exposed to increasing concentrations of ACh and dFBr. **A)** Co-application of dFBr and 100 μ M ACh response traces for β 2D179A receptors expressed via the LS receptor preparation. **B)** Co-application of dFBr and 10 μ M ACh response traces for β 2T177A receptors expressed via the HS receptor preparation. Response traces were recorded from a single oocyte. The solid bar above the response trace indicates the time the oocyte was exposed to co-application of varying concentrations of dFBr and ACh.

4.4.3. β 2 C-loop Mutations.

Alanine mutations were made at D217 and D218 in the C-loop of the β 2 subunit. These amino acids are located on the + face of the receptor and thus in the putative binding domain for dFBr. In the GABA_A receptor, α 1S204 and α 1T206 are equivalent to D217 and D218 of the β 2 nAChR subunit. These residues are thought to be within the GABA_AR allosteric binding site for benzodiazepines (Amin et al., 1997; Wagner and Czajkowski, 2001). In addition to the similar location of these residues to the benzodiazepine binding site, β 2D217 and β 2D218 were hypothesized to be potentially important to the allosteric mechanism of dFBr due to their presence in the C-loop region. Since C-loop residues have been shown to be important for mediating agonist responses at the orthosteric site, we postulated that a similar effect of inducing C-loop closure might be required for dFBr action at the allosteric site (Sala et al., 2005; Weltzin and Schulte, 2010b).

4.4.3.1. *Effects of β 2 C-loop Mutation on ACh Induced Responses.*

Figure 4.6A and B show concentration-response curves obtained for wild-type and mutant receptors using the LS and HS receptor preparations respectively. ACh was applied alone at varying concentrations (0.1 – 3000 μ M) for the experiments shown in both A and B. Minimal effects were observed in the LS receptor preparation (Figure 4.6A, Table 4.1). The pEC_{50} and n_H values obtained using β 2D217A and β 2D218A were similar to wild-type receptors (Table 4.1).

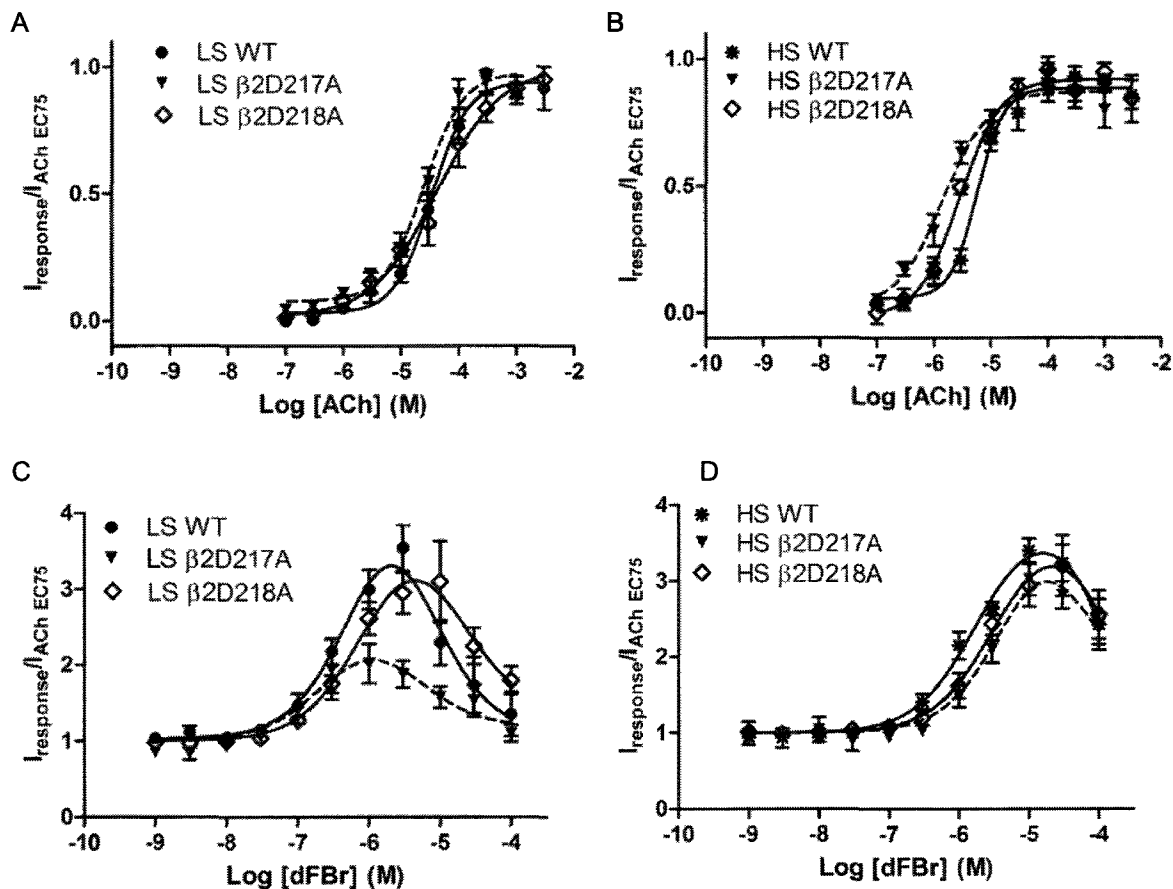


Figure 4.6. ACh and dFBr dose-response curves for β 2+ face C-loop mutant and wild-type (WT) receptors expressed using the low- (LS) and high- (HS) sensitivity receptor preparations.

Xenopus oocytes were prepared using the HS and LS receptor preparations (HS mRNA injected at a ratio of 1 α :5 β ; LS mRNA injected at a ratio of 5 α :1 β). Expressing oocytes were exposed to increasing concentrations of ACh and dFBr. **A and B)** ACh dose-response curves for wild-type and β 2+ face C-loop mutant receptors expressed using the LS and HS receptor preparations. Individual peak amplitudes were normalized to the I_{max} on the same oocyte. **C and D)** Dose-response curves for co-application of varying concentrations of dFBr and 100 μ M ACh for wild-type and β 2+ face C-loop mutant receptors expressed using the LS and HS receptor preparations. The ACh and dFBr dose-response values were determined using non-linear curve fitting as described in the methods and are reported in Table 4.1 and 3.2. Data points represent at least 4 replicate values obtained from a minimum of two oocytes harvested from different frogs. Error bars indicate \pm SEM.

β 2D218A receptors expressed in the HS receptor preparation also produced no change in pEC_{50} or n_H values for ACh stimulation (Figure 4.6B, Table 4.2). A slight, but statistically significant shift in pEC_{50} (1.1 fold) was observed for the β 2D217A mutant ($p < 0.0001$) with no concurrent decrease in n_H (Figure 4.6B, Table 4.2).

4.4.3.2. Effects of β 2 C-loop Mutations on dFBr Potentiation.

Mutation of β 2D217 to alanine had no significant effect on pEC_{50} , pIC_{50} or I_{max} values for dFBr potentiation and inhibition in either the LS or HS receptor preparations (LS: Figure 4.6C, Table 4.1; HS: Figure 4.6D, Table 4.2). In the LS preparation, the β 2D217A dFBr dose-response curve appeared to have a reduced I_{max} and be shifted to the left but differences were not significantly different from wild-type receptors.

The β 2D218A mutation produced no effect on the dFBr dose-response curve in either the LS or HS receptor preparations compared to wild-type receptors (Figure 4.6C and D). No significant alterations to pEC_{50} , pIC_{50} or I_{max} values were observed (Table 4.1 and 4.2).

The lack of any substantial effect of the β 2D217A and β 2D218A mutations of dFBr effects was surprising due to its presence in a key region of the C-loop and its equivalent position in the GABA_A benzodiazepine binding pocket (Amin et al., 1997; Wagner and Czajkowski, 2001). These data do not strongly support a role of the C-loop in dFBr interaction although other residues within the C-loop may be involved.

4.4.3.3. ACh Response Profiles of β 2 C-loop Mutations.

β 2D217A and β 2D218A response profiles appeared similar to wild-type receptors expressed using both the LS and HS receptor preparations (for traces see appendix A).

4.4.4. β 2 A-loop Mutations.

β 2 subunit amino acids at position D116, Y120 and Y127A in the A-loop region were mutated to alanine and evaluated for their effects on stimulation by ACh and/or the potentiating effects of dFBr (Figure 4.7). β 2Y120 was chosen since it is equivalent to α H101 located in the GABA_A benzodiazepine binding site (Wieland et al., 1992). The Aspartate at position 116 was chosen since it is highly conserved in both GABA and nAChRs (Figure 4.1 and 4.2). Similarly, at an aromatic amino acid is conserved at position 127 in both GABA and nAChRs (Figure 4.1 and 4.2).

4.4.4.1. Effects of β 2 A-loop Mutation on ACh Induced Responses.

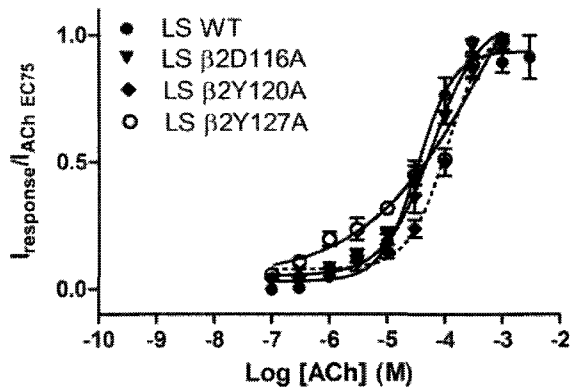
Figure 4.7A and B show concentration-response data obtained for wild-type and mutant receptors using the LS and HS receptor preparations respectively. Minimal effects were observed

on the ACh dose-response in the LS preparation (Figure 4.7A, Table 4.1). The pEC_{50} value obtained using $\beta 2D116A$ on LS or HS receptors were not significantly different then for wild-type. For the $\beta 2Y120A$ and $\beta 2Y127A$ LS mutants, a significant change in pEC_{50} ($p=0.0021$ and $p=0.0026$ respectively) of 1.1 and 1.4 fold was observed. (Figure 4.7A, Table 4.1). A similar, significant shift 1.2 fold was observed for $\beta 2Y127A$ on the HS preparation ($p < 0.0001$) while no significant change was observed for $\beta 2Y120A$. No significant change in n_H was observed for $\beta 2D116A$ or $\beta 2Y120A$ in the LS preparation, although the n_H of 0.4 ± 0.2 for the $\beta 2Y127A$ mutant was significantly different then 1.4 ± 0.3 for wild-type receptors (Table 4.1). In the HS preparation, n_H decreased to 0.4 ± 0.1 for $\beta 2Y120A$ and 0.5 ± 0.1 for $\beta 2Y127A$, significant decreased from the 1.9 ± 0.3 observed in wild-type receptors (Table 4.2).

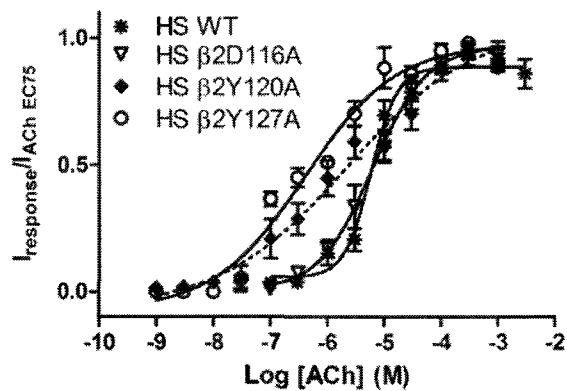
Figure 4.7. ACh and dFBr dose-response curves for β 2+ face A-loop mutant and wild-type (WT) receptors expressed using the low- (LS) and high- (HS) sensitivity receptor preparations.

Xenopus oocytes were prepared using the high and LS receptor preparations (HS mRNA injected at a ratio of 1 α :5 β ; LS mRNA injected at a ratio of 5 α :1 β). Expressing oocytes were exposed to increasing concentrations of ACh and dFBr. **A)** ACh dose-response curves for wild-type and β 2+ face A-loop mutant receptors expressed using the LS receptor preparation. Individual peak amplitudes were normalized to the I_{max} on the same oocyte. **B)** ACh dose-response curves for wild-type and β 2+ face A-loop mutant receptors expressed using the HS receptor preparation. Individual peak amplitudes were normalized to the I_{max} on the same oocyte. **C)** Dose-response curves for co-application of varying concentrations of dFBr and 100 μ M ACh for wild-type and β 2+ face A-loop mutant receptors expressed using the LS receptor preparation. Insert: A graph with the same y-axis as in figure D for easy comparison. **D)** Dose-response curves for co-application of varying concentrations of dFBr and 10 μ M ACh for wild-type and β 2+ face A-loop mutant receptors expressed using the HS receptor preparation. The ACh dose-response values were determined using non-linear curve fitting as described in the methods and are reported in Table 1 and 2. The dFBr dose-response values were determined using non-linear curve fitting as described in the methods and are reported in Table 4.1 and 4.2. Data points represent at least 4 replicate values obtained from a minimum of two oocytes harvested from different frogs. Error bars indicate \pm SEM.

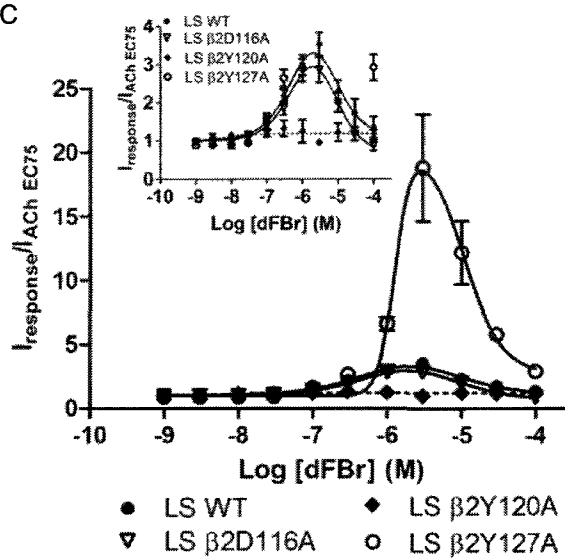
A



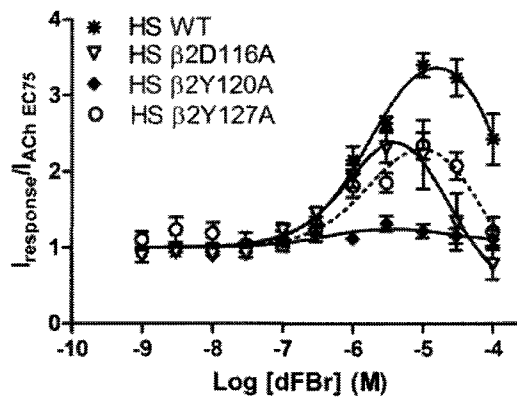
B



C



D



4.4.4.2. Effects of $\beta 2$ A-loop Mutations on dFBr Potentiation.

The $\beta 2D116A$ mutation expressed in the LS receptor preparation produced no change in pEC_{50} , pIC_{50} or I_{max} values for dFBr potentiation and inhibition compared to wild-type receptors, although a slight non-significant decrease in the HS I_{max} was observed (Figure 4.7C, Table 4.1). Similar to the LS preparation, co-application of dFBr and 10 μM ACh on $\beta 2D116A$ in a HS preparation had no significant effect on dFBr's pEC_{50} or pIC_{50} values although the observed I_{max} was significantly reduced ($p = 0.0087$) from 3.6 ± 0.3 to 2.6 ± 0.2 (Figure 4.7D, Table 4.2).

The $\beta 2Y120A$ mutation expressed in the LS preparation only mildly enhanced ACh induced currents ($I_{max} = 1.6 \pm 0.2$) and no inhibition by dFBr was observed (Figure 4.7C). Co-exposure to 0.1-1 μM dFBr and 100 μM ACh induced the maximum amount of potentiation. The pEC_{50} for dFBr potentiation of $\beta 2Y120A$ in the LS preparation was not significantly different from wild-type receptors although the observed I_{max} was significantly reduced ($p = 0.0020$) compared to 3.4 ± 0.4 obtained on wild-type receptors in this preparation (Table 4.1). In the HS receptor preparation, a bell-shaped dose-response curve showing both potentiation and inhibition was observed on mutant $\beta 2Y120A$ (Figure 4.7D). Responses were minimally potentiated by dFBr with the maximum potentiation ($I_{max} = 1.3 \pm 0.1$) observed at co-application of 3 μM dFBr and 10 μM ACh. dFBr concentrations in excess of 3 μM weakly inhibits ACh potentiated currents (Figure 4.7D). No significant shifts were seen in dFBr pEC_{50} and pIC_{50} values were observed in the HS preparation compared to those obtained on wild-type receptors, although the observed I_{max} was significantly reduced ($p < 0.0001$) compared to wild-type receptors (3.6 ± 0.3) (Table 4.2).

$\beta 2Y127A$ receptors expressed in the LS receptor preparation also produced a bell-shaped dose-response curve; however, both the shape and magnitude of the curve was dramatically altered for this receptor (Figure 4.7C). $\beta 2Y127A$ mutant receptors were significantly and maximally potentiated by an enormous 2000% by 10 μM dFBr co-applied with 100 μM ACh ($I_{max} = 20.0 \pm 3$, $p = 0.0018$) (Table 4.1). Similar to wild-type, receptors were inhibited at dFBr concentrations $> 3 \mu M$ (Figure 4.7C). Visual inspection of Figure 4.7C showed an apparently large increase in the slope of the dFBr potentiation phase compared to wild-type receptors. The rapid change in dFBr potentiated ACh currents made accurate determination of pEC_{50} and pIC_{50} values difficult, although the dFBr pEC_{50} and pIC_{50} values seemed comparable to wild-type receptors (Table 4.1). In the HS preparation, the $\beta 2Y127A$ mutant produced a bell-shaped dFBr dose-response curve that was similar to wild-type receptors with no significant changes in pEC_{50} or pIC_{50} values (Figure 4.7D, Table 4.2). Maximum potentiation of 240% was observed with co-application of 10 μM dFBr and 10 mM ACh ($I_{max}=2.4 \pm 0.1$), a significant reduction in I_{max} ($p = 0.0087$) compared to 3.6 ± 0.3 for wild-type receptors in the HS preparation (Table 4.2).

These findings suggest that the A-loop is important for dFBr interactions with $\alpha 4\beta 2$ nAChR expressed in either the LS or HS preparations. $\beta 2D116A$ is the only residue not to affect the ACh dose-response curve, unlike $\beta 2Y120A$ and $\beta 2Y127A$ receptors in the LS and HS preparations. All of the examined A-loop mutations alter the dFBr concentration-response curve in the LS preparation, while only mutations $\beta 2Y120A$ and $\beta 2Y127A$ affect the dFBr dose-response curve in the HS preparation.

4.4.4.3. Response Profiles Obtained with Co-application of dFBr and ACh on A-loop Mutant Receptors.

The response traces for the A-loop mutations in both the LS and HS preparation appeared to be similar to wild-type receptors (see appendix A for traces).

4.4.5. $\alpha 4$ D- and E- β -Sheet Mutations.

The minus face of the putative allosteric binding domain for dFBr was hypothesized to be composed of the $\alpha 4$ D- and E- β -sheets based on homology to the orthosteric nAChR binding site and the benzodiazepine binding site of GABA_A receptors. Two amino acids, in equivalent locations to the GABA_A benzodiazepine binding site residues $\gamma M130$ (E-loop) and $\gamma F77$ (D-loop) were chosen for alanine mutation on the $\alpha 4$ subunit (Buhr et al., 1997a; Buhr and Sigel, 1997). These correspond to the $\alpha 4$ subunit amino acids K140 and W88 respectively.

4.4.5.1. Effects of $\alpha 4$ D- and E- β -Sheet Mutations on ACh Induced Responses.

Figure 4.8A and B shows ACh dose-response data obtained for wild-type and mutant receptors expressed using the LS and HS receptor preparations. For $\alpha 4W88A$ receptors in the LS preparation, pEC_{50} and n_H values are similar to wild-type receptors (Table 4.1). In contrast, for the HS preparation the curve is shifted significantly to the left and the pEC_{50} is increased significantly from 5.2 ± 0.2 (wild-type) to 6.2 ± 0.2 ($\beta 2W88A$) (1.4 fold shift) ($p = 0.0012$) (Table 4.2). Similar to LS mutant receptors, no effect in n_H is observed on the HS preparation.

For the $\alpha 4K140A$ mutation, the dose-response curve shifts to the left in both the LS and HS preparations (Figure 4.8B). For the LS preparation the pEC_{50} is increased significantly from 4.5 ± 0.1 (wild-type) to 7.0 ± 0.1 ($\alpha 4K140A$) ($p < 0.0001$) compared to LS wild-type receptors (Table 4.1). $\alpha 4K140A$ expressed via the HS preparation, the pEC_{50} is also significantly increased from 5.2 ± 0.1 (wild-type) to 7.2 ± 0.1 ($\alpha 4K140A$) compared to HS wild-type receptors ($p < 0.001$) (Table 4.2). The n_H values are similar to wild-type receptors in both the LS and HS preparations (Table 4.1 and 4.2).

4.4.5.2. Effects of α 4 D- and E- β -Sheet Mutations on dFBr Potentiation.

Mutation of α 4K140 to an alanine produces receptors insensitive to potentiation by dFBr in both the LS and HS preparations. In the preparations, inhibition was observed at high dFBr concentrations (Figure 4.8C and D). The pIC_{50} value for dFBr inhibition was not significantly different from LS wild-type receptors.

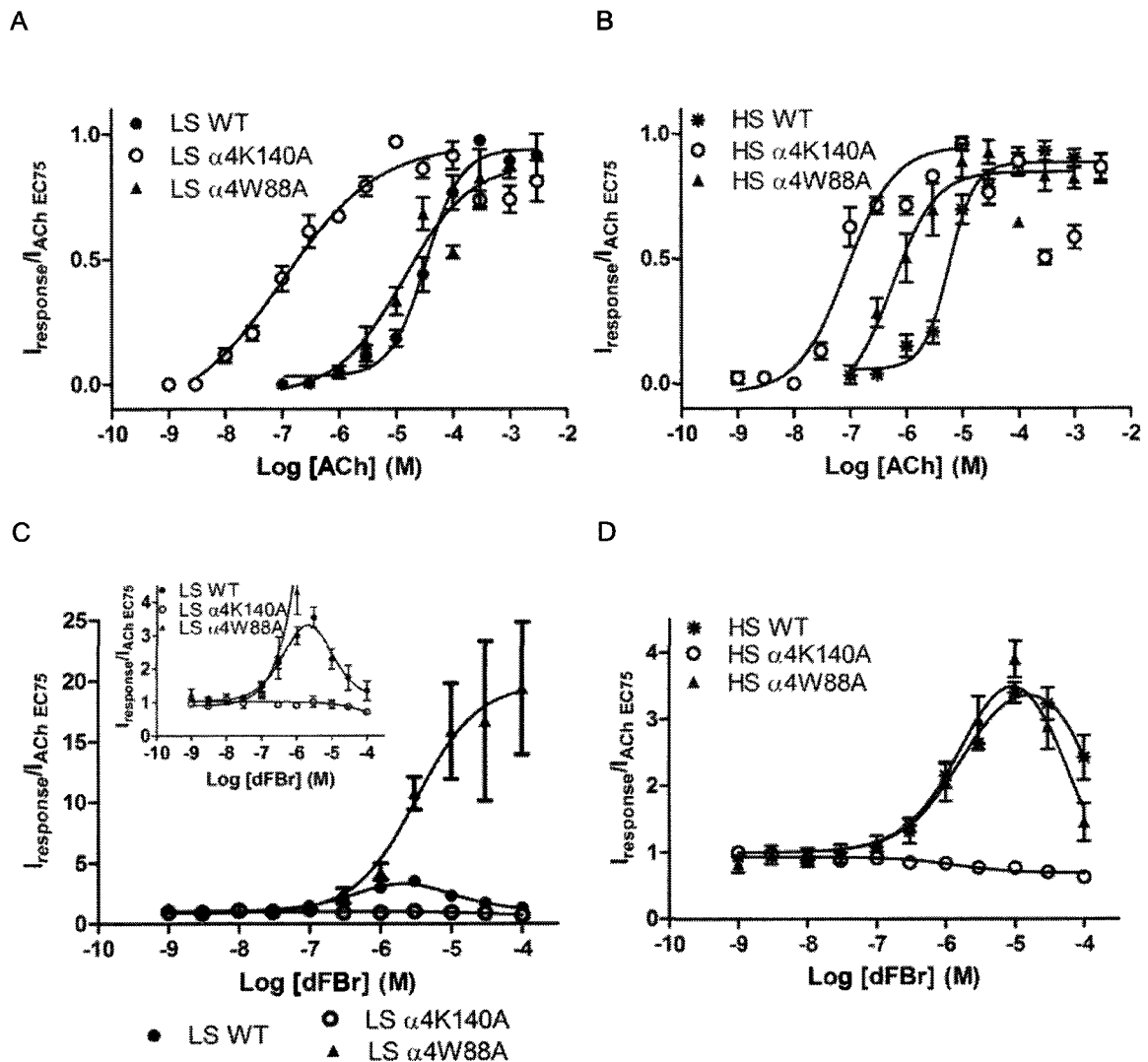


Figure 4.8. ACh and dFBr dose-response curves for α 4- face mutant and wild-type (WT) receptors expressed using the low- (LS) and high- (HS) sensitive receptor preparations.

Xenopus oocytes were prepared using the high and low-sensitivity receptor preparations (HS mRNA injected at a ratio of $1\alpha:5\beta$; LS mRNA injected at a ratio of $5\alpha:1\beta$). Expressing oocytes were exposed to increasing concentrations of ACh and dFBr. **A and B)** ACh dose-response curves for wild-type and α 4- face mutant receptors expressed using the LS and HS receptor preparations. Individual peak amplitudes were normalized to the I_{max} on the same oocyte. **C and D)** Dose-response curves for co-application of varying concentrations of dFBr and the EC75 ACh for wild-type and α 4- face mutant receptors expressed using the LS and HS receptor preparations. Insert: A graph with the same y-axis as in figure D for easy comparison. The ACh and dFBr dose-response values were determined using non-linear curve fitting as described in the methods and are reported in Table 4.1 and 4.2. Data points represent at least 4 replicate values obtained from a minimum of two oocytes harvested from different frogs. Error bars indicate \pm SEM.

Mutation of $\alpha 4W88$ to an alanine amplified I_{max} in the presence of dFBr from 3.4 ± 0.4 (wild-type) to 21 ± 4 ($\alpha 4W88A$) ($p < 0.0001$) in the LS receptor preparation, although the pEC_{50} for dFBr potentiation was not significantly different from wild-type receptors (Figure 4.8C, Table 4.1). Maximum dFBr potentiation of 2100% was observed at dFBr concentration $> 30 \mu M$, similar to the $\beta 2Y127A$ A-loop mutation in the LS preparation. In the LS preparation, no inhibition was observed for $\alpha 4W88A$ in the concentration range of dFBr tested. In the HS preparation the $\alpha 4W88A$ mutant had little effect on dFBr dose-responses curves when compared to those obtained using wild-type receptors (Figure 4.8D). No significant shifts in pEC_{50} , pIC_{50} or I_{max} observed values were seen (Table 4.2).

ACh concentration-response results for the mutant $\alpha 4K140A$ was different from wild-type receptors in both the LS and HS preparations, while the $\alpha 4W88A$ results were only affected in the HS preparation. These findings suggested that these residues may be involved in ACh induced conformational change and may depend on the $\alpha 4\beta 2$ receptor preparation. It is difficult to determine if these residues are also involved in dFBr interactions with the receptor. Because $\alpha 4W88A$ in the LS preparation did not affect ACh results but did eliminate the bell-shaped dose-response of dFBr, we suggest that this residue is possibly located in the dFBr binding site.

4.4.5.3. Response Profiles Obtained With Co-application of dFBr and ACh on $\alpha 4$ Mutant Receptors.

The dFBr concentration-response traces for $\alpha 4K140A$ in both the LS and HS receptor preparation appeared similar to wild-type receptors with the exception to increases in the peak response (see appendix A for traces). The $\alpha 4W88A$ expressed in the HS preparation response profiles appeared similar to wild-type receptors (see appendix A for traces). In the LS preparation, $\alpha 4W88A$ traces appeared to look more like $\alpha 7$ nAChR traces (Figure 4.9). At low, increasing dFBr concentrations co-applied with $100 \mu M$ ACh the response peak sharpens and there was a decrease in the desensitization. At dFBr potentiating concentrations, the peak response was sharper and the desensitization lagging phase was decreased but the current does not return to the baseline. At inhibiting concentrations, the peak response continued to sharpen and the lagging phase decreased sharply and returned to the baseline current (Figure 4.9).

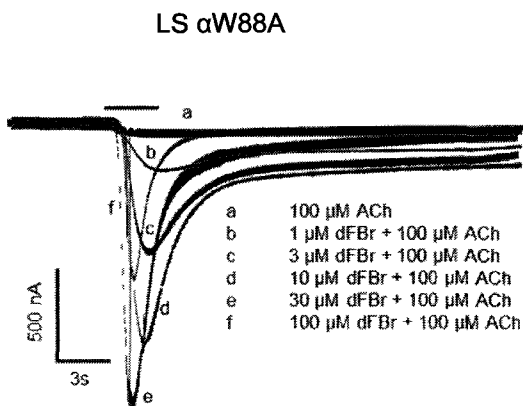


Figure 4.9. Response profiles for co-application of varying concentrations of dFBr and ACh for α -4 face mutant W88A expressed using the low- (LS) sensitive receptor preparation.

Xenopus oocytes were prepared using the low-sensitivity receptor preparations (LS mRNA injected at a ratio of 5 α :1 β). Expressing oocytes were exposed to increasing concentrations of dFBr and co-application of 100 μ M ACh. Response traces were recorded from a single oocyte. The solid bar above the response trace indicates the time the oocyte was exposed to co-application of varying concentrations of dFBr and ACh.

4.5 Discussion.

The primary goal of this study is to test the hypothesis that the plus face of the β 2 subunit and the minus face of the α 4 subunit form the binding domain for dFBr and/or mediate its potentiating effects. To test this hypothesis, we conducted a site directed mutagenesis study of amino acids located in this domain. Residues previously shown to be conserved or important to ligand binding in LGIC receptors were chosen for mutation. Amino acids in loops A, B and C on the β 2 subunit (+face) and D and E on the α 4 subunit (- face) were mutated to alanine. All of the mutants tested appeared to express well in *Xenopus* oocytes although some seem to produce smaller macroscopic currents, possibly due to lower expression levels. Receptors were expressed in both LS and HS preparations and ACh EC_{50} values were either unaltered or only slightly affected in most cases suggesting the receptor stoichiometry is likely unchanged as a result of the mutation.

β 2T177A, β 2D179A, β 2D217A, β 2D218A, β 2D116A and α 4W88A receptors expressed in the LS preparation produces minimal effects on ACh responses compared to wild-type receptors. β 2T177A, β 2D218A, β 2D116A and β 2Y120 mutant receptors expressed in the HS receptor preparation also produced only minimal effects on ACh dose-response curves. Small changes in ACh pEC_{50} 's due to mutations were likely to occur within in any region of the protein, it is the

degree of change that is important. In the LS preparations $\beta 2T177A$, $\beta 2D179A$, $\beta 2Y120A$, $\beta 2Y127A$, $\alpha 4K140A$ and $\alpha 4W88A$ receptors produced large effects on potentiation by dFBr including decreases and increases in efficacy of potentiation and shifts in both EC_{50} and IC_{50} values. In the HS preparation, $\beta 2W176A$, $\beta 2T177A$, $\beta 2D179A$, $\beta 2D116A$, $\beta 2Y120A$, $\beta 2Y127A$, $\alpha 4K140A$ and $\alpha 4W88A$ receptors produced large changes in the dFBr concentration-response data. These data suggest involvement of these amino acids in either the binding of dFBr or in mediating dFBr's potentiating effects. The elimination of dFBr potentiation in mutants such as $\alpha 4K140A$ or $\beta 2Y120A$ suggests that these amino acids may be directly involved.

We postulate that the dFBr binding site is located on the + face of the $\beta 2$ subunit and involves $\beta 2T177$ in $\alpha 4\beta 2$ receptors expressed in either the LS or HS receptor preparation. In the LS preparation, $\beta 2W176A$, $\beta 2T177A$, $\beta 2D179A$ and $\alpha 4W88A$ significantly altered the potentiating effects of dFBr but only minimally altered the ACh dose-response curves. In the HS receptor preparation $\beta 2T177A$, $\beta 2D116A$ and $\beta 2Y120A$ receptors showed significant effects on dFBr potentiation despite the minimal effects on ACh stimulation.

4.5.1 Stoichiometries of Receptors in LS and HS $\alpha 4\beta 2$ nAChR Preparations.

Injection of different concentrations of $\alpha 4:\beta 2$ mRNA or DNA has been shown to cause the expression of two different receptor populations (Nelson et al., 2003; Zhou et al., 2003; Briggs et al., 2006; Moroni et al., 2006; Zwart et al., 2006; Tapia et al., 2007). Previous studies have suggested that the HS receptor preparation predominantly forms receptors with two $\alpha 4$ and three $\beta 2$ subunits in the pentameric arrangement $\alpha\beta\alpha\beta\beta$ ($(\alpha 4)_2(\beta 2)_3$) (Nelson et al., 2003; Zhou et al., 2003; Briggs et al., 2006; Moroni et al., 2006; Zwart et al., 2006; Tapia et al., 2007). This stoichiometry would produce receptors in the HS preparation containing two $\alpha+/\beta-$ clefts, two $\beta+/\alpha-$ clefts and one $\beta+/\beta-$ cleft (see Figure 1.4 in introduction). Several lines of evidence suggest that receptors formed in the LS receptor preparation are predominantly composed of three $\alpha 4$ and two $\beta 2$ subunits in the arrangement $\alpha\beta\alpha\beta\alpha$ ($(\alpha 4)_3(\beta 2)_2$) (Nelson et al., 2003; Zhou et al., 2003; Briggs et al., 2006; Moroni et al., 2006; Zwart et al., 2006; Tapia et al., 2007). If this stoichiometry is correct, the receptors in the LS preparation would contain two $\alpha+/\beta-$ clefts, two $\beta+/\alpha-$ clefts and one $\alpha+/\alpha-$ cleft. It is likely that other arrangements of subunits are also expressing in both the HS and LS preparation although possibly to a lesser extent.

The presumed HS and LS stoichiometries have not yet been conclusively demonstrated. Studies have shown that receptors expressed using the LS receptor preparation have an ACh EC_{50} of $\sim 60-90 \mu M$ and HS receptor preparations have an ACh EC_{50} of $\sim 1.8-4 \mu M$ (Zwart and Vijverberg, 1998; Moroni et al., 2008). These values are similar to what we observed for the HS and LS preparations, indicating that our receptor expression systems likely form comparable

receptors to those used in previous studies (Nelson et al., 2003; Zhou et al., 2003; Briggs et al., 2006; Moroni et al., 2006; Zwart et al., 2006; Tapia et al., 2007).

In general, mutant receptors expressed using the HS receptor preparation produced greater changes in ACh dose-response data than mutant receptors expressed using the LS preparation. One explanation for this phenomenon may lie in the possible different stoichiometric arrangements of subunits in the two different preparations. As described above, the HS preparation may contain receptors containing two $\alpha 4$ and three $\beta 2$ subunits. Thus receptors would contain three rather than two mutant subunits and these mutations would be present at three of the five subunit interfaces (one $\beta 2+\beta 2-$ subunit interface and two $\beta 2+\alpha 4-$ subunit interfaces). In the LS preparation $\beta 2$ mutations would only be present at two of the interfaces.

Differences in mutant and wild-type ACh dose-response data, particularly in the HS receptors might be explained by alteration in receptor gating. Previous studies using muscle AChRs have demonstrated that single point mutations can reduce receptor open state stabilities (Akk, 2002; Purohit and Auerbach, 2010). Purohit and Auerbach (2010) show that mutation of $\alpha Y93$ and $\alpha W149$ in mouse muscle AChR increased spontaneous and monoligand open events, indicating a change in receptor gating. Mutation of $\delta W57$ has also been shown to alter channel gating by single channel analysis (Akk, 2002). The homologous residues to Torpedo $\alpha Y93$, $\alpha W149$ and $\delta W57$ are $\beta 2 Y120$, $\beta 2 W176$ and $\alpha 4 W88$ respectively. Effects similar to those observed in Torpedo receptors may be responsible for the effects we observed on mutant $\alpha 4 \beta 2$ nAChRs.

Unwin has previously hypothesized that the localized twisting of the *Torpedo* $\alpha 6$ subunit in response to ACh application must also affect the neighboring subunits (Unwin, 1995). Current crystallography structures of the acetylcholine binding protein have shown various structural arrangements of the C-loop in binding clefts without ligand (Brejc et al., 2001; Celie et al., 2005). A study by Teissere and Czajkowski (2001) provides further support that non-orthosteric clefts are structurally altered by agonist binding to their receptors. Teissere and Czajkowski (2001) have shown that mutating $\gamma Y72C$, $\gamma D75C$ and $\gamma F78C$ located within the benzodiazepine binding site in GABA_A receptors caused a shift in the GABA EC₅₀ values less than four fold. SCAM studies have additionally shown that a cysteine substituted for $\gamma A79$ in the GABA receptor is more accessibility to MTSEA-biotin modification during GABA binding and channel gating (Teissere and Czajkowski, 2001). Authors suggest that their data confirms that structural rearrangements occur within the benzodiazepine binding site in response to GABA binding in its orthosteric site. These results are similar to our current findings that mutations in interfaces not involved in binding ACh can alter ACh stimulation of the receptor. If dFBr acts similar to the benzodiazepine

drug class, then dFBr may be exerting a similar modifying effect on the normal processes of receptor gating mediated through the non-orthosteric interfaces. Alternatively, a possibility that we cannot rule out is that the mutations made in on allosteric subunit faces could cause structural rearrangements in the orthosteric binding site.

In summary, data obtained in our mutagenesis studies suggest a role of non-orthosteric subunit interfaces in ACh receptor gating and desensitization. This is the first data supporting a role of this region of the nAChR in mediating responses to ACh.

4.5.2 The $\beta 2+$ and $\alpha 4$ - Subunits Contain the dFBr Allosteric Binding Site.

Wild-type receptors expressed in the LS and HS receptor preparations responded similarly to dFBr. In the LS receptor preparation, $\beta 2W176A$, $\beta 2T177A$, $\beta 2D179A$ (B-loop) and $\alpha 4W88A$ (D- β -sheet) significantly affected the ability of dFBr to potentiate ACh responses but had only minimally modified the ACh dose-response relationships. In the HS receptor preparation $\beta 2T177A$ (B-loop), $\beta 2D116A$ (A-loop) and $\beta 2Y120A$ (A-loop) significantly altered the dFBr potentiation but with only minimally effects on the ACh dose-response. All of these mutations are at positions where homologous amino acids in the GABA_AR benzodiazepine binding site have been shown to participate in the interaction of benzodiazepines (Duncalfe et al., 1996; Amin et al., 1997; Buhr et al., 1997a; Buhr et al., 1997b; Wingrove et al., 1997; Wagner and Czajkowski, 2001). These data are consistent with an effect of dFBr on the nAChR similar to the action of benzodiazepines on the GABA_A receptor.

4.5.3 Summary.

Our data supports a role for the non-orthosteric cleft in ACh activation of the $\alpha 4\beta 2$ receptor. In particular, the $\beta 2+/\alpha$ - cleft appears to play a role in normal receptor function in response to ACh. This region of the receptor, particularly the $\beta 2$ subunit, also appears to be involved in mediating the effects of dFBr as a PAM. We hypothesize that dFBr may exert its effects by altering the normal conformational changes in the receptor that involve the non-orthosteric clefts. Amino acids expressed in the LS preparation include $\beta 2W176A$, $\beta 2T177A$, $\beta 2D179A$ and $\alpha 4W88A$, while in the HS preparation residues $\beta 2T177A$, $\beta 2D116A$, $\beta 2D116A$ and $\beta 2Y120A$ appear to be involved in dFBr actions. Results from this study enhance our understanding of non-orthosteric clefts of $\alpha 4\beta 2$ nAChRs response mechanisms to the orthosteric ligand ACh. In addition, residues involved in dFBr actions have been resolved, paving the way for the design of therapeutic ligands acting at this novel site.

4.6 References.

Adams CE and Stevens KE (2007) Evidence for a role of nicotinic acetylcholine receptors in schizophrenia. *Front Biosci* **12**:4755-4772.

Akk G (2002) Contributions of the non-alpha subunit residues (loop D) to agonist binding and channel gating in the muscle nicotinic acetylcholine receptor. *J Physiol* **544**:695-705.

Amin J, Brooks-Kayal A and Weiss DS (1997) Two tyrosine residues on the alpha subunit are crucial for benzodiazepine binding and allosteric modulation of gamma-aminobutyric acidA receptors. *Mol Pharmacol* **51**:833-841.

Aubert I, Araujo DM, Cecyre D, Robitaille Y, Gauthier S and Quirion R (1992) Comparative alterations of nicotinic and muscarinic binding sites in Alzheimer's and Parkinson's diseases. *J Neurochem* **58**:529-541.

Bertrand D and Gopalakrishnan M (2007) Allosteric modulation of nicotinic acetylcholine receptors. *Biochem Pharmacol* **74**:1155-1163.

Brejč K, van Dijk WJ, Klaassen RV, Schuurmans M, van Der Oost J, Smit AB and Sixma TK (2001) Crystal structure of an ACh-binding protein reveals the ligand-binding domain of nicotinic receptors. *Nature* **411**:269-276.

Briggs CA, Gubbins EJ, Marks MJ, Putman CB, Thimmapaya R, Meyer MD and Surowy CS (2006) Untranslated Region Dependent Exclusive Expression of High-Sensitivity Subforms of $\{\alpha\}4\{\beta\}2$ and $\{\alpha\}3\{\beta\}2$ Nicotinic Acetylcholine Receptors. *Mol Pharmacol*.

Buhr A, Baur R and Sigel E (1997a) Subtle changes in residue 77 of the gamma subunit of $\alpha1\beta2\gamma2$ GABAA receptors drastically alter the affinity for ligands of the benzodiazepine binding site. *J Biol Chem* **272**:11799-11804.

Buhr A, Schaerer MT, Baur R and Sigel E (1997b) Residues at positions 206 and 209 of the $\alpha1$ subunit of gamma-aminobutyric AcidA receptors influence affinities for benzodiazepine binding site ligands. *Mol Pharmacol* **52**:676-682.

Buhr A and Sigel E (1997) A point mutation in the $\gamma2$ subunit of gamma-aminobutyric acid type A receptors results in altered benzodiazepine binding site specificity. *Proc Natl Acad Sci U S A* **94**:8824-8829.

Butt CM, Hutton SR, Marks MJ and Collins AC (2002) Bovine serum albumin enhances nicotinic acetylcholine receptor function in mouse thalamic synaptosomes. *J Neurochem* **83**:48-56.

Celie PH, Kasheverov IE, Mordvintsev DY, Hogg RC, van Nierop P, van Elk R, van Rossum-Fikkert SE, Zhmak MN, Bertrand D, Tsetlin V, Sixma TK and Smit AB (2005) Crystal structure of nicotinic acetylcholine receptor homolog AChBP in complex with an alpha-conotoxin PnIA variant. *Nat Struct Mol Biol* **12**:582-588.

Court J, Martin-Ruiz C, Piggott M, Spurden D, Griffiths M and Perry E (2001) Nicotinic receptor abnormalities in Alzheimer's disease. *Biol Psychiatry* **49**:175-184.

Duncalfe LL, Carpenter MR, Smillie LB, Martin IL and Dunn SM (1996) The major site of photoaffinity labeling of the gamma-aminobutyric acid type A receptor by [3H]flunitrazepam is histidine 102 of the alpha subunit. *J Biol Chem* **271**:9209-9214.

Gotti C, Moretti M, Meinerz NM, Clementi F, Gaimarri A, Collins AC and Marks MJ (2008) Partial deletion of the nicotinic cholinergic receptor alpha 4 or beta 2 subunit genes changes the acetylcholine sensitivity of receptor-mediated $^{86}\text{Rb}^+$ efflux in cortex and thalamus and alters relative expression of alpha 4 and beta 2 subunits. *Mol Pharmacol* **73**:1796-1807.

Harvey RJ, Thomas P, James CH, Wilderspin A and Smart TG (1999) Identification of an inhibitory Zn^{2+} binding site on the human glycine receptor alpha1 subunit. *J Physiol* **520 Pt 1**:53-64.

Hsiao B, Dweck D and Luetje CW (2001) Subunit-dependent modulation of neuronal nicotinic receptors by zinc. *J Neurosci* **21**:1848-1856.

Hsiao B, Mihalak KB, Repicky SE, Everhart D, Mederos AH, Malhotra A and Luetje CW (2006) Determinants of zinc potentiation on the alpha4 subunit of neuronal nicotinic receptors. *Mol Pharmacol* **69**:27-36.

Joshi PR, Suryanarayanan A and Schulte MK (2004) A vertical flow chamber for *Xenopus* oocyte electrophysiology and automated drug screening. *J Neurosci Methods* **132**:69-79.

Kim JS, Padnya A, Weltzin M, Edmonds BW, Schulte MK and Glennon RA (2007) Synthesis of desformylfluorabromine and its evaluation as an alpha4beta2 and alpha7 nACh receptor modulator. *Bioorg Med Chem Lett* **17**:4855-4860.

Lester HA, Dibas MI, Dahan DS, Leite JF and Dougherty DA (2004) Cys-loop receptors: new twists and turns. *Trends Neurosci* **27**:329-336.

Lippiello PM (2006) Nicotinic cholinergic antagonists: a novel approach for the treatment of autism. *Med Hypotheses* **66**:985-990.

Marks MJ, Stitzel JA, Grady SR, Picciotto MR, Changeux JP and Collins AC (2000) Nicotinic-agonist stimulated ($^{86}\text{Rb}^+$) efflux and [(3)H]epibatidine binding of mice differing in beta2 genotype. *Neuropharmacology* **39**:2632-2645.

Martin-Ruiz CM, Lee M, Perry RH, Baumann M, Court JA and Perry EK (2004) Molecular analysis of nicotinic receptor expression in autism. *Brain Res Mol Brain Res* **123**:81-90.

Moretti M, Mugnaini M, Tessari M, Zoli M, Gaimarri A, Manfredi I, Pistillo F, Clementi F and Gotti C (2010) A comparative study of the effects of the intravenous self-administration or subcutaneous minipump infusion of nicotine on the expression of brain neuronal nicotinic receptor subtypes. *Mol Pharmacol* **78**:287-296.

Moroni M, Vijayan R, Carbone A, Zwart R, Biggin PC and Bermudez I (2008) Non-agonist-binding subunit interfaces confer distinct functional signatures to the alternate stoichiometries of the alpha4beta2 nicotinic receptor: an alpha4-alpha4 interface is required for Zn^{2+} potentiation. *J Neurosci* **28**:6884-6894.

Moroni M, Zwart R, Sher E, Cassels BK and Bermudez I (2006a) $\alpha_4\beta_2$ nicotinic receptors with high and low acetylcholine sensitivity: pharmacology, stoichiometry, and sensitivity to long-term exposure to nicotine. *Mol Pharmacol* **70**:755-768.

Moroni M, Zwart R, Sher E, Cassels BK and Bermudez I (2006b) $\alpha_4\beta_2$ nicotinic receptors with high and low acetylcholine sensitivity: pharmacology, stoichiometry and sensitivity to chronic exposure to nicotine. *Mol Pharmacol*.

Mudo G, Belluardo N and Fuxe K (2007) Nicotinic receptor agonists as neuroprotective/neurotrophic drugs. Progress in molecular mechanisms. *J Neural Transm* **114**:135-147.

Nelson ME, Kuryatov A, Choi CH, Zhou Y and Lindstrom J (2003) Alternate stoichiometries of $\alpha_4\beta_2$ nicotinic acetylcholine receptors. *Mol Pharmacol* **63**:332-341.

Nordberg A (2001) Nicotinic receptor abnormalities of Alzheimer's disease: therapeutic implications. *Biol Psychiatry* **49**:200-210.

Picciotto MR, Caldarone BJ, Brunzell DH, Zachariou V, Stevens TR and King SL (2001) Neuronal nicotinic acetylcholine receptor subunit knockout mice: physiological and behavioral phenotypes and possible clinical implications. *Pharmacol Ther* **92**:89-108.

Purohit P and Auerbach A (2010) Energetics of gating at the apo-acetylcholine receptor transmitter binding site. *J Gen Physiol* **135**:321-331.

Sala F, Mulet J, Reddy KP, Bernal JA, Wikman P, Valor LM, Peters L, Konig GM, Criado M and Sala S (2005) Potentiation of human $\alpha_4\beta_2$ neuronal nicotinic receptors by a *Flustra foliacea* metabolite. *Neurosci Lett* **373**:144-149.

Sigel E (2002) Mapping of the benzodiazepine recognition site on GABA(A) receptors. *Curr Top Med Chem* **2**:833-839.

Taly A, Corringer PJ, Guedin D, Lestage P and Changeux JP (2009) Nicotinic receptors: allosteric transitions and therapeutic targets in the nervous system. *Nat Rev Drug Discov* **8**:733-750.

Tapia L, Kuryatov A and Lindstrom J (2007) Ca^{2+} permeability of the $(\alpha_4)_3(\beta_2)_2$ stoichiometry greatly exceeds that of $(\alpha_4)_2(\beta_2)_3$ human acetylcholine receptors. *Mol Pharmacol* **71**:769-776.

Teissere JA and Czajkowski C (2001) A (β) -strand in the $(\gamma)_2$ subunit lines the benzodiazepine binding site of the GABA A receptor: structural rearrangements detected during channel gating. *J Neurosci* **21**:4977-4986.

Unwin N (1995) Acetylcholine receptor channel imaged in the open state. *Nature* **373**:37-43.

Wagner DA and Czajkowski C (2001) Structure and dynamics of the GABA binding pocket: A narrowing cleft that constricts during activation. *J Neurosci* **21**:67-74.

Weltzin MM and Schulte MK (2010a) Pharmacological characterization of the allosteric modulator desformylflustrabromine and its interaction with $\alpha_4\beta_2$ neuronal nicotinic acetylcholine receptor orthosteric ligands. *J Pharmacol Exp Ther* **334**:917-926.

Weltzin MM and Schulte, MK (2010b) Allosteric modulation of high and low affinity alpha4beta2 nicotinic acetylcholine receptors by HEPES, in *Society for Neuroscience*, San Diego.

Wieland HA, Luddens H and Seeburg PH (1992) A single histidine in GABAA receptors is essential for benzodiazepine agonist binding. *J Biol Chem* **267**:1426-1429.

Wingrove PB, Thompson SA, Wafford KA and Whiting PJ (1997) Key amino acids in the gamma subunit of the gamma-aminobutyric acidA receptor that determine ligand binding and modulation at the benzodiazepine site. *Mol Pharmacol* **52**:874-881.

Zhou Y, Nelson ME, Kuryatov A, Choi C, Cooper J and Lindstrom J (2003) Human alpha4beta2 acetylcholine receptors formed from linked subunits. *J Neurosci* **23**:9004-9015.

Zwart R, Broad LM, Xi Q, Lee M, Moroni M, Bermudez I and Sher E (2006) 5-I A-85380 and TC-2559 differentially activate heterologously expressed alpha4beta2 nicotinic receptors. *Eur J Pharmacol*.

Zwart R and Vijverberg HP (1998) Four pharmacologically distinct subtypes of alpha4beta2 nicotinic acetylcholine receptor expressed in *Xenopus laevis* oocytes. *Mol Pharmacol* **54**:1124-1131.

CHAPTER 5: Allosteric Modulation of High- and Low- Sensitivity alpha4beta2 Nicotinic Acetylcholine Receptors by HEPES.

5.1 Abstract.

A number of new positive allosteric modulators (PAMs) have been reported that enhance responses of neuronal alpha7 and alpha4beta2 nicotinic acetylcholine receptor (nAChR) subtypes to orthosteric ligands. PAMs represent promising new leads for the development of therapeutic agents for disorders involving alterations in nicotinic neurotransmission such as Autism, Alzheimer's and Parkinson's disease. During our recent studies of alpha4beta2 PAMs, we identified a novel effect of 4-(2-hydroxyethyl)-1-piperazineethanesulfonic acid (HEPES). The effects of HEPES were evaluated in phosphate buffered recording solutions using two-electrode voltage clamp techniques and alpha4beta2 and alpha7 nAChR subtypes expressed in *Xenopus laevis* oocytes. Acetylcholine induced responses of high-sensitivity alpha4beta2 receptors were potentiated 190% by co-exposure to HEPES. Responses were inhibited at higher concentrations (bell-shaped dose-response curve). Coincidentally, at concentrations of HEPES typically used in oocyte recording (5-10 mM), the potentiating effects of HEPES are matched by its inhibitory effects thus producing no net effect. Mutagenesis results suggest HEPES potentiates the high-sensitivity stoichiometry of the alpha4beta2 receptors through action at the beta+/beta- interface and is dependent on residue beta2D218. On low-sensitivity alpha4beta2 receptors, HEPES produced only inhibition of ACh induced responses. HEPES was not observed to potentiate or inhibit acetylcholine induced responses on alpha7 nAChRs.

Our data may alter the interpretation of previous PAM studies due to the common use of HEPES as a buffering agent in electrophysiological recording buffer. We performed experiments using previously published alpha4beta2 potentiating agents to document these effects.

5.2 Introduction.

Nicotinic acetylcholine receptors (nAChR), GABA_A, 5HT_{3A} and glycine receptors are members of the Cys-loop super family of ligand gated ion channels. Alterations in expression of nAChRs have been implicated in neurological disorders including Alzheimer's disease (Court et al., 2001; Nordberg, 2001), Parkinson's disease (Aubert et al., 1992), Autism (Martin-Ruiz et al., 2004; Lippiello, 2006), Schizophrenia (Adams and Stevens, 2007) and nicotine addiction (Picciotto et al., 2001). In addition, mutations in the $\alpha 4$ (CHRNA4) and $\beta 2$ (CHRN2) subunit genes cause autosomal nocturnal frontal lobe epilepsy (Weiland et al., 2000).

Studies have provided suggestive evidence that both the high- (HS) and low- (LS) ACh sensitivity $\alpha 4\beta 2$ nAChR stoichiometries are expressed in the mammalian brain (Marks et al., 2000; Butt et al., 2002; Gotti et al., 2008) and can be altered by chronic exposure to nicotine (Moretti et al., 2010). In the brain, most $\alpha 4\beta 2$ nAChRs act presynaptically or preterminally to modulate neurotransmitter release (Wonnacott, 1997). The composition of the human $\alpha 4\beta 2$ stoichiometries has not been elucidated in neurons.

In heterologous expression systems, both HS and LS receptors have been observed and these are attributed to a predominance of either the $(\alpha 4)_2(\beta 2)_3^*$ or $(\alpha 4)_3(\beta 2)_2^*$ stoichiometries even though it is acknowledged that other stoichiometries may also be present. The expression of different $\alpha 4\beta 2$ stoichiometries in *Xenopus laevis* oocytes can be influenced by injecting higher concentrations of mRNA for one subunit over the other (Zwart and Vijverberg, 1998; Moroni and Bermudez, 2006; Moroni et al., 2006a; Tapia et al., 2007). These stoichiometries differ in their functional pharmacology, desensitization kinetics, unitary conductance and calcium permeability. The presumed HS stoichiometry has a high acetylcholine (ACh) sensitive (Nelson et al., 2003). The LS stoichiometry possess a lower ACh sensitive and reduced sensitivity to up-regulation by agonists, desensitizes more rapidly and has a higher Ca²⁺ permeability than the HS receptors (Nelson et al., 2003; Tapia et al., 2007).

This study investigates allosteric modulation of HS and LS $\alpha 4\beta 2$ nAChRs and $\alpha 7$ nAChRs by 4-(2-hydroxyethyl)-1-piperazineethanesulfonic acid (HEPES). HEPES is a popular buffering agent originally developed 1966 by Normon Good and colleagues as one of a series of related buffers with pKa values around physiological pH (Good et al., 1966). Collectively known as "Good's buffers", these compounds were thought to be physiologically inert. Over the years there has been accumulating evidence that HEPES is a fairly reactive molecule which interacts with *in vitro* experimentation. HEPES has been shown to stimulate the production of ATP, decrease the uptake of P-glycoprotein, effect cell membrane and block both chloride ion channels

and mammalian 5-hydroxytryptamine transporters (Li et al., 2002). These findings suggest that HEPES may not be a benign molecule.

Our results indicate a specific interaction of HEPES with the HS $\alpha 4\beta 2$ nAChR. HEPES dose-response curves on HS receptors activated by acetylcholine (ACh) are triphasic with a potentiation phase followed by two distinct inhibitory phases. LS $\alpha 4\beta 2$ receptors are not potentiated but show a single inhibitory phase at high HEPES concentrations equivalent to the second inhibitory phase observed on high-sensitivity receptors. Mutagenesis of the $\beta 2$ D218 to an alanine in the C-loop region of the + face of the $\beta 2$ subunit abolishes the potentiation phase and the first inhibitory phase on HS receptors but leaves the third, low-sensitivity inhibitory phase intact. This mutation does not alter inhibition by HEPES on the LS subtype. The apparent selectivity for the HS receptor combined with mutagenesis data indicates the involvement of the $\beta 2+$ face and suggests that at the $\beta +/\beta -$ cleft contains the HEPES allosteric potentiation binding site.

The ability of HEPES to modulate $\alpha 4\beta 2$ nAChRs may alter the interpretation of previous studies of $\alpha 4\beta 2$ modulators due to the wide use of HEPES in electrophysiological recording buffers. We have included a re-analysis of two such modulators (desformylflustrabromine (dFBr) and Zn^{2+}) in this study to demonstrate how the presence of HEPES in the recording buffer may hinder interpretation of experimental data.

5.3 Materials and Methods.

5.3.1 Receptors and mRNA.

The cDNA sequences for human $\alpha 4$ (NCBI Reference Sequence: NM_000744.5), $\beta 2$ (NCBI Reference Sequence: NM_000748.2) and $\alpha 7$ (NCBI Reference Sequence: NM_000746.3) nAChR subunits were used to synthesize a full length cDNA for each subunit. cDNA synthesis was conducted by GeneArt Inc. (Burlingame, CA). The $\beta 2$ cDNA was inserted into the pcDNA3.1/Zeo(+) mammalian expression vector with restriction enzymes Not I and Xho I and the $\alpha 4$ cDNA was inserted into the pcDNA3.1/hygromycin mammalian expression vector with restriction enzymes Hind III and BamHI (vectors procured from Invitrogen, Carlsbad, CA; restriction enzymes purchased from New England Biolabs). The constructs were transformed into AG1 super-competent cells (Stratagene) for production of cDNA. The cDNA for $\alpha 7$ nAChR subunit was inserted with restriction enzymes Sal I and Xba into the pBudCE4.1 expression vector (Invitrogen). Synthetic cRNA transcripts for $\alpha 4$, $\beta 2$ and $\alpha 7$ subunits were prepared using the T7 mMESSAGE mMACHINE™ High Yield Capped RNA Transcription Kit (Ambion, Austin,

TX). All constructs were fully sequenced and confirmed to be identical to the published sequences for each subunit.

The β 2D218A mutation was created using the QuickChange[®] mutagenesis kit as described previously (Agilent Technologies, Inc. Santa Clara, CA) (Venkataraman et al., 2002; Moroni et al., 2008). The resulting DNA was used to transform AG1 super-competent cells and individual colonies were screened to identify those producing mutant β 2 cDNA. To facilitate screening of mutant receptors, a silent Sac II restriction site was engineered into the mutant cDNA. The mutation was confirmed by commercial DNA sequencing (Sequetech, Mountain View, CA).

5.3.2 Test Compounds.

4-(2-hydroxyethyl)-1-piperazineethanesulfonic acid (HEPES), Acetylcholine (ACh), Tris (hydroxymethyl)-aminomethane hydrochloride, Tris (hydroxymethyl) aminomethane, potassium dihydrogen phosphate, potassium phosphate dibasic, ZnCl and other salts and buffering agents were obtained from Sigma-Aldrich, Inc (MO). Desformylflustrabromine-HCl (dFBr) was synthesized by Dr. Richard Glennon (Virginia Commonwealth University) according to a previously published procedure (Kim et al., 2007).

5.3.3 *Xenopus laevis* Oocytes and Receptor Expression.

Xenopus laevis frogs and frog food were purchased from Nacso (Fort Atkinson, WI). Ovarian lobes were surgically removed from Finquel anesthetized *Xenopus laevis* frogs and washed twice in Ca²⁺-free Barth's buffer (82.5 mM NaCl; 2.5 mM KCl; 1 mM MgCl₂; 5 mM HEPES, pH 7.4) then gently shaken with 1.5 mg/mL collagenase (Sigma type II, Sigma-Aldrich Inc., MO) for 20min at 20–25°C. Stage V and VI oocytes were selected for microinjection. No more than four surgeries were conducted on each frog. A recovery period greater than six weeks was allowed in between surgeries (*Xenopus* protocols conform to those approved by the University of AK Fairbanks Intuitional Animal Care and Use Committee; approval number 08-71).

For expression of high- (HS) and low- (LS) sensitivity subtypes, oocytes were injected with 50 nL cRNA. Injected oocytes were incubated at 19°C for 24-72h prior to their use in voltage clamp experiments. For expression of primarily HS receptors 50 nL of a mixture containing 250 ng/ μ L of α 4 cRNA and 50 ng/ μ L of β 2 cRNA was injected (5:1 ratio of α 4 to β 2). Expression of LS receptors was achieved by injecting 50 nL of a mixture of 50 ng/ μ L α 4 cRNA and 250 ng/ μ L β 2 cRNA (1:5 ratio of α 4 to β 2). Expression of α 7 nACh was achieved by injecting 50 nL of 250 ng/ μ L of α 7 cRNA. The EC₅₀ values obtained for ACh induced currents on the HS and LS subtypes obtained from these injection ratios were verified by electrophysiology assays as

described below and found to compare well with published values for the $(\alpha_4)_2(\beta_2)_3$ (HS) and $(\alpha_4)_3(\beta_2)_2$ (LS) receptors (Zwart and Vijverberg, 1998; Moroni et al., 2006a). EC_{50} values and response profiles indicated the expression of predominantly the HS or LS receptor subtypes although it is likely that both are present in each experiment (see results section).

5.3.4 Two-Electrode Voltage Clamp.

Recordings were performed using an automated two-electrode voltage-clamp system incorporating an OC-725C oocyte clamp amplifier (Warner Instruments, Hamden, CT) coupled to a computerized data acquisition (Datapac 2000, RUN technologies, Mission Viejo, CA) and autoinjection system (Gilson, Middleton, WI). Recording and current electrodes with resistance 1–4 M Ω were filled with 3 M KCl. Details of the chambers and methodology employed for electrophysiological recordings have been described earlier (Joshi et al., 2004). Oocytes were held in a vertical flow chamber of 200 μ L volume, clamped at a holding potential of -60 mV and perfused with various ND-96 recording buffers. Three different ND-96 recording buffers were used in these experiments: **HEPES-ND96** (96 mM NaCl, 2 mM KCl, 1.8 mM CaCl₂, 1 mM MgCl₂, 5 mM HEPES); **Tris ND-96** (96 mM NaCl, 2 mM KCl, 1.8 mM CaCl₂, 1 mM MgCl₂, 5 mM Tris-HCL); **phosphate ND-96** (96 mM NaCl, 2 mM KCl, 1.8 mM CaCl₂, 1 mM MgCl₂, 2 mM phosphate). The pH for all three buffers was 7.4. Osmolarity differences between the three recording buffers were minimal based on calculated osmolarities (HEPES buffer: 214.4 mOsm, Phosphate Buffer: 212.4 mOsm, Tris buffer: 219.4 mOsm). While it is clear that osmolarity differences can affect ion channel function, all running buffers, wash solutions and test solutions containing agonists or modulators (including HEPES) were made from common stock solutions to minimize any effects on osmolality. In addition, oocytes were equilibrated in the appropriate buffer for at least seven minutes prior to exposure to agonists. To assure that observed effects were not a result of slight pH changes on addition of test compounds, the pH of every buffer and test solution was verified using a calibrated pH meter. Addition of HEPES to phosphate and Tris buffers did not alter the pH for HEPES concentrations less than 100 mM thus pH changes were not observed for most solutions. In the case of solutions containing 100 mM and 300 mM HEPES or Tris, pH decreased slightly to 7.3. The pH of these solutions were corrected to pH 7.4 using NaOH (typically >200 μ L/100 μ L of test solution of 1M NaOH). Oocytes were perfused with the different recording buffers at a rate of 20 mL/ min. Test compounds were dissolved in buffer and injected into the chamber at 20 mL/min using a Gilson auto-sampler injection system (Joshi et al., 2004).

5.3.5 Electrophysiology Dose-Response Experiments.

Dose-response curves for the endogenous nAChR agonist Acetylcholine·Cl, (ACh) (Sigma-Aldrich) were determined for both HS and LS receptors at concentrations ranging from 0.1 μ M- 3 mM in all three buffer systems. The ACh dose-response curves on α 7 nAChR were conducted at concentration ranges from 0.1 μ M - 1 mM in HEPES buffer and 0.001 μ M - 1 mM ACh in the phosphate buffer. Dose-response curves for HEPES and Tris-HCl were determined by co-application with either 10 μ M ACh (EC_{75}) for HS receptors, 100 μ M ACh (EC_{75}) for LS receptors with HEPES or Tris-HCl at concentrations ranging from 0.01 μ M – 300 mM. The α 7 nAChR dose-responses curves for HEPES were determined by co-application with 1 mM ACh for nAChR at HEPES concentrations ranging from 0.01 μ M – 300 mM. HEPES and Tris dose-response curves were performed with phosphate ND-96 as the recording buffer. The effects of dFBr on Tris inhibition was determined by co-exposure of varying concentrations of ligand co-applied with 1 μ M dFBr.

Verification of HEPES as an allosteric modulator was achieved by conducting ACh dose/response curves co-applied with 100 μ M HEPES. Zn^{2+} was confirmed as a modulator by co-applying a range of Zn^{2+} concentrations (0.001 μ M – 1 mM) with either 10 μ M ACh (high-sensitivity receptors) or 100 μ M (low-sensitivity receptors). Changes in dFBr efficacy was evaluated by dose-response curves of increasing dFBr concentrations ranging from 0.001 μ M – 100 μ M dFBr co-applied with 10 μ M ACh for high receptors or 100 μ M ACh for low-sensitivity receptors. To verify that the phosphate ND-96 buffer did not alter receptor I_{max} , a series of buffers with different phosphate concentrations (0.5 mM, 1 mM and 2 mM phosphate) were tested at the ACh I_{max} concentrations (300 μ M ACh for high-sensitivity receptors and 1 mM ACh for low-sensitivity).

In order to compare responses from different oocytes, individual responses to drug application were normalized to control responses elicited using 10 μ M ACh for HS receptors or 100 μ M ACh for low-sensitivity receptors. Data were collected from at least four replicate experiments using oocytes obtained from at least two different frogs.

5.3.6 Data Analysis and Statistics.

Dose-response curves were fit using non-linear curve fitting and GraphPad Prism Software (San Diego, CA) with standard built-in algorithms. pEC_{50} ($-\log EC_{50}$) and EC_{50} values were determined by fitting concentration/response data to a single site binding model:

$$I = \frac{b + (I_{max} - b)}{1 + 10^{(LogEC_{50} - Log[L])*nH}} \quad (1)$$

Where I is the current elicited on application of agonist, b is the baseline current in the absence of ligand, L is the ligand concentration and nH is the Hill slope. The EC_{50} value is the concentration of agonist producing currents equal to one half the maximal current (I_{max}). I_{max} values for ACh were evaluated to compare the changes in apparent efficacy as a result of co-application by HEPES, Tris, dFBr or Zn^{2+} .

Dose-response curves were fit using a non-linear curve fitting algorithm and GraphPad Prism Software (San Diego, CA). PAMs often produce bell-shaped dose-response curves with both potentiating and inhibiting phases. HEPES, dFBr and Zn^{2+} displayed this typical dose-response profile. pEC_{50} ($-\log EC_{50}$) and pIC_{50} ($-\log IC_{50}$) values were determined in these cases by simultaneously fitting both the potentiation and inhibition phases using equation 2. Similar equations have been used previously to examine bell-shaped PAM data (Harvey et al., 1999; Hsiao et al., 2001; Hsiao et al., 2006; Kim et al., 2007; Weltzin and Schulte, 2010).

$$I = I_{maxcalc} + \left(\frac{(Plateau1 - I_{maxcalc})}{1 + 10^{((LogEC_{50} - LogX) * nH_1)}} \right) + \left(\frac{(Plateau2 - I_{maxcalc})}{1 + 10^{((LogX - LogIC_{50}) * nH_2)}} \right) \quad (2)$$

I is the current elicited on application of agonist, $I_{maxcalc}$ is the calculated maximum induced current of both the potentiation and inhibition curves. *Plateau 1* is the initial current prior to addition of the modulator and *Plateau 2* is the plateau after the inhibition of the agonist response at high concentrations of the modulator. The EC_{50} value is the concentration of modulator producing currents equal to one half the calculated maximum current ($I_{maxcalc}$) during co-application with agonist. The IC_{50} is the concentration of modulator required to inhibit the response to $1/2 I_{maxcalc}$.

Equation 2 describes the sum of two Hill equations and is considered an appropriate model for two interacting binding sites (Kim et al., 2007; Weltzin and Schulte, 2010; Pandya and Yakel, 2011). This is in contrast to use of the product of Hill Equations described by Kasai et al. which is more appropriate for two independent binding sites (Kasai, 1998). Since the simultaneous action of ACh and the potentiator alter the protein conformation (channel opening) to expose a site for binding of the inhibitor (open channel block), the two processes are not independent and a summation model seems more appropriate.

Simultaneous fitting of two Hill equations can prove difficult if the EC_{50} and IC_{50} values are close together due to the inability to collect data near the value of $I_{maxcalc}$. In these cases, insufficient data is present to fully define the curve and some constants must be approximated for the fit to converge and the appropriate EC_{50} and IC_{50} values determined. In order to overcome these limitations, Hill slopes for potentiation and inhibition were typically fixed at +1 and -1 respectively unless otherwise indicated.

Despite our hypothesis of interdependence of the potentiating and inhibiting binding site, it is possible that a distinct mechanism of inhibition is present and the two binding sites may, in fact, be independent. Separate potentiating and inhibiting sites not allosterically linked as postulated by Moroni et al. (2008) for Zn²⁺ would be best fit by a multiplicative model. We thus compared curve fits using the summation model to the multiplicative model. Comparison of the two models showed that the fits were significantly ($p = 0.0192$; $F=5.679$). The summation model better fit the data and hence we used this model, consistent with our hypothesis of dependent sites, to calculate the data provided in the results section (see Results section for statistical analysis of these curve fits).

Inhibition curves were fit using non-linear curve fitting and GraphPad Prism Software (San Diego, CA) with standard built-in algorithms. pIC_{50} ($-\log EC_{50}$) values were determined by fitting concentration/response data to a log(inhibitor) verses response binding model:

$$I = Plateau2 + \left(\frac{(Plateau1 - Plateau2)}{(1 + 10^{(LogX - LogIC_{50}) * n_H})} \right) \quad (3)$$

Where I is the current elicited on application of agonist and modulator, *Plateau 1* is the current elicited by the agonist prior to addition of the inhibitor. *Plateau 2* is the current at saturating concentrations of inhibitor. The IC_{50} is the concentration of modulator that inhibits the current by $1/2 I_{max}$. In order to permit comparison of data from different oocytes, responses for all test compounds were normalized to the currents obtained with 10 μ M ACh for HS receptors and 100 μ M ACh for LS receptors.

Statistical comparisons of pEC_{50} or pIC_{50} values used an unpaired t-test with p values calculated based on the null hypothesis. One way ANOVA was used to compare I_{max} values in different ND-96 recording buffers for both high and low-sensitivity receptors.

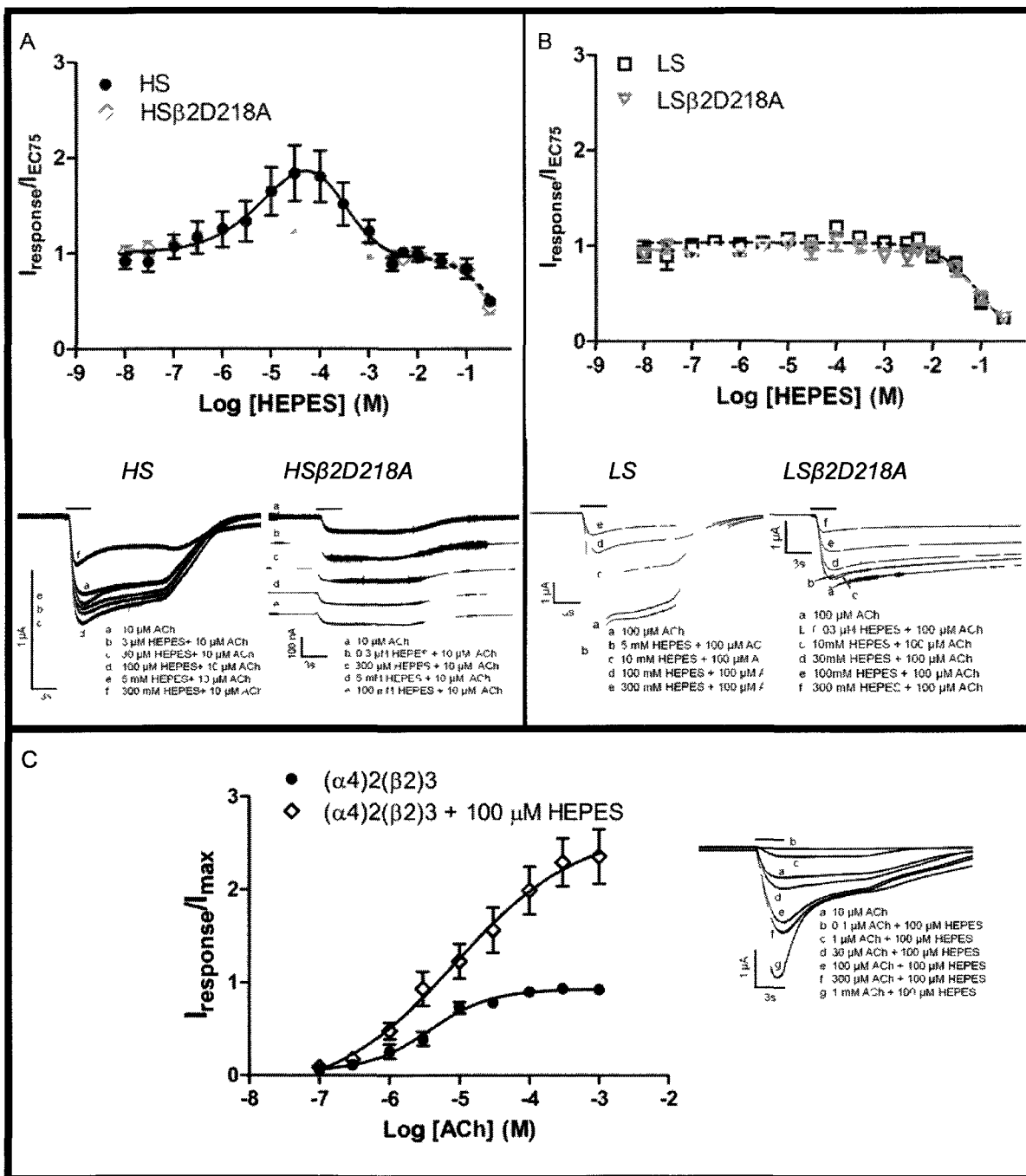
5.4 Results.

5.4.1 HEPES is an Allosteric Modulator of the High-sensitivity $\alpha 4\beta 2$ nAChR.

To explore the effects of HEPES on HS and LS preparations of $\alpha 4\beta 2$ receptors, increasing concentrations of HEPES (0.01 μM - 300 mM) were co-applied with ACh at a concentration equal to the ACh EC_{75} (10 μM for HS receptors or 100 μM for LS receptors) in a phosphate buffered ND-96 recording solution (pH 7.4) on oocytes expressing predominantly HS or LS $\alpha 4\beta 2$ stoichiometries. Test solutions were monitored for any changes in pH. No changes in pH were observed at HEPES concentrations < 100 mM. For concentrations \geq 100 mM a slight decrease to pH 7.3 was observed and the solution adjusted to pH 7.2 using NaOH as described in the methods. With co-application of < 300 μM HEPES (potentiating concentrations) and 10 μM ACh on HS receptors, the response profile showed a slight sharpening of the response peak, larger overall responses and a faster return to the baseline (Figure 5.1A – responses b-d). Application of > 300 μM HEPES and 10 μM ACh further sharpened the response peak but also decreased the overall amplitude of the response (Figure 5.1A – responses b-d). In addition a possible tail current is evident at HEPES concentrations >100 μM (Figure 5.1A, trace f), suggesting a possible open-channel block by HEPES. On LS receptors, increasing concentrations of HEPES co-applied with 100 μM ACh inhibited responses with a decrease in the overall amplitude of the response and a decrease in sharpness of the peak (Figure 5.1B – responses b-e). No significant potentiation was evident when HEPES was co-applied with ACh on LS receptors.

Figure 5.1 HEPES dose-response curves on high- and low- sensitivity receptors.

HEPES and the appropriate concentration of ACh were co-applied to *Xenopus* oocytes expressing HS (mRNA injected at a ratio of 1 α :5 β) or LS receptors (mRNA injected at a ratio of 5 α :1 β). Responses were obtained from *Xenopus* oocytes under voltage clamp conditions ($V_m = -60$ mV). The peak currents were measured and responses normalized to currents elicited by ACh applied alone to the same oocyte. Each data point represents the combined data from at least four different experiments from a minimum of two different oocytes harvested from different frogs. Error bars indicate \pm SEM. pEC_{50} , pIC_{50} , I_{max} and Hill slope (n_H) were calculated using non-linear curve fitting algorithms. Response traces were recorded from a single oocyte expressing HS and LS receptors. The solid bar above the response trace indicates the time the oocyte was exposed to HEPES and ACh (3s). The response trace scale bars is 1 μ A on the y-axis and 3s on the x-axis. **A) Top:** Co-application of HEPES and 10 μ M ACh concentration response curves on HS and HSB2D218A receptors. **Bottom:** Response traces for co-application of varying concentrations of HEPES and 10 μ M ACh on HS (*left*) and HSB2D218A (*right*) receptors. **B) Top:** Co-application of HEPES and 100 μ M ACh concentration response curves on LS and LSB2D218A receptors. **Bottom:** Response profiles for co-application of HEPES and 100 μ M ACh concentration response curves on LS (*left*) and LSB2D218A (*right*) receptors. **C) Left:** Co-application of 100 μ M HEPES and 10 μ M ACh on HS receptors. **Right:** Response traces for co-application of 100 μ M HEPES and 10 μ M ACh on HS receptors.



Bell-shaped dose-response curves were obtained when peak amplitudes from response traces were plotted against HEPES concentration (0.01 μ M- 300 mM HEPES co-applied with 10 μ M ACh on high-sensitivity receptors) (Figure 5.1A). Concentrations of HEPES < 300 μ M potentiated ACh induced currents by 180% (the calculated I_{max} was 2.7 ± 3.1). The pEC_{50} value for HEPES potentiation was 5.2 ± 0.9 ($EC_{50} = 7.1 \mu$ M). HEPES concentrations > 300 μ M produced a biphasic inhibition of the ACh induced responses. The first inhibitory phase appeared to inhibit only the HEPES potentiated portion of the response and plateaued at 1.0 (the normalized, unpotentiated response amplitude using 10 μ M ACh). A second phase inhibited the response amplitude below 1.0. The pIC_{50} value for the first inhibitory phase was 3.4 ± 0.4 ($IC_{50} = 430 \mu$ M) (Figure 5.1A) while the pIC_{50} of the second inhibitory phase was estimated to be 0.4 ± 0.8 ($IC_{50} \sim 420$ mM). The second inhibitory component of HEPES inhibition on HS receptors was fit using equation 3 and the curve is indicated by a black, dashed line in Figure 5.1A to distinguish it from the separate bell-shaped curve used to fit dose-response data for HEPES concentrations less than 3 mM. On LS receptors, HEPES produced only a single phase inhibitory response with a $pIC_{50} = 1.0 \pm 0.2$ ($IC_{50} = 90$ mM) (Figure 5.1B). This is similar to data from previous studies which determined the HEPES dissociation rate to be 100 mM on the AChBP, a structural homolog of nAChRs (Brejc et al., 2001). Coincidentally, minimal net effects of HEPES are seen at concentrations between 5 - 10 mM (typical concentration in HEPES recording buffers). This may be one reason why the functional effects of HEPES potentiation have gone unobserved for so many years. Comparison of data from oocytes expressing predominantly LS and HS receptors suggest that HEPES selectively potentiates the HS population compared to the LS stoichiometry. The application of HEPES alone to $\alpha 4\beta 2$ nAChR expressing oocytes produced no induced current (data not shown).

HEPES positive modulation was further investigated by applying the maximum potentiating concentration of HEPES (100 μ M) over a range of ACh concentrations (0.1 μ M – 1 mM) to the HS preparation. The response profiles displayed overall larger responses and sharper response peaks compared to those obtained by exposure to ACh alone (Figure 5.1C). Results show no significant change in pEC_{50} values for stimulation by ACh in the presence of 100 μ M HEPES ($p = 0.1687$). In the absence of HEPES, the pEC_{50} for ACh stimulation was 5.4 ± 0.1 ($EC_{50} = 3.7 \mu$ M). In the presence of 100 μ M HEPES the pEC_{50} was 5.1 ± 0.3 ($EC_{50} = 8.6 \mu$ M). Application of 100 μ M HEPES produced a 285% potentiation of the ACh induced I_{max} currents (Figure 5.1C). The Hill slope for ACh stimulation appeared to decrease with application of 100 μ M HEPES (from 0.97 ± 0.11 to 0.49 ± 0.25), but differences were not significant ($p=0.1773$).

Based on the observation that HEPES selectively potentiates receptors in the HS preparation (presumably due to high expression levels of the HS stoichiometry), it appears that

allosteric modulation by HEPES may be HS specific. Comparison of the HS and LS $\alpha 4\beta 2$ nAChRs reveals that the high-sensitivity subtype ($(\alpha 4)_2(\beta 2)_3$) may contain a $\beta +/\beta -$ interface which is not present in the low-sensitivity subtype ($(\alpha 4)_3(\beta 2)_2$). In contrast, the LS receptors contains an $\alpha +/\alpha -$ interface which may not be present in the HS receptor. Both receptor stoichiometries contain $\beta +/\alpha -$ interfaces. Since potentiation by HEPES was only seen in oocytes expressing HS receptors, we hypothesized that the $\beta +/\beta -$ interface likely contains the binding site involved in HEPES potentiation. As determined from bell-shaped dose-response curves, the EC_{50} for HEPES potentiation at this site is approximately 7.1 μM (see section above results). By comparing the sequence of AChBP and the $\beta 2$ subunit, we hypothesized that HEPES potentiation of ACh responses could involve unique residues found in an allosteric binding cleft in a region comparable to the orthosteric binding site for ACh. Two cysteine residues located in the C-loop of the orthosteric site (C187 and C188, AChBP numbering) of the AChBP and α nAChR subunits are involved in ligand binding. We hypothesized that the C-loop on the principal face of the $\beta 2$ subunit might form an allosteric binding domain for HEPES. In particular, one of the two vicinal aspartates found in the C-loop (D218) on the principal face of the $\beta 2$ subunit ($\beta 2+$) may contribute to HEPES- interactions ($\beta 2$ numbering; D188 in the AChBP sequence. Amino acids are numbered from the initial methionine of the unprocessed subunit. To find the amino acid position in the mature form subtract 30 residues from the number for $\alpha 4$ and 25 residues for $\beta 2$ (Moroni et al., 2008). The D218 residue described here is in the identical position to that hypothesized by Moroni to form part of the Zn^{2+} inhibitory binding site (Moroni et al., 2008).

To examine the possibility that the $\beta +$ face may be involved in HEPES binding, a alanine mutation of $\beta 2D218$ was constructed and injected into oocytes with a 1:5 or 5:1 ratio of $\alpha 4$: $\beta 2D218A$ mRNA (Figure 5.1 A and B, right panels). For the HS preparation, $\beta 2D218A$ responses obtained by application of ACh alone showed similar response kinetics compared to wild-type receptors but the induced current in mutated receptors was much smaller than wild-type receptors. This observation may suggest that some alteration in receptor function, conductance and/or expression may be occurring with $\beta 2D218A$ receptors (Figure 5.1A, bottom. Right and left set of responses, trace a). Dose-response curves for ACh stimulation of oocytes expressing HS $\beta 2D218A$ receptors produced an EC_{50} value of 2.1 μM (Figure 5.2C and Table 5.1). This was similar to that obtained for wild-type (3.7 μM) receptors with the identical injection ratio (1:5). The Hill slopes were also similar for HS wild-type receptors (1.0 ± 0.2) and HS $\beta 2D218A$ receptors (0.9 ± 0.3). These results indicate that the 1:5 injection ratio $\beta 2D218A$ receptors are likely assembling similar to the HS wild-type receptors and are predominantly HS receptors with a presumed stoichiometry of $(\alpha 4)_2(\beta 2D218A)_3$.

For oocytes injected with a 5:1 ratio of $\alpha 4:\beta 2D218A$, ACh alone response amplitudes appeared to decrease with a loss of the sharp response peak and altered desensitization (Figure 5.1B, bottom, right and left set of response traces, trace a). Results of the $\beta 2D218A$ LS dose-response curves for ACh stimulation produced an EC_{50} value of 58 μM , similar to those obtained for wild-type receptors with the 5:1 injection ratio (32 μM) (Figure 5.2D and Table 5.1). The Hill slopes were also similar for the LS wild-type (1.2 ± 0.2) and $\beta 2D218A$ receptors (0.8 ± 0.2) (Figure 5.2 and Table 5.1). These results suggests that the 5:1 injection ratio $\beta 2D218A$ receptors assembled similar to wild-type receptors with the presumed $(\alpha 4)_3(\beta 2D218A)_2$ LS stoichiometry. Modified response kinetics suggests the $\beta 2D218A$ mutation alters receptor function, conductance and/or expression.

We evaluated the effects of HEPES on HS and LS $\beta 2D218A$ nAChRs preparations. Oocytes injected with either a 1:5 or 5:1 ratio of $\alpha 4:\beta 2D218A$ mRNA were exposed to increasing concentrations of HEPES (0.001 μM -300 mM) and ACh (10 μM the 1:5 ratio or 100 μM for the 5:1 ratio) in phosphate buffered ND-96 recording solution. In contrast to wild-type receptors, the $\beta 2D218A$ mutant abolished HEPES potentiation in the HS preparation (Figure 5.1A, dose-response curve). Inhibition by HEPES at high concentrations (> 3 mM) was evident in both HS and LS preparations of $\beta 2D218A$ receptors and was similar to that observed for wild-type receptors. For HS $\beta 2D218A$ receptors, HEPES inhibited ACh responses with a calculated $pIC_{50} = 0.23 \pm 0.7$ ($IC_{50} = 590$ mM). For LS $\beta 2D218A$ receptors the pIC_{50} for inhibition of ACh responses was 0.78 ± 0.23 ($IC_{50} = 170$ mM). These data are not statistically different from the inhibition observed on wild-type receptors at high concentrations of HEPES ($p = 0.9144$ for HS and $p = 0.4304$ for LS receptors).

The differences in response profiles on both the HS and LS $\beta 2D218A$ receptors compared to wild-type receptors suggest that the $\beta 2D218$ residue may play a role in receptor function. However, the eradication of HEPES potentiation by this mutation suggests that the binding site for HEPES potentiation involves D218 on the $\beta 2+$ face.

5.4.2 Minimal Changes Were Observed in ACh Dose-Response Curves When HEPES and Phosphate ND-96 Recording Buffers.

To ensure that the effects seen with HEPES buffer were not attributable to the presence of phosphate in the phosphate buffered ND-96, ACh dose-response curves were compared on high and low-sensitivity receptors in both HEPES and phosphate containing buffers (Figure 5.2). Responses to ACh on the high-sensitivity oocyte preparation appeared similar in both phosphate and HEPES buffer. Different amplitudes can be observed in the responses shown in Figure 5.2 (A

and C) but these can be attributed to different expression levels in the different oocytes tested. For LS preparations, slight variations in response characteristics were observed mostly with respect to the sharpness of the peak response at higher ACh concentrations (Figure 5.2, B and D).

Figure 5.2 ACh dose-response curves in HEPES and phosphate ND-96 recording buffer.

Xenopus oocytes expressing high-sensitivity $\alpha 4\beta 2$ nAChR (HS) (mRNA injected at a ratio of 1 α :5 β) or low-sensitivity receptors (LS) (mRNA injected at a ratio of 5 α :1 β) were exposed to increasing concentrations of ACh in HEPES (**A and B**) or Phosphate (**C and D**) recording buffer. Individual peak amplitudes were normalized to the I_{\max} on the same oocyte. Response traces were recorded from a single oocyte expressing HS and LS receptors. The solid bar above the response trace indicates the time the oocyte was exposed to varying concentrations of ACh. pEC_{50} and n_H values (see table 5.1) were determined using non-linear curve fitting as described in the methods. Data points represent at least 4 replicate values obtained from a minimum of two oocytes harvested from different frogs. Error bars indicate \pm SEM.

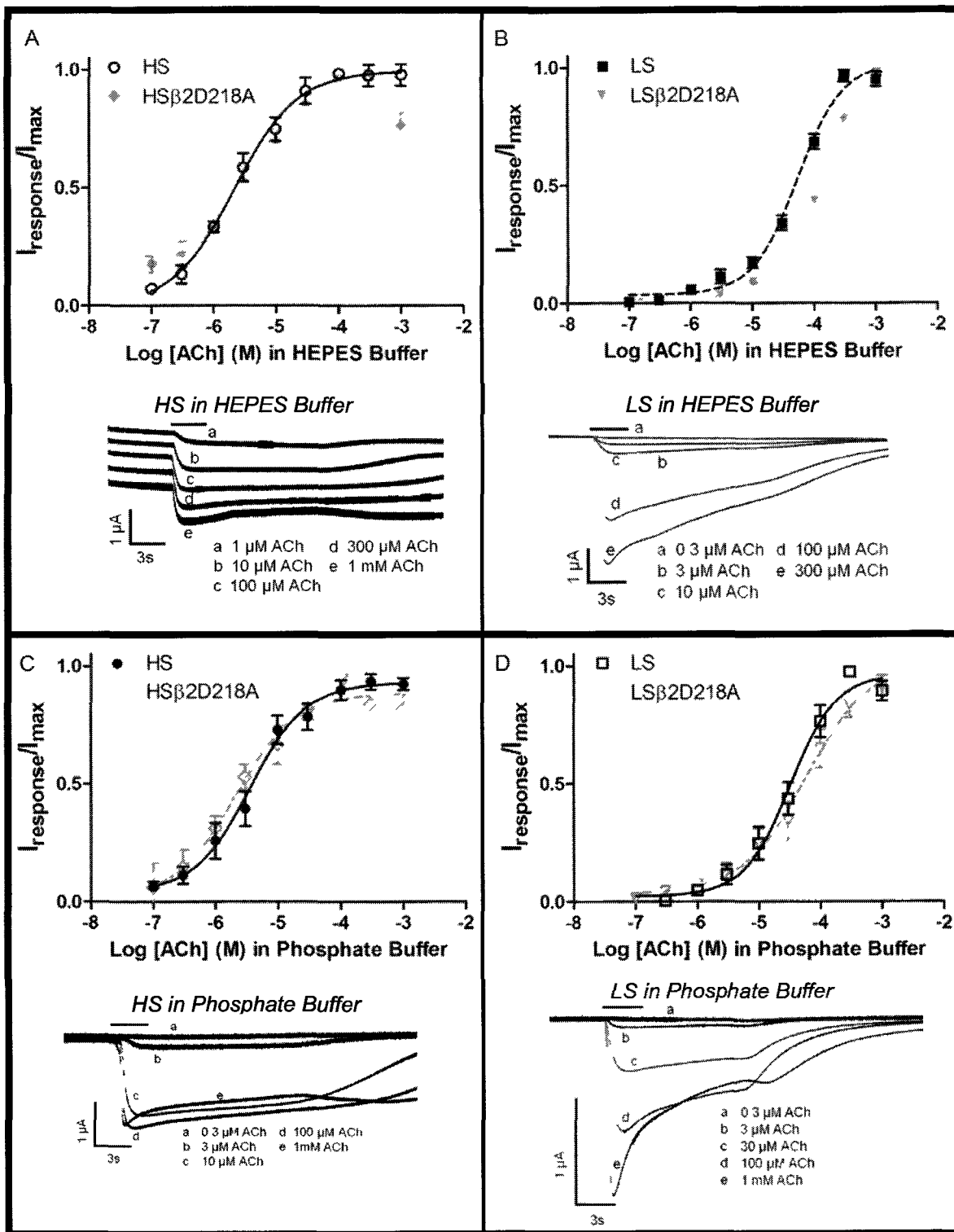


Table 5.1. Summary of the calculated results determined from ACh dose-response curves in HEPES and phosphate ND-96 recording buffer.

Receptor	Buffer	pEC ₅₀ ± SEM (EC ₅₀ μM)	nH ± SEM
HS	HEPES	5.7 ± 0.1 (2.2)	0.9 ± 0.2
HSβ2D218A	HEPES	5.5 ± 0.1 (3.5)	1.1 ± 0.3
LS	HEPES	4.3 ± 0.1 (54)	1.2 ± 0.1
LSβ2D218A	HEPES	3.83 ± 0.04 (150)	1.0 ± 0.1
HS	Phosphate	5.4 ± 0.1 (3.7)	1.0 ± 0.2
HSβ2D218A	Phosphate	5.7 ± 0.2 (2.1)	0.9 ± 0.3
LS	Phosphate	4.5 ± 0.1 (32)	1.2 ± 0.2
LSβ2D218A	Phosphate	4.2 ± 0.2 (58)	0.8 ± 0.2

ACh dose-response curves determined from peak currents showed no effect of buffer composition on ACh pEC₅₀ ($p = 0.2365$) and Hill slope ($p = 0.7478$) for HS receptors (Figure 5.2A and C, and Table 5.1). A slight, but significant change in pEC₅₀ for ACh stimulation was observed for LS receptors ($p = 0.0277$) although there was no significant change in Hill slopes ($p = 0.9162$) (Figure 5.2B and D, and Table 5.1). Mutation of β2D218 to alanine had no effect on ACh pEC₅₀ values for HS receptors in either phosphate or HEPES buffers (Figure 5.2 A and C, and Table 5.1) ($p = 0.3891$). For LS receptors, the pEC₅₀ values for ACh stimulation were significantly different in both phosphate and HEPES buffer ($p = 0.0246$) (Figure 5.2 B and D, and Table 5.1). The Hill slopes for ACh stimulation of the β2D218A HS and LS receptors in either the HEPES or phosphate buffers were not significantly different (HS receptors $p = 0.6733$; LS receptors $p = 0.3760$) (Figure 5.2 and Table 5.1).

As seen in Figure 5.2, the phosphate buffered ND-96 had minimal or no effect on ACh EC_{50} values for either receptor preparation. To further evaluate possible effects of the phosphate buffer, I_{max} values obtained at saturating concentrations of ACh in different concentrations of phosphate buffer were determined. Varying concentrations of phosphate buffer ranging from 0.5 mM to 2 mM were used to prepare phosphate ND-96 recording solutions. The pH for each recording buffer was 7.4. The I_{max} currents induced by ACh for each stoichiometry (300 μ M and 1 mM for HS and LS receptors respectively) were measured for each phosphate buffer. Each phosphate concentration course was run on the same oocyte. Alterations in the ACh induced current in different buffers containing different concentrations of phosphate would indicate interactions of phosphate with the receptors and/or ligands. We saw no change in the ACh induced I_{max} current for any concentration of phosphate buffer between the HS (ANOVA $p = 0.6751$) and LS (ANOVA $p = 0.8921$) $\alpha 4\beta 2$ receptors (results not shown). No induced responses were seen with application of different phosphate solutions when applied alone (without agonist). These data show no apparent effect of the phosphate buffer on $\alpha 4\beta 2$ receptors making it a good choice for evaluation of $\alpha 4\beta 2$ receptor function.

5.4.3 Tris Buffer

As a result of our discovery that HEPES modulates $\alpha 4\beta 2$ nAChR function, we also considered whether or not the commonly used Tris buffer had any effect on $\alpha 4\beta 2$ receptors. Like HEPES, Tris is a polar molecule that is a member of the family of Good's buffers and is used as a physiological buffering agent. We examined the effect of Tris on ACh induced responses on HS and LS subtypes of the $\alpha 4\beta 2$ nAChR. Increasing concentrations of Tris (0.01 μ M - 300 mM) were co-applied with either 10 μ M or 100 μ M ACh to HS and LS oocytes preparations using a phosphate ND-96 recording buffer. We found that Tris inhibits both HS ($pIC_{50} = 2.0 \pm 0.1$; $IC_{50} = 10$ mM) and LS $\alpha 4\beta 2$ nAChRs ($pIC_{50} = 2.2 \pm 0.1$; $IC_{50} = 6.8$ mM) (Figure 5.3). The pIC_{50} values were not significantly different from each other ($p = 0.2590$).

To examine possible effects of Tris buffer on a high efficacious PAM, we used the $\alpha 4\beta 2$ selective compound desformylflustrabromine (dFBr) (Sala et al., 2005; Kim et al., 2007). dFBr was co-applied with ACh and Tris in phosphate buffered ND-96 recording solution. Potentiation of Tris and ACh induced responses by 1 μ M dFBr did not significantly change the Tris pIC_{50} of high-sensitivity receptors ($pIC_{50} = 2.2 \pm 0.1$; $IC_{50} = 6.8$ mM) ($p = 0.3422$) (Figure 5.3A). For LS receptors, pIC_{50} values with and without 1 μ M dFBr ($pIC_{50} = 1.3 \pm 0.2$; $IC_{50} = 47$ mM) were significantly different from each other (Figure 5.3B). dFBr produced potentiation of ~360% when co-applied with 10 μ M ACh and Tris (Tris concentrations < 300 μ M) on HS receptors (Figure 5.3A). On the HS receptors, co-application of 1 μ M dFBr, Tris (Tris concentrations < 1000 μ M)

and ACh produced responses potentiated by 280% compared to Tris and ACh alone (Figure 5.3B). dFBr potentiation was reduced by ~50% at Tris concentrations > 1 mM on HS receptors and > 30 mM on LS nAChRs. Application of Tris alone did not induce currents. Given that Tris did inhibit ACh induced currents on HS receptors at concentrations greater than 1 mM and inhibited dFBr potentiation by ~50% at Tris concentrations >1 mM, we found Tris to be an inadequate buffer agent.

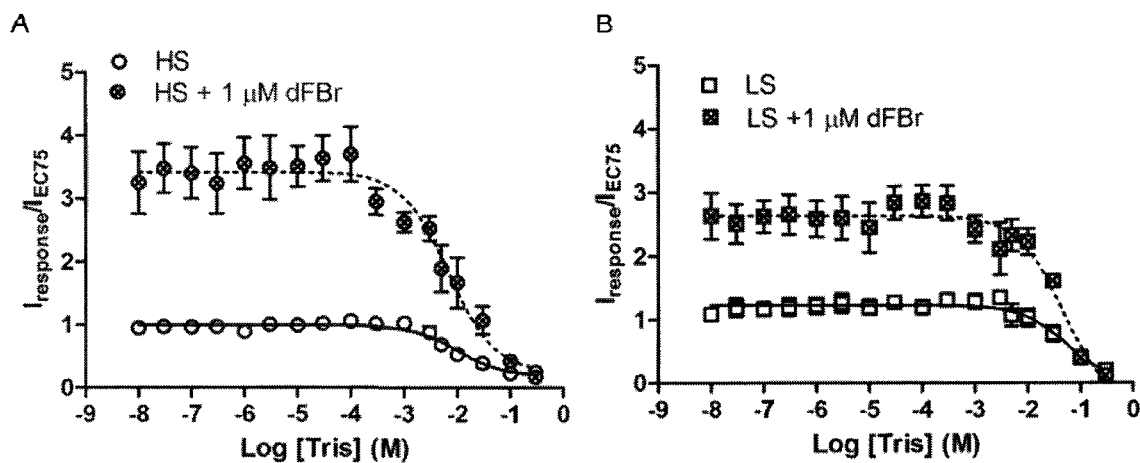


Figure 5.3 Tris concentration response curves for co-application of ACh and 1 μM dFBr on high- (HS) and low- (LS) sensitivity $\alpha 4\beta 2$ receptors.

Xenopus oocytes expressing HS (mRNA injected at a ratio of 1 α :5 β) or LS (mRNA injected at a ratio of 5 α :1 β) receptors were exposed to increasing concentrations of Tris and ACh (at concentrations equal to the EC_{75}). Responses were potentiated with 1 μM of the high efficacious allosteric modulator desformylflustrabromine (dFBr). Individual peak amplitudes were normalized to those elicited by the identical concentration of ACh alone on the same oocyte. pEC_{50} , pIC_{50} and n_H values were determined using non-linear curve fitting as described in the methods. Data points represent at least 4 replicate values obtained from a minimum of two oocytes harvested from different frogs. Error bars indicate \pm SEM.

5.4.4 The $\alpha 7$ nAChR is Unaffected by HEPES.

The $\alpha 7$ nAChR is one of the most common nAChRs found in the central nervous system. The expression of $\alpha 7$ nAChRs are altered in many neurological disorders including Alzheimer's disease and Schizophrenia (Levin and Rezvani, 2007). The effects we observed on $\alpha 4\beta 2$ stoichiometries led us to investigate possible interactions of HEPES's with the $\alpha 7$ nAChR subtype. ACh dose-response curves were determined from peak currents obtained from oocytes expressing $\alpha 7$ receptors in either HEPES or phosphate ND-96 recording buffers (Figure 5.4A). For ACh stimulation, pEC_{50} values were identical in both HEPES and phosphate buffers (HEPES:

$pEC_{50} = 3.8 \pm 0.1$; $EC_{50} = 146 \mu\text{M}$. Phosphate buffer: $pEC_{50} = 3.8 \pm 0.1$; $EC_{50} = 177 \mu\text{M}$ ($p = 0.5893$). The Hill slopes were 1.1 ± 0.2 and 0.79 ± 0.13 for the HEPES and phosphate recording buffers respectively ($p = 0.2061$).

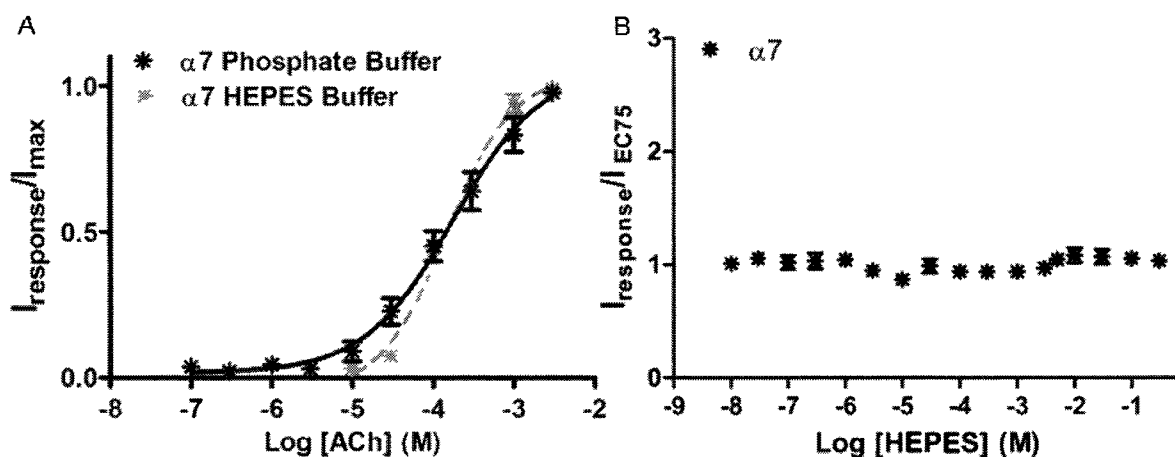


Figure 5.4 $\alpha 7$ ACh dose-response curves obtained using HEPES or phosphate ND-96 recording buffers.

Xenopus oocytes expressing $\alpha 7$ receptors were exposed to increasing concentrations of ACh in HEPES or phosphate recording buffer (A). Individual peak amplitudes were normalized to the I_{max} on the same oocyte. pEC_{50} and n_H values were determined using non-linear curve fitting as described in the methods. B) Increasing concentrations of HEPES co-applied with 1 mM ACh on $\alpha 7$ receptors. Responses were normalized to 1 mM ACh in both the HEPES and phosphate buffer. Data points represent at least 4 replicate values obtained from a minimum of two oocytes harvested from different frogs. Error bars indicate \pm SEM.

To investigate the effects of HEPES on the $\alpha 7$ nAChR, we co-applied varying concentrations of HEPES (0.01 μM - 300 mM) with 1 mM ACh (ACh EC_{75}) to oocytes expressing $\alpha 7$ receptors. Unlike $\alpha 4\beta 2$ stoichiometries, HEPES showed no effect on $\alpha 7$ receptors. Figure 5.4B shows no potentiation or inhibition of responses induced by 1 mM ACh for HEPES concentrations up to 300 mM. This is further evidence of the selectivity of HEPES potentiation to HS $\alpha 4\beta 2$ receptors.

5.4.5 HEPES Effects Other PAM Interactions with $\alpha 4\beta 2$ nAChR.

In light of our study showing that HEPES modulates $\alpha 4\beta 2$ nAChR, we hypothesized that HEPES may have altered the results of previous studies using other modulators. We investigated the possible differences in observed effects of the previously tested $\alpha 4\beta 2$ PAMs desformylflustrabromine and Zn^{2+} using both HEPES and phosphate ND-96 recording buffers.

5.4.5.1 Desformylflustrabromine Modulation of High- and Low-sensitivity $\alpha 4\beta 2$ Receptors in HEPES ND-96 Recording Buffer.

Desformylflustrabromine (dFBr) is novel PAM that potentiates ACh induced currents of $\alpha 4\beta 2$ nAChR by 265% at concentrations $< 10 \mu\text{M}$ and inhibits at concentrations $> 10 \mu\text{M}$ (Sala et al., 2005; Kim et al., 2007; Weltzin and Schulte, 2010a). This compound appears to potentiate $\alpha 4\beta 2$ nAChRs by shifting the equilibrium between open and desensitized conformations (Weltzin and Schulte, 2010a). Inhibition caused by application of high concentrations of dFBr has been shown to be the result of open channel block (Weltzin and Schulte, 2010a). These experiments were conducted using a 5 mM HEPES- ND-96 recording buffer. Given the current findings it is possible that the results found with dFBr have been altered by the presences of HEPES.

Differences in dFBr potentiation of ACh induced responses on HS and LS $\alpha 4\beta 2$ nAChR in a HEPES and phosphate buffered ND-96 recording solution were investigated. A range of dFBr concentrations (0.001 μM - 100 μM) were co-applied with either 10 μM or 100 μM ACh on oocytes expressing HS and LS $\alpha 4\beta 2$ nAChRs respectively. Both receptor types were potentiated by dFBr. Results showed that in HEPES ND-96 recording buffer, the pEC_{50} values for dFBr on the two receptor types were not significantly different ($p = 0.4040$) (Figure 5.5 A and Table 5.2).

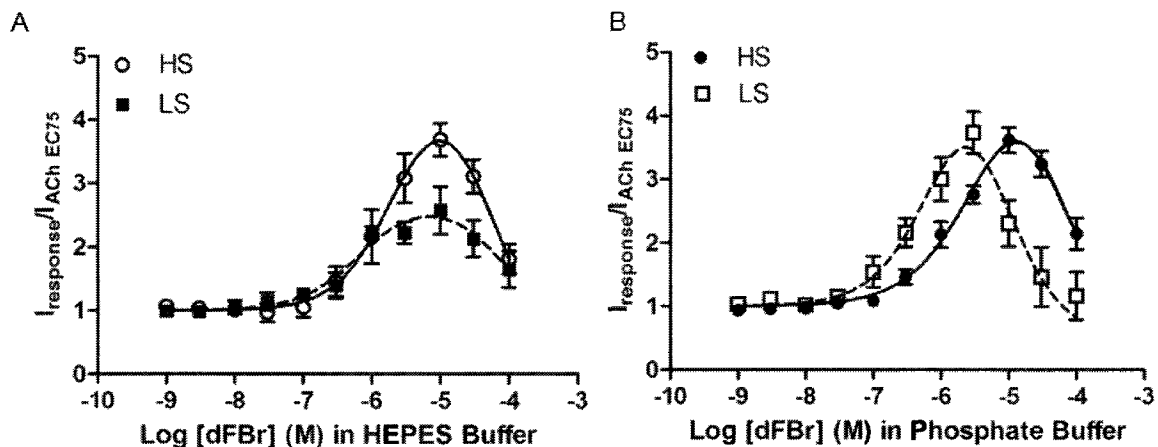


Figure 5.5 dFBr concentration responses curves for high- (HS) and low- (LS) sensitivity $\alpha 4\beta 2$ nAChR obtained using HEPES or phosphate ND-96 buffers.

Responses were obtained from *Xenopus* oocytes under voltage clamp conditions ($V_m = -60$ mV). *Xenopus* oocytes expressed either HS (mRNA injected at a ratio of $1\alpha:5\beta$) or LS (mRNA injected at a ratio of $5\alpha:1\beta$) receptors. **A)** Dose-response curves obtained from co-application of dFBr and ACh (concentration equal to the ACh EC_{75}) on HS and LS $\alpha 4\beta 2$ nAChR in HEPES buffer. **B)** Dose-response curves obtained from co-application of dFBr and ACh (concentration equal to the ACh EC_{75}) on HS and LS $\alpha 4\beta 2$ nAChR in phosphate recording buffer. Individual peak amplitudes were normalized to the response obtained using an identical concentration of ACh alone (equal to the ACh EC_{75}). pEC_{50} , pIC_{50} and n_H values (see Table 5.2) were determined using non-linear curve fitting as described in the methods. Data points represent at least 4 replicate values obtained from a minimum of two oocytes harvested from different frogs. Error bars indicate \pm SEM.

Table 5.2. Summary of calculated results from dFBr concentration responses curves for high- (HS) and low- (LS) sensitivity $\alpha 4\beta 2$ nAChR obtained using HEPES or phosphate ND-96 buffers.

Receptor	Buffer	pEC ₅₀ (EC ₅₀ μ M)	I _{max}	pIC ₅₀ (IC ₅₀ μ M)
HS	HEPES	5.6 \pm 0.5 (2.5)	370%	4.3 \pm 0.8 (50)
LS	HEPES	6.2 \pm 0.4 (0.63)	260%	4.0 \pm 1.3 (100)
HS	Phosphate	5.5 \pm 0.3 (3.2)	360%	4.1 \pm 0.1 (79)
LS	Phosphate	5.9 \pm 1.1 (1.3)	370%	5.2 \pm 0.6 (6.3)

The amount of potentiation produced by dFBr on the ACh induced currents using a HEPES ND-96 recording buffer was greater on the HS receptors compared to the LS stoichiometry. The LS receptors were potentiated 260% while the HS receptors were potentiated by 370%. This finding suggest that either; 1) dFBr has a higher efficacy on the HS receptor; 2) The potentiating effects of HEPES and dFBr produce an additive effect on the HS stoichiometry; or 3) competition between HEPES and dFBr is causing a reduction in the apparent efficacy on the LS stoichiometry.

dFBr Modulation of High- and Low-sensitivity $\alpha 4\beta 2$ Receptors in Phosphate ND-96 Recording Buffer.

To evaluate possible differences of dFBr-receptor interactions without the conflicting actions of HEPES, dFBr dose-response curves were performed in a phosphate buffered ND-96 recording solution. Varying concentrations of dFBr (0.001 μ M - 100 μ M) were co-applied with either 10 μ M or 100 μ M ACh on oocytes expressing HS or LS receptors. Results showed that the amount of dFBr potentiation of ACh induced responses using phosphate buffer was similar for HS (360%) and LS (370%) receptors (Figure 5.5B and Table 5.2). The pEC₅₀ values for dFBr potentiation were also not significantly different between HS and LS receptors tested in phosphate buffered ND-96 (Figure 5.5B and Table 5.2) ($p = 0.6362$). The pEC₅₀ values for dFBr

potentiation of HS ($p = 0.7459$) and LS ($p = 0.8377$) nAChRs were also not significantly different from those determined in HEPES ND-96 recording buffer although the degree of potentiation of HS receptors by dFBr was decreased in HEPES relative to phosphate buffer (Figure 5.5 and Table 5.2).

No significant difference in pIC_{50} values were observed for inhibition of ACh induced currents by application of high ($> 10 \mu\text{M}$) dFBr concentrations using either HEPES or phosphate buffer on HS or LS receptors (HS, $p = 0.7683$); LS, $p = 0.4040$) (Figure 5.5 A and B and Table 5.2). In addition no change was observed in dFBr pIC_{50} values for HS or LS receptors in HEPES buffer ($p = 0.8485$). An increase in the pIC_{50} value on the LS receptors was seen compared to the HS receptor in phosphate buffered ND-96 ($p = 0.0435$) (Figure 5.5B and Table 5.2).

5.4.5.2 Zn^{2+} Modulation of Low and High-sensitivity $\alpha 4\beta 2$ Receptors in HEPES ND-96 Recording Buffer.

Zn^{2+} has been reported to be a selective LS receptor PAM and an allosteric inhibitor of HS receptors (Hsiao et al., 2001; Hsiao et al., 2006; Moroni et al., 2008). Based on data showing decreased inhibition of HS $\beta 2D218A$ receptors by Zn^{2+} and enhanced potentiation of LS $\beta 2D218A$ receptors, Moroni et al., (2008) have suggested that Zn^{2+} inhibits $\alpha 4\beta 2$ receptors by binding to an allosteric inhibitory site at the $\beta +/\alpha -$ interface. Thus $\beta 2D218$ is apparently involved with binding of Zn^{2+} . Mutation of a $\alpha 4H195$, located on the – face of the α subunit, abolished potentiation of the LS receptor by Zn^{2+} . In combination with the apparent selective potentiation of the LS receptor, this suggested that the potentiation site was located at the $\alpha +/\alpha -$ interface on the LS stoichiometry. These experiments and others have used a 10 mM HEPES ND-96 recording solution to study the modulation of nAChRs by Zn^{2+} (Hsiao et al., 2001; Hsiao et al., 2006; Moroni et al., 2008). As for dFBr above, we re-evaluated Zn^{2+} modulation in non HEPES containing buffers to determine if HEPES might have altered the results of these studies.

In a HEPES ND-96 recording buffer, dose-response curves resulting from co-application of Zn^{2+} (0.001 μM -1 mM) and 10 μM ACh on HS nAChRs produced inhibition of ACh induced currents (Figure 5.6A and Table 5.3). Mutation of $\beta 2D218A$ of this receptor produced a significant 1.3 fold decrease in the pIC_{50} value for Zn^{2+} inhibition (Figure 5.6A and Table 5.3) ($p = 0.0362$). These results are consistent with previous results of Moroni et al. (2008) and appear to suggest that residue $\beta 2D218A$ is involved in Zn^{2+} inhibition on the HS $\alpha 4\beta 2$ receptor.

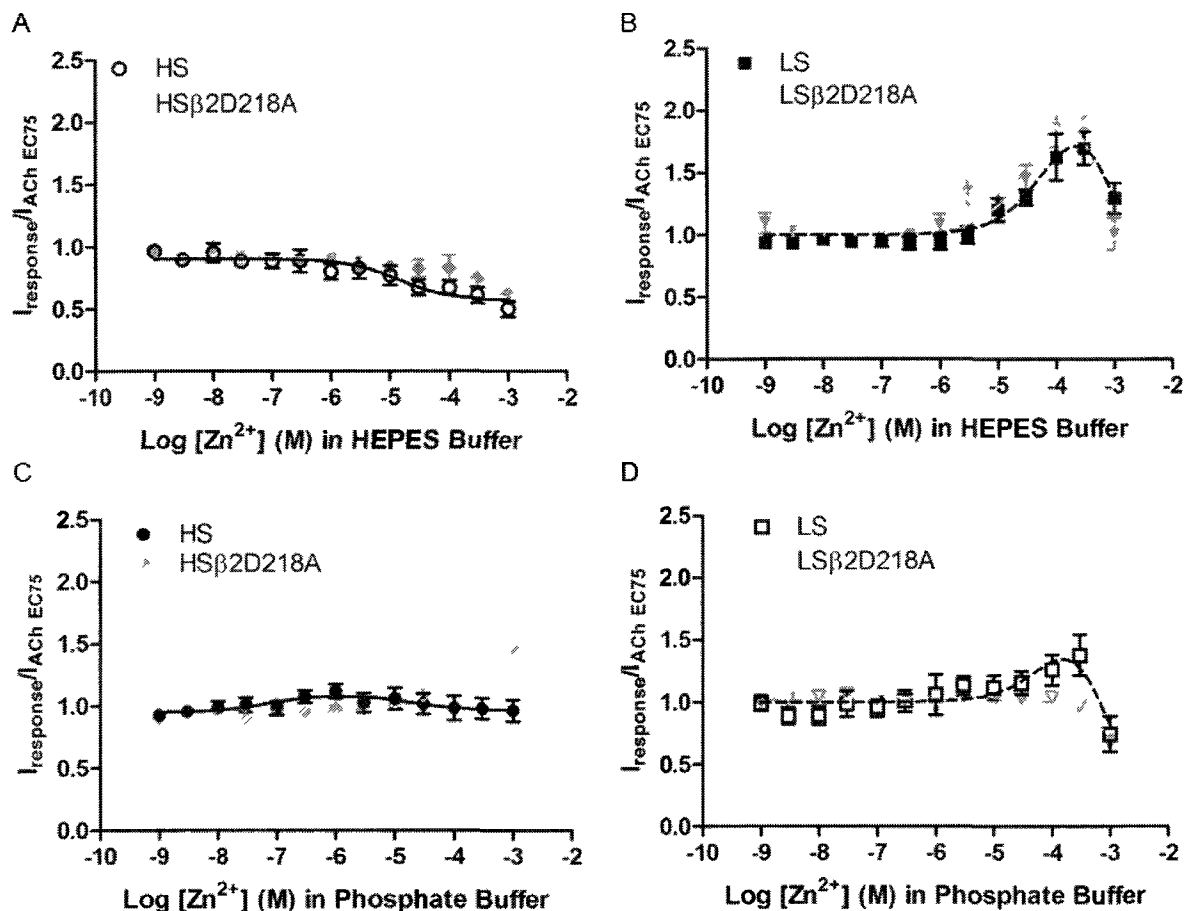


Figure 5.6 Zn^{2+} concentration response curve obtained by co-application of Zn^{2+} and ACh on high- (HS) and low- (LS) sensitivity $\alpha 4\beta 2$ nAChR using HEPES or phosphate ND-96 buffer.

Responses were obtained from *Xenopus* oocytes under voltage clamp conditions ($V_m = -60$ mV) using *Xenopus* oocytes expressed either HS (mRNA injected at a ratio of $1\alpha:5\beta$) or LS (mRNA injected at a ratio of $5\alpha:1\beta$) receptors. **A)** Dose-response curves resulting from co-application of Zn^{2+} and ACh (EC_{75} concentration) on HS and HS β 2D218A receptors in HEPES buffer. **B)** Dose-response curves resulting from co-application of Zn^{2+} and ACh (EC_{75} concentration) on LS and LS β 2D218A receptors in HEPES buffer. **C)** Dose-response curves resulting from co-application of Zn^{2+} and ACh (EC_{75} concentration) on HS and HS β 2D218A receptors in phosphate recording buffer. **D)** Dose-response curves resulting from co-application of Zn^{2+} and ACh (EC_{75} concentration) on LS and LS β 2D218A receptors in phosphate recording buffer. Individual peak amplitudes were normalized to those obtained using a concentration of ACh equal to the ACh EC_{75} on the same oocyte. pEC_{50} , pIC_{50} and n_H values (see Table 5.3) were determined using non-linear curve fitting as described in the methods. Data points represent at least 4 replicate values obtained from a minimum of two oocytes harvested from different frogs. Error bars indicate \pm SEM.

Table 5.3. Summary of calculated results from Zn²⁺ concentration responses curve obtained by co-application of Zn²⁺ and ACh on high- (HS) and low- (LS) sensitivity α 4 β 2 nAChR using HEPES or phosphate ND-96 buffer.

Receptor	Buffer	pEC ₅₀ ± SEM (EC ₅₀ μM)	I _{max}	pIC ₅₀ ± SEM (IC ₅₀ μM)
HS	HEPES	-	-	4.9 ± 0.3 (13)
HSβ2D218A	HEPES	-	-	3.6 ± 0.5 (250)
LS	HEPES	4.0 ± 0.7 (100)	170%	2.9 ± 2.7 (1260)
LSβ2D218A	HEPES	4.2 ± 0.4 (63)	190%	3.2 ± 0.6 (630)
HS	Phosphate	7.1 ± 0.9 (0.079)	110%	4.7 ± 1.1 (20)
HSβ2D218A	Phosphate	3.6 ± 0.5 (250)	-	-
LS	Phosphate	3.8 ± 0.8 (160)	140%	3.2 ± 1.7 (630)
LSβ2D218A	Phosphate	-	0%	2.6 ± 0.6 (2500)

Co-application of Zn²⁺ (0.001 μM – 1 mM) and 100 μM ACh in HEPES ND-96 recording solution on the HS receptor produced a bell-shaped dose-response curve (Figure 5.6B). Zn²⁺ potentiated ACh induced responses at concentrations ≤ 300 μM. Zn²⁺ concentrations ≥ 300 μM inhibited ACh induced currents. On oocytes expressing LSβ2D218A receptors, dose-response curves resulting from co-application of Zn²⁺ (0.001 μM - 1 mM) and 100 μM ACh in the HEPES ND-96 recording buffer showed no significant differences in the pEC₅₀ (p = 0.8896) or pIC₅₀ (p = 0.9054) when compared to wild-type LS receptors (Figure 5.6B and Table 5.3). The I_{max} appears to increase from 170% to 190% with the mutant, consistent with previous results (Moroni et al., 2008). The increase in Zn²⁺ potentiation observed with the β2D218A is not likely explained by shifts in the ACh dose-response curve.

5.4.5.3 Zn^{2+} Modulation of High- and Low-sensitivity $\alpha\beta 2$ Receptors in Phosphate ND-96 Recording Buffer.

In phosphate ND-96 buffer, co-application of Zn^{2+} and 10 μM ACh on the HS $\alpha\beta 2$ receptors produced a slight bell-shaped dose-response curve (Figure 5.6C and Table 5.3). Mutation of $\beta 2D218$ to alanine resulted in an apparent rightward shift of the dose-response curve and enhancement of the observed potentiated I_{max} when responses were obtained in phosphate ND-96 buffer. The clear enhancement of potentiation was not observed in HEPES buffer. The inhibition observed in HEPES buffer for the $\beta 2D218A$ mutation could result from either inhibition by HEPES or saturation of a shared Zn^{2+} /HEPES binding site by the high concentrations of HEPES present in the buffer. In phosphate buffer, this inhibition is not present thus potentiation is observed. It is unclear why potentiation is enhanced by the $\beta 2D218A$ mutation compared to wild-type when recorded in phosphate buffer but this could be the result of a differential rightward shift in the EC_{50} and IC_{50} for Zn^{2+} potentiation and inhibition.

The concurrent application of Zn^{2+} (0.001 μM - 1 mM) and 100 μM ACh on oocytes expressing LS receptors produced bell-shaped dose-response curves in both the HEPES and phosphate ND-96 recording buffer. The pEC_{50} ($p = 0.8394$) and pIC_{50} ($p = 0.9204$) values were not significantly different between the two buffers (Figure 5.6B and D and Table 5.3). Zn^{2+} potentiation was reduced in the phosphate buffer (140%) compared to the HEPES buffer (190%) (Figure 5.6D). In contrast, mutation of $\beta 2D218A$ produced dramatically different effects dependent on buffer composition. Mutation of $\beta 2D218$ to alanine produced slight enhancement of potentiation when responses were recorded in HEPES buffer but abolished Zn^{2+} potentiation when using phosphate buffer. This is not easily explained by independent actions of HEPES or Zn^{2+} since simple additive effects would not likely produce these results. The data from both wild-type and mutant receptors recorded in both buffers suggest a possible synergistic activity of HEPES and Zn^{2+} that compensates for the effects of the $\beta 2D218A$ mutation. Loss of Zn^{2+} potentiation by the $\beta 2D218A$ mutation in phosphate buffer suggests a role for this residue in Zn^{2+} mediated potentiation of ACh induced currents on LS receptors. pIC_{50} values found using HEPES or phosphate buffered ND-96 were not significantly different ($p = 0.7593$) (Figure 5.6 and Table 5.3). Moroni et al., (2008) previously suggested that the α^+/α^- interface contains the Zn^{2+} potentiation site. These results appear confounded by the presence of HEPES in the recording buffer. Our results suggest a role of the β^+ face in Zn^{2+} mediated potentiation.

5.5 Discussion.

5.5.1 HEPES Modulation of $\alpha 4\beta 2$ nAChR.

This study investigates the effects of HEPES on HS and LS $\alpha 4\beta 2$ and $\alpha 7$ nAChRs. Our results demonstrate HEPES selectively potentiates the HS stoichiometry compared to the LS $\alpha 4\beta 2$ and $\alpha 7$ nAChRs. The HS receptor is thought to have a $(\alpha 4)_2(\beta 2)_3$ stoichiometry with a unique $\beta +/\beta -$ binding cleft. The putative LS receptor is thought to have a $(\alpha 4)_3(\beta 2)_2$ stoichiometry and does not have a $\beta +/\beta -$ cleft although both HS and LS receptors contain a $\beta +/\alpha -$ binding cleft. Mutagenesis data showed that mutation of the $\beta 2D218$ residue in the $\beta +$ C-loop region abolished HEPES potentiation. These findings ascertain the HEPES potentiation site is located at the $\beta +/\beta -$ cleft of the HS $\alpha 4\beta 2$ receptor site and involves the $\beta 2D218$ residue.

The first inhibitory phase of HEPES inhibition of the HS stoichiometry plateaus at a normalized response of one, suggesting HEPES can only inhibit the potentiated response at these concentrations (100 μ M - 3 mM). The IC_{50} s of the first (LS receptors) and second (HS receptors) HEPES inhibitory phases are similar and are unaffected by the $\beta 2D218A$ mutation. This could mean the inhibitory phases utilize similar mechanisms.

It is unclear from our data what the mechanism or binding site(s) are for HEPES inhibition. The two phase inhibition on the HS receptor suggests multiple mechanisms. Such mechanisms could include an allosteric inhibitory site, competition at the orthosteric site or open-channel block. Conceivably at least one inhibitory mechanism is competition at the orthosteric site since in the crystal structure of AChBP, HEPES was found to bind at the same location as other orthosteric ligands. In addition the IC_{50} values for HEPES inhibition are similar to that observed for HEPES binding to the AChBP. A second possibility is that HEPES is acting as an open-channel blocker at high concentrations. Hump currents, also known as rebound or tail currents, are inward currents which occur during the desensitized phase of the response on washout of the ligand and have been previously linked to open-channel block (Liu et al., 2008). At the concentrations tested, a possible tail current was seen at 300 μ M HEPES. This could suggest that at high HEPES concentrations, open-channel block could be the inhibition mechanism of HEPES (Figure 5.1A and B).

5.5.2 HEPES Effects on $\alpha 7$ nAChRs.

We also investigated the effects of HEPES on $\alpha 7$ nAChRs to determine if similar modulatory effects of HEPES were present. A small insignificant decrease was found in the Hill slope of the ACh dose-response experiments in the Phosphate buffer compared to HEPES buffer. The $\alpha 7$ ACh pEC_{50} values found using the HEPES and Phosphate buffer systems were not

different from one another. In addition $\alpha 7$ receptors were not affected by application of HEPES. Due to seeing no effects of buffer composition on $\alpha 7$ nAChR we suggest that either HEPES or Phosphate buffer systems are adequate for investigating $\alpha 7$ nAChR.

5.5.3 HEPES as a Therapeutic Lead Drug.

Several ligands have different affinities and efficacies for the $\alpha 4\beta 2$ stoichiometries including cytosine, ACh, nicotine and epibatidine (Moroni et al., 2006). To our knowledge, the S-enantiomer of mecamylamine (Taragacept® TC-5213) is the only ligand to show selective activation of the HS channels and inhibition of the LS channels (Taly et al., 2009). In the current study we show that HEPES is a selective PAM of HS receptors when compared to the LS stoichiometry and $\alpha 7$ nAChRs. Stoichiometric selective drugs based on HEPES could provide significant benefits for elucidation of mechanisms involving changes in expression or location of specific stoichiometries of $\alpha 4\beta 2$ receptors. Such ligands could also prove useful in the diagnosis and treatment of CNS disorders. Our laboratory is currently engaged in structure function studies designed to develop novel analogs of HEPES for these purposes.

5.5.4 Mounting Evidence That Good's Buffers Interact with Physiological Systems.

Over the years, Good's buffers have been shown to alter physiological systems. HEPES has been shown to stimulate the production of ATP and decrease the uptake of P-glycoprotein in Caco-2 and MDCK-MDR1 cells (Luo et al., 2010). The hyperpolarization-activated transient currents of human and rat 5-hydroxytryptamine transporters (SERT) expressed in *Xenopus* oocytes were blocked by HEPES with alterations in SERT kinetics (Li et al., 2002). The SERT currents decreased 10-50% by HEPES at concentrations greater than 1 mM. Additionally, HEPES has been shown to affect cell membrane (Poole et al., 1982) and block chloride ion channels (Yamamoto and Suzuki, 1987).

Tris buffer and similar compounds have been revealed to alter physiological responses. Studies suggest that Tris inhibits the function of enzymes such as aminopeptidase and alpha-amylase (Desmarais et al., 2002; Ghalanbor et al., 2008). In addition, Tris, TES and related buffer compounds have been shown to react with nerve agents to form new products (Gab et al., 2010).

To add to this growing list of the physiological and biochemical effects of Good's buffer's, the current study demonstrates alteration of nAChR function by HEPES and Tris. HEPES potentiates and inhibits ACh induced responses on $\alpha 4\beta 2$ nAChRs in a stoichiometric dependent manner. We've also demonstrated that Tris inhibits ACh currents on both HS and LS $\alpha 4\beta 2$ receptor stoichiometries at concentrations > 3 mM. Application of 10 mM Tris inhibited dFBr potentiated ACh induced currents by > 50%.

5.5.5 HEPES Competition with Other PAMs.

Positive allosteric modulators (PAMs) have recently become alluring targets in the search for potential therapeutic agents. PAMs generally function to increase the sensitive and/or efficacy of endogenous ligands such as ACh. Since many electrophysiological studies use a HEPES recording buffer, the discovery that HEPES is an allosteric modulator of $\alpha 4\beta 2$ nAChR presents a concern regarding data interpretation. HEPES potentiation or inhibition may alter the responses of the compound in question. These concerns are especially pertinent with the study and development of other modulators.

We investigated the effects of buffer composition on the sensitive and efficacy of the PAMs dFBr and Zn^{2+} . The affinities and efficacies of these PAMs were altered by Tris and HEPES buffers. A previous study comparing Tris and HEPES buffers showed that the GABA_A PAM, thymol, displayed biphasic behavior in a HEPES buffer while only inhibition was seen when using a Tris buffer (Garcia et al., 2008). Similarly in our laboratory, dFBr appears to be more efficacious for the HS versus LS $\alpha 4\beta 2$ receptors when using a HEPES buffer. But in the absence of HEPES no difference is evident. Despite the apparent difference in the dFBr and HEPES binding sites (dFBr to the $\beta +/\alpha$ -cleft and HEPES to the $\beta +/\beta$ - cleft), the independent modulatory effects of dFBr and HEPES both alter the apparent efficacy, potency and inhibition of dFBr on the LS receptors. The complications arising from HEPES interaction with $\alpha 4\beta 2$ receptors is further illustrated by our re-analysis of the effects of Zn^{2+} on HS and LS receptors. In their original study, Moroni et al. (2008) concluded that Zn^{2+} inhibited $\alpha 4\beta 2$ receptors at the $\beta +/\alpha$ - binding interface while potentiating at the $\alpha +/\alpha$ - interface. This conclusion was based on the observation that Zn^{2+} was selective for the LS stoichiometry with a unique $\alpha +/\alpha$ - cleft along with mutagenesis studies implicating $\beta 2D218$ in inhibition and $\alpha H195$ in potentiation. It is likely that HEPES inhibition of the HS receptor obscured the observation of Zn^{2+} potentiation. Since the HS receptor lacks the $\alpha +/\alpha$ -binding cleft, it must be concluded that the $\alpha +/\alpha$ - cleft is not necessary for potentiation. With data obtained in the absence of HEPES, it seems more likely that the potentiation site is at the $\beta +/\alpha$ -cleft and the inhibitory site is at the $\beta +/\beta$ - cleft. This also explains our observation that Zn^{2+} potentiation increases with the $\beta 2D218$ mutation in phosphate buffer since $\beta 2$ would be expected to alter both potentiation and inhibition.

5.5.6 Summary.

Our data have shown HEPES to be a potentially valuable lead molecule for a new class of stoichiometric selective ligands of $\alpha 4\beta 2$ receptors. Continued work in this direction will likely elucidate features of both ligand and receptor responsible for this selectivity. In addition we have shown that HEPES buffer can interfere in physiological systems involving nAChRs and would

recommend against using this buffer for the study of nAChRs. While phosphate buffer appears to be suitable in some cases, our discovery of changes induced in phosphate buffer on $\alpha 7$ receptors suggests caution in replacing HEPES with phosphate in all situations. While it might be tempting to switch to another Good's buffer in place of HEPES, our data with Tris suggests that this may also be potentially troublesome. Many Good's buffers share common structural features with HEPES and may exert effects on nAChRs. A thorough characterization of these buffers is currently being performed to identify suitable replacements.

5.6 References.

- Adams CE and Stevens KE (2007) Evidence for a role of nicotinic acetylcholine receptors in schizophrenia. *Front Biosci* **12**:4755-4772.
- Aubert I, Araujo DM, Cecyre D, Robitaille Y, Gauthier S and Quirion R (1992) Comparative alterations of nicotinic and muscarinic binding sites in Alzheimer's and Parkinson's diseases. *J Neurochem* **58**:529-541.
- Brejč K, van Dijk WJ, Klaassen RV, Schuurmans M, van Der Oost J, Smit AB and Sixma TK (2001) Crystal structure of an ACh-binding protein reveals the ligand-binding domain of nicotinic receptors. *Nature* **411**:269-276.
- Butt CM, Hutton SR, Marks MJ and Collins AC (2002) Bovine serum albumin enhances nicotinic acetylcholine receptor function in mouse thalamic synaptosomes. *J Neurochem* **83**:48-56.
- Court J, Martin-Ruiz C, Piggott M, Spurden D, Griffiths M and Perry E (2001) Nicotinic receptor abnormalities in Alzheimer's disease. *Biol Psychiatry* **49**:175-184.
- Desmarais WT, Bienvenue DL, Bzymek KP, Holz RC, Petsko GA and Ringe D (2002) The 1.20 Å resolution crystal structure of the aminopeptidase from *Aeromonas proteolytica* complexed with tris: a tale of buffer inhibition. *Structure* **10**:1063-1072.
- Gab J, John H, Melzer M and Blum MM (2010) Stable adducts of nerve agents sarin, soman and cyclosarin with TRIS, TES and related buffer compounds--characterization by LC-ESI-MS/MS and NMR and implications for analytical chemistry. *J Chromatogr B Analyt Technol Biomed Life Sci* **878**:1382-1390.
- Garcia DA, Vendrell I, Galofre M and Sunol C (2008) GABA released from cultured cortical neurons influences the modulation of t-[(35)S]butylbicyclopentylphosphorothionate binding at the GABAA receptor Effects of thymol. *Eur J Pharmacol* **600**:26-31.
- Ghalanbor Z, Ghaemi N, Marashi SA, Amanlou M, Habibi-Rezaei M, Khajeh K and Ranjbar B (2008) Binding of Tris to *Bacillus licheniformis* alpha-amylase can affect its starch hydrolysis activity. *Protein Pept Lett* **15**:212-214.
- Good NE, Winget GD, Winter W, Connolly TN, Izawa S and Singh RM (1966) Hydrogen ion buffers for biological research. *Biochemistry* **5**:467-477.
- Gotti C, Moretti M, Meinerz NM, Clementi F, Gaimarri A, Collins AC and Marks MJ (2008) Partial deletion of the nicotinic cholinergic receptor alpha 4 or beta 2 subunit genes changes the acetylcholine sensitivity of receptor-mediated 86Rb+ efflux in cortex and thalamus and alters relative expression of alpha 4 and beta 2 subunits. *Mol Pharmacol* **73**:1796-1807.
- Harvey RJ, Thomas P, James CH, Wilderspin A and Smart TG (1999) Identification of an inhibitory Zn²⁺ binding site on the human glycine receptor alpha1 subunit. *J Physiol* **520** Pt 1:53-64.
- Hsiao B, Dweck D and Luetje CW (2001) Subunit-dependent modulation of neuronal nicotinic receptors by zinc. *J Neurosci* **21**:1848-1856.
- Hsiao B, Mihalak KB, Repicky SE, Everhart D, Mederos AH, Malhotra A and Luetje CW (2006) Determinants of zinc potentiation on the alpha4 subunit of neuronal nicotinic receptors. *Mol Pharmacol* **69**:27-36.
- Joshi PR, Suryanarayanan A and Schulte MK (2004) A vertical flow chamber for *Xenopus* oocyte electrophysiology and automated drug screening. *J Neurosci Methods* **132**:69-79.
- Kasai M (1998) A comment on the analysis of bell-shaped dose-response curves. *Japanese J of Physiology*. **48**: 91-93.

Kim JS, Padnya A, Weltzin M, Edmonds BW, Schulte MK and Glennon RA (2007) Synthesis of desformylflustrabromine and its evaluation as an $\alpha 4\beta 2$ and $\alpha 7$ nACh receptor modulator. *Bioorg Med Chem Lett* **17**:4855-4860.

Levin ED and Rezvani AH (2007) Nicotinic interactions with antipsychotic drugs, models of schizophrenia and impacts on cognitive function. *Biochem Pharmacol* **74**:1182-1191.

Li M, Farley RA and Lester HA (2002) Voltage-dependent transient currents of human and rat 5-HT transporters (SERT) are blocked by HEPES and ion channel ligands. *FEBS Lett* **513**:247-252.

Lippiello PM (2006) Nicotinic cholinergic antagonists: a novel approach for the treatment of autism. *Med Hypotheses* **66**:985-990.

Liu Q, Yu KW, Chang YC, Lukas RJ and Wu J (2008) Agonist-induced hump current production in heterologously-expressed human $\alpha 4\beta 2$ -nicotinic acetylcholine receptors. *Acta Pharmacol Sin* **29**:305-319.

Luo S, Pal D, Shah SJ, Kwatra D, Paturi KD and Mitra AK (2010) Effect of HEPES buffer on the uptake and transport of P-glycoprotein substrates and large neutral amino acids. *Mol Pharm* **7**:412-420.

Marks MJ, Stitzel JA, Grady SR, Picciotto MR, Changeux JP and Collins AC (2000) Nicotinic-agonist stimulated ($^{86}\text{Rb}^{+}$) efflux and [^3H]epibatidine binding of mice differing in $\beta 2$ genotype. *Neuropharmacology* **39**:2632-2645.

Martin-Ruiz CM, Lee M, Perry RH, Baumann M, Court JA and Perry EK (2004) Molecular analysis of nicotinic receptor expression in autism. *Brain Res Mol Brain Res* **123**:81-90.

Moretti M, Mugnaini M, Tessari M, Zoli M, Gaimarri A, Manfredi I, Pistillo F, Clementi F and Gotti C (2010) A comparative study of the effects of the intravenous self-administration or subcutaneous minipump infusion of nicotine on the expression of brain neuronal nicotinic receptor subtypes. *Mol Pharmacol*.

Moroni M and Bermudez I (2006) Stoichiometry and Pharmacology of Two Human $\alpha 4\beta 2$ Nicotinic Receptor Types. *J Mol Neurosci* **30**:95-96.

Moroni M, Vijayan R, Carbone A, Zwart R, Biggin PC and Bermudez I (2008) Non-agonist-binding subunit interfaces confer distinct functional signatures to the alternate stoichiometries of the $\alpha 4\beta 2$ nicotinic receptor: an $\alpha 4$ - $\alpha 4$ interface is required for Zn^{2+} potentiation. *J Neurosci* **28**:6884-6894.

Moroni M, Zwart R, Sher E, Cassels BK and Bermudez I (2006) $\alpha 4\beta 2$ nicotinic receptors with high and low acetylcholine sensitivity: pharmacology, stoichiometry, and sensitivity to long-term exposure to nicotine. *Mol Pharmacol* **70**:755-768.

Nelson ME, Kuryatov A, Choi CH, Zhou Y and Lindstrom J (2003) Alternate stoichiometries of $\alpha 4\beta 2$ nicotinic acetylcholine receptors. *Mol Pharmacol* **63**:332-341.

Nordberg A (2001) Nicotinic receptor abnormalities of Alzheimer's disease: therapeutic implications. *Biol Psychiatry* **49**:200-210.

Pandya A and Yakel JL (2011) Allosteric Modulator Desformylflustrabromine Relieves the Inhibition of $\alpha 2\beta 2$ and $\alpha 4\beta 2$ Nicotinic Acetylcholine Receptors by β -Amyloid(1-42) Peptide. *J Mol Neurosci*. **45**:42-7.

Picciotto MR, Caldarone BJ, Brunzell DH, Zachariou V, Stevens TR and King SL (2001) Neuronal nicotinic acetylcholine receptor subunit knockout mice: physiological and behavioral phenotypes and possible clinical implications. *Pharmacol Ther* **92**:89-108.

Poole CA, Reilly HC and Flint MH (1982) The adverse effects of HEPES, TES, and BES zwitterion buffers on the ultrastructure of cultured chick embryo epiphyseal chondrocytes. *In Vitro* **18**:755-765.

Sala F, Mulet J, Reddy KP, Bernal JA, Wikman P, Valor LM, Peters L, Konig GM, Criado M and Sala S (2005) Potentiation of human $\alpha 4\beta 2$ neuronal nicotinic receptors by a Flustra foliacea metabolite. *Neurosci Lett* **373**:144-149.

Taly A, Corringier PJ, Guedin D, Lestage P and Changeux JP (2009) Nicotinic receptors: allosteric transitions and therapeutic targets in the nervous system. *Nat Rev Drug Discov* **8**:733-750.

Tapia L, Kuryatov A and Lindstrom J (2007) Ca^{2+} permeability of the $(\alpha 4)_3(\beta 2)_2$ stoichiometry greatly exceeds that of $(\alpha 4)_2(\beta 2)_3$ human acetylcholine receptors. *Mol Pharmacol* **71**:769-776.

Venkataraman P, Venkatachalan SP, Joshi PR, Muthalagi M and Schulte MK (2002) Identification of critical residues in loop E in the 5-HT₃ASR binding site. *BMC Biochem* **3**:15.

Weiland S, Bertrand D and Leonard S (2000) Neuronal nicotinic acetylcholine receptors: from the gene to the disease. *Behav Brain Res* **113**:43-56.

Weltzin MM and Schulte MK (2010) Pharmacological Characterization of the Allosteric Modulator Desformylflustrabromine and its Interaction with $\{\alpha\}_4\{\beta\}_2$ nAChR Orthosteric Ligands. *J Pharmacol Exp Ther*.

Wonnacott S (1997) Presynaptic nicotinic ACh receptors. *Trends Neurosci* **20**:92-98.

Yamamoto D and Suzuki N (1987) Blockage of chloride channels by HEPES buffer. *Proc R Soc Lond B Biol Sci* **230**:93-100.

Zwart R and Vijverberg HP (1998) Four pharmacologically distinct subtypes of $\alpha 4\beta 2$ nicotinic acetylcholine receptor expressed in *Xenopus laevis* oocytes. *Mol Pharmacol* **54**:1124-1131.

CHAPTER 6: Discussion and Conclusions.

6.1 General Overview

Ligand gated ion channels (LGIC) are distributed throughout the peripheral and central nervous system (Taly et al., 2009) where they play a critical role in synaptic transmission at the junctions between nerve cells (synapses) and between nerve and muscle cells by regulating the passage of ions into the cell (Gotti et al., 2006). LGIC receptors are thus of critical importance to learning and memory, gene transcription and muscle contraction. The nicotinic acetylcholine receptor (nAChR) that is discussed in this thesis is one member of this Cys-loop super family of LGICs. Previous studies have demonstrated that dysregulation of nAChRs may underlie multiple neurological disorders including Alzheimer's disease (Court et al., 2001; Nordberg, 2001), Schizophrenia (Adams and Stevens, 2007), Parkinson's disease (Aubert et al., 1992), Autism (Martin-Ruiz et al., 2004; Lippiello, 2006) and nicotine addiction (Picciotto et al., 2001).

The development of novel ligands targeted at LGICs is thought to have high therapeutic potential for the treatment of neurological disorders. In particular, nAChR selective ligands could be useful in treating pathological conditions where nicotinic tone is altered. This thesis has focused on our research developing of a novel class of nicotinic receptor ligands typically described as positive allosteric modulators (PAMs). These ligands bind at an allosteric binding domain on nAChRs and enhance the endogenous neurotransmitter acetylcholine (ACh). This is in contrast to ligands that bind to the orthosteric site and either activate the receptor (competitive full and partial agonists) or block the binding of ACh (competitive antagonists). Many competitive ligands have been developed for nAChRs (for review see (Romanelli et al., 2007)), however positive allosteric modulators have been more elusive. Nonetheless, PAMs are likely to have many advantages over competitive ligands. Since PAMs typically alter responses elicited by the endogenous transmitter but are incapable of activating receptors directly they would enable retention of synaptic control via release of endogenous neurotransmitter. Additionally, some PAMs also preserve the overall response kinetics of the receptors while amplifying the peak responses. This is in contrast to competitive ligands which tend to block or desensitize receptors and reduce acetylcholine mediated synaptic currents. By PAMs exerting their effects only on ACh release and maintaining a normal, yet amplified signal (reviewed in (Bertrand and Gopalakrishnan, 2007)), the result of PAM action is likely to be similar to what might be obtained by increasing receptor numbers at the synapse, the basis of learning and memory. The success of a related class of PAMs for the GABA_AR, the benzodiazepines, illustrates the potential value of this approach. Benzodiazepines are commonly used clinically for the treatment of seizure disorders. Discovery of nAChR PAMs could produce similar benefits in the treatment of other

neurological disorders such as Alzheimer's disease where decline in nAChR numbers are evident.

Despite nAChRs wide distribution throughout the human body and the potential medical application, there are currently no allosteric modulators therapeutically used that selectively target nAChR subtypes. Based on preliminary molecular modeling and sequence comparisons between members of LGICs, we formed the general hypothesis that there are selective allosteric modulators for $\alpha 4\beta 2$ nAChRs and they bind in a similar region as benzodiazepines on GABA_ARs.

This thesis describes the discovery and development of two unique PAMs selective for the $\alpha 4\beta 2$ nAChR subtype. The lead compounds desformylflustrabromine (dFBr) and 4-(2-hydroxyethyl)-1-piperazineethanesulfonic acid (HEPES) were evaluated for their ability to potentiate $\alpha 7$ and both high- and low- ACh sensitivity $\alpha 4\beta 2$ receptors. dFBr was previously shown to act as a selective $\alpha 4\beta 2$ PAM with no potentiating action on the $\alpha 7$ subtype (Sala et al., 2005; Kim et al., 2007). HEPES was previously thought to have no effect on nAChRs and is a common buffer in physiological preparations (Good et al., 1966) although it is observed bound to the orthosteric site in the crystal structure of the AChBP (Brejc et al., 2001).

Chapter 3 of this thesis presented data obtained in the first pharmacological characterization of synthetic dFBr, its effects on nAChR responses to partial and full agonists and its influence on receptor kinetics determined using two-electrode voltage clamp and human receptors expressed in *Xenopus* oocytes. Our studies show different degrees of potentiation for partial and full agonists and shed light on the mechanisms that may underlie the potentiating effect of dFBr. Chapter 4 describes a continuation of these studies aimed at identifying potential involvement of the plus face of the $\beta 2$ subunit and the minus face of the $\alpha 4$ subunit in mediating the effects of dFBr.

In Chapter 5, we turned our attention to our second lead molecule, HEPES. We evaluated HEPES as a PAM for high and low ACh sensitivity $\alpha 4\beta 2$ receptors. Our data show a selectivity of HEPES for the high-ACh sensitivity $\alpha 4\beta 2$ receptor compared to the low-ACh sensitivity subtype. Since HEPES is commonly used as an electrophysiological buffer we also investigated other Good's buffers as well as phosphate for effects on $\alpha 4\beta 2$ and $\alpha 7$ receptor function. Our data suggest that phosphate recording buffers should be preferred over HEPES type buffers due to our observed potentiating and/or inhibitory action of these compounds on nAChRs. This is particularly true in the study of nAChR PAMs where HEPES type buffers may confound interpretation of electrophysiological data.

6.1.1 Pharmacological Characterization of Synthetic dFBr.

The characterization of dFBr pharmacology described in chapter 3 was aimed at determining if the effects of dFBr were dependent on the type of stimulating agonist (partial or full) and on the order and timing of dFBr application. Effects of dFBr were examined using two-electrode voltage clamp and human $\alpha 4\beta 2$ nAChRs expressed in *Xenopus laevis* oocytes. Our data indicate that responses to both partial and full agonists can be potentiated by dFBr. Responses to low-efficacy agonists were potentiated significantly more than responses to high-efficacy agonists ($9.9 \pm 0.05\%$ versus 2.7 ± 0.01 fold change). The agonists ACh, choline and nicotine EC_{50} values were enhanced and reduced respectively with the co-application of dFBr. In contrast, antagonist pIC_{50} values were unaffected by co-application of dFBr. The order of addition of dFBr did not appear to affect potentiation and pre-exposure to dFBr, and did not alter the rise time of the responses when compared to co-exposure with ACh. We also applied dFBr at different points during the ACh response curve. Our data indicate that dFBr could be applied at any point during the ACh-induced response and still elicit an amplified response. Addition of dFBr during the desensitizing phase of the response produced spikes equivalent in height to dFBr when co-applied with ACh, but required more rapid rise times to peak. This peak declined rapidly when compared to the original desensitized response amplitude on continuous application of dFBr. Thus, dFBr appears to “rescue” receptors from desensitization. While precise mechanisms await future single channel analysis, this data may indicate that dFBr shifts receptor equilibrium from a desensitized to an open conformation or, alternatively, permit receptors to enter an alternate open conformation.

We also investigated the inhibitory component of the biphasic dFBr potentiation/inhibition kinetics. In contrast to potentiation, inhibition of ACh-induced responses by dFBr was dependent on membrane potential suggesting it may involve open-channel block by dFBr and ACh. Our data indicates distinct mechanisms for the potentiation and inhibitory components of dFBr action. Since both potentiation and inhibition appear to be mediated by distinct mechanisms, it seems reasonable that alteration of the chemical structure of dFBr may lead to analogs capable of larger potentiation with little or no inhibitory action, or analogs with EC_{50} and IC_{50} values sufficiently different to permit tailoring of the potentiation effect by controlling dFBr concentration.

The results from the study have aided the field in understanding how $\alpha 4\beta 2$ nAChR are modulated biphasically by dFBr. The ability of dFBr to modulate full and partial agonists especially with regards to ACh, nicotine and choline may be a useful quality in developing therapeutic treatment strategies for diseases such as Alzheimer’s disease, nicotine addiction and Autism. The enhancement of choline efficacy by dFBr further suggests that dFBr may be able to

prolong a cholinergic response via choline. In this study we have begun to reveal the mechanism of dFBr potentiation and its ability to reactivate desensitized receptors. The ability of dFBr to reactivate desensitized receptors may be an appealing property especially with regards to smoking cessation, an addiction that up-regulates and desensitizes nAChR. The findings that dFBr inhibition involves open-channel block demonstrates that a single ligand can have several unique functions on a receptor. In addition, because the inhibition mechanism may be separate from the potentiation component, this suggests that the inhibitory actions of dFBr could be removed in future dFBr analogues. Although due to dFBr's apparent ability to potentiate choline-evoked currents and thus alter the time course of cholinergic transmission, inhibition by dFBr may be an advantage to maintaining the temporal relationship.

6.1.2 Putative Binding Domain for Desformylflustrabromine.

In chapter 3, we investigated the involvement of non-orthosteric subunit interfaces of $\alpha 4\beta 2$ receptors in the potentiation of ACh induced responses by dFBr. Amino acids on the non-orthosteric $\beta 2+$ and $\alpha 4-$ subunit faces were mutated to alanine and the receptors were expressed in *Xenopus laevis* oocytes. Residues were chosen for mutation based on sequence homology with amino acids identified as important for binding of benzodiazepine in the GABA_A receptor. Selection of mutations and receptor locations were designed to test our hypothesis that dFBr binds at the subunit interfaces not utilized by binding ACh or competitive nAChR ligands (the non-orthosteric subunit interfaces). Acetylcholine and dFBr induced responses were recorded using two-electrode voltage clamp techniques. The effects of mutations can be classified into fundamentally three distinct categories:

1. Mutations that alter the dose response relationship for ACh in the absence of dFBr.
 - a. Low-sensitivity preparation: $\beta 2W176A$, $\beta 2Y120A$, $\beta 2Y127A$ and $\alpha 4K140A$.
 - b. High-sensitivity preparation: $\beta 2W176A$, $\beta 2D179A$, $\beta 2D217A$, $\beta 2Y120A$, $\beta 2Y127A$, $\alpha 4K140A$, $\alpha 4W88A$.
2. Mutations that alter the ability of dFBr to potentiate ACh induced responses with minimal effect on responses to ACh alone.
 - a. Low-sensitivity preparation: $\beta 2T177A$, $\beta 2D179A$ and $\alpha 4W88A$.
 - b. High-sensitivity preparation: $\beta 2T177A$, $\beta 2D116A$ and $\beta 2Y120A$.
3. Mutations that had no effect on either ACh alone or ACh co-applied with dFBr.
 - a. Low-sensitivity preparation: $\beta 2D217A$, $\beta 2D218A$, $\beta 2D116A$.

b. High-sensitivity preparation: β 2D218A.

Mutations altering the ACh response in the absence of dFBr indicate a potential involvement of the mutated subunit faces (β 2+ or α 4-) in mediation of the native ACh response. Since these subunit faces do not form part of the orthosteric site, our data suggest that conformational changes in these regions of the receptor may be involved in normal function of the receptor, a finding that has never before been demonstrated.

The novel discovery that allosteric clefts play a role in the ACh induced receptor conformational changes leading to activation and desensitization has not been previously demonstrated. One possibility for the basis of these effects might be that the C-loop within allosteric clefts moves as part of the conformational changes that occur on channel opening and/or desensitization. We hypothesize that this movement of the C-loop, possibly by closure similar to what occurs in the orthosteric cleft, might be involved in the conformational change leading to stabilization of a desensitized conformation. Mutations altering responses to ACh might also alter dFBr potentiation; however, since this effect would be obscured by the concurrent effects on ACh responses it is not possible to make any conclusions regarding dFBr interaction with these amino acids.

The second category of mutations that alter the effects of dFBr with little or no change in ACh dose response curves suggests that this set of mutations is involved in the interaction of dFBr with the receptor or with its effect on receptor function. The β 2+ and α 4- faces both appear to play a role in mediating dFBr's effects. Our original hypothesis, that dFBr may bind at the non-orthosteric β 2+ binding face, is supported by these data. The importance of this region in normal receptor function as illustrated by our data suggest that dFBr may alter receptor mechanism by either facilitating or inhibiting the normal function of the receptor at the β 2+/ α 4-subunit interface. As described above, we hypothesize that movement of the C-loop in this region of the receptor may be involved in stabilization of the desensitized conformation of the receptor. If dFBr binding prevents C-loop closure, the desensitized conformation would likely be destabilized leading to a shift in equilibrium to the open conformation. Such an effect might explain the ability of dFBr to rescue desensitized receptors. Removal of dFBr might be expected to restore this equilibrium thus decreasing rapidly the number of receptors back to the unpotentiated levels we observe in experiments where dFBr is applied during the desensitizing phase of the response. Further studies to determine if dFBr actually binds to this region or simply alters the normal conformational changes that occur will require additional studies, perhaps using cysteine scanning mutagenesis and the substituted cysteine accessibility method (SCAM).

6.1.3 Allosteric Modulation of High- and Low- ACh Sensitivity $\alpha 4\beta 2$ Nicotinic Acetylcholine Receptors by HEPES.

In Chapter 5, we present our discovery that 4-(2-hydroxyethyl)-1-piperazineethanesulfonic acid (HEPES) is a PAM selective for high ACh sensitive $\alpha 4\beta 2$ nAChRs. These experiments were prompted by our observation that mutation of $\beta 2D218A$ increased the potentiating effects of dFBr and our observation that HEPES was present in the orthosteric cleft of the homologous AChBP. We postulated that the enhancement of dFBr action might be the result of a blocking of the allosteric site by HEPES. If $\beta 2D218$ interacted with HEPES but not dFBr, then mutation of $\beta 2D218$ to an alanine might decrease affinity for HEPES, enabling dFBr to bind, producing an apparent enhanced effect by dFBr. The effects of HEPES were evaluated in phosphate buffered recording solutions using two-electrode voltage clamp techniques and $\alpha 4\beta 2$ and $\alpha 7$ nAChR subtypes expressed in *Xenopus laevis* oocytes. Varying concentrations of HEPES co-applied with 10 μ M ACh produced a bell-shaped dose-response curve on $\alpha 4\beta 2$ nAChR expressed using the high-ACh sensitivity receptor preparation similar to the kinetics observed for dFBr. Co-exposure of 100 μ M HEPES and 10 μ M ACh produced responses potentiated 190% compared to ACh alone. When concentrations in excess of 100 μ M were used, responses to ACh were inhibited by HEPES. Coincidentally, at concentrations of HEPES typically used in oocyte recording (5-10 mM), the potentiating effects of HEPES are matched by its inhibitory effects thus producing no apparent effect. This may explain why this effect had not previously been observed despite the common use of HEPES in recording media. Mutagenesis of $\beta 2D218$ to alanine blocked the potentiating effects of HEPES suggesting it acts by binding to the plus face of the $\beta 2$ subunit. In contrast to the high-ACh sensitivity $\alpha 4\beta 2$ receptor preparation, receptors expressed using the low-ACh sensitivity preparations were not potentiated by HEPES. The remarkable selectivity of HEPES for a single receptor stoichiometry makes it of interest as a lead compound for highly selective PAMs but also an excellent research tool for the study of allosteric modulation in nAChRs. Understanding the selectivity of HEPES compared to dFBr may reveal new classes of PAMs with varied selectivity for different nAChR subtypes. The apparent competition between HEPES and dFBr strengthens the argument that dFBr is actually binding to subunit interfaces containing the plus face of the $\beta 2$ subunit (our postulated dFBr binding site).

More recent data not presented in this thesis has continued our evaluation of Good's buffers with similar in chemical structure. We have evaluated EPPS (3-[4-(2-Hydroxyethyl)-1-piperazinyl]propanesulfonic acid), PIPES (piperazine-N,N'-bis(2-ethanesulfonic acid), POPSO, MES (2-(N-morpholino)ethanesulfonic acid), MOPS (3-(N-morpholino)propanesulfonic acid),

CHES (N-Cyclohexyl-2-aminoethanesulfonic acid), CAPS (N-cyclohexyl-3-aminopropanesulfonic acid) and CAPSO (N-cyclohexyl-2-hydroxyl-3-aminopropanesulfonic acid) on high- and low- ACh sensitivity preparations. The co-application of varying concentrations of the test compounds EPPS, POPSO, MOPS and CHES with 10 μ M ACh on high-sensitivity receptors produced currents that were biphasically potentiated. Application of POPSO on low-sensitivity receptors produced a bell-shaped dose-response curve where 100 μ M ACh induced currents were both potentiated and inhibited. MES and CAPS inhibited ACh induced currents of receptors expressed in the high-sensitivity receptor preparation. Ligands MOPS, CAPS and CAPSO inhibited ACh induced currents on low-sensitivity receptors. EPPS, MES and CHES had no effect on ACh stimulated responses on low-sensitivity receptors while CAPSO had no influence on high-sensitivity receptors. PIPES was the only tested compound to have no effect on ACh induced currents on either receptor preparation. Tris inhibits both high ($pIC_{50} = 2.0 \pm 0.1$; $IC_{50} = 10$ mM) and low-sensitivity $\alpha 4\beta 2$ nAChRs ($pIC_{50} = 2.2 \pm 0.1$; $IC_{50} = 6.8$ mM). In contrast, no effect was observed for phosphate buffers.

While these experiments are incomplete and do not yet enable us to determine accurate structure function relationships, they do lay the groundwork for future studies to develop improved HEPES type PAMs. In addition, these new data suggest that HEPES type buffers are unsuitable for electrophysiological studies of nAChRs.

The effects of HEPES and Good's buffers on nAChR function likely alters the interpretation of previous PAM studies due to the common use of HEPES as a buffering agent in electrophysiological recording buffers. From our experiments, it is clear that phosphate buffer represents the safest choice for performing electrophysiological studies of nAChRs. It is possible that similar effects of HEPES will be documented in the future for other LGIC receptor subtypes.

6.2 Future Directions.

The investigation of dFBr has so far focused on characterizing dFBr functionally and pharmacologically at the macroscopic level. The goal is to develop dFBr or an analogue of dFBr into a therapeutic ligand. For the therapeutic development of dFBr or a similar ligand to occur, further understanding how dFBr modulates the receptor at the microscopic and whole body system needs to be determined.

6.2.1 Single Channel Studies.

To investigate dFBr at the microscopic level, single channel and patch clamp techniques will be necessary. These techniques would elucidate the mechanisms of action of dFBr

potentiation and inhibition by evaluating its effects on conformational stability on single receptor proteins. Single channel analysis is currently the most direct method available to obtain detailed information regarding the kinetic behavior of ion channels. Application of potentiating concentrations of dFBr and ACh could produce increases in the mean open times of the channel or, alternatively, alter the bursting frequency of the receptor compared to ACh only. These results would provide further evidence that the mechanism of dFBr potentiation involves stabilization of the open conformation of the receptor. Single channel studies would also be helpful in elucidating the mechanism of inhibition by dFBr. These experiments would need to be conducted at holding potentials where open-channel block by dFBr and ACh does not occur. Application of inhibiting concentrations of dFBr and ACh under these conditions might result in reduced open time probabilities or altered bursting rates. Combining these studies with site directed mutagenesis would likely provide novel insights into dFBr mechanisms at the single channel level and would also be extremely valuable at determining the role of the $\beta 2+/\alpha 4-$ interface in normal receptor function.

6.2.2 More Mutations and Scanning Cysteine Accessibility Method (SCAM).

Further work is needed to fully characterize the dFBr binding site. The work covered in this thesis provided the initial groundwork. Additional mutations that might provide insight into dFBr binding include: $\alpha 4W82F$, $\alpha 4N86A$, $\alpha 4W88F$, $\alpha 4K90A$, $\alpha 4K90R$, $\alpha 4V135A$, $\alpha 4T136A$, $\alpha 4T136S$, $\alpha 4H137A$, $\alpha 4H137R$, $\alpha 4L138A$, $\alpha 4L138V$, $\alpha 4T139A$, $\alpha 4T139S$, $\alpha 4K140R$, $\alpha 4T152A$, $\alpha 4T152I$, $\alpha 4P153A$, $\alpha 4P153D$, $\alpha 4P154A$, $\beta 2M126A$, $\beta 2Y127A$, $\beta 2T139S$, $\beta 2S175A$, $\beta 2S175T$, $\beta 2W176F$, $\beta 2T177A$, $\beta 2T177S$, $\beta 2T178A$, $\beta 2Y178F$, $\beta 2D179A$, $\beta 2D179Q$, $\beta 2N215A$, $\beta 2N215E$, $\beta 2D218Q$, $\beta 2S219A$, $\beta 2S219T$, $\beta 2T220A$, $\beta 2T220S$, $\beta 2Y221A$ and $\beta 2Y221F$. In addition, mutations that produced little or no effect on dFBr or ACh effects should be mutated to cysteine to determine if these would be suitable sites for SCAM. SCAM utilizes the ability to modify cysteine residues not involved in disulfide bonds with exogenous thiol reagents during the course of an experiment. Amino acids are substituting with cysteine then modified by the formation of thiol esters in the presence and absence of ligand. Changes in the rate of modification in the presence of the ligand help determine if the presence of the ligand alters the accessibility of the target amino acid. Decreased accessibility in the presence of dFBr would further support the hypothesis that the substituted amino acid is located within the ligand binding site. Ideally, cysteine mutations should be made on all key binding loops within the putative binding domain to confirm the location of the dFBr and HEPES binding domains. SCAM can also be used to identify portions of the receptor that move during the receptor cycle thus helping to identify the role of these regions in normal receptor functions. This approach could enable testing of the hypothesis that the C-loop of

the $\beta 2+$ face closes during receptor activation/desensitization and whether or not dFBr alters this closure.

6.2.3 The Development of the dFBr Binding Site on AChBP.

One of the goals of Dr. Marvin Schutte's laboratory is to develop high throughput drug screening techniques. A potential candidate for a high throughput screening platform is the Acetylcholine Binding Protein (AChBP). Kinetic and affinity data for ligands interacting with the AChBP can be evaluated using Scintillation Proximity Assay (SPA) and Surface Plasmon Resonance (SPR). AChBP has similar pharmacology sensitivity to nAChR. The construction of AChBP proteins that are more similar to LGICs via mutagenesis may facilitate the drug screening process and lead to a better understanding of ligand binding sites.

One direction that the dFBr project can take is to develop an AChBP homologue that binds dFBr similarly to $\alpha 4\beta 2$ nAChR. This would involve mutating AChBP residues to the equivalent of dFBr binding site residues. dFBr analogues could then be screened on the dFBr sensitive AChBP rapidly using techniques such as the SPR. This would greatly enhance the rate at which we are able to evaluate dFBr analogues and develop an understanding of this drug class. In addition, a dFBr sensitive AChBP homolog will be useful in studying the specific amino acid interactions that occur for the binding of dFBr to $\alpha 4\beta 2$ nAChR. Crystal structures of the dFBr sensitive AChBP unbound and bound with dFBr could be resolved and be used to further understand the binding orientation and protein structural rearrangements induced by dFBr. The development of this protein will help verify binding site models of the $\alpha 4\beta 2$ receptor and provide a platform for high throughput screening of the new dFBr class of modulatory agents.

6.2.4 Receptor Selectivity.

dFBr selectivity has been thoroughly investigated by us on $\alpha 4\beta 2$ and $\alpha 7$ nAChR and by others on $\alpha 3\beta 2$ receptors (Pandya and Yakel, 2011). The selectivity appears localized to receptors that contain the $\beta 2$ subunit. However, many more subtypes of nAChR exists including the $\alpha 3\beta 2$, $\alpha 4\beta 2$, $\alpha 3\beta 4$ subtypes. While Sala et al., (2005) evaluated several subtypes and suggested that dFBr was selective for $\alpha 4\beta 2$ receptors, we observed differences in both potency and efficacy of synthetic dFBr compared to their results using dFBr purified from natural sources. This suggests that dFBr selectivity may be broader than was initially observed. Thus the true selectivity of dFBr is unknown. The effect of dFBr on other nAChR subtypes need to be evaluated. In addition, it would be interesting to determine if dFBr also interacts with other LGIC receptors. Our laboratory has performed preliminary studies indicating dFBr does not potentiate

serotonin responses on 5-HT_{3A}R but the LGIC family is large and many other possibilities exist. The development of radiolabeled dFBr might facilitate these studies by enabling large receptor binding studies to be performed using high throughput approaches. The development of radiolabeled dFBr is currently underway in our collaborators' laboratory.

6.2.5 dFBr Analogues.

The lead compound in these studies, dFBr, is a natural product and is unlikely to be suitable in its current form as a therapeutic agent. A number of potential problems are likely to be encountered when administering dFBr for the treatment of neurological disorders. These include poor pharmacokinetics, transit across the blood brain barrier (BBB), therapeutic efficacy and selectivity. To overcome these difficulties, a number of steps are typically involved in optimizing the structure of the ligand. These include:

1. Optimization of the pharmacophore structure (increased potency and selectivity).
2. Evaluation of biological distribution and optimization for target tissue (increased BBB transit and partitioning into brain).
3. Improved chemical stability in vivo (optimized pharmacokinetics).
4. Decreased toxicity (evaluation of non-LGIC effects – selectivity).
5. Evaluation and enhancement of therapeutic efficacy.

The first step in this process involves evaluation in receptor expression systems as described in this thesis. Steps 2-5 involve the use of animal models and eventually human subjects. Each step involves numerous structurally varied analogs. This is likely to be a long process that will take place in several laboratories before commercially available compounds become available. We are currently in Stage 1 although interest by other laboratories and the recent release of synthetic dFBr by Tocris is likely to facilitate future animal studies. The release of synthetic dFBr is largely the result of our efforts and is based on the data presented in this thesis. We are also in the process of developing and characterizing dFBr analogues to optimize the dFBr pharmacophore. Our collaborators have synthesized 26 different analogues which we have analyzed. Results have shown that 12 of the 26 analogues potentiate α 4 β 2 nAChRs 250-290%. These 12 compounds selectively potentiated α 4 β 2 and not α 7 nAChR. An optimized ligand would be expected to have high selectivity for α 4 β 2 receptors, higher potency, increased efficacy and lack of inhibitory effects. Improved characterization of the dFBr binding site is expected to enhance our ability to optimize the pharmacophore by enabling receptor homology modeling of the binding site and docking of potential ligands. This will lead to "rational drug

design” for dFBr ligands. As we progress further toward ligands with better BBB transit, *in vivo* stability and therapeutic efficacy this fundamental data on dFBr’s requirements for selective interaction will guide further modification of the structure without loss of $\alpha 4\beta 2$ selectivity.

6.2.6 Further Studies of HEPES Potentiation.

One unexpected finding that arose from the work in this thesis is the discovery that HEPES selectively modulates high ACh sensitive $\alpha 4\beta 2$ receptors compared to low ACh sensitive $\alpha 4\beta 2$ receptors and $\alpha 7$ nAChRs. This is one of the only ligands available that can selectively modulate high ACh sensitive $\alpha 4\beta 2$ receptors. To our knowledge, S-enantiomer of mecamylamine (TC-5213), is the only other ligand shown to show *in vivo* selective activation of the high-sensitivity channels and inhibition of the low sensitivity $\alpha 4\beta 2$ nAChRs (Taly et al., 2009). The development of stoichiometric selective ligands would be useful in determining the distribution of these receptor populations throughout the central and peripheral nervous system in normal and diseased tissues. In addition such selective ligands could be highly valuable therapeutic ligands to treat disorders where dysregulation of one receptor stoichiometry occurs.

To develop HEPES or HEPES analogues as useful ligands, several steps are necessary. Like the path that dFBr has and will continue to travel, HEPES must also go through this process. This includes the development and evaluation of HEPES analogues on $\alpha 4\beta 2$ and other nAChR subtypes, understanding of HEPES mechanisms, characterization of its binding site and testing in animal models and ultimately human subjects. One obstacle in the development of HEPES analogs is the low hydrophobicity of the parent compound, a problem not likely with dFBr analogs with a calculated LogP value of -4.87. This problem could make penetration of the BBB more difficult to engineer into HEPES compared to dFBr.

6.3 Summary.

The work described in this thesis has contributed significantly to advancement of our understanding of nAChR function in general and specifically to the development of an entirely new class of nAChR ligand. The long term impact is likely to be significant as this drug class is developed. In addition, the discovery of the effects of HEPES on nAChRs is likely to help prevent misleading experimental results due to the complicating factors of using HEPES in recording buffers. HEPES may additionally prove to be a valuable lead in the development of a new, even more selective ligand for characterization of $\alpha 4\beta 2$ receptors in brain. This body of work also aided in the mechanistic understanding of how non-orthosteric clefts may be involved in the receptor mechanism.

Therapeutic applications of the discoveries made in this thesis are also likely to be broad. Development of a novel $\alpha 4\beta 2$ modulator has important application in the treatment of some of the most serious diseases facing us today. Alzheimer's disease (Prevention, 2010a) and Autism (Prevention, 2010b) are rapidly increasing in our population and smoking continues to underlie some of the most debilitating diseases including cardiovascular disease, stroke and cancer (Prevention, 2010c). The development of new drugs to treat these diseases is crucial and compounds like dFBr and HEPES target the specific receptor identified as important in these disorders, the $\alpha 4\beta 2$ receptors. We have begun the complicated endeavor of revealing the mechanism behind dFBr's potentiation and inhibition actions on $\alpha 4\beta 2$ receptors and we have located and characterized the $\alpha 4\beta 2$ dFBr and HEPES binding sites. This will greatly facilitate the development of novel dFBr and HEPES analogues ultimately leading to a completely novel therapeutic agent.

6.4 References.

- Adams CE and Stevens KE (2007) Evidence for a role of nicotinic acetylcholine receptors in schizophrenia. *Front Biosci* **12**:4755-4772.
- Aubert I, Araujo DM, Cecyre D, Robitaille Y, Gauthier S and Quirion R (1992) Comparative alterations of nicotinic and muscarinic binding sites in Alzheimer's and Parkinson's diseases. *J Neurochem* **58**:529-541.
- Bertrand D and Gopalakrishnan M (2007) Allosteric modulation of nicotinic acetylcholine receptors. *Biochem Pharmacol* **74**:1155-1163.
- Brejč K, van Dijk WJ, Klaassen RV, Schuurmans M, van Der Oost J, Smit AB and Sixma TK (2001) Crystal structure of an ACh-binding protein reveals the ligand-binding domain of nicotinic receptors. *Nature* **411**:269-276.
- Court J, Martin-Ruiz C, Piggott M, Spurden D, Griffiths M and Perry E (2001) Nicotinic receptor abnormalities in Alzheimer's disease. *Biol Psychiatry* **49**:175-184.
- Good NE, Winget GD, Winter W, Connolly TN, Izawa S and Singh RM (1966) Hydrogen ion buffers for biological research. *Biochemistry* **5**:467-477.
- Gotti C, Zoli M and Clementi F (2006) Brain nicotinic acetylcholine receptors: native subtypes and their relevance. *Trends Pharmacol Sci* **27**:482-491.
- Kim JS, Padnya A, Weltzin M, Edmonds BW, Schulte MK and Glennon RA (2007) Synthesis of desformylflustrabromine and its evaluation as an alpha4beta2 and alpha7 nACh receptor modulator. *Bioorg Med Chem Lett* **17**:4855-4860.
- Lippiello PM (2006) Nicotinic cholinergic antagonists: a novel approach for the treatment of autism. *Med Hypotheses* **66**:985-990.
- Martin-Ruiz CM, Lee M, Perry RH, Baumann M, Court JA and Perry EK (2004) Molecular analysis of nicotinic receptor expression in autism. *Brain Res Mol Brain Res* **123**:81-90.
- Nordberg A (2001) Nicotinic receptor abnormalities of Alzheimer's disease: therapeutic implications. *Biol Psychiatry* **49**:200-210.
- Pandya A and Yakel JL (2011) Allosteric Modulator Desformylflustrabromine Relieves the Inhibition of alpha2beta2 and alpha4beta2 Nicotinic Acetylcholine Receptors by beta-Amyloid(1-42) Peptide. *J Mol Neurosci*.
- Picciotto MR, Caldarone BJ, Brunzell DH, Zachariou V, Stevens TR and King SL (2001) Neuronal nicotinic acetylcholine receptor subunit knockout mice: physiological and behavioral phenotypes and possible clinical implications. *Pharmacol Ther* **92**:89-108.
- Prevention CfDca (2010a) Alzheimer's Disease, in *Healthy Aging*, Centers for Disease Control and Prevention, Atlanta.
- Prevention CfDca (2010b) Autism Spectrum Disorders (ASDs), in, Centers for Disease Control and Prevention, Atlanta.
- Prevention CfDca (2010c) Health Effects, in *Smoking & Tobacco Use*, Centers for Disease Control and Prevention, Atlanta.
- Romanelli MN, Gratteri P, Guandalini L, Martini E, Bonaccini C and Gualtieri F (2007) Central nicotinic receptors: structure, function, ligands, and therapeutic potential. *ChemMedChem* **2**:746-767.

Sala F, Mulet J, Reddy KP, Bernal JA, Wikman P, Valor LM, Peters L, König GM, Criado M and Sala S (2005) Potentiation of human $\alpha 4\beta 2$ neuronal nicotinic receptors by a *Flustra foliacea* metabolite. *Neurosci Lett* **373**:144-149.

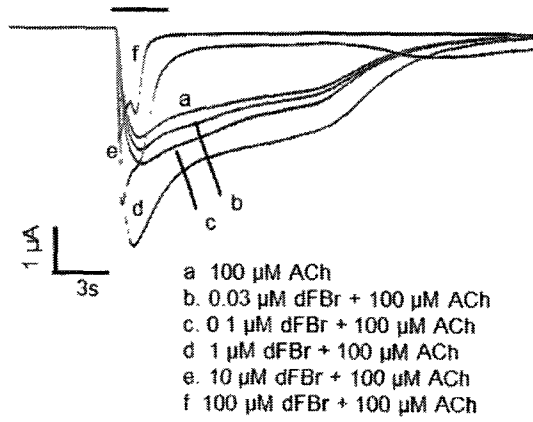
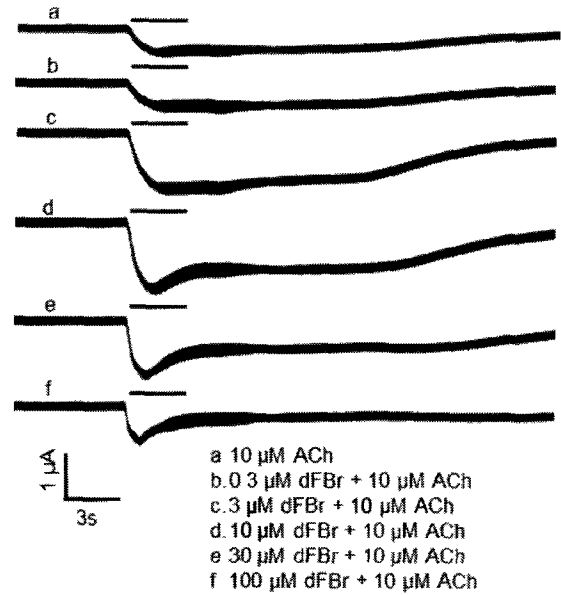
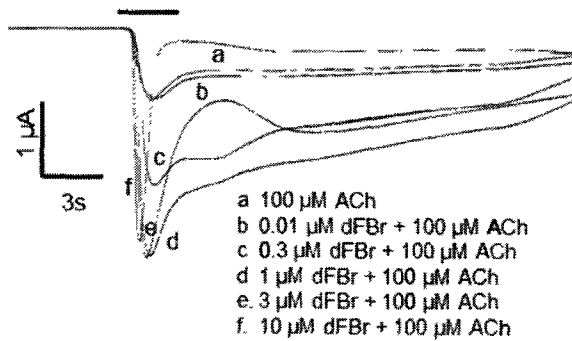
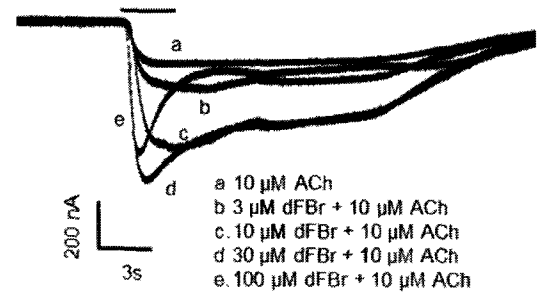
Taly A, Corringer PJ, Guedin D, Lestage P and Changeux JP (2009) Nicotinic receptors: allosteric transitions and therapeutic targets in the nervous system. *Nat Rev Drug Discov* **8**:733-750.

Appendix A.1 Response profiles for co-application of varying concentrations of dFBr and ACh for $\beta 2+$ face B-loop mutant receptors expressed using the low (LS) and high (HS) sensitive receptor preparations.

Xenopus oocytes were prepared using the high and low sensitive receptor preparations (HS mRNA injected at a ratio of $1\alpha:5\beta$; LS mRNA injection at a ratio of $5\alpha:1\beta$). Expressing oocytes were exposed to increasing concentrations of ACh and dFBr. **A)** Co-application of dFBr and 100 μM ACh response traces for $\beta 2\text{W}176\text{A}$ receptors expressed via the low sensitive receptor preparation. **B)** Co-application of dFBr and 10 μM ACh response traces for $\beta 2\text{W}176\text{A}$ receptors expressed via the high sensitive receptor preparation. **C)** Co-application of dFBr and 100 μM ACh response traces for $\beta 2\text{T}177\text{A}$ receptors expressed via the low sensitive receptor preparation. **D)** Co-application of dFBr and 10 μM ACh response traces for $\beta 2\text{D}179\text{A}$ receptors expressed via the high sensitive receptor preparation. Response traces were recorded from a single oocyte. The solid bar above the response trace indicates the time the oocyte was exposed to co-application of varying concentrations of dFBr and ACh. For figures A, B and F, the response traces are offset for clarity.

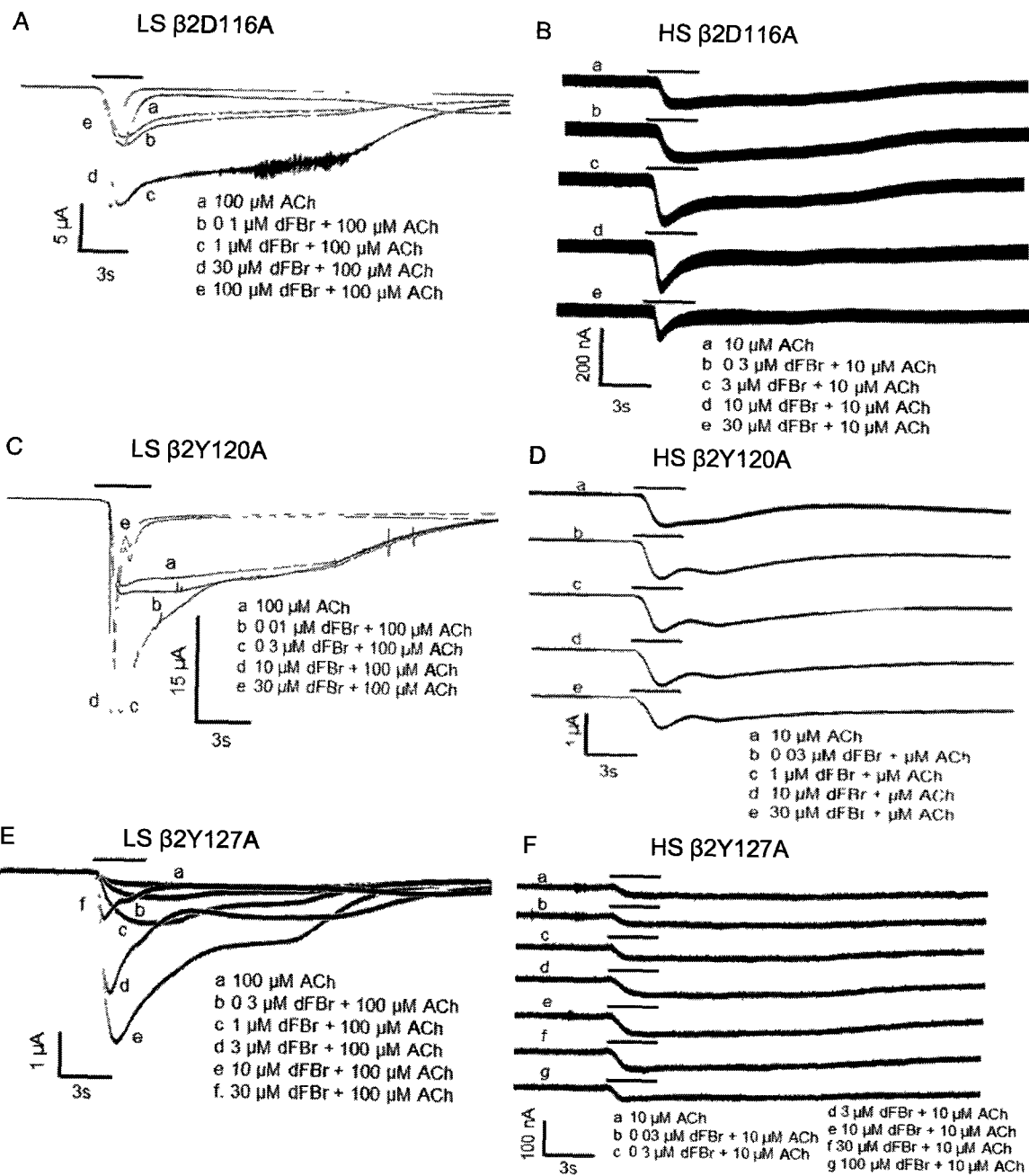
Appendix A.2 Response profiles for co-application of varying concentrations of dFBr and ACh for $\beta 2+$ face C-loop mutant receptors expressed using the low (LS) and high (HS) sensitive receptor preparations.

Xenopus oocytes were prepared using the high and low sensitive receptor preparations (HS mRNA injected at a ratio of 1 α :5 β ; LS mRNA injection at a ratio of 5 α :1 β). Expressing oocytes were exposed to increasing concentrations of ACh and dFBr. **A)** Co-application of dFBr and 100 μ M ACh response traces for $\beta 2D217A$ receptors expressed via the low sensitive receptor preparation. **B)** Co-application of dFBr and 10 μ M ACh response traces for $\beta 2D217A$ receptors expressed via the high sensitive receptor preparation. **C)** Co-application of dFBr and 100 μ M ACh response traces for $\beta 2D218A$ receptors expressed via the low sensitive receptor preparation. **D)** Co-application of dFBr and 10 μ M ACh response traces for $\beta 2D218A$ receptors expressed via the high sensitive receptor preparation. Response traces were recorded from a single oocyte. The solid bar above the response trace indicates the time the oocyte was exposed to co-application of varying concentrations of dFBr and ACh. For figure B, the response traces are offset for clarity.

A LS β 2D217AB HS β 2D217AC LS β 2D218AD HS β 2D218A

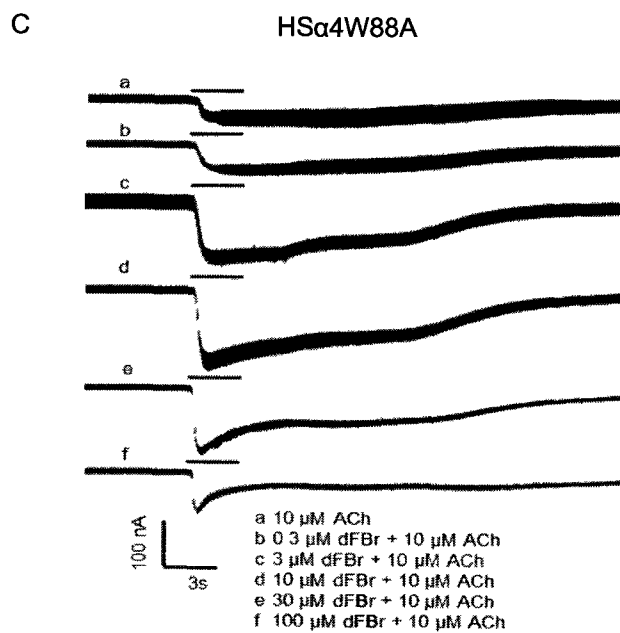
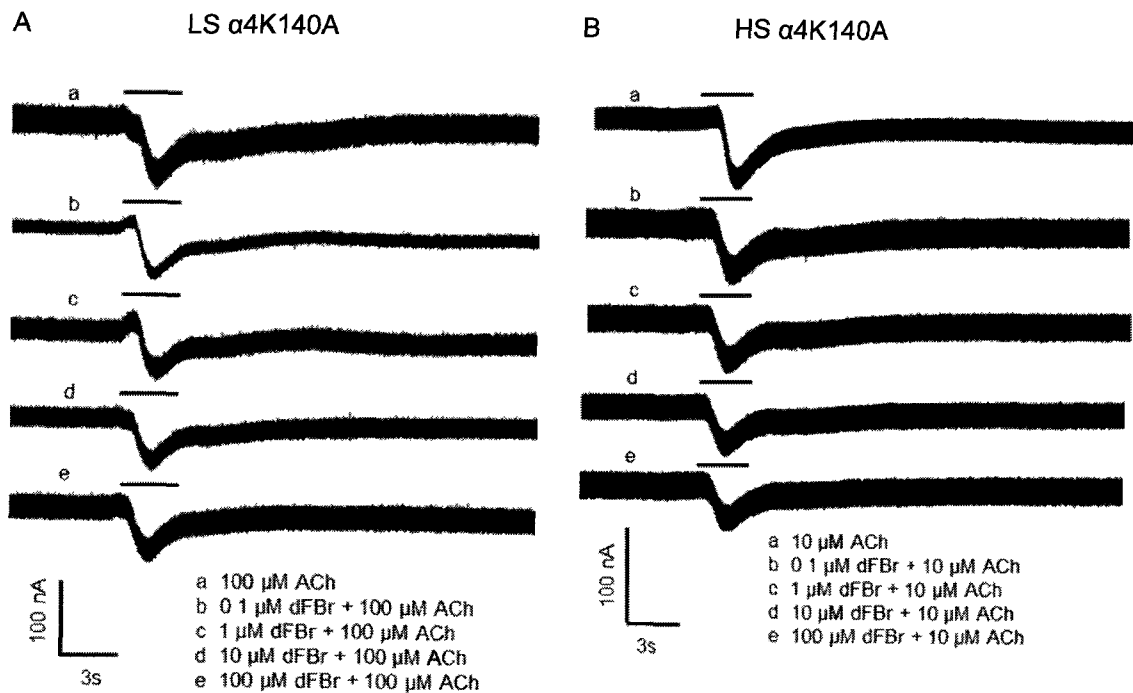
Appendix A.3 Response profiles for co-application of varying concentrations of dFBr and ACh for β 2+ face A-loop mutant receptors expressed using the low (LS) and high (HS) sensitive receptor preparations.

Xenopus oocytes were prepared using the high and low sensitive receptor preparations (HS mRNA injected at a ratio of 1 α :5 β ; LS mRNA injection at a ratio of 5 α :1 β). Expressing oocytes were exposed to increasing concentrations of ACh and dFBr. **A)** Co-application of dFBr and 100 μ M ACh response traces for β 2D116A receptors expressed via the low sensitive receptor preparation. **B)** Co-application of dFBr and 10 μ M ACh response traces for β 2D116A receptors expressed via the high sensitive receptor preparation. **C)** Co-application of dFBr and 100 μ M ACh response traces for β 2Y120A receptors expressed via the low sensitive receptor preparation. **D)** Co-application of dFBr and 10 μ M ACh response traces for β 2Y120A receptors expressed via the high sensitive receptor preparation. **E)** Co-application of dFBr and 100 μ M ACh response traces for β 2Y127A receptors expressed via the low sensitive receptor preparation. **F)** Co-application of dFBr and 10 μ M ACh response traces for β 2Y127A receptors expressed via the high sensitive receptor preparation. Response traces were recorded from a single oocyte. The solid bar above the response trace indicates the time the oocyte was exposed to co-application of varying concentrations of dFBr and ACh. For figures B, D and F, the response traces are offset for clarity.



Appendix A.4 Response profiles for co-application of varying concentrations of dFBr and ACh for α 4- face mutant receptors expressed using the low (LS) and high (HS) sensitive receptor preparations.

Xenopus oocytes were prepared using the high and low sensitive receptor preparations (HS mRNA injected at a ratio of 1 α :5 β ; LS mRNA injection at a ratio of 5 α :1 β). Expressing oocytes were exposed to increasing concentrations of ACh and dFBr. **A)** Co-application of dFBr and 100 μ M ACh response traces for α 4K140A receptors expressed via the low sensitive receptor preparation. **B)** Co-application of dFBr and 10 μ M ACh response traces for α 4K140A receptors expressed via the high sensitive receptor preparation. **C)** Co-application of dFBr and 10 μ M ACh response traces for α 4W88A receptors expressed via the high sensitive receptor preparation. Response traces were recorded from a single oocyte. The solid bar above the response trace indicates the time the oocyte was exposed to co-application of varying concentrations of dFBr and ACh. For figures A, B and C, the response traces are offset for clarity.



Appendix B: IACUC Assurance



(907) 474-7600
 (907) 474-5044 fax
 iyacuc@uaf.edu
 www.uaf.edu/iacuc

Institutional Animal Care and Use Committee

505 N. Koyukuk Dr. Suite 212 P.O. Box 757270 Fairbanks, Alaska 99775-7270

February 6, 2009

To: Marvin Schulte, PhD
 Principal Investigator

From: Erich H. Folinsow, PhD
 IACUC Chair

Re: IACUC Assurance Application

The University of Alaska Fairbanks Institutional Animal Care and Use Committee (IACUC) reviewed the following Assurance at their December 1, 2008, meeting. This Assurance was approved pending receipt of a revised assurance addressing the committee's questions. The assurance received on January 29, 2009 was determined to be satisfactory; therefore I am pleased to issue approval.

Protocol#: 08-71

Title: *Allosteric Modulation of Ligand Gated Ion Channels*

Received: November 24, 2008 (orig)
 January 29, 2009 (rev)

Approved: February 6, 2009

Review Due: February 6, 2010

The PI is responsible for acquiring and maintaining all required permits and permissions prior to beginning work on this assurance. Failure to obtain or maintain valid permits is considered a violation of an IACUC assurance, and could result in revocation of IACUC approval.



INSTRUCTIONS REGARDING AN APPROVED *ASSURANCE OF ANIMAL CARE*

Communication of Assurance

All lab animals and captive wildlife used under this *Assurance* must be identified with the assigned IACUC number by using cage cards, door cards, or some ready method of identifying pens or paddocks with this *Assurance*.

Access to the Approved Assurance

It is required that a readily accessible copy of the approved *Assurance* be kept in the laboratory and/or office. The PI is responsible for ensuring that all personnel working on this project read, understand and follow the methods and procedures identified in this *Assurance*.

Life Span of the Assurance and Reporting Requirements

All *Assurances* are valid for 12 months after approval and must be kept current with respect to new methods or techniques as they evolve. Notification from the IACUC will be sent the month prior to the annual anniversary of the approval of the *Assurance* of a Continuing Review Form due. The Continuing Review Form serves as an annual report to the IACUC regarding this *Assurance*. Continuing Reviews may occur for 2 years after the initial approval date. In the third year a Rationale for Continued Use of Animals must be completed and a new *Assurance* application must be submitted if the work is to be ongoing.

Formal Training Requirement for Personnel Working with Live Vertebrates

Personnel working with live vertebrates must complete the appropriate module(s) of the University's web-based training program in animal care and use. All individuals performing manipulations on vertebrates (handling, capture, blood collection, surgery, etc.) must demonstrate proper training, experience, and capability. A principal investigator is responsible for ensuring that all individuals working on his/her protocol have completed both the required IACUC web-based training modules and appropriate protocol-specific training. It is the Institution's responsibility to ensure that proper training is made available. Contact the Office of Research Integrity for more information about UAF training programs.

Notify Funding Agencies about IACUC Protocol Review

Please notify the Research Integrity Administrator if a letter confirming IACUC review and approval is required by a funding agency. Please provide the necessary contact information to the Administrator: fy2iacuc@uaf.edu

Additional Information

Visit the IACUC web site, <http://www.uaf.edu/iacuc>, or contact any member of the IACUC or the Office of Research Integrity.





Institutional Animal Care and Use Committee

909 N. Koyuk Dr. Suite 200 • Box 757270 Fairbanks, Alaska 99777-2070

Phone: 907-475-7600
Fax: 907-474-5630
fyiac@uaf.edu
www.uaf.edu/fyac

February 11, 2011

To: Marvin Schulte, PhD
Principal Investigator

From University of Alaska Fairbanks IACUC
Re [144916-5] Allosteric Modulation of Ligand Gated Ion Channels

The IACUC has reviewed the Progress Report by Designated Member Review and the Protocol has been approved for an additional year

Received	February 8, 2011
Initial Approval Date	February 8, 2009
Effective Date	February 11, 2011
Expiration Date	February 8, 2012

This action is included on the February 16, 2011 IACUC Agenda.

If you have any questions about how to submit the required information through IRBNet please contact the Office of Research Integrity for assistance (email fyoni@ualf.edu or call x7800/x7832)